REMOVAL OF HEAVY METALS FROM WATER BY FUNCTIONALIZED CARBON NANOTUBES WITH DEEP EUTECTIC SOLVENTS: AN ARTIFICIAL NEURAL NETWORK APPROACH

SEEF SAADI FIYADH

INSTITUTE FOR ADVANCED STUDIES
UNIVERSITY OF MALAYA
KUALA LUMPUR

2019

REMOVAL OF HEAVY METALS FROM WATER BY FUNCTIONALIZED CARBON NANOTUBES WITH DEEP EUTECTIC SOLVENTS: AN ARTIFICIAL NEURAL NETWORK APPROACH

SEEF SAADI FIYADH

THESIS SUBMITTED IN FULFILMENT OF THE REQUIREMENTS FOR THE DEGREE OF DOCTOR OFPHILOSOPHY

INSTITUTE FOR ADVANCED STUDIES
UNIVERSITY OF MALAYA
KUALA LUMPUR

2019

UNIVERSITY OF MALAYA

ORIGINAL LITERARY WORK DECLARATION

Name of Candidate: Seef Saadi Fiyadh

Matric No: HHC150018

Name of Degree: Doctor of philosophy

Title of Project Paper/Research Report/Dissertation/Thesis ("this Work"):

REMOVAL OF HEAVY METALS FROM WATER BY FUNCTIONALIZED CARBON NANOTUBES WITH DEEP EUTECTIC SOLVENTS: AN ARTIFICIAL NEURAL NETWORK APPROACH

Field of Study: Materials engineering (Nanotechnology)

I do solemnly and sincerely declare that:

(1) I am the sole author/writer of this Work;
(2) This Work is original;
(3) Any use of any work in which copyright exists was done by way of fair dealing and for permitted purposes and any excerpt or extract from, or reference to or reproduction of any copyright work has been disclosed expressly and sufficiently and the title of the Work and its authorship have been acknowledged in this Work;
(4) I do not have any actual knowledge nor do I ought reasonably to know that the making of this work constitutes an infringement of any copyright work;
(5) I hereby assign all and every rights in the copyright to this Work to the University of Malaya ("UM"), who henceforth shall be owner of the copyright in this Work and that any reproduction or use in any form or by any means whatsoever is prohibited without the written consent of UM having been first had and obtained;
(6) I am fully aware that if in the course of making this Work I have infringed any copyright whether intentionally or otherwise, I may be subject to legal action or any other action as may be determined by UM.

Candidate's Signature Date:

Subscribed and solemnly declared before,

Witness's Signature Date:

Name:
Designation:

REMOVAL OF HEAVY METALS FROM WATER BY FUNCTIONALIZED CARBON NANOTUBES WITH DEEP EUTECTIC SOLVENTS: AN ARTIFICIAL NEURAL NETWORK APPROACH

ABSTRACT

Water is a vital nutrient, it is the most valuable resource for the existence and maintenance of life. Heavy metals are the most challenging pollutants that require continues monitoring and creative solutions to be removed from polluted water. The multi-wall carbon nanotubes (MW-CNTs) is a sophisticated adsorbent for heavy metals removal from water, but it needs a functionalization using chemicals and non-environmental friendly acids by a complicated process. This research uses the deep eutectic solvents (DESs) as a novel functionalization agent for CNTs. DESs, as novel solvents involved in chemistry, were recently involved in different applications due to their advantages towards green chemistry. Different molar ratios of salts to hydrogen bond donors (HBDs) were used to prepare the DESs. The selected DESs were used as CNTs functionalization agents to form novel adsorbents for mercury ions (Hg^{2+}), lead ions (Pb^{2+}) and arsenic ions (As^{3+}) removal from water. A screening process was conducted for the removal of the selected heavy metal using the adsorption process. Three kinetic models were used to identify the adsorption rate and mechanism, the pseudo-second order best described the adsorption kinetics. The adsorption process is complicated due to the interactive effect of many parameters. The relationship between the parameters in the adsorption process (i,e; contact time, adsorbent dosage, pH and initial concentration) is nonlinear; thus, there is a necessity for mapping such a complicated process by a powerful modelling technique. Therefore, artificial neural network (ANN) was proposed as a novel modelling technique for this particular nano-adsorption system as a less complicated modelling method within the sophisticated biological networks. This technique is selected for the treatment such a non-linear function relationship among the variables. The ANN techniques do not require

any mathematical induction since ANN analysing the dataset and recognize their correlations from inputs and outputs series of the dataset without any presumption about their interrelations and characteristics. Different ANN algorithms have been used in this study such as feed forward backpropagation algorithm, layer recurrent algorithm, adaptive neuro fuzzy inference system and NARX neural network. Moreover, various indicators were implemented to evaluate the ANN model's productivity including relative root mean square error (RRMSE), mean square error (MSE), root mean square error (RMSE), mean absolute percentage error (MAPE) and relative error (RE). The sensitivity study for the parameters in the experimental work was achieved. Three algorithms are used for the modelling of Pb^{2+} ions, the maximum relative error (RE) for the layer recurrent is 18.67%, whereby, for the feed-forward back-propagation RE is 11.62%. The best result achieved for Pb^{2+} removal using ANFIS algorithm is with RE 7.078%. For As^{3+} removal using different adsorbents, two algorithms were applied for the modelling, the feed-forward back-propagation maximum RE achieved is 5.97% while, the NARX algorithm achieved better accuracy with maximum RE of 5.79%. The NARX algorithm is used for the modelling of Hg^{2+} removal. The maximum RE obtained is 3.49%. The modelling results revealed that NARX algorithm is the best compared to the used algorithms in term of accuracy.

Keywords: Heavy metals removal; carbon nanotubes; deep eutectic solvents; water treatment; artificial neural network.

PENYINGKIRAN LOGAM BERAT DARIPADA AIR MENGGUNAKAN NANOTIUB KARBON FUNGSIAN KHAS DENGAN PELARUTAN EUTEKTIK MENDALAM: SATU KAEDAH RANGKAIAN SARAF BUATAN

ABSTRAK

Air, satu nutrien penting, ia merupakan sumber yang sangat bernilai bagi kewujudan dan kelestarian hidup. Logam berat merupakan bahan pencemar merbahaya yang memerlukan pemantauan berterusan dan penyelesaian kreatif untuk dikeluarkan daripada air tercemar. Karbon Tiub nano (CNTs) telah terbukti sebagai penyerap canggih untuk menghilangkan logam berat, tetapi memerlukan fungsian dengan asid tidak mesra alam dan bahan kimia melalui proses yang rumit. Kajian ini menggunakan kaedah ejen fungsian novel untuk CNT, iaitu pelarut eutektik dalam (DES), dengan kata lain, cecair ionik analog. DES sejak akhir-akhir ini terlibat dalam banyak aplikasi kerana kemampuannya bertindak sebagai pelarut novel dalam kimia. DES ini telah disediakan menggunakan nisbah molar yang berbeza bagi penderma bon hidrogen (HBDs) kepada garam. DES yang terpilih telah digunakan sebagai ejen fungsian dengan CNT asli untuk membentuk penyerap novel bagi menyingkirkan ion-ion plumbum (Pb^{2+}), ion arsenik (As^{3+}), dan ion raksa (Hg^{2+}) daripada air. Proses penyaringan dijalankan untuk penyingkiran logam berat terpilih menggunakan proses penjerapan. Tiga model kinetik telah digunakan untuk mengenal pasti mekanisme dan kadar penjerapan, *pseudo-second order* adalah terbaik untuk menggambarkan penjerapan kinetik. Hubungan antara parameter dalam proses penjerapan (misal: catatan masa, kepekatan awal, pH dan dos penjerap) adalah tidak linear, maka pemodelan ini sesuai untuk pemetaan proses yang sedemikian rumit. Oleh itu, rangkaian neural tiruan (ANN) sebagai teknik pemodelan baru telah dicadangkan oleh kajian ini sebagai kaedah pemodelan yang kurang rumit dalam rangkaian biologi yang canggih. Teknik pengganti ini dipilih untuk mewakili hubungan fungsi tidak linear dalam kalangan pembolehubah. Teknik ANN tidak

memerlukan sebarang induksi matematik kerana ANN menganalisis contoh-contoh dan mengiktiraf korelasi antara input dan siri output dataset tanpa apa-apa anggapan tentang hubungan dan ciri-ciri mereka. Algoritma ANN yang berbeza telah digunakan dalam kajian ini seperti, algoritma *backpropagation feed forward*, algoritma *layer recurrent*, sistem *adaptive neuro fuzzy inference* dan rangkaian neural NARX. Tambahan pula, pelbagai indikator telah dilaksanakan untuk menilai produktiviti model ANN termasuk *relative root mean square error* (RRMSE), *mean square error* (MSE), *root mean square error* (RMSE), kesilapan peratusan mutlak (MAPE) dan ralat relatif (RE) . Kajian kepekaan terhadap parameter dalam kerja eksperimen ini telah dicapai. Tiga algoritma digunakan bagi pemodelan ion Pb^{+2}, ralat relatif maksimum (RE) bagi *layer recurrent* adalah 18.67%, yang mana, untuk RE *feed-forward back-propagation* adalah 11.62%. Hasil terbaik yang dicapai untuk penyingkiran Pb^{2+} menggunakan algoritma ANFIS adalah 7.078%. Untuk penyingkiran As^{3+} penyerap yang berlainan telah digunakan, dua algoritma telah digunakan bagi pemodelan, maksimum RE untuk feed-forward back-propagation yang dicapai ialah 5.97% dan algoritma NARX mencapai ketepatan yang lebih baik dengan RE maksimum 5.79%. Algoritma NARX digunakan untuk pemodelan penyingkiran Hg^{2+}, ralat relatif maksimum yang diperoleh adalah 3.49%. Hasil keputusan model menunjukkan bahawa algoritma NARX adalah yang terbaik berbanding dengan algoritma lain dari segi ketepatannya.

Kata Kunci: Penyingkiran logam berat; nanotube karbon; iaitu pelarut eutektik dalam; rawatan air; rangkaian neural tiruan.

ACKNOWLEDGEMENTS

In the name of Allah, the Most Gracious and the Most Merciful All the praise and absolute thankfulness are to Almighty Allah for providing me with this opportunity and for granting me the patience and the capability to complete this work successfully.

I would like to express my sincere appreciation and gratitude to my supervisors Dr. Mohammed Abdulhakim AlSaadi and Prof. Dr. Ahmed Hussein Kamel Ahmed Elshafie for their endless support and guidance, and mostly for their patience and encouragement through the period of this study. I would like to present my appreciation to my parents for their help and patience through all the stages of my life, also special thanks to my uncle Abdul Salam Fiyadh Omran, and my brother Dr. Sabah Saadi Fayaed and his son Yazen Sabah Saadi for their support.

I would like to express my sincere appreciation to my friend Dr. Mohamed Khalid Mohamed Saied for his support during my study. A special thanks to Dr. Salman Ali Al Jumaili for his support.

Finally, not to forget the supports of my friends for their help and encouragements, specially my friend Musatafa Noori Salih.

TABLE OF CONTENTS

LIST OF FIGURS

LIST OF TABELS

LIST OF SYMBOLS AND ABBREVIATIONS

CNTs	Carbon nanotubes
SWCNTS	Single-wall carbon nanotubes
MWCNTs	Multi-wall carbon nanotubes
WHO	World health organization
ILs	Ionic liquids
DES	Deep eutectic solvents
ANN	Artificial neural network
LR	Layer recurrent
FF-NN	Feed-forward neural network
BP	Backpropagation
ANFIS	Adaptive neuro fuzzy interface system
Pb^{+2}	Lead ions
AS^{+3}	Arsenic ions
Hg^{+2}	Mercury ions
TEG	Tri ethylene glycol
MTPB	Methyl triphenyl phosphonium bromide
BTPC	Benzyl triphenyl phosphonium chloride
ATPB	Allyl triphenyl phosphonium bromide
TAB	Tetra-n-butyl ammonium bromide
DAC	N, N-diethyl ethanol ammonium chloride

The rest of the symbols and abbreviations are identified within the text.

CHAPTER 1: INTRODUCTION

1.1 Overview

Water is the most essential component to life existence and maintenance. It is a major challenge to supply pure water to all human civilization, since more than 700 million people currently face difficulty in accessing pure water sources (WHO, 2014). While the continued consumption for the pure water occurs with increasing population activities. Pollution is also contributing to the depletion of pure water resources. Water pollution may occur from natural sources or human industrial activities. There are different types of pollution, including organic compounds, heavy metals, oils, and radioactive metals. Therefore, the demand for new effective ways to eliminate any contaminates in water, especially harmful compounds, is crucial (Abbas et al., 2016).

Heavy metals are the most challenging pollutants that require continues monitoring and creative solutions to be removed from polluted water. Whatever the heavy metals source in nature or from human activities, their removal or control keep attracting great concern based on environmental and economic considerations. In addition, heavy metals are destructive to human health and thus, it is recommended to be removed from or minimized in water to the allowable limits. Different techniques have been developed to reduce heavy metals concentration in water supplies, such as adsorption, coagulation, precipitation, and ion exchange.

Nanotechnology has become a promising approach to develop the techniques of environmental remediation. Nanotechnology is defined as emerging applications working on nanometre scale to produce devices, materials, and systems with new characteristics and purposes by governing the shape and size of matters (Mansoori & Soelaiman, 2005; Ramsden, 2009). The global interest in the nanotechnology has developed huge momentum because of its potential applications in several fields, such as

medicine (Kiparissides & Kammona, 2015; Müller et al., 2015; Usui et al., 2008), food industry (Duncan, 2011) and energy (Hussein, 2015). This nanotechnology momentum presents the opportunities for leap scenarios in the development and alteration of conventional remediation technologies.

Carbon nanotubes (CNTs), could be either single-walled SWCNTs or multi-walled MWCNTs which have gained a high attention because of their electrical, mechanical, chemical, and physical properties (Koziol et al., 2007). They can be considered as advantages alternatives of the other traditional adsorbents as they can remove both organic contaminants and heavy metals with greater adsorption efficiency because of their binding site that are more available comparing to the other traditional adsorbents such as the activated carbon (Ji, Chen, Duan, & Zhu, 2009).

In the last decades, ionic liquids (ILs) were involved in many applications due to their physicochemical properties and solvation, which has lead them to be considered as designer solvents. Nevertheless, ILs have many flaws, specifically their relatively cost processes of synthesis and associated with waste disposal. Lately, (Abbott, Capper, Davies, Rasheed, & Tambyrajah, 2003) introduced the so called deep eutectic solvents (DESs) for the development of cheaper replacement for ILs (Abbott et al., 2003; Andrews, Jacques, Qian, & Rantell, 2002). DESs are an evolving class of solvents that are considered ionic liquid analogues, and sometimes as fourth generation of (ILs) (Cvjetko Bubalo, Vidović, Radojčić Redovniković, & Jokić, 2015).

Along with their mesmerizing solvation properties, they are chemically stable with suitable physical properties, including low vapor pressure and high boiling point. DESs are a combination of two or more than two compounds, the combination of these elements have a melting point lower than the individual element (Cooper et al., 2004; Hayyan, Mjalli, Hashim, & AlNashef, 2010). Consequently, DESs have numerous advantages

comparing to the conventional ILs, that can be concluded as easiness of synthesis, physical properties variety with diverse molar ratios, and reasonable components price (M. Hayyan et al., 2013; Hayyan, Looi, Hayyan, Wong, & Hashim, 2015). Lately, ILs and DESs were applied in several nanotechnology related fields. The first combination of nanotechnology and ionic liquids was introduced by (Deshmukh, Rajagopal, & Srinivasan, 2001). Next, ILs and DESs were used as a media for synthesis of nanoparticles (M. Chakrabarti et al., 2015; Karimi, Eshraghi, & Jahangir, 2016; Xiong, Tu, Ge, Wang, & Gu, 2015; Xu et al., 2016).

Moreover, DESs were employed in many related fields of nanotechnology, including the electrolyte in a nanostructure sensor (Zheng, Ye, Yan, & Gao, 2014), the electrolyte in nanoparticle deposition (Abbott, El Ttaib, Frisch, McKenzie, & Ryder, 2009), in a nanodroplet embedded in a microstructure (C.-D. Gu & J.-P. Tu, 2011). The DESs is the key for CNTs functionalization to use it as adsorbent of heavy metals using the adsorption process. The relationship between the involved parameters in the adsorption process is nonlinear, thus the modelling of this kind of process is complicated.

Therefore, new modelling technique such as artificial neural network (ANN) has been used as a less complicated model method in the sophisticated biological network. The substitute technique of modelling, artificial neural network system (ANN), is selected in order to represent the non-linear function relationship among variables. The artificial neural network (ANN) techniques do not require any mathematical induction since the (ANN) analyses examples and recognizes the correlations in the inputs and outputs series of dataset without any presumption about their interrelations and characteristics (Sumantra Mandal, Sivaprasad, Venugopal, & Murthy, 2009). The (ANN) speciality to identify and generalize the pattern of any non-linear and complex development makes it an influential modelling means. Neural network has the ability to extract complicated data that is beyond the capability to be observed by a human or any computer technique.

Experiments have been successfully performed to use (ANN) to model the adsorption of lead ions by pistachio Vera L. shells (Yetilmezsoy & Demirel, 2008b), the Laneset Red G removal on Chara contraria (Mjalli, Al-Asheh, & Alfadala, 2007), Laneset Red G on walnut husk removal efficiency (Çelekli, Birecikligil, Geyik, & Bozkurt, 2012), and the intercalated tartrate-Mg-Al layered double hydroxides as an adsorbent (Yamin Yasin, Faujan Bin H. Ahmad, Mansour Ghaffari-Moghaddam, & Mostafa Khajeh, 2014a). Many studies were recently conducted on the prediction of water quality system modelling (Chibole, 2013; G. Wu & Xu, 2011). Moreover, there are some research have been applied on different areas for example, modelling the fermentation media optimization (K. M. Desai, S. A. Survase, P. S. Saudagar, S. S. Lele, & R. S. Singhal, 2008), modelling of a microe-wave-assisted extraction method (M. M. a. M. Khajeh, 2011).

1.2 Problem statement

Eventually, one of the greatest challenges facing humanity in this century is the conservation of water resources. The lack of water in many parts of the world and rampant pollution has led to the exertion of enormous pressure on resources and motivated the establishment of new techniques to provide good water quality for human life and other organisms. Due to the heavy metals high toxicity even at low concentration, the removing of heavy metals contamination from water has become a great concern. Many traditional techniques were used for heavy metals removal from water, including coagulation, ion exchange, precipitation, reverse osmosis, and oxidation. However, these techniques have some negatives sides in terms of cost effectiveness and limitations in removing different kinds of pollutants. Thus, the modified technologies are needed or new alternatives are required. The adsorption technique is considered as most effective techniques comparing to the other methods for heavy metals ions removal since it excels at separating small amounts of pollutants from large amounts of contaminated water.

Furthermore, adsorption has advantages over other techniques due to the simplicity of operation, the wide range of available adsorbents, and the ability to remove soluble organic, inorganic and biological pollutants from water. However, adsorption also suffers from limitations, including low adsorption capacity for some adsorbents, complicated scale up for industrial production processes, and the high cost associated with relatively high adsorption capacity, such as nano-based adsorbents (Ali, 2012).

It is well known that CNTs are considered of the most promising adsorbent compared to other nano-based adsorbents. However, in the aqueous solution, the CNTs applications are significantly hindered by their low dispersion due to the graphitic surface hydrophobicity and the strong intermolecular Vander Waals interaction between tubes, that lead to loose bundles/ aggregates formation which reduce the effective surface area (Vuković et al., 2010). To overcome these drawbacks and improve the CNTs efficiency, CNTs can be functionalized by chemical treatment methods in which the pristine CNTs can gain functional groups on the surface after being treated with certain chemicals. CNTs functionalization is subject to the purpose of the specific application, since each functional group adds different characteristics and serves different types of applications. Therefore, CNTs activation is the key role in improving the CNTs adsorption capacity due to the modification in the surface functional groups and surface morphology (Han, Zou, Li, Li, & Shi, 2006). The conventional functionalization usually involves strong acids and harsh chemicals, which involve complicated processes and environmentally harmful. Thus, the need for new functionalization agents, green solvents, environmentally friendly and economical is crucial for new applications development (Hayyan, Abo-Hamad, AlSaadi, & Hashim, 2015; Martinez et al., 2003).

DESs could be a successful option to replace conventional acids and other chemicals that require a complicated process to modify the surface of CNTs. Furthermore, DESs are green, biodegradable, economical, and simple to synthesize solvents. Combining the

sophisticated properties of CNTs and DESs as a green novel functionalization agent was one of the motivations of this research. This research is attempt to modify mathematical model describes and predict the behaviour of the adsorption process of CNT-DES-Functionalized adsorbent in contaminated water.

In general, removal of heavy metals by adsorption process is considered as a complicated process due to the interactive influence of many variables including, adsorbent dosage, contact time, initial heavy metal concentration and pH. The conventional linear method for modelling of this kind of process is hectic. Therefore, artificial neural networks (ANNs) techniques could be a powerful tool able to recognize a given data and process them towards their target outputs. The ANN capability to generalize and learn the behaviour of any non-linear and complex process makes it not only a powerful tool but robust and viable technique. ANNs consist of a massive parallel architecture which can solve the complicated problems by the assistance of highly connected neurons organised in layers. Recently, ANNs technique is used for various engineering applications (Ghosal & Gupta, 2016; S Mandal, Mahapatra, Sahu, & Patel, 2015; Zafar, Van Vinh, Behera, & Park, 2016).

1.3 Research objectives

The objectives of this study are:

1- To utilize the deep eutectic solvent-functionalized MWCNTs for the removal of heavy metals contaminants from water.

2- To study the effect of different parameters (pH, contact time, adsorbent dosage and initial concentration) on the adsorption capacity and investigate the adsorption kinetics by determining their coefficients.

3- To investigate the potential of artificial intelligence (AI) model for simulation of the adsorption capacity of the DES-functionalized MWCNTs for heavy metals removal from water.

4- To develop a prediction models using ANNs techniques for different heavy metals removal and investigate its potential on the adsorption kinetics models.

1.4 Methodology of research

The stages of this research illustrated in Figure 1.1, and can be summarised as following:

1- Syntheses the DESs based on the specified HBD-salt ratios.

2- CNTs oxidation by $KMnO_4$ using a sonicating system at 65˚C for 2 h.

3- Functionalizing the CNTs using the Synthesized DESs.

4- Utilizing the DESs-functionalized CNTs for the removal of heavy metals from water namely, arsenic, lead and mercury.

5- Utilizing the collected data from the experimental work in (ANN) systems towards the modelling of the heavy metal adsorption capacity of the DES-functionalized CNTs.

6- Selecting the best suitable algorithms for the modelling.

7- Develop and optimize the ANN model structure in terms of node and layers number, and the type of transfer function.

8- Applying different indicators to check the model accuracy such as, MES, RRMSE, RMSE, MAPE, RE and R^2.

9- Investigate the adsorption kinetics data of the adsorptions systems using ANN model outputs.

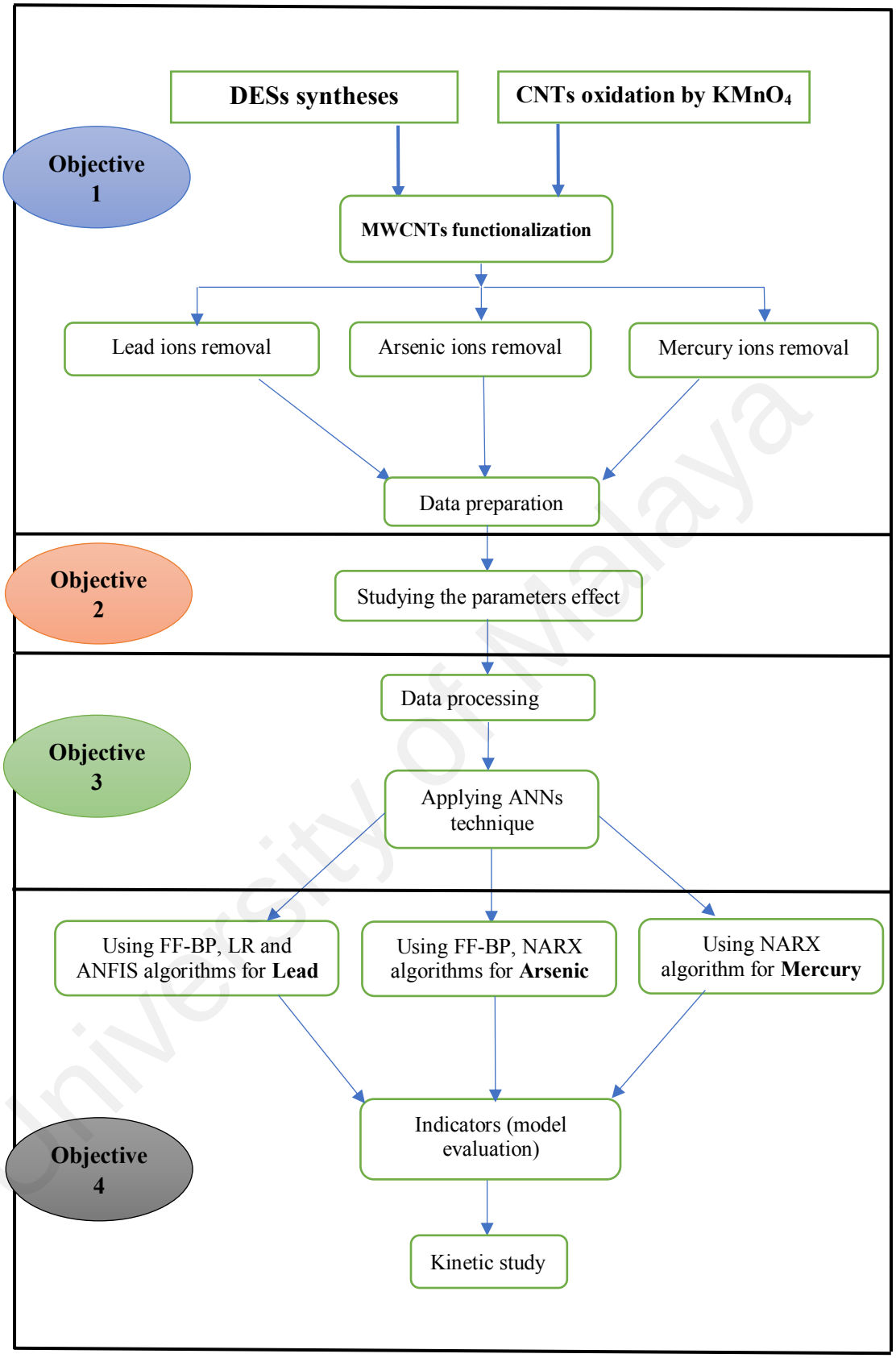

Figure 1. 1: The flow work

1.5 Thesis outline

The format of this thesis followed the article style format approved by the University of Malaya. This style gives the author a flexibility to present the work in the form of various independent articles arranged in a sequence of chapters. The research objectives are comprehensively satisfied though these articles with a smoothly flowing research story. The work in this thesis has been submitted to ISI journals in the form of seven technical articles. Upon the writing of this thesis, seven articles have been published in ISI journals. The outline of this thesis is as follows:

Chapter 1 (Introduction): Includes a brief background on water treatment and the use of nanomaterials as adsorbents of heavy metals. Moreover, a brief background on the artificial neural network (ANN). The purpose of this research is mentioned, followed by the objectives of the research and finally a brief description of the methodology.

Chapter 2 (Literature Review): This chapter covers a literature survey of nanotechnology in water treatments. A comprehensive review on the functionalization of CNTs to remove Pb^{2+}, As^{3+} and Hg^{2+} from water is presented. In addition, this chapter includes a brief review of the involvement of DESs in nanotechnology related fields. Finally, a background on the applications of artificial neural network (ANN).

Chapter 3 (Article 1: The modeling of lead removal from water by deep eutectic solvents functionalized CNTs: artificial neural network (ANN) approach): In this chapter, DESs functionalization agent for CNTs was used for the removal of lead ions from water solution. Two ANN types were designed in this work, the FF-BP and LR, both methods are compared based on their predictive proficiency in terms of the (MSE), (RMSE), (RRMSE), (MAPE) and (R^2) based on the testing dataset. This chapter is published in the water science and technology journal.

Chapter 4 (Article 2: The modeling of lead removal from water using deep eutectic solvents functionalized CNTs: Feed-Forward Neural network (FF-NN) and adaptive neuro fuzzy interface system (ANFIS) modelling approach): In this chapter, CNTs was functionalization by DESs for lead ions removal from water solution. Two ANN types were designed in this work the Feed-Forward Neural network (FF-NN) and adaptive neuro fuzzy interface system (ANFIS), both methods are compared based on their predictive proficiency in terms of the (MSE), (RMSE), (RRMSE), (MAPE) and (R^2) based on the testing dataset.

Chapter 5 (Article 3: The modelling of arsenic removal from water by deep eutectic solvents functionalized CNTs: Artificial Neural Network (ANN) approach): In this chapter, a novel adsorbent was developed by using deep eutectic solvent system as functionalization agent of carbon nanotubes (mK-CNTs) for the removal of arsenic ions from water. Artificial neural network (ANN) approach is used to predict arsenic removal from water. Different indicators are used to determine the efficiency and accuracy of the NARX neural network model which are (MSE), (RMSE), (RRMSE), (MAPE). This chapter is published in the desalination and water treatment journal.

Chapter 6 (Article 4: BTPC based DES-functionalized CNTs for As^{3+} removal from water :(NARX) neural network approach): In this chapter, the benzyltriphenyl-phosphonium chloride-based DES was developed for the functionalization of carbon nanotubes for arsenic ions removal from water. The nonlinear autoregressive network with exogenous inputs (NARX) neural network strategy is used for the modelling and predicting the adsorption capacity of functionalized carbon nanotubes, three kinetic models are used to identify the adsorption rate and mechanism. Different indicators are used to determine the efficiency and accuracy of the NARX neural network model which

are (MSE), (RMSE), (RRMSE), (MAPE). This chapter is published at the Journal of Environmental Engineering.

Chapter 7 (Article 5: Arsenic removal from water using N, N- diethylethanol ammonium chloride-based DES-functionalized CNTs: (NARX) neural network approach): In this chapter, the N, N- diethylethanol ammonium chloride-based DES-functionalized CNTs is used for arsenic ions removal from water solution. The nonlinear autoregressive network with exogenous inputs (NARX) neural network strategy is used for the modelling and predicting of the adsorption capacity of functionalized carbon nanotube. Different indicators are used to determine the efficiency and accuracy of the NARX neural network model which are (MSE), (RMSE), (RRMSE), (MAPE). This chapter is published at Journal of Water Supply: Research and Technology-Aqua.

Chapter 8: (Article 5: Mercury removal from water using tetra-n-butyl ammonium bromide (TAB) based DES-functionalized CNTs: (NARX) neural network approach): In this chapter, tetra-n-butyl ammonium bromide (TAB) based DES was used for CNTs functionalization for mercury removal from water. The NARX neural network modelling technique is used for the modelling of the adsorption capacity of the functionalized CNTs using different parameters and based on experimental data. Three kinetics models such as Pseudo first-order, Pseudo second order and Intraparticle diffusion are applied on the experimental and predicted data. This chapter is published at Environmental Progress & Sustainable Energy.

Chapter 9: (Allyl triphenylphosphonium bromide-based DES-functionalized CNTs for mercury removal from water: artificial neural network modelling approach): In this chapter, the Allyl triphenylphosphonium bromide-based DES-functionalized CNTs is used for mercury ions removal from water. The NARX neural network modelling technique is used for the modelling of the adsorption capacity of the functionalized CNTs.

Three kinetics models such as Pseudo first-order, Pseudo second order and Intraparticle diffusion are applied on the experimental and predicted data. Different indicators are used for checking the model accuracy and efficiency including (MSE), (RMSE), (RRMSE), (MAPE), (RE) and correlation coefficient R^2.

Chapter 10: (conclusion and recommendations): In this chapter, a conclusion and the findings of this research are summarised and the recommendations for future work are listed in this chapter.

CHAPTER 2: LITERATURE REVIEW

2.1 Introduction

The most important and indispensable substance for the life forms on earth is water for existing organism. Regrettably, with the population, civilization and industrialization growth, the quality of the available water resources is continuously deteriorating. Moreover, there is a fundamental problem that around 700 million of people are unable to access to the sources of pure water (Ali & Gupta, 2006; Supply & Programme, 2014; Tchobanoglous & Burton, 1991). There are various pollutants types such as: heavy metals, radioactive nucleating metals, organic, etc. These pollutants are harmful to the living beings consequently, the purification of water has become the major concern of global and researchers nowadays. Different methods were used for the water purification such as the adsorption, reverse osmosis, precipitation and coagulation.

The adsorption process for heavy metals removal is a complicated process due to the involvement of various variables such as pH, heavy metal concentration, contact time and adsorbent dosage. The conventional linear method for modelling of heavy metals removal process using the adsorption technique is hectic. Therefore, artificial neural networks (ANNs) technique is a powerful tool, which is able to recognize a given data set into their target outputs. The ANN capability to generalize and learn the behaviour of any non-linear and complex process makes it a powerful tool. ANNs consist of a massive parallel architecture, which can solve the complicated problems by the assistance of highly connected neurons organised in layers.

A literature review conducted in this chapter on the carbon nanotube application, the techniques of heavy metals removal, types of adsorbent used and its functionalization agents, and the ANN techniques and its applications.

2.2 Heavy metals: negative impact and water remediation

The poisonous heavy metals expressed to any relatively metalloid and dense metals which is distinguished for its potential toxicity (S. Srivastava & Goyal, 2010). In general, heavy metals have an atomic weight range of 63.5 to 200.6 and a density greater than 5 g/cm^3 (Fu & Wang, 2011; N. Srivastava & Majumder, 2008). The contamination of heavy metals is fundamentally caused by the modern chemical industries, fertilizer, metal plating facilities, manufactures of batteries, pesticides and papers, fossil fuel, tannery, natural resources, production and metallurgical of different plastics. Various kind of harmful materials are nowadays available in the water resources such as chromium, nickel, mercury, zinc, lead and arsenic (Jiang Gong et al., 2014; C. Luo, Tian, Yang, Zhang, & Yan, 2013; Nriagu, 1988; Yamauchi & Yamamura, 1983). Because they have high toxicity, heavy metals are extremely hazardous even at low concentration.

2.2.1 Lead

The presence of lead (Pb) in water may led to various health problems, lead has a huge concern in the world nowadays due to its physiological effects specially to the children (Ngueta et al., 2014). Lead (Pb) is one of the poisonous elements to the humans and animals, their exposure to lead can cause brain disorder and disorganize the nerve system (Gad & Pham, 2014). Lead can go into the water resources by the pluming materials corrosion, also it enters the water resources through the industries disposals (Tong, Schirnding, & Prapamontol, 2000). Its stated that drinking water is the major source of lead into human body (Abbas et al., 2016).

2.2.2 Arsenic

Arsenic (As) is the most poisonous heavy metal that has been perceived as very lethal heavy metal since long time, it can cause many side effects to the living organisms. It can be found in a different forms and toxicity levels. Several water resources were

contaminated either through human activities or naturally (Black, 1999; B. K. Mandal & Suzuki, 2002). The maximum allowable level of arsenic in the drinking water is 10 µg/L, it is determined by the World Health Organization (WHO) (Smedley & Kinniburgh, 2001; Tawabini, Al-Khaldi, Khaled, & Atieh, 2011). The exposure to arsenic has been linked to several lethal and dangerous diseases such as urinary tract, bladder and skin cancer (Ng, 2005; Sharma & Sohn, 2009).

2.2.3 Mercury

Mercury (Hg) is one of the heavy metals that can be found in either vapour or liquid phase; it is one of the most toxic heavy metals in nature. The renal organ, gastrointestinal (GI) and neurologic systems are the most affected once exposed to mercury. Mercury (Hg) could be found in three forms such as inorganic salt, organic salt and metallic element (Goldman, Shannon, & Health, 2001). These elements exist in the soil, fresh water and seawater (Hassett-Sipple, Swartout, & Schoeny, 1997). Moreover, mercury could be found in the industries waste products such as production of wiring devices, various switches, fossil fuels dental work, lighting and control and measuring devices (A. Gupta, Vidyarthi, & Sankararamakrishnan, 2014). The maximum allowable mercury concentration in water is 1µg/L stated by the World Health Organization (WHO), due to its tremendously effects at a very low concentration (Mohan, Gupta, Srivastava, & Chander, 2001).

2.2.4 Remediation techniques of heavy metals removal

Different methods have been used to remove heavy metals from water such as: oxidation (Thomas M Gihring, Gregory K Druschel, R Blaine McCleskey, Robert J Hamers, & Jillian F Banfield, 2001), reverse osmosis (Ning, 2002), ion exchange (J. Kim & Benjamin, 2004), precipitation (Monique Bissen & Fritz H Frimmel, 2003), coagulation (P. R. Kumar, Chaudhari, Khilar, & Mahajan, 2004), flotation and

photocatalysis. However, these methods have some drawbacks such as the hazardous west produced with the precipitation method, which is also required, a further treatment. The ion exchange method drawback is the recyclability, regardless the high efficiency of the method. The generation and cost, along with the residuals materials disposable are the membrane filtration method limitations. The flocculation and coagulation technique suffer from the generated sludge volume. The photocatalytic method drawback is the long duration. The electrodialysis methods has high efficiency but, the lake is the high energy consumption and high operation cost (Abbas et al., 2016). Due to some drawback of the mentioned methods, the developing of alternative method or modified technologies is required (Payne & Abdel-Fattah, 2005; Tuutijärvi, Lu, Sillanpää, & Chen, 2009). The adsorption technique is the most suitable method comparing to the other conventional methods due to its high efficiency in removing of heavy metals ions from water even at low concentration, adsorbents availability, regeneration possibility and the process simplicity (Mobasherpour, Salahi, & Ebrahimi, 2012; Rao, Lu, & Su, 2007). Further details regarding the adsorption technique are presented in the following subsection.

2.2.4.1 Adsorption technique of heavy metals removal

The adsorption method has been considered as a suitable technique to remove the heavy metals ions from water due to the ability to remove the pollutants even at a very low concentration, low energy consumption and row materials availability to make different adsorbent types (Ali, 2012). The adsorption technique defined as the soluble liquid and gas attachment onto the adsorbent surface (Kaneko, 1994). Relying on the attachment categories the adsorption type could be categories as physisorption, once the absorbent and adsorbate concerned molecules comes with the van der Waals force. The chemisorption is defined once the concerned molecular is attached to the adsorbent surface with a strong chemical bonding. The adsorption quality is depending on the adsorption capacity, which is affected by the adsorbent surface characteristics; for

example, surface charge, surface area and the functional groups gives active sites at different pollutants.

Different adsorbents types have been reported for the heavy metals removal such as: modified chitosan (Justi, Fávere, Laranjeira, Neves, & Peralta, 2005), manganese oxides (E.-J. Kim, Lee, Chang, & Chang, 2013), peanut hulls (Brown, Jefcoat, Parrish, Gill, & Graham, 2000), peat (Ho & McKay, 1999), sewage sludge ash (Ho & McKay, 1999), granular biomass (Hawari & Mulligan, 2006), fly ash (Weng & Huang, 2004), extracellular polymeric substances (J. Yang et al., 2015), landfill clay (Ghorbel-Abid & Trabelsi-Ayadi, 2015), activated carbon (Kadirvelu, Thamaraiselvi, & Namasivayam, 2001; Kobya, Demirbas, Senturk, & Ince, 2005; Sounthararajah, Loganathan, Kandasamy, & Vigneswaran, 2015) and many others. However, the mentioned adsorbents have some limitations such as low adsorption capacity and removal efficiency (Abbas et al., 2016); therefore, the need for a new adsorbent is important. The nanotechnology revolution gives a wide path for a new adsorption processes. The carbon nanotubes have been described as the greatest adsorbent nano-based due to the remarkable chemical and physical properties (Thostenson, Ren, Chou, & technology, 2001). The carbon nanotubes are a stable material and it is considered as a poor adsorbent but, by adding to the CNT surface a new functional group the selectivity, sensitivity and adsorption efficiency to the heavy metals will be increased. The CNTs surface activation and functionalization is needed to make an affinity for many kinds of pollutants.

2.3 Heavy metals removal using functionalized CNTs

Carbon nanotubes (CNTs) are first presented by (Iijima, 1991). The CNTs contains one or more graphite sheets wrapped around itself forming as cylindrical with a length more than 20 μm and less than 100 nano-meter (nm) radius (Zhu et al., 2002). There are two types of carbon nanotube, multi wall carbon nanotube (MWCNTs) which contains

more than one graphene sheets and single wall carbon nanotube (SWCNTs) which contains one graphene sheet, Figure 2.1 shows the SWCNTs and MWCNTs. The CNTs are categorised into three types: chiral nanotubes, zigzag and armchair, it depends on the CNTs sheet shaped in two-dimension. The zigzag as shown in Figure 2.2 a, which is typically form a hexagons pattern as it moves around the tubule body. The armchair, which can be described as one of the two-cyclohexane conformers, the carbon atom hexagon can be defined by the hexagons shape as it moves around the tubule body; the armchair form is illustrated in Figure 2.2 b. The third form of the CNTs is presented in Figure 2.2 c, which is identified as a chiral form. The mentioned types usually occur in the SWCNT. The term chiral denote handedness which indicates that the tubes could be twist in any direction. The chiral shape of the SWCNTs is similar to the form of zigzag and armchair (Baughman, Zakhidov, & De Heer, 2002).

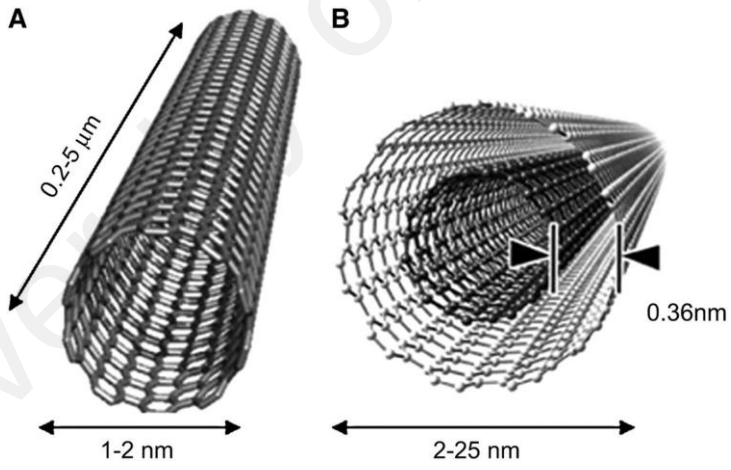

Figure 2. 1: The structure of multi-walled and single CNTs

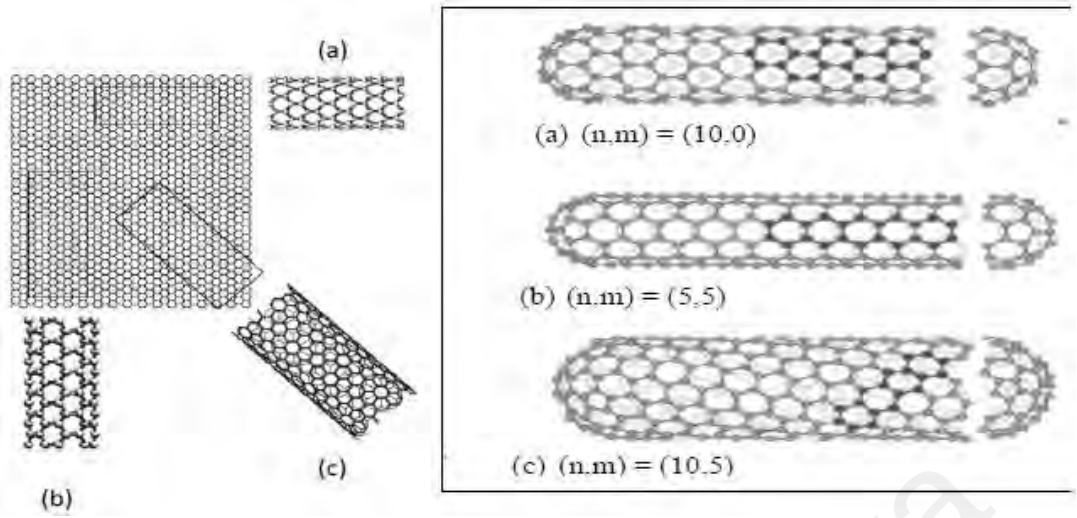

Figure 2. 2: Patterns of CNT. (a) Zigzag Single-Walled Nanotube, (b) Armchair Single-Walled Nanotube, (c) Chiral Single-Walled Nanotube

The MWCNTs contains a group of a graphene cylinder nested together. The TEM examination discovered the inter shell spacing which are varied from 0.335 nm to 0.34 nm, supplementing diminishing tube diameter. It is stated that the smallest diameter biggest spacing is in the high cover, subsequent in an unwelcome force, and associated to the decreasing diameter in the CNTs shell (Gogotsi, 2006; Saito, Dresselhaus, & Dresselhaus, 1998). The bulk graphite crystal spacing value of 0.34 nm is nearly that of CNTs (Saito et al., 1998). It is stated by (Ru, 2000), that the interlayer spacing mean value is 0.3444 ± 0.001 nm. Moreover, the CNTs value size are larger in a few percent than the bulk graphite crystal (Ru, 2000). There is a spacing between the layers which is denoted by d = 3.39 Å, which is based on the theoretical computation and it is greater than the observed for graphite. Using the TEM image experimentally, the MWCNTs found to have a spacing of d = 3.4 Å (Ebbesen & P M, 1992). The magical CNTs structure results in an awesome chemical and physical properties. Because of the bond between the carbon atoms in the sp^2 direction, the CNTs become one of the strongest materials in the world. It is stated by (Bindiganavale, 2009) that the strength and Young's modulus

are greater more than the steel by 10-100 times. (Popov, 2004) stated the specific heat and thermal conductivity by using the phonons. The SWCNTs thermal conductivity was 8-350 K as reported by (Hone, Whitney, Piskoti, & Zettl, 1999); while, for the MWCNTs was 4-300 K as stated by (Yi, Lu, Dian-Lin, Pan, & Xie, 1999). Moreover, by comparing the CNTs to the other materials conductivities the CNTs have a higher electrical conductivity (Collins & Avouris, 2000). The conductivity statues of the CNTs are effected by the hexagonal rings arrangement along the tubular surface even it is a semiconductor or metallic. The chiral vectors (n, m) of the SWCNTs, are responsible for the semiconducting or metallic properties, where m and n are the two integers. The m and n variance are responsible for the semiconducting and metallic state but, in a multiple three differences in the m-n results in the CNTs metallic state. Moreover, it is possible to attach the nanotube with various chiralities, to form a nanotube heterojunction, that can form a various of nanoscale molecular components of the electronic device (Arnold, Green, Hulvat, Stupp, & Hersam, 2006).

2.3.1 CNTs and their Functionalization

Due to the extraordinary chemical, physical and electrical properties, CNTs are involved in many applications including medical science, environmental engineering, electrical engineering and material science. However, there are some significant limitation of CNTs because of the interactive forces which take place between the carbonic nanostructures leading to the aggregation, difficult manipulation and poor dispersibility. Furthermore, the carbon nanotube chemical active sites principally are located around the defected positions such as pentagons those oriented opposite to the tube body which generally consist of hexagon only and this might give CNTs a great ability for interaction with other compounds (Andrews et al., 2002; Fischer, 2002; T. Lin, Bajpai, Ji, & Dai, 2003; X. Lu & Chen, 2005; Niyogi et al., 2002; Sun, Fu, Lin, & Huang, 2002; Thostenson, Ren, & Chou, 2001). The CNTs functionalization is the key point to

enhance the CNTs efficiency, depending on the chemical and physical properties which is mainly effected by the particle size, surface nature and chemical composition. The CNTs functionalization by adding a functional group on the CNTs surface is considered as an essential modification for improving CNTs and affects their special characteristics. However, there are two classes of functionalization, covalent and non-covalent. The functional groups, which covalently attached by chemical reaction with CNTs skeleton a string covalent functionalization takes place. While, the non-covalent functionalization is a term used for the case when functional groups coat the CNTs walls (Karousis, Tagmatarchis, & Tasis, 2010). Regarding to the CNTs first class functionalization which implemented in many application, Chen et al., (1998) have reported the SWCNTs functionalization by using the chlorine (Cl) for the side wall with soluble dichlorocarbene reaction. Eventually, 2% saturation of carbon atoms resulted in spectacular change to the structure of electronic band (J. Chen et al., 1998). The oxidation reaction is the common functionalization method. This method conducted by CNTs acidification via refluxing in boiling acid, such as sulfuric acid, nitric acids or both as a mixture (Esumi, Ishigami, Nakajima, Sawada, & Honda, 1996). The other oxidation type arises by a strong oxidant, for example $KMnO_4$ (Salam, 2013; R. Yu et al., 1998). In the oxidative procedures, adding carboxylic groups to CNTs it results in considerable number of functional groups, that can be used for further functionalization and application (Hirsch & Vostrowsky, 2007). The carboxyl (–COOH) or hydroxyl (–OH) groups are the most active functional groups could be found on the CNTs surfaces (P.-C. Ma, Siddiqui, Marom, & Kim, 2010). Moreover, the functional groups attachment effects the CNTs hydrophobic nature, following by a hydrophilic structure because of the polar groups on the CNTs surface which allows the CNTs to be dispersible in the organic solvents. The less nucleophilic and alky1 amines derivatives is presented by Haddon et al. (1998) as the oxidative functionalization agent to treat the SWCNTs. The octadecy1 amine effects gained from

acid functionality will cause a soluble SWCNTs (J. Chen et al., 1998; Hamon et al., 1999). The CNTs have been used with the biomolecules (Coleman, Khan, & Gun'ko, 2006), arylation and alkylation (Stephenson, Sadana, Higginbotham, & Tour, 2006), esterification (Haddon, 2002), polymer grafting (P. Liu, 2005; Mittal, Dhand, Rhee, Park, & Lee, 2015), thiolation (Hirsch & Vostrowsky, 2007), and silanation (P. C. Ma, Kim, & Tang, 2006). Lately, the ionic liquids (ILs) gained a great attention as a green solvent because of their special characteristics. The ILs were presented as nanomaterials functionalization agents, the first ionic liquid and nanotechnology combination was introduced by Deshmukh (Deshmukh et al., 2001). The IL anion roles on the MWCNTs solubility in the organic solvents and water by an anion exchange series on the treated MWCNTs by ILs was investigated by (Park et al., 2006). ILs is used as a replacement for the organic solvents and strong acids used as a functionalization agent. The ILs advantage comparing to the organic solvent that the ILs are non-distractive reaction while, the organic solvent strategy retains the properties of CNTs (Polo-Luque, Simonet, & Valcárcel, 2013). As long as, the CNTs have the ability to accept several types of functional groups, the CNTs have occupied nearly all the science fields. Due to the CNTs specific structure, morphology and surface area, CNTs are used as great adsorbents due to their adsorption sites. CNTs have the adequacy to many pollutants such as: trihalomethanes (C. Lu, Chung, & Chang, 2005), fluoride (Y.-H. Li et al., 2003), 1,2-dichlorobenzene (Peng et al., 2003), lead (Y.-H. Li et al., 2002), zinc (C. Lu & Chiu, 2006), cadmium (Y.-H. Li et al., 2003), ozone (Yim & Liu, 2004), hydrogen (Dillon, Jones, Bekkedahl, & Kiang, 1997), ammonia (Bauschlicher Jr & Ricca, 2004), methane, nitrogen (Bienfait et al., 2004), dioxin (Long & Yang, 2001). Consequently, the CNTs become the interest of the researchers and resulted in many publications than other adsorbents (Ali, 2012). The use of the ILs have some disadvantages therefore, the need for new functionalization agent is crucial, the DESs could be the option to replace the

ILs. The DESs have some advantages such as; it is a green material, biodegradable, economical, and simple to synthesize solvents. The deep eutectic solvents (DESs) is one of the ionic liquid analogues which is presented by Abbot et al. in 2003 (Abbott et al., 2003) as a cheaper replacement for developed ionic liquids (ILs). Generally, DESs made up from two or more compounds. In contrast, DES has several advantages comparing to the conventional ILs such as, diversity of physical properties and different molar ratios, easy to synthesis and cheaper price of compounds. The adsorption process is used for the removal of heavy metals using the functionalized CNTs as adsorbent material.

2.3.2 Deep eutectic solvents (DESs) as functionalization agent

At the previous two decades, the interest in the ionic liquids (ILs) application has been increased, with respect to functional liquids, biotechnology, catalysts, and electrochemistry process technology, the ILs solvents contain ions only. The ILs synthesis can be divided to two separate categories, which can be shaped from the organic salts and metal halides of the eutectic mixtures, they consist a separated anion (E. L. Smith, Abbott, & Ryder, 2014). The ILs application depending on their chemical and physical properties (Q. Zhang, Zhang, & Deng, 2011). Therefore, there are some limitations in the use of ILs includes the waste disposal and high cost (Phadtare & Shankarling, 2010). Subsequently, the new solvents that is easy to synthesis, reasonable price and environmentally are needed, Abbot et al. (2003) presented the deep eutectic solvents (DES) as a replacement of ILs (Abbott et al., 2003). Mostly, DESs are a combination of two or more compounds which have a melting point lower than the individual component (Abbott, Capper, Davies, & Rasheed, 2004; Hayyan et al., 2010). Moreover, DESs are organized by mixing a hydrogen bond donor (HBD) and salt, DESs can be prepared from different salts types (organic and inorganic) with many HBDs types (Q. Zhang, Vigier, Royer, & Jérôme, 2012).

DESs can be divided into three distinct types. Class (A) DESs are composed of an ionize salt and a HBD. This class is the most heavily studied, the choline chloride and urea mixture is the example of this type of DES as shown in Figure 2.3. The second, class (B) which include a metal salt and ionize salt, for example zinc chloride and choline chloride (Abbott, Boothby, Capper, Davies, & Rasheed, 2004). Class (C) is the third class, which is considered as a complex type comparing to the other classes, it is prepared by a mixture of ammonium salt, urea and carbohydrate with different ratios, such as choline chloride: d-fructose DES (A. Hayyan et al., 2012).

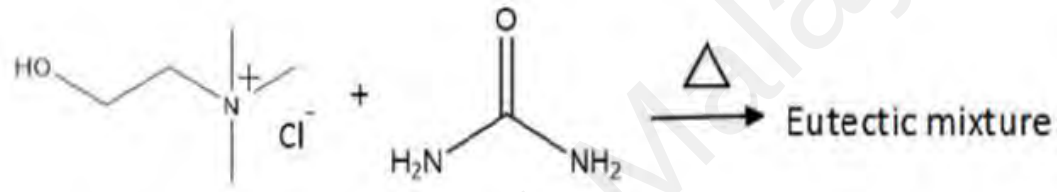

Figure 2. 3: ChCl:U eutectic mixture

The DESs physicochemical properties are almost like the conventional ILs properties (A. Hayyan et al., 2013). In general, both the ILs and DESs are similar in term of high viscosity, starting materials, non-volatility and non-flammability. Besides, DESs are the fourth generation of ILs (Cvjetko Bubalo et al., 2015). Nevertheless, the DESs have several advantages comparing to the ILs, such as negligible or low toxicity profiles, lower cost, simplicity in synthesis and sustainability in economic benefits and environmental (A. Hayyan et al., 2013; Hayyan, Abo-Hamad, et al., 2015). In addition, the DESs components are economically, easy to synthesis in a large scale. Moreover, the DESs syntheses are performed by mixing the components simply, that reduce the tedious work and waste disposal (Q. Zhang et al., 2012).

2.3.2.1 (DESs) applications

The present growth in the patents and research papers regarding to the DESs application and synthesis revealed the DESs important roles as a future solvent. DESs established first as a solvent for electroplating application and electrodeposition (Abbott & McKenzie, 2006). Therefore, DESs development as electroplating media using different kind of metals was a significant focus (E. L. Smith et al., 2014). The DESs are used widely in the purification and biodiesel production field, Hayyan et al. 2010 presented this method for separating the glycerol form biodiesel (Hayyan et al., 2010).

Because of the CH_3 and CO_2 concern, that are the main greenhouse gases discharge these days, the adsorption and separation of the CH_3 and CO_2 gases was increased. The DESs capability to dissolve the CO_2 is similar to the ILs (Q. Zhang et al., 2012). Li et al. (2008) used the urea and ChCl mixture to inspect the CO_2 solubility with different condition such as molar ratio, pressure and temperature (X. Li, Hou, Han, Wang, & Zou, 2008). Moreover, the DESs advantages in the gas storage field contain the unique which provided by DESs for coordinatively unsaturated metal centers and porosity creation that increase the gas storage capacity (Férey, 2008; Jian Zhang, Wu, Chen, Feng, & Bu, 2009). The use of ChCl: glycerol was presented by Yang et al. (2013) to absorb SO_2 with considering the molar ratio, pressure and temperature (D. Yang et al., 2013). Salas et al. (2014) studied the DESs effect on the pore structure composition by using two DESs-based hierarchical carbon monoliths, that effect on the CO_2 adsorption role. DESs based carbon displays a good selectivity toward CO_2 and adsorption capacity (López-Salas et al., 2014). DESs are used in the field of enzymatic, as presented by many publications regarding the DESs use in the biotransformation. The DESs use in the field of biotransformation presented the first time by Gorke et al. (2008) to examine the hydrolases catalytic activity in the DESs (Gorke, Srienc, & Kazlauskas, 2008). Furthermore, the lipase-catalyzed reaction processes were wieldy examined (Singh,

Lobo, & Shankarling, 2011; Sonawane, Phadtare, Borse, Jagtap, & Shankarling, 2010; H. Zhao, Baker, & Holmes, 2011).

2.3.2.2 DESs and Nanotechnology

The first ILs application presented by Deshmukh et al. (2001) in the field of nanotechnology at a room temperature, IL was implemented to synthesis the Pd–biscarbene mixtures and stabilize clusters (Deshmukh et al., 2001). Later, some studies including patents and papers published related to the ILs in nanotechnology. Lately, the DESs were used as ILs replacement in many nanotechnology applications fields.

It`s known that the main limitation for the nanomaterials is their propensity aggregate. Hence, the reach complete nanomaterials potential, the necessity for an environment which promises a perfect dispersion is crucial. Based on ASTM standards, the good stability criteria need the zeta potential absolute value more than 40 mV (Fan, Shi, Tian, Wang, & Yin, 2012). Therefore, the DESs were utilized as dispersant environment for the nanoparticles synthesis. The use of ChCl:malonic acid presented by Oh and Lee (2014) as structure directing agent and reaction media for synthesising of gold nanoparticle (Oh & Lee, 2014).

The acrylic acid: ChCl DES used a solvent microporous poly (acrylic acid)–carbon nanotube mixture synthesis, the researchers revealed that using green DES in the synthesising method resulted in nanocomposite environmental and biological application production (Mota-Morales et al., 2013). In the meantime, the use of ChCl:tris (hydroxymethyl) propane DES presented by Mąka et al. (2014) as a curing agent of epoxy resin for GNP/DES/ epoxy resin production. The DES presence effect positively the epoxy composites electrical volume resistivity (Mąka, Spychaj, & Kowalczyk, 2014).

In the electrochemistry field, the nanomaterials and DES rule are clear. The use of ChCl: urea was reported by Zheng et al. (2014) as quercetin sensors electrolyte, and they used the MWCNT electrode which demonstrated to be more convenient and easier than the use of ILs- CNTs composite (Zheng et al., 2014). The uniform Pt nanoflowers produced by using the DESs with electrochemically shaped methods, that shows a higher stability and electrocatalytic activity (Wei et al., 2012). The DES ChCl: ZnCl was encapsulated with 1:1 molar ratio in SWCNTs presented in Figure 2.4. This technique included the SWCNTs thermal treatment to remove the ending cups, the produced result was characterized with different techniques (Shimou Chen et al., 2009).

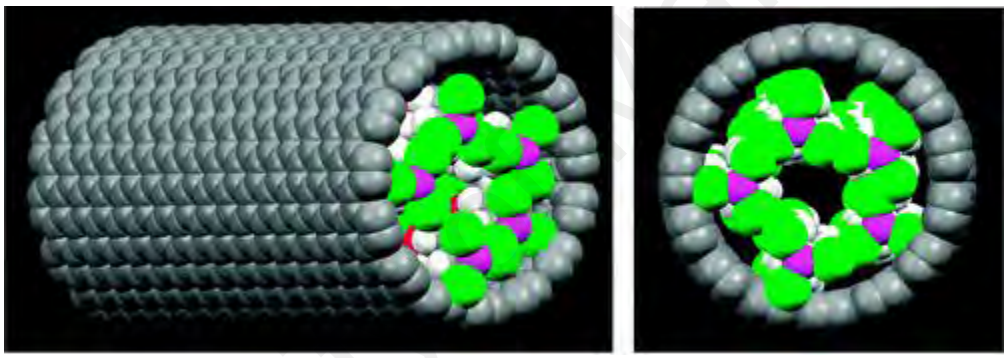

Figure 2. 4: DES encapsulated SWCNT

Gu and Tu (2011) presented a new technique to enable thermos chromism and dissolve metal complexes. The new technique included two DESs, ChCl:ethylene glycol and ChCl:urea, for dissolving many metal chlorides. NiCl2-6H2O displayed outstanding and stable thermochromic performance with a temperature started from ambient until 150 °C. The researchers recommended that their findings have probability in the development of high performance thermochromic materials for fabrication facile (C.-D. Gu & J.-P. Tu, 2011).

The DESs was used as graphene functionalization agent, many DESs types were used to examine the DESs effect on the surface of graphene. The findings reveal that the graphene functionalized with DESs have a great performance with many applications because of the effect of the functional groups introduced to the graphene surface (Hayyan, Abo-Hamad, et al., 2015). The most and effective material used in the water treatment field is carbon nanotube (CNTs) for the removal of several types of pollutants (Abbas et al., 2016; Ibrahim, Hayyan, AlSaadi, Hayyan, & Ibrahim, 2016). However, there are some limitations in the CNTs application due to various flaws in solubility, difficulty in manipulation, and aggregation.

2.3.3 Arsenic (As) ions adsorption using functionalized CNTs

Arsenic (As) removal is complicated comparing to the other heavy metals, the adsorption techniques considered as one of the effective method for arsenic removal from water. The removal of (As) using the CNTs as adsorbent are less comparing to the other heavy metals. The CNTs oxidization by HNO_3 and H_2SO_4 mixture using the sonication for 3 h at 40 ˚C was presented by (Veličković et al., 2013). The Oxidized MWCNTs was dispersed in EDA–ethylenediamine with the (1-[Bis (dimethylamino) methylene]-1H-1,2,3-triazolo pyridinium 3-oxid hexafluorophosphate) and methanol presence to be as coupling agent via sonication for 4h at 40˚C. The maximum adsorption capacity of the Oxidized MWCNTs was 12 mg/g and the adsorption model was fit to the Freundlich model (Veličković et al., 2013). Based on the previous studied, it is known that the arsenic has rapport with various kinds of metal oxides for different adsorbent based (Andjelkovic et al., 2014; Cui, Li, Gao, & Shang, 2012; Z.-C. Di et al., 2006; Feng et al., 2012; Ghosh, Poinern, Issa, & Singh, 2012; K. Gupta et al., 2011; Mak, Rao, & Lo, 2009; Martinson & Reddy, 2009; Mohmood et al., 2013; Patel, Byun, & Yavuz, 2012; M. A. Ramos, Yan, Li, Koel, & Zhang, 2009; Selvakumar et al., 2011; Tresintsi et al., 2013; Tuutijärvi et al., 2009). Moreover, the iron oxide (Fe-MWCNT) composite was used by Tawabini et al.

(2011) for arsenic (As^{3+}) removal, and the maximum removal capacity was 84.8% at pH ranged from 7-8 and the model of adsorption fitted with Langmuir isotherm and a pseudo-second-order rate for the kinetic model (Tawabini et al., 2011).

2.3.4 Lead (Pb) ions adsorption using functionalized CNTs

There are many techniques were proposed for the removal of Pb ions from water, due to the high effect of Pb ions. One of the proposed method for Pb removal was the adsorption process (H. Wang, Zhou, Peng, Yu, & Chen, 2007). Different adsorbents types were used for the Pb removal from water such as: sawdust, maize cobs, rice husks (Abdel-Ghani, Hefny, & El-Chaghaby, 2007), granulated blast-furnace slag (Dimitrova & Mehandgiev, 1998), giru clay and kaolinitic clay (Orumwense, 1996) and aquatic plant (Axtell, Sternberg, & Claussen, 2003). Moreover, the activated carbon is the most used adsorbent that can be initiate from various sources (Goel, Kadirvelu, Rajagopal, & Garg, 2005; Imamoglu & Tekir, 2008; Netzer & Hughes, 1984; Sekar, Sakthi, & Rengaraj, 2004; Tao, Zhang, Li, & Ding, 2015). The most effective adsorbents are the nanoparticles due to its special properties including catalytic potential, large surface area, high reactivity, small size (Ali, 2012). In the water treatment field, the most used nanomaterial is carbon nanotubes (CNTs). It is notable, that the common functionalization is oxidation using $KMnO_4$ or acids. The acidified CNTs with HNO_3 adsorption capacity reached to 85 mg/g with 50 mg/L initial concentration of Pb^{2+} within 6h, and the Pb^{2+} able to generate via decreasing the solution pH to 2.0 (H. Wang et al., 2007). The treated CNTs with HNO_3 to remove Pb^{2+} was stated by (Tofighy & Mohammadi, 2011), the maximum adsorption capacity was 101.5 mg/g. Moreover, the MnO_2 attachments on the MWCNTs by adding $KMnO_4$ to the CNTs at 70 ˚C with the addition of NaOH, the maximum reaction speed of adsorption increased to 5 min (Salam, 2013). Besides, the redox process was used for the Mn coating on the CNTs surface (Richter, Berndt, Eckelt, Schneider, &

Fricke, 1999). The adsorption capacity of the MnO_2/CNTs is depending on the pH of the solution, it increased from 77% to 98% with increasing the pH value from 2 to 4.

The MWCNTs was coated by using the modified magnetic amino CoFe2O4 ($CoFe_2O_4$-NH_2) by one-pot polyol method Zhou et al. (2014). The mixture was improved by using the chitosan (CTS), later the prepared mixture (MNP-CTS) used as adsorbent for the removal of Pb^{2+} and tetra bromo bisphenol A (TBBPA), the MNP-CTS adsorption capacity reached to 140 mg/g. Most of the adsorbent of heavy metals was highly depending on the pH of solution (Zhou et al., 2014). In addition, the dioxide/MWCNTs (TiO2/MWCNTs) adsorption capacity reached to 137.0 mg/g for Pb^{2+} at pH 6.0 (X. Zhao, Jia, Song, Zhou, & Li, 2010).

The sugarcane bagasse/MWCNTs mixture was presented by Hamza et al. (2013), and the adsorption capacity reached to 56.6 mg/g at temperature of 28 ºC and 4 pH solution, the best isotherm model fit to Langmuir model. (Hamza, Martincigh, Ngila, & Nyamori, 2013) reported that the removal efficiency is effected by the solution pH value, the adsorption capacity increased from 23.4 % to 99.8% by increasing the pH from 1 to 4.5. In addition, the saturated CNTs on bamboo charcoal (CNT/BC) adsorption capacity was 47.4 mg/g at pH 5 (Huang, Zhang, Wang, Lv, & Kang, 2012). The solid humic acid (HA) and MWCNTs (HAMWCNTs) are used as Pb^{2+} adsorbents from water was reported by Lin et al. (2012). The CNTs have a weak positive charge, nevertheless, after the coating by HA the charge reached to zero. Then, the CNTs surface was negatively charged with adding acidic functional groups that led to an increase in the CNTs adsorption capacity, because of the increasing in the electrostatic attraction. Three adsorbents were described by the isotherm Langmuir model, the adsorption capacity reached to 318 mg/g at 25% for the HA-CNTs and 333 mg/g at 50% for the HACNTs (D. Lin et al., 2012).

The surface area and CNTs structure are very important in the heavy metals removal, the adsorption capacity increase by decreasing the CNTs outer diameter. While, the CNTs oxidization by NaClO will results in an increase in the outer diameter thus, the CNTs adsorption capacity is increased. This confirm that the MWCNTs surface area and oxygen groups have impact on the adsorption capacity. Moreover, the negative charge increased on the oxidized surface which result in an increased in the adsorption capacity, the phonic groups have a large effect on the adsorption capacity due to the phonic groups affinity to the Pb^{2+} ions. Consequently, the mechanism of adsorption involved both physisorption and chemisorption (F. Yu, Ma, & Wu, 2011; F. Yu, Wu, Ma, & Zhang, 2013). The Pb^{2+} ions removal by using the CNTs as an adsorbent was reported by Kabbashi et al, 2009. Contact time, adsorbent dosage, pH and agitation speed were examined. The maximum removal of Pb^{2+} reached to 96.03% at 80 min, 40 mg/L 5 pH and 50 r/min agitation speed (Nassereldeen A Kabbashi et al., 2009). The graphene- CNT adsorption capacity was in the range of 230 to 415 mg/g, the $FeSO_4$ and CNT amounts are the two important parameters for the removal efficiency, stated by (M. Zhang, Gao, Cao, & Yang, 2013). The synthesized Zeolite carbon nanotubes (ZCNTs) was used as a new technique for the removal of Pb^{2+} ions, with 55.74 mg/g of adsorption capacity, the ZCNTs kinetics model was the pseudo-second-order with a Langmuir isotherm model (Venkata Ramana et al., 2013). In addition, the hyperchromic effect on the carboxylic CNTs for the Pb^{2+} removal was investigated by examining the reaction order of the absorbance (Tan et al., 2012).

New adsorption techniques were used for the removal of Pb^{2+} from water solution such as the electrochemical adsorption. The SWCNT and stainless-steel net (SWCNT@SSN) was used as a cathode and anode, the cathode surface and Pb^{2+} were attracted to each other, and the maximum removal reached to 97.2% for 20 mg dm^{-3} initial

concentrations and 99.6% for 159 mg dm^{-3} initial concentrations (Y. Liu, Yan, Yuan, Li, & Wu, 2013).

2.3.5 Mercury (Hg) ions adsorption using functionalized CNTs

The removal of mercury (Hg) from water is important to maintain pure drinking water. Many conventional methods have been used to decrease Hg concentration in water, such as, photoreduction, coagulation, membrane separation, reverse osmosis, ion-exchange, precipitation, and solvent extraction (Bandaru et al., 2013). However, some of these techniques either required large amount of chemical or high energy (F.-S. Zhang, Nriagu, & Itoh, 2005). Therefore, new methods for Hg removal are crucial. Adsorption method is a suitable technique in the comparing to the other used conventional methods, thus, Hg removal using adsorption technique is the most studied (Chandra & Kim, 2011; Chiarle, Ratto, & Rovatti, 2000).

Consequently, in this section the mercury removal using the CNTs as adsorbent is highlighted. The functionalized CNTs with amino thiol increased the CNTs adsorption capacity for Hg^{2+} removal. The SWCNTs-SH adsorption efficiency reached to 91% with five-fold usage (Bandaru et al., 2013). Moreover, the magnetite nanocomposite/ thiol-functionalized MWCNTs using grafting mercaptopropyl triethoxysilane (MPTS) on the (CNTs/Fe_3O_4) surface to generate MPTS-CNTs/Fe3O4 nanocomposites for Pb^{2+} and Hg^{2+} removal. The adsorption capacity at pH 6.5 reached to 65.40 and 65.52 mg/g for Pb^{2+} and Hg^{2+}, respectively. The adsorption capacity increases with increasing the pH value, the optimal pH for maximum adsorption was 6.5 mg/g, due to the competition between the H^{+} and metals ions, due to the metals ions tendency to hydrate M(OH)2 with higher pH values (C. Zhang, Sui, Li, Tang, & Cai, 2012). El-Sheikh et al. (2011), presented the geometrical dimension effects on the non- oxidized and oxidized MWCNTs on the Hg^{2+} removal from water (El-Sheikh, Al-Degs, Al-As' ad, & Sweileh, 2011). Chen

et al. (2014) reported on the use of MWCNTs functionalized by $KMnO4/H_2SO_4$ and MWCNTs with HNO_3. The pseudo second order was the best fit for the experimental data, and the mechanism of adsorption was chemisorption based on the Elovich model. Moreover, the Langmuir equation was the best describe for the isotherm models, the functionalized MWCNTs adsorption capacity was higher than the pristine MWCNTs (P. H. Chen, Hsu, Tsai, Lu, & Huang, 2014). The Sulfur containing MWCNTs (SMWCNTs) was reported by Pillay et al. (2013) for Hg^{2+} removal from water, the maximum adsorption capacity was 72.8 mg/g and the isotherm model fit to Langmuir equation.

2.4 Artificial Neural Network (ANN)

Artificial neural network (ANN) is a system identification method to assist studying the phenomena's that are not agreeable for the analytical modelling. The (ANNs) development started at 1943 (McCulloch & Pitts, 1943),encouraged in a desire for understanding the brain of human and imitate its function, the structure of the artificial neural network is presented in Figure 2.5.

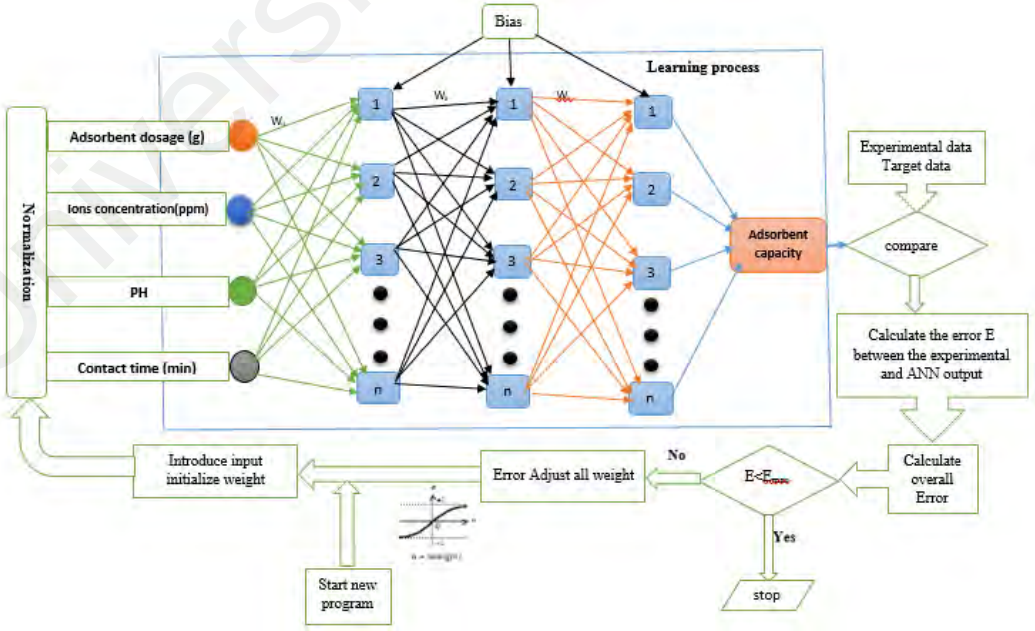

Figure 2. 5: Neural network structure

Recently, a huge renaissance in the development of sophisticated algorithms as a computation tools. Many researchers have been reported on the (ANNs) potential as a computational tool that compute, represent and acquire a mapping one input to the another (P. D. Wasserman, 1989). Scientifically, the ANN is considered as an approximator, the capability in the identifying the relationship by given data set, it is probable for the (ANNs) to solve a complicated problem for example nonlinear modelling, pattern recognition, association and classification. The (ANNs) idea was projected by McCulloch and Pitts (1943), the (ANNs) development technique was by (Hopfield, 1982). A huge growth of interest in the computational machine since (Rumelhart, Hinton, & McClelland, 1986) rediscovered a mathematically strict framework such as the back-propagation algorithm. Therefore, (ANNs) has been utilized in many areas such as financing, image processing, robotics, cybernetics, acoustics, computer science, electrical engineering, biomedical engineering, neurophysiology, physics and others.

The (ANNs) technique was used in a wide range in alloy design, process design, material characterization and process control (O. Lourie, Wagner, Zhang, & Iijima, 1999). The neural network structure, inputs and output normalization, data representation and suitable activated function have an influence on the performance and efficiency of neural network (Berhan et al., 2004). The transfer functions that can be use such as linear, log sigmoid or tangent sigmoid.

The back-propagation (BP) algorithm is achieved as following, the input data are supplied to network with calculated errors then, the sensitivity were propagated from the outcome layer to the input layer, the biases and weights were updatable parameters (Cai et al., 2001). This technique has shown to be valuable in classification and modelling problems, where the required properties are estimated as inputs vast array function

(Mallat, 1989). The epochs and neuron number used during the training phase are optimized by using the MSE to improve the performance of the network. The weights of network are randomly assigned initially, the appropriate selection at the training process is important in the minimizing of the estimated error. In general, there is no specific technique to create an inclusive priori estimation of training set cases pre-knowing the convergence and outcome of training process set; therefore, different strategies of training with different sets of data need to be applied initially for the algorithm validation. The training set must comprise the information which defines the behaviour within the range of inputs and outputs. This is required for the trained neural network to simplify the response which is involved in the training set; then, examining the trained network and its outcome is by comparing the trained and untrained full range (verification) data.

The development of neural network is based on some rules such as the process of the information occur at the nodes or called the neurons, the connection link between the nodes is the weight that associated in the connection link and the type of activation function. The characterization of neural network is based on its structure which present the connection pattern between the nodes, the activation function and the method of the connection weight (Fausett & Fausett, 1994). The typical neural network structure contains of a number of nodes organized according to specific design. Moreover, the ANNs categorization can be based on the processing and information direction flow, the nodes are arranged in a layers in the feedforward network starting from input layer to the output layer (Govindaraju, 2000). There are two methods of training whether in classification and regression, the supervised and unsupervised. In the supervised method, the network is trained by changing the weight value between the connections that can assume the value(s) of outputs. While, in the unsupervised training method there is no target outputs from the trained inputs (Esfe, Afrand, Yan, & Akbari, 2015).

2.4.1 ANN applications

The neural network techniques have been used in many applications of science. The ANN was used in the solar researches community, Yadev and Zhang present an inclusive review on the modelling of the solar radiation with different ANN algorithms such as radial basis function (RBFNN), NARX-NN, ANFIS and GRNN (Yadav & Chandel, 2014; Jianyuan Zhang, Zhao, Deng, Xu, & Zhang, 2017).

Genuino et al. (2017) used the ANN for the modelling and optimization of humic acid (HA) removal from the municipal solid waste biochar with studying the effect of KOH concentration, precipitant volume, contact time and extractant dose (Genuino, Bataller, Capareda, & de Luna, 2017). The ANN techniques were applied effectively for the optimization process and prediction such as membrane processes (Hazrati, Moghaddam, & Rostamizadeh, 2017), oxidation processes (AOPs) (Aghaeinejad-Meybodi, Ebadi, Shafiei, Khataee, & Rostampour, 2015).Tehlah et al. (2016) used the ANNs technique for developing two ANN models, for prediction and optimization of refined palm oil process, three inputs were involved in the first model pressure (P), column temperature (T) and feed flow rate (F), while, the second model two parameters were included the model pressure (P) and column temperature (T) (Tehlah, Kaewpradit, & Mujtaba, 2016). Shirazian et al. (2017) applied the ANNs modelling method for twin-screw extruder modelling, different ANN configurations were used with various number of hidden layer, activation function types and nodes number for determining the optimal condition of efficient prediction model (Shirazian, Kuhs, Darwish, Croker, & Walker, 2017). Pombeiro et al. (2017) used the ANN techniques for the prediction of electricity consumption for the intelligent building which needs a continuous monitoring, different parameters are considered in the modelling such as the occupancy which was estimated using the WiFi traffic, weather conditions, and time-of-day (Pombeiro, Santos, Carreira, Silva, & Sousa, 2017).

The wellhead choke liquid critical-flow rates as a function of gas-liquid ratio, choke size and wellhead pressure was predicted using the ANNs technique, different parameters were involved in the modelling such as temperature, oil specific gravity and gas specific gravity (Choubineh et al., 2017). Moreover, the ANNs modelling techniques was used for the concrete properties prediction by using normal aggregate (Ince, 2004; Kewalramani & Gupta, 2006; S.-C. Lee, 2003; Ni & Wang, 2000; Sobhani, Najimi, Pourkhorshidi, & Parhizkar, 2010). In addition, some studies on the modelling of the concrete compressive strength using a recycled aggregate and the ANNs technique for the prediction of the compressive strength (Šipoš, Miličević, & Siddique, 2017).

The pile settlement behaviour was also modelled using the ANNs method by using the cone penetration test (CPT) data for the training, validation and testing the ANNs model (Nejad & Jaksa, 2017). Hamad et al. (2017) modelled the road traffic noise by using the ANNs modelling methods, the parameters used were roadway temperature, average speed, classification and traffic volume and noise level, 240 data set were used in the modelling with 16 feed-forward back-propagation of ANN models were prepared in the study (Hamad, Khalil, & Shanableh, 2017).

Some of other researchers used the artificial neural network for the modelling in different fields includes pure refrigerants surface tension (Nabipour & Keshavarz, 2017), carbon aerogels pore structure (Z. Yang, Qiao, & Liang, 2017), heat reflux extraction (Olalere, Abdurahman, bin Mohd Yunus, & Alara, 2017), TiO_2 reinforced composites and Nano TiB_2 (Akbari, Shirvanimoghaddam, Hai, Zhuiykov, & Khayyam, 2017), olive oil ultrasound-assisted bleaching (Asgari, Sahari, & Barzegar, 2017), solar system (Abujazar, Fatihah, Ibrahim, Kabeel, & Sharil, 2018), MgO/oil nano-lubricants (Esfe, Bahiraei, Hajmohammad, & Afrand, 2017) and wave resource characterization (Sánchez et al., 2017).

2.4.2 ANN and remediation of water treatment

The artificial neural network (ANN) is a mathematical approximation method for the empirical model's developments. Kim et al. (2015) developed a model using the ANN methods for forecasting and prediction the of water quality variables such as TP, TN, DO and pH, the ANN showed high accuracy (S. E. Kim & Seo, 2015). The mean value estimation of four variables involved in the quality of water by using the ANN method, the authors reveals that ANN method cannot promise that the ANN model will show a best result, without choosing the suitable method. Moreover, the results indicate that the single best ANN model shows lower ability of generalization than the ensemble ANN model (Khalil, Ouarda, & St-Hilaire, 2011). The graphene nanofluid thermal conductivity modelling was presented by Vakili et al. (2016) by using the multilayer perceptron (MLP) ANN technique, the prediction results shows high certainty and accuracy of the ANN model (Vakili, Yahyaei, & Kalhor, 2016). The prediction of membrane fouling for the nanofiltration of drinking water using the ANN method was presented by Shetty et al. (2003), the ANN inputs comprised the physical and independent variables such as flow rate and the parameters of water quality (total dissolve solids (TDS), UV254 and pH) (Shetty & Chellam, 2003).

Moreover, ANN was applied for the prediction of lead ions separation percent (SP) from the wastewater by using the electrodialysis (ED), the involved variables in the process were voltage, flow rate and temperature. The optimum nodes and hidden layers number used (4:6:2:1), for SP prediction and ED cell current efficiency (CE) (Sadrzadeh, Mohammadi, Ivakpour, & Kasiri, 2009). Furthermore, the ANN used for the modelling of lead ions removal from water using the electrodialysis (ED) cell as adsorbent, the voltage, flow rate, temperature and lead ions concentration were used as the inputs variables (Sadrzadeh, Mohammadi, Ivakpour, & Kasiri, 2008). The Fenton process performance was investigated using the ANN system in landfill leachate treatment, three

targets were used for this purpose to cover different post-treatment products aspects including mass removal efficiency (MRE), sludge and supernatant and mass content ratio (MCR). The coagulation was observed as dominant mechanism for all the responses, the average error (AE), root mean square error (RMSE) and correlation coefficient (R^2) were proposed for the model evaluation, the ANN model showed a satisfactory result (Sabour & Amiri, 2017).

Won et al. (2016) presented a study using the ANN for the modelling of water quality using Chlorophyll-a, Turbidity, TP, TN, Electric Conductivity, pH, DO and Temperature as the process parameters at Cheongpyeong dam downstream. The ANN purpose of use is to reduce the influence of stochastic component, periodicity and trend, for enhancing the ANN model performance the stratified sampling method was used (won Seo, Yun, & Choi, 2016). The ANN system was used to develop a model for water bloom to avoid erupting water bloom and adopt the emergency response measures, also to give a technical basis to improve the lake and river environmental system (Zeng, Song, Liu, & Wang, 2010).

The ANN applications were applied to predict the dissolved oxygen (DO) in the Danube River, the number of input dataset used were 1912 monitoring for 17 parameters of water quality which were divided into regular set including low variability and normally distributed data, and extreme set which include monitoring records of outlier values. It is reviled that the phosphorus concentration, biological oxygen demand (BOD), pH and temperature are mostly effect the level of dissolved oxygen (Tomić, Antanasijević, Ristić, Perić-Grujić, & Pocajt, 2018).

Hong et al (2018) designed a robust model using ANN model technique for the estimation of heavy metals build-up in the urban roads, based on the results the map distribution of heavy metal load and the risk of comprehensive ecological map were

generated. The generated maps can give a conception platform to recognize the area priority where can reuse a safe storm water, moreover, the maps could be used as the urban land use planning tool for effective storm context (Hong, Zhu, & Liu, 2017). The ANN modelling system are used in many other aspects including the adsorption of heavy metals using the adsorption technique, some of these studies are reviewed in the following section.

2.4.3 ANN and adsorption

The ANNs techniques is suitable for prediction the trends of experimental data in water treatments such as for dyes removal from water solution by adsorption technique (Ghaedi & Vafaei, 2017). The dye compounds removal by using Penicillium YW 101 biomass as adsorbent, the process variable importance such as contact time, temperature, pH and initial concentration was investigated using ANN modelling method (Y. Yang et al., 2011). The removal of amido Black 10B from water solution by using the polyaniline/ SiO2 nanocomposite as an adsorbent by using the adsorption technique, different parameters were studied including initial dye concentration, solution pH, adsorbent dosage and adsorption time, the ANN technique was used for the optimization (Tanzifi et al., 2018). Yetilmezsoy et al. (2008) developed an ANN model for prediction the adsorption capacity of Antep pistachio (Pistacia Vera L) shells that used as adsorbents for lead Pb^{2+} removal from water solution by adsorption technique, the operational parameters effects including contact time, temperature, initial pH, Pb^{2+} initial concentration and adsorbent dosage were examined to find the optimum condition for Pb^{2+} ions removal (Yetilmezsoy & Demirel, 2008a). The ANN was applied to model and evaluate the heavy metals biosorption, the black cumin adsorbent was used in the process to remove lead ions from water. The process variable effect were investigated including temperature, biosorbent mass and pH (Bingöl, Hercan, Elevli, & Kılıç, 2012).

Yasin et al. (2014) developed an eco-friendly environmentally for lead ions removal from water solution, the ANN and genetic algorithm (GA) techniques were used for the optimization and simulation of lead ions, the intercalated tartrate-Mg–Al layered double hydroxides as lead absorbent. The Levenberg–Marquardt (LM) algorithm was used for the training of ANN model, the model inputs variable were lead ion concentration, adsorbent dosage, pH of solution and contact time (Yamin Yasin, Faujan Bin H Ahmad, Mansour Ghaffari-Moghaddam, & Mostafa Khajeh, 2014b).

The ANN technique showed a high accuracy for the modelling of zinc ions removal (Zn^{2+}) from leachate. Turan et al. (2011) developed an ANN model for (Zn^{2+}) ions removal using hazelnut shell as adsorbent. The operation parameters effect such as temperature, contact time, adsorbent dosage and pH were examined for optimizing the maximum adsorption condition of (Zn^{2+}) ions, by comparing the experimental and ANN model results the coefficient of correlation was ($R^2 = 0.99$) which demonstrate that the ANN is able to predict the zinc removal efficiently (N Gamze Turan, Başak Mesci, & Okan Ozgonenel, 2011). Another study was presented for the removal of Cu^{+2} from water, the operational parameters effect such as contact time, pH, adsorbent dosage and temperature were studied. The ANN system was implemented for the prediction of percentage removal of Cu^{2+} from water, firstly, the model was developed using three-layers with 4, 8 and 4 neurons at the first, second and third layers respectively. In addition, the radial basis function (RBF) was also used and its accuracy was compared to the other network types, the coefficient of correlation of the ANN model was ($R^2 = 0.999$) which demonstrate a high accuracy of the ANN model (N Gamze Turan, Basak Mesci, & Okan Ozgonenel, 2011).

Furthermore, other researchers used the ANN to develop a model for prediction of copper ions removal by waste flax meal as adsorbent, the effect of pH, amount of biosorbent

dosage and metal ions concentration were investigated (Podstawczyk, Witek-Krowiak, Dawiec, & Bhatnagar, 2015). Esfahani et al. (2015) conducted a batch experiment and used the ANN modelling method for the removal of chromium from water using bare ZVIN and S-ZVIN and evaluate their efficiency, the influence of variables which involved in the experiment was investigated, the ANN model was able to predict the chromium experimental data satisfactory with coefficient of correlation ($R^2 = 0.9803$) (Esfahani, Hojati, Azimi, Farzadian, & Khataee, 2015). Another study was conducted for the removal of Pb^{2+} and Cu^{2+} from water by using rice straw as adsorbent, the ANN was used to determine the optimum variable values to find the maximum efficiency of removal, the root mean squared error (RMSE) was used as an indicator to define the model topology (Khandanlou et al., 2016).

The removal of cobalt and manganese was presented by Khajeh et al. (2017), the tea waste solid-phase used as the adsorbent, the ANN was implemented to for the optimization and modelling of tea waste extraction process, the inputs variables that used were eluent and sample flow rates, eluent concentration, eluent volume, concentration of PAN (complexing agent), tea waste amount, and pH (M. Khajeh, Sarafraz-Yazdi, & Moghadam, 2017). Hamid et al. (2016) observed in their study the influence of sorbent dosage, concentration of Cu^{2+}ions and temperature on the removal of Cu^{2+} from water using the surface-oxidized cellulose nanowhiskers (CNWs) as Cu^{2+} absorber from water, this study reveals that the modified CNWs have a higher surface per unit mass comparing to the unmodified CNWs. The ANN system was employed for the optimization and creating a predictive model for Cu^{2+} performance evaluation. Different indicators were used to evaluate the ANN model such as the root mean squared error (RMSE), absolute average deviation (AAD) and the determination coefficient (R^2) (Hamid, Jenidi, Thielemans, Somerfield, & Gomes, 2016).

The different operating parameters effect including contact time, adsorbent dosages, Pb^{2+} ion concentration and pH of solution were examined for the optimization the optimum condition of Pb^{2+} ions removal from water using six different bio-sorbents. Applicability of ANN examined, three training algorithms (Scaled Conjugate Gradient, Levenberg–Marquardt and Backpropagation) with different transfer functions in the hidden layer and linear transfer function at the output layer were used (Singha, Bar, & Das, 2015). ANN is a suitable tool for analysis and modelling systems that is interest response which depends of various variables and the relationship between dependant and independent factors in the system is unknown. The ANN was applied successfully for metals biosorption in the recent years (Ahmad, Haydar, Bhatti, & Bari, 2014; Roy, Mondal, & Das, 2014; Shojaeimehr, Rahimpour, Khadivi, & Sadeghi, 2014).

2.5 Summary

A historical background on the heavy metals impact in water and its effects on the living organisms, such as the effect of lead, arsenic and mercury. The remediation techniques of the heavy metals removal are discussed carefully, such as the adsorption technique for the removal of heavy metals. In addition, the removal of heavy metals using the functionalized CNTs as adsorbent was presented especially for the adsorption of arsenic, lead and mercury. The CNTs functionalization agent, deep eutectic solvents (DES) and its application as a functionalization agent and its application in the nanotechnology are reviewed in the chapter.

An overview on the artificial neural network (ANN) historical background and its applications were presented. The ANN and its remediation in the water treatment field are highlighted. Moreover, a review is conducted on the recent developments in the ANN and its modifications to be used for the modelling of heavy metals removal processes.

Some studies on the use of ANN modelling methods that used for the modelling of heavy metals removal process were presented as well.

CHAPTER 3: THE MODELING OF LEAD REMOVAL FROM WATER BY DEEP EUTECTIC SOLVENTS UNCTIONALIZED CNTS: ARTIFICIAL NEURAL NETWORK (ANN) APPROACH

3.1 Introduction

The removal of heavy metal ions from water has been a crucial step to curb the resulting environmental problem. Any presence of heavy metals in water is recognized as a threat to both the human health and aquatic organisms (J. Wang & Chen, 2006). In addition, the properties of heavy metals to be non-biodegradable and has the tendency to build up in living organism may lead to various disease. Heavy metals may be present in the solution as free ions or in the form of molecules, and chelate metal ligands in any water streams (Salisu, Sanagi, Abu Naim, Wan Ibrahim, & Abd Karim, 2016). Lead is known to be one of the primary toxins of the heavy metals, discharge into the environment by battery manufacturing, metal electroplating, pigment and dye industries (Majumdar et al., 2010). The consumption of each such contaminate water may affect kidney, brain, liver and central nervous system which subsequently will lead to irreversible brain damage, weakness of muscles and nervous disorders (Geetha, Latha, Pillai, & Koshy, 2015). Research has been done to prove that the adsorption technique is one of the effective methods to extract metal ions from water solution (Pimentel et al., 2007). The effectiveness of adsorption is majorly dependent on the selection of appropriate process condition, including the mass of sorbent, duration of the process, pH and temperature of the system (E. Lourie & Gjengedal, 2011). Many studies have been done on different materials to be used as an adsorbent to extract metal cations from water, for example, activated carbon (J. P. Chen & Wu, 2004), clay minerals (J. U. K. Oubagaranadin & Z. V. P. Murthy, 2010), biomaterials (V. K. Gupta, A. Rastogi, V. K. Saini, & N. Jain, 2006) and pistachio vera shells (Yetilmezsoy & Demirel, 2008b). However, these adsorbents have not proven satisfying results.

Researchers have suggested carbon nanotubes (CNT) to be used as most effective adsorbents to extract numerous pollutants such as dyes, metal ions phenols, aniline, drugs and other contaminants (Ibrahim et al., 2016). The qualities of CNTs such as large surface area, diameter and the shorter equilibrium time than other materials contribute to its applications. CNTs have the potential to be used in variety of applications due to its distinctive electrical, physical and chemical properties.

CNTs have been successfully used to extract various heavy metals, for instance chromium, copper, zinc, lead, cadmium, arsenic and mercury (Ihsanullah et al., 2016). Researchers have reported that carbon nanotubes are efficient and is significantly adsorb lead more than copper and cadmium in the suitable pH value. Besides, the presence of different ions, the strength of ions and the pH value are the major criteria that influences the adsorption of Pb^{2+} (Nassereldeen A. Kabbashi et al., 2009).

Moreover, CNTs proved a great affinity for interaction with different compounds (Ihsanullah et al., 2016). Therefore, functionalization is the key to improve the activity of CNTs. The conventional functionalization usually involves hash acids and non-environmentally friendly chemicals with complicated processes. Consonantly, the need for environmentally friendly functionalization agents with simple chemical processes is crucial (AlOmar, Alsaadi, Jassam, Akib, & Ali Hashim, 2017).

Recently, deep eutectic solvents (DESs) have gain an enormous amount of interest due to its involvement in many applications. DESs was first introduced as a low-cost development or replacement of ionic liquids (ILs). DESs have many advantages over ILs in team of availability of the row martials and easy to synthesis with minimum environmentally harmful waste (AlOmar, Hayyan, et al., 2016). Therefore, DESs have conquer many fields of science. Lately, DESs involvement in many nanotechnologies related fields including media for synthesis of nanoparticles (M. H. Chakrabarti et al.,

2015; P. H. Chen et al., 2014; Jia et al., 2015; Xu et al., 2016), electrolyte in nanostructure sensors (Zheng et al., 2014), and electrolyte in nanoparticle deposition (Abbott et al., 2009; C. Gu & J. Tu, 2011; Renjith, Roy, & Lakshminarayanan, 2014). Functionalization agent of CNTs (AlOmar, Alsaadi, Hayyan, Akib, & Hashim, 2016; AlOmar, Alsaadi, Hayyan, et al., 2017). AlOmar et,al. 2016 have used choline chloride based DESs as a functionalization agent of CNTs to prepare a sufficient adsorbent of Pb^{2+} ions. Consequently, the dataset prepared from that work has been implemented for the modelling in this work (AlOmar, Alsaadi, Hayyan, et al., 2016b).

New techniques such as artificial neural network (ANN) has been considered as less complicated model in the sophisticated biological network. The substitute technique of modelling, artificial neural network system (ANN), is been selected in order to represent the non-linear function relationship among variables. The artificial neural network (ANN) techniques do not require any mathematical induction since the ANN analyses examples and recognizes the patterns in a series of inputs and outputs of dataset without any prior assumptions about their characteristics and interrelations (Sumantra Mandal et al., 2009). The speciality of the ANN to generalize and identify the pattern of any non-linear and complex development makes it an influential modelling means. Neural network has the ability to extract complicated data that is beyond the capability to be observed by a human or any computer technique. Experiments have been successfully performed to use ANN to model the adsorption of lead ions by pistachio Vera L. shells (Yetilmezsoy & Demirel, 2008b), the removal of Laneset Red G on Chara contraria (Mjalli et al., 2007), Laneset Red G on walnut husk removal efficiency (Çelekli et al., 2012), and the intercalated tartrate-Mg-Al layered double hydroxides as an adsorbent (Yasin et al., 2014a). Several studies have recently been conducted on water quality prediction models (Chibole, 2013; G. Wu & Xu, 2011). Moreover, there are some research have been applied on different areas for example, modeling the fermentation

media optimization (Kiran M. Desai et al., 2008), modeling of a microe-wave-assisted extraction method (M. M. a. M. Khajeh, 2011).

3.1.1 Problem statement

The Artificial neural network (ANN) is used to predict the adsorbent capacity of Pb^{2+} from water by using a set of experimental data that have been prepared in advance. The main advantages of using the ANN are their precision, salient and efficacy in apprehending the non-linear relationship current between the variables of multi-input or output in complicated system. Moreover, the availability in abundance and easy handing, the ANN is economically and the best option to predict Pb^{2+} adsorption. From an economical perspective, ANN can be utilised as a substitute of CNTs that is relatively higher in cost to study the adsorption process. Furthermore, the adsorption prediction model can play a key role in providing relevant information related to the input variables. In addition to that, the development of such models can be considered as low-cost and reduce the engineering effort.

3.1.2 Objective

The aims of this study are: (1) to create an ANN model to establish the relationship that exists between the adsorbent dosage, concentration of Pb^{2+}, pH and contact time to predict the DES-CNTs adsorption capacity of Pb^{2+} from water solution based on the experimental data set prepared in lab scale (AlOmar, Alsaadi, Hayyan, et al., 2016b). (2) The adsorption capacity of the DES-CNTs adsorbent for Pb^{2+} will be predicted by using ANN model and compare it with the experimentally measured values. (3) Two neural network types will be designed and compared based on the performance of the network.

3.2 Materials and methods

3.2.1 Experimental

In a previous study, a novel Pb^{2+} adsorbent was prepared based on pristine CNTs oxidized with $KMnO_4$, and then functionalized by choline chloride: tri ethylene glycol (salt: HBD) 1:2 DES (TEG). The preparation of the adsorbent was in two stages, the primary oxidation involved sonication of P-CNTs with $KMnO_4$ for 2 h @ 65 °C, later the resulted oxidized CNTs (K-CNTs) was sonicated with DES for 3 h @ 65 °C to produce KTEG-CNTs. The adsorbent was comprehensively characterized by indicting the RAMAN shift using Raman spectroscopy. The functional groups associated with the functionalization process was analysed using FT-IR. The surface charge, surface area and surface morphology was investigated by Zeta potential, IBT surface area, FESEM and TEM respectively. The structural phase was also investigated by conducting the XRD profile.

Moreover, batch adsorption study was performed at ambient condition. Adsorbent dosage, initial concentration, pH value and contact time were taken as variables to the response of adsorption capacity of KTEG-CNTs. 158 points were taken to study the influence of each parameter and the interaction among them on the adsorption capacity. The restriction taken for each parameter is listed in Table 3.1. The work flow is demonstrated in Figure 3.1.

Table 3. 1: The range of input and output parameters

Parameters	Minimum	Maximum
Adsorbent Dosage (g)	5	20
Initial Concentration of Pb^{2+} (ppm)	3	60
PH	2.7	7
Contact Time (min)	3	900
Uptake Capacity (mg/g) (output)	7.12	294.5

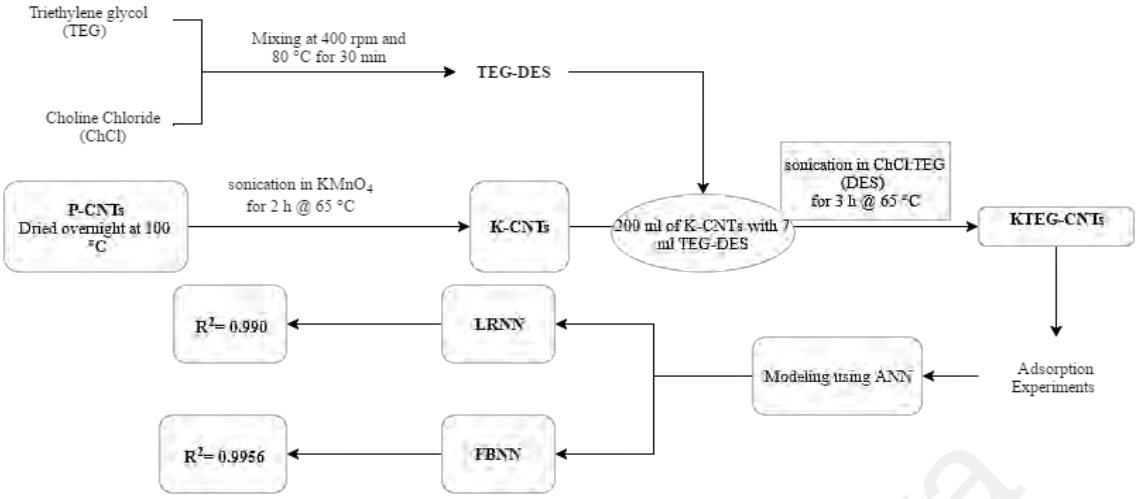

Figure 3. 1: The work flow

3.3 Design of Artificial neural networks (ANN) structure

The NN Toolbox R2014a of MATLAB is a mathematical software that was used to predict the adsorption capacity of functionalized carbon nanotube to adsorb Pb^{2+} from water solution. A total of 158 experimental datasets were prepared and used to create the ANN model. The experimental variables are initial concentration of Pb^{2+}, adsorbent dosage, pH and contact time.

Artificial neural network (ANNs) is a sophisticated statistical approach that created to behaves similar to the nervous system of human by developing a logical model containing of inter-connective neurons system in a computing network (Hemmat Esfe, Afrand, Yan, & Akbari, 2015; Kurt & Kayfeci, 2009). The neural network is used to resolve complicated test models such as pattern recognition, classification and estimation.

The supervised and the unsupervised are the two major types of ANNs that can be used in classification or regression. At the supervised model, the network is trained in order to adjust the optimum weight values between neurons that makes it able to produce the desired output value(s) after taking different number of instructing data from the previous experimental examples. Whereby, for the unsupervised model, there is no

preferred design value during the introducing of the input to the structure. The supervised method was applied in this work.

The 158-present data were allocated into training and testing sets, where it comprises of four (4) input and one (1) output, and the testing files contained only the output parameter that were not operated for the training processes. The data were subdivided as defined percentages to prepare separate data sets for training and testing processes of the ANN model. Nevertheless, the division is organised on the basis that the training data forms the major share of the latter. Subsequently, the data were switched within the spreadsheet and analysis was done to invalidate the presence of existing combination of trend and the inherent characteristics within the data (GK, Nale, & Muluneh; Sarangi & Bhattacharya, 2005; B. Zhang & Govindaraju, 2003).

A total of two types of neural network were designed to analyse the feed-forward back-propagation (BP) and the layer recurrent, as to develop ANN. The number of neuron(s), layer(s), training and testing sets and the type of transfer function need to be determine carefully.

The suitable training algorithm can only be determined upon the identification of the complexity of the problem, the number of data point in the training set, the value of biases and weights in the network and the maximum error target. Six training function as presented in Table 3.2, were used and compared based on their performance to select the best suitable training function in both the feed-forward back-propagation (BPNN) and the layer recurrent. For all training function, three hidden layers were selected for the feedforward Backpropagation (BP) and five hidden layers for the layer recurrent (LRNN), the number of hidden layers were selected by try and error to design the best NN structure.

Table 3. 2: The selected training functions

Name of training function	Training function
Quasi-Newton back-propagation	Trainbfg
Bayesian regularization back-propagation	Trainbr
Powell Beale conjugate gradient back-propagation	Traincgb
Polak Ribi-ere conjugate gradient back-propagation	Traincgp
Fletcher Reeves conjugate gradient back-propagation	Traincgf
Levenberg Marquardt back-propagation	Trainlm

Similarly, to select the optimum number of hidden neurons to be used in the network is one of the major challenges for neural networks, using imprudent hidden neurons will lead to overfitting problem, this will cause to the network an over-estimate the complexity of the goal problem. It significantly effects the generalization performance, which cause a significant deviation in predictions. In the network optimization, 2 hidden neurons were used as the first hypothesis up to fifteen for both the feedforward backpropagation (BP) and the layer recurrent (LR). In this perception, the determining of the optimum number of hidden neurons to avoid over-fitting problem is critical in function estimation using NN. The transfer function is one of the most important factors in the model creation, in this study a three-different transfer function are used (TANSIG, PURELIN and LOGSIG) to choose the optimum one for the model.

3.3.1 Feed-forward Back-propagation (BP)

The feed-forward Back-propagation is usually used learning algorithm in ANN application, which used the back-propagation system as the gradient decent technique to minimize network error. Each layer in the BPANN has several neurons and each neuron transmits input values and processes to the next layer. As shown in Figure 3.2, the value of the input variable is multiplied by the connection weights w_{ii} which connects the input to the hidden layer.

The FFBP models consist of input layers, hidden layers and output layer in a multilayer neural network. The input layer consists of I nodes, the hidden layer contains a J node(s) and the output layer consists of the K nodes. Consequently, the Z_K can be written as:

$$z_k = f(b_{ok} + \sum_{j=1}^{J} b_{jk} . f(a_{oj} + \sum_{i=1}^{I} a_{ij} . x_i)) \tag{3.1}$$

The f is the transfer function in the equation 1 or its the activation function, b_{jk} and a_{ij} (i= 1,2,3, I; j=1,2, 3, J; k=1,2, 3, k) are the weight values, xi is the input number, and a_{oj} and b_{ok} are the deviation. The f function in equation (1) is a type of mapping rule to transfer the neurons from the weighted input to output, also it is a strategy type to introduce the nonlinear into the FBNN network (Kothari & Agyepong, 1996).

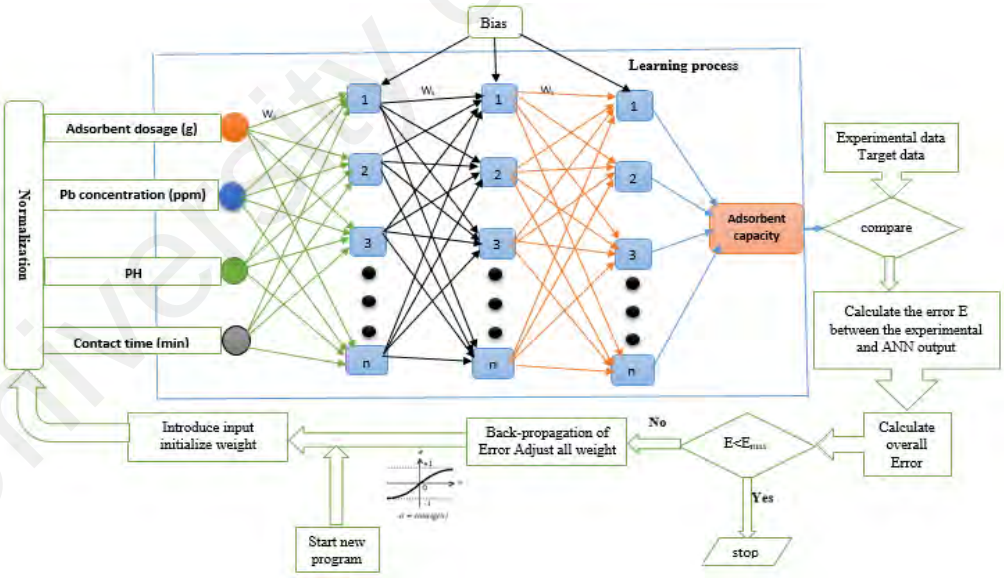

Figure 3. 2: Feed-forward back-propagation neural network structure

There are plenty of Feed-forward Back-propagation Neural Network (FBNN) transfer function in the backpropagation unit. The following transfer function selected principles used as a monotonous non-decreasing, differentiable and continuous function. In this

work the most universal binary logistic sigmoid transfer function is used and it is written as following:

$$f(x) = \frac{1}{1+e^{-x}} \tag{3.2}$$

The optimal parameters can be selected by adjusting the weight values of the network as the FBNN owned by a supervisory learning algorithm technique (A. H. El-Shafie & El-Manadely, 2011), and optimum means the different between the target values or actual values t_k and the network output z_k achieved the minimum or the target that is:

$$E = \frac{1}{2}\sum_{k=1}^{k}(z_k - t_k)^2 \tag{3.3}$$

To produce an output vector Y= (y_1, y_2,…, y_p) for the ANN which is close as possible to target vector T= (t_1,t_2,…t_p) a learning, also named as training process, is employed to find the optimum bias vectors V and the optimum weight matrices W, that reduce the error which been established in advance that typically has the from:

$$E = \sum_{P}\sum_{p}(y_i - t_i)^2 \tag{3.4}$$

Here, y_i = ANN output; t_i is the target output T; p = the output value of nodes and P= training patterns number. The training is a process which the connection weights of the ANN are adapted by a continuous process of stimulation through the situation in which the network is embedded.

The input data is normalized in the range of (0 to 1) form to avoid the overfitting, the adopted FBNN model structure, it is realized that all the unite at the same layer does not connect to each another, and the connections between the developed layers can be expressed based on the weighted coefficient (A. El-Shafie, Taha, & Noureldin, 2007).

The weighted signals and bias from the input neurons are summed by the hidden neurons and then projected through the transfer function. In the (FFBP) algorithm, the inputs forwarded into the network until the end of the network, output are initiated and compared to the target value and the error is calculated (Hemmat Esfe et al., 2015; Kurt & Kayfeci, 2009).

The back-propagation learning is to establish the relationship between the target data and the input data that is usually assigned with a random initial weight and later updating them by comparing the results between the actual and target values. In diversity of research using neural computations, consist of different transfer functions were possible to use depending upon problem nonlinearity and the complexity of data, in order to design the proper network.

3.3.2 Layer recurrent

The artificial recurrent neural network (RNNs) preform a great and different classes of computational modeling which is usually created by more or less detailed analogy with the biological brain module. In the layer-recurrent, many abstract neurons and also may called processing elements or units which are interconnected by likewise distracted synaptic links or connection, which enable activation to pass through the network.

The (LRNN) is almost the same as the (FNN) except that both the hidden and output layer of the (LRNN) has recurrent connection associated with a tab delay which is different with the (FNN). In addition to the input space, the RNN works on an internal state space, which is a trace of what has already been processed by the network. Neurons in RNN can be connected to any other neurons in the same or a previous layer. The recurrent neural network (RNNs) consist of input layer, hidden layer, and output layer, with activation function, feedback connection weights, and interconnection weights. Figure 3.3 illustrates the flow of the input samples in the LRNN architecture. The first

hidden layer of the LRNN are connected to the inputs and the following layer which assemble the networks output and has a connection from the previous layer. The input weights of the hidden layer come from the input samples, and the following layer has a weight comes from the preceding hidden layer. Though, the hidden layer does not directly affect with the external environment, they have great influence on the following layer or the output layer of the ANN.

The LRNN is categorized by the appearance of a backward connection in the hidden and output layers providing backward connection initiated from each output of hidden layer connected to one of the weights of the input layer by the context unit. Moreover, the backward connection from the output of the hidden layer as presented in Figure 3.3, is occupied from the real output during the training process of the LRNN.

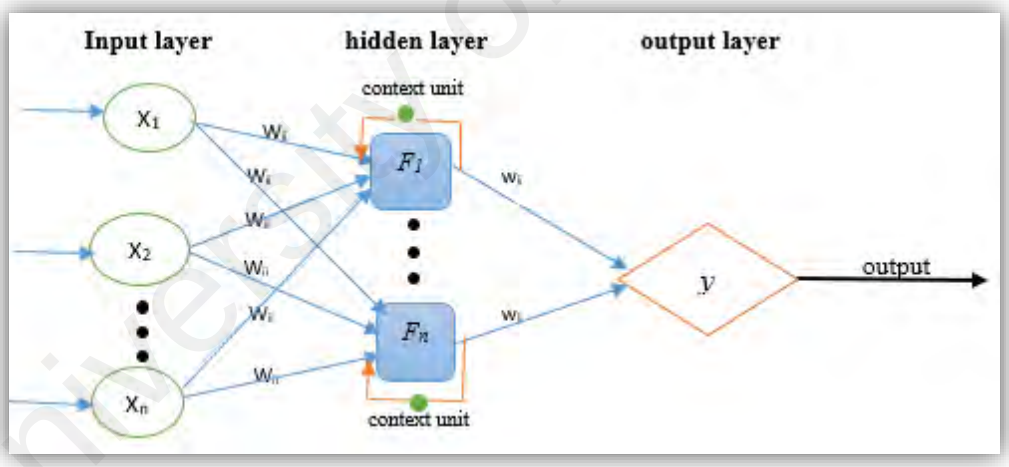

Figure 3. 3: The architecture system of the LRNN

The selection of proper network parameters such as the hidden layer's number, the neurons number in each layer, and the function of transfer types which is one of the most important network parameters considered for the architecture.

3.4 Evaluation indicators for simulation models

Two competing neural networks have been developed, the feedforward back-propagation and layer recurrent for modeling was used in this study. The total of 158 experimental data were divided into two subsets of testing and training (K. M. Desai, S. A. Survase, P. S. Saudagar, S. Lele, & R. S. Singhal, 2008; J.-W. Lee, Suh, Hong, & Shin, 2011) for developing ANN model. The experimental variables are Pb^{2+} concentration, adsorbent dosage, pH, and contact time. The assessment of multicriteria was carried out. Therefore, the (FNN) and (RNN) models performance was determined by comparing the actual data and the simulated data. The simulation behaviour of each model was evaluated by using the root mean square error (RMSE), relative error (RE), mean square error (MSE), relative root mean square error (RRMSE) and the mean absolute percentage error (MAPE). Formulas for calculation MSE, RMSE, RE, RRMSE, and MAE were given below and as follow:

$$MSE = \frac{1}{n}\sum_{i=1}^{n}\left(D_{a(t)} - D_{f(t)}\right)^2 \tag{3.5}$$

$$RMSE = \left[\frac{1}{n}\sum_{t=1}^{n}\left(D_{a(t)} - D_{f(t)}\right)^2\right]^{\frac{1}{2}} \tag{3.6}$$

$$RRMSE = \left[\frac{1}{n}\sum_{t=1}^{n}\left(\frac{D_{a(t)} - D_{f(t)}}{D_{a(t)}}\right)^2\right]^{\frac{1}{2}} \tag{3.7}$$

$$MAPE = \frac{1}{n}\sum\nolimits_{t=1}^{n}\left|\frac{\left(D_{a(t)} - D_{f(t)}\right)}{D_{a(t)}}\right| \times 100 \tag{3.8}$$

$$R^2 = 1 - \frac{SS_{res}}{SS_{tot}} \tag{3.9}$$

$$RE = \frac{D_{a(t)} - D_{f(t)}}{D_{a(t)}} \times 100 \quad (3.10)$$

Where:

$D_{a(t)}$ = the actual value.

$D_{f(t)}$ = the simulated value.

SS_{res} = the regression sum of squares.

SS_{tot} = the sum of squares of residuals.

Generally, MSE, RMSE, RE, MAPE and RRMSE equations were selected to indicate the models performance, were based on the obtained result by comparing the evaluated error of the actual and simulated model. The best model the model with the smallest error is considered.

3.5 Results and Discussion

In this section, the used methods to select the optimal neuron number, training function, performance of the selected model, model performance evaluation and the relative error between the predicted and the actual results are discussed.

3.5.1 Model performance evaluation

The functioning of every model was presented by using the MSE, RMSE, RRMSE and MAPE. The values of each simulated method are tabulated in Table 3.3.

Table 3. 3: Evaluation indicators

	FBNN	LRNN
MSE	1.66×10^{-4}	7.2×10^{-4}
RMSE	1.28×10^{-2}	2.68×10^{-2}
RRMSE	5.76×10^{-2}	7.46×10^{-2}
MAPE	4.101	5.605

With reference to the MSE values of every model listed in Table 3.3, it is observed that the MSE of FBNN model is 1.66×10^{-4} which is a practical value and reflects the

efficacy and higher accuracy in comparison to the LRNN model to simulate the relationship between initial concertation of Pb^{2+}, adsorbent dosage, pH and contact time to analyse the adsorbent capacity of KTEG-CNTs.

A simulation model is categorised to be reasonable and accurate if the MAPE value is below 30 % and 5 % respectively. Based on this acceptance criteria, the MAPE value for FBNN that is 4.10 % is considered as accurate, whereas the MAPE value of 5.60 % for LRNN does not fall in the range of accuracy.

It is evident that the FBNN provides better result in comparison to LRNN. Furthermore, the FBNN model had resulted in RMSE and RRMSE value of 1.28×10^{-2} and 5.76×10^{-2} respectively which is lesser than the results obtained in LRNN model. The probability of error in simulated value is low with the result of RMSE and RRMSE getting closer to zero. Therefore, these criteria further confirm that the FBNN method provide higher degree of accuracy in comparison to the LRNN method.

3.5.2 Training and testing dataset

This section discusses the part of a typical multilayer network workflow. In common practice, the data is first partitioned into two sets. The first set is termed as training set that is used to record the gradient and modify the network weights and biases. Testing set is the second subset, which is not applied during the training but is functional to compare various models and plot the errors of test sets. Generally, each backpropagation training group starts with several initial weights and biases, and various division of data into training and testing sets. These different conditions can lead to varied solutions for the same problem. In this study, different training and testing percentage used to find the optimal set with minimum error, the used sets are presented in Table 3.4.

Table 3. 4: The training and testing sets

		MSE	
Training %	Testing %	FBNN	LRNN
70	30	2.44×10^{-2}	1.08×10^{-1}
75	25	9.73×10^{-3}	9.41×10^{-2}
80	20	5.87×10^{-3}	2.96×10^{-2}
85	15	1.66×10^{-4}	7.22×10^{-4}
90	10	6.67×10^{-2}	8.45×10^{-2}

The used data in this study is 158 were separated into training and testing sets, different sets of data were used as presented in Table 4 to find the optimal set for model creation. At 70% training and 30 % testing the MSE for the FBNN is 2.44×10^{-2} and for the LRNN is 1.08×10^{-1} whereby, when increasing the percentage of the training set to 75 % with 25 % for the test set, the MSE decreased to 9.73×10^{-3} for the FBNN and 9.41×10^{-2} for the LRNN. Furthermore, the percentage of training increased to 80 % with decreased the percentage of the test set to 20 % there was an improvement in the result of the MSE it shows 5.87×10^{-3} for FBNN and 2.96×10^{-2} for the LRNN. The minimum MSE for the FBNN and LRNN was at 85 % at the training and 15% at the test set with 1.66×10^{-4} for the FBNN and 7.22×10^{-4} for the LRNN. While, by increasing the training set to 90 % for the training and 10 % for testing the MSE showed a higher value with 6.67×10^{-2} for the FBNN and 8.45×10-2 for LRNN. Hence, the optimal split is 85% for the training and 15 % for the test. The results demonstrate that FBNN model is more accurate than LRNN as the values of the MSE for all the sets for the FBNN lower than the MSE for LRNN.

3.5.3 Neurons number optimization

The best structure of the ANN model and its specification difference are determined with reference to the smallest value of MSE of the test dataset. With increasing the number of the neurons, the network generates different MSE values for the testing dataset. Figure 3.4 illustrate the relationship between the number of neurons in each

hidden layer and MSE obtained. For the feedforward backpropagation, 3 hidden layers were used. The MSE value of the network result is higher for the 2 neurons (MSE 7.43×10^{-2}) and 3 (7.60×10^{-2}) hidden layer neurons, than those with 4 shows a higher drop to (MSE 6.51 10-2). While, for 5 (MSE 5.03×10^{-2}), 6 (MSE 4.25×10^{-2}) and 7 (MSE 3.54×10^{-2}). The value of the MSE reduced significantly from 3.54×10^{-2} to 1.48×10^{-2} with the application of 8 hidden neurons and continue to decrease with subsequent rise in the neurons number from 8 to 10. Therefore, the neural network consisting of 10 hidden neurons with MSE value of 1.66×10^{-4} was selected as the best case based on the MSE value.

Furthermore, when the neurons number increase to 13, the MSE value displayed a slight increment from 1.66×10^{-4} to 4.98×10^{-3}. Subsequently, with further addition in the neurons number from 13 to 15, the result of the MSE is sharply increased. The increment might be assign to the MSE characteristics input vector used and performance index used in this work.

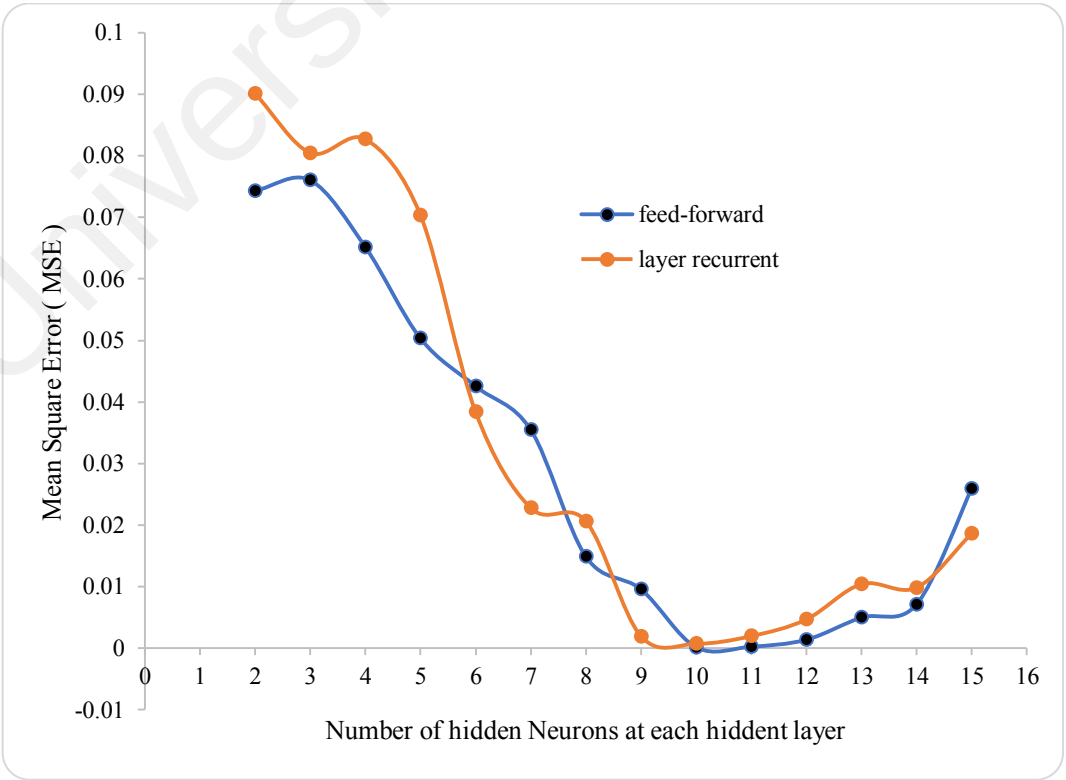

Figure 3. 4: The neurons number at each hidden layer with the MSE value

While for layer recurrent as shown in Figure 3.4, the number of hidden neurons was tested on 5 hidden layers as the best for the structure of the network. 2 hidden neurons were used at the first try and showed (9.01×10^{-2} MSE), while for 3 neurons the MSE decreased to (8.04×10^{-2}) and, for 4 the MSE increased (8.27×10^{-2}). While, when using 5 neurons there is a decline in the MSE with (7.03×10^{-2}), however, increasing the neurons to 6 the MSE showed a slightly decrease to (3.83×10^{-2}), the number of hidden neurons were later increased to 7 and 8 hidden neurons to improve the stabilization of the network, the MSE decreased to (2.27×10^{-2} and 2.06×10^{-2}) respectively, with the increasing of neurons to 9 the MSE reached to (1.94×10^{-3}). Furthermore, with 10 neurons the MSE decreased to 7.22×10^{-4} which shows the best stabilization of the network. With 11 and 12 neurons, the MSE resulted displayed a higher value which are 1.96×10^{-3} and 4.68×10^{-3} respectively. Finally, with 13, 14 and 15 neurons, the MSE rises to 1.04×10^{-2}, 9.84×10^{-3} and 1.86×10^{-2} respectively. This confirm that using 10 neurons at each hidden layer shows the best performance of the network.

3.5.4 Selection of the training function for FBNN and LRNN

It is laborious work to find the fastest training algorithm for the given problem due to the complexity of the problem that depends on various factors. This section discusses on the comparison of the various training algorithms. Networks are trained on six different training functions and identified the based on the R^2 value and the MSE. Six training functions shown in Table 5 were used and compared to select the best suitable training function in both the feedforward backpropagation (BP) and the layer recurrent (LR).

For the feed-forward back-propagation, the comparison study resulted that the Bayesian regularization backpropagation (trainrb) had resulted in smallest value of MSE in comparison to different sets of algorithms such as the Levenberg Marquardt

backpropagation (trainlm) algorithm. As shown in Table 3.5, the smallest MSE was obtained about 1.66×10^{-4}, and 0.9956 of R^2 for trainbr function presented in Figure 3.5 which reflects a great performance of the network.

Table 3. 5: The training function, R^2 and MSE

Training function	Feedforward backpropagation MSE	R^2	layer recurrent MSE	R^2
Trainbfg	9.03×10^{-3}	0.7465	1.28×10^{-2}	0.856
Trainbr	1.66×10^{-4}	0.9956	7.22×10^{-4}	0.990
Traincgb	2.97×10^{-3}	0.9021	4.44×10^{-3}	0.956
Traincgf	4.63×10^{-2}	0.4931	2.89×10^{-2}	0.663
Traincgp	2.30×10^{-2}	0.6915	1.32×10^{-2}	0.891
Trainlm	6.79×10^{-4}	0.9766	2.82×10^{-3}	0.968

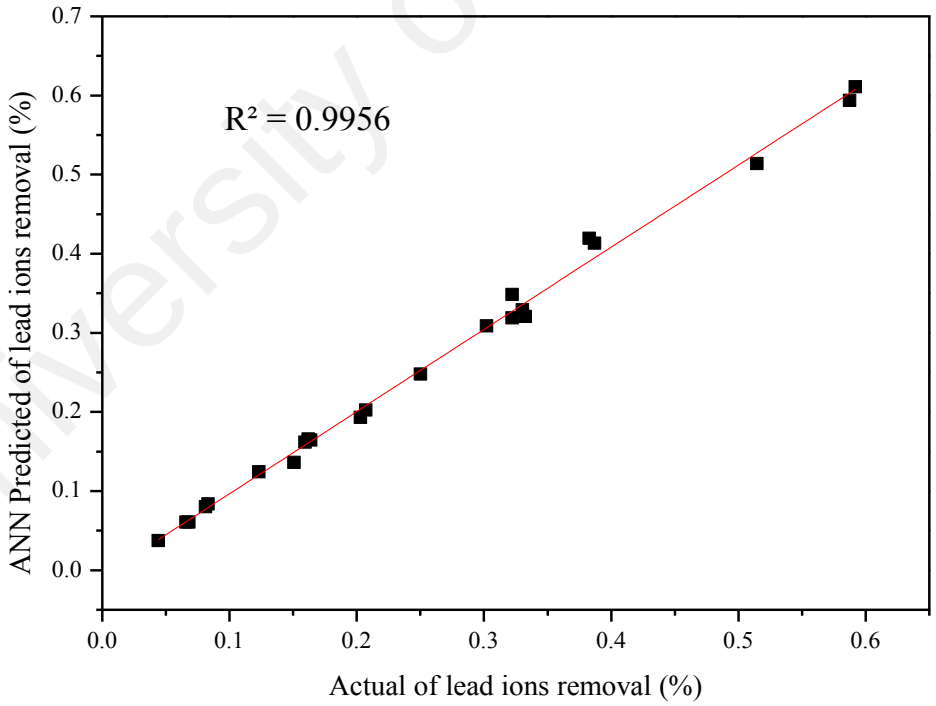

Figure 3. 5: The R^2 of feedforward neural network

This was followed by the trainlm with a MSE of 6.79×10^{-4}. However, both trainrb and trainlm shows a great behaviour comparing to the other algorithms such as trainbgf, traincgb, traincgf and traincgp. The structure and the combinatorial characteristic of the test data influences the results optimality initiated by some BP algorithms. Therefore, the problem complexity was solved by the results of several analysis of training algorithms used for the comparison.

Whereby, for the layer recurrent the first try is using trainbfg as training function with tansig transfer function and gave a result of the MSE is 1.28×10^{-2}. While for the trainbr training function the MSE is decreased to 7.22×10^{-4}, which shows a great performance of the network. However, by using a different training function such as traincgb and traincgf, the MSE is 4.44×10^{-3} and 2.89×10^{-2} which are greater than the MSE of trainbr training function. While, the MSE for the traincgp is 1.32×10^{-2}. The performance of the trainlm also showed a great value of the MSE 2.82×10^{-3} which can be considered as one of the best suitable training function for the network. It can be realized that the trainbr training function is the best suitable for both feed-forward backpropagation and layer recurrent network.

3.5.5 Relative error indication

Relative error is one of the indications of error in the model prediction values comparing the predicted values to the actual values, measurements and calculation can be characterized with regard to their precision and accuracy. The term accuracy can be defined as how closely the predicted value matches the actual value, whereas precision is referred to how closely values matches with each other. The highest relative error value is found to be 14.93 % for the FBNN model and 18.67 % for the LRNN model calculated by equation (10) which is considered as an acceptable value.

Based on the results shown in Figure 3.6, it is observed that occurred error for all the testing dataset is less than 14.93 % for the FBNN whereby, the maximum error for the LRNN is less than 18.67 % for the LRNN. Which indicate that the FBNN model is more accurate than the LRNN model.

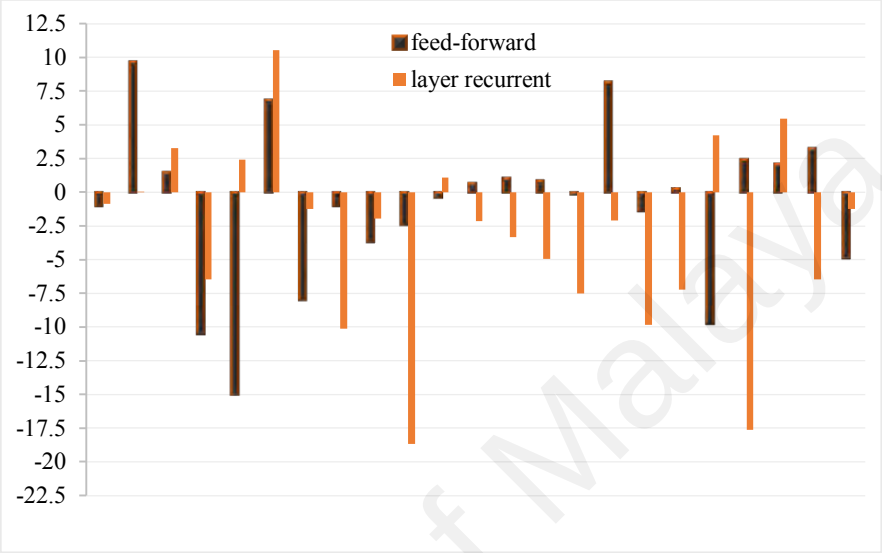

Figure 3. 6: Illustrates the accuracy of the hybrid model

This proves the effectiveness and reliability of the proposed approach to extract features from input data. The hybrid FBNN algorithm network model is able to provide a perfect prediction of KTEG-CNTs as Pb^{2+} absorber from water. The uncertainty in this work might come from the accuracy of the initial concentration of Pb^{2+}, amount of adsorbent dosage, and the aqueous solution pH adjustment, as the amount of the materials used is very small amount. Also, the humidity and the temperature of the room is not considered in this study which might affect the accuracy of the results.

3.5.6 The effect of pH on the adsorption capacity

The pH is one of the very important factors which can affect the quantity and the form of Pb^{2+} in water, and the interactions between the adsorbent and Pb^{2+}, and the quantity and the form of the adsorbent surface sites (H. Chen & Wang, 2007).

The pH effect on adsorption capacity studied by mixing 12.5 mg adsorbent dosage with 5 mg/L concertation at 15 min contact time with range pH values from 2 to 7. The experiment results present that the pH of the solution was found as an important factor effecting the adsorption efficiency. The pH increment led to significant increase in adsorption capacity until pH 5.0, then the adsorption capacity became steady with increasing pH. It is well known that at pH greater than 7.0, the dominant species of Pb^{2+} are $Pb(OH)^{+}$ and $Pb(OH)_2$. This complexation may occur due to the extensive presence of OH- at this pH level which resulted in a precipitation form (V. K. Gupta, Agarwal, & Saleh, 2011). In addition, the decreasing of H^{+} plays a significant role in the mechanism of Pb^{2+} adsorption due to the decreasing of competition on the active sides of the adsorbent. The agreement of the ANN model predictions as a pH function is presented in Figure 3.7. From Figure 3.7, it can be noticed that the ANN model outputs showed almost the same behaviour as the experimental data, this can prove that the ANN model can predict the adsorption capacity of Pb^{2+} removal from water satisfactorily.

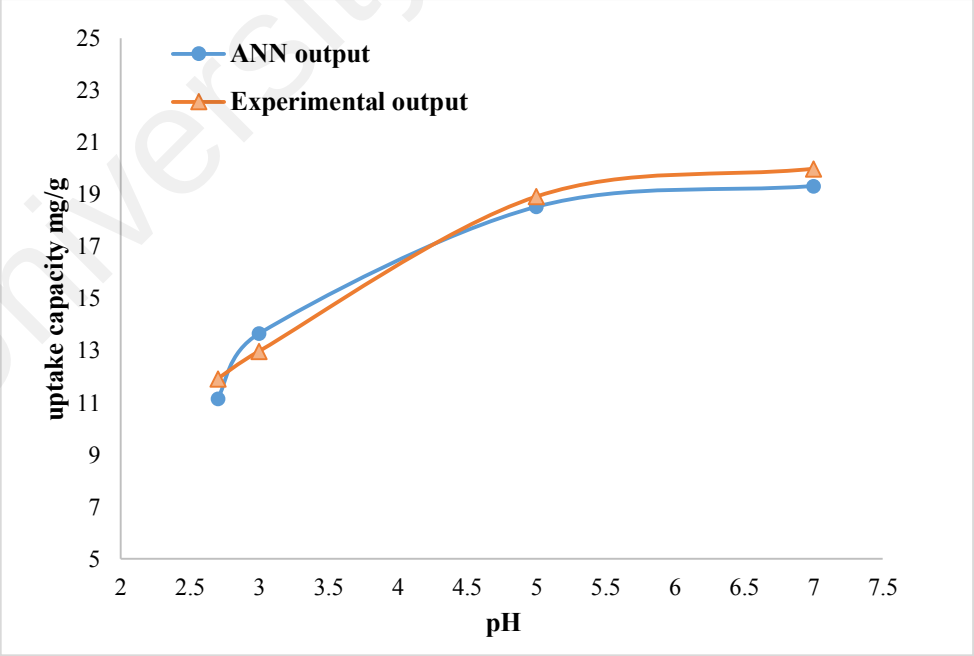

Figure 3. 7: Agreement between ANN and experimental outputs with various pH values

3.5.7 The effect of adsorbent dosage on the adsorption capacity

The Adsorbent dosage is one of the important parameters involved in the adsorption process. Adsorbent dosage effect on the Pb^{2+} removal is examined by keeping the involved factors as constant, at time 10 minutes, pH 5.0, and 5 mg/L of Pb^{2+} initial concentration. The Pb^{2+} removal capacity is decreased from 47.46 mg/m to 19.704 mg/g after increasing the adsorbent dosage from 5 mg to 12.5 mg and 19.704 mg/g to 12.392 mg/g after increasing the adsorbent dosage from 12.5 mg to 20 mg.

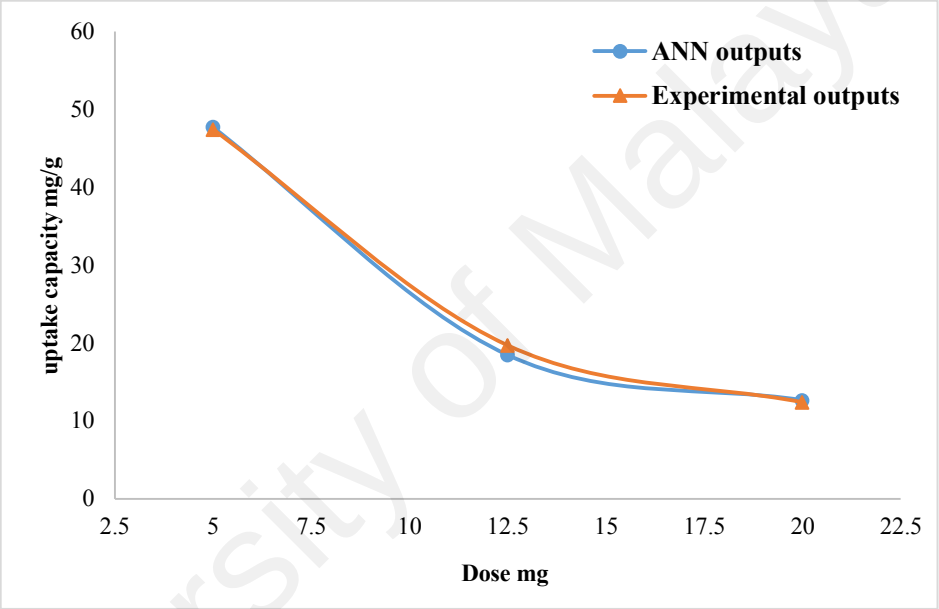

Figure 3. 8: Experimental and ANN output as the function of adsorbent dosage

The decrease in the uptake capacity with increasing in the adsorbent dosage might be attributed to the increase in the adsorbent surface area following in an increase of more active sites (B. Das, Mondal, Bhaumik, & Roy, 2014; M. S. Kumar & Phanikumar, 2013). The ANN technique is used for the modeling and prediction of the obtained data from the experimental work, the prediction results show a good agreement with the experimental result trend. The ANN outputs and the experimental results as the function of adsorbent dosage versus the uptake capacity are presented in Figure 3.8.

3.5.8 The effect of initial concentration

The initial concentration being one of the factors involved in this work, the effect of initial concentration of Pb^{2+} ions is studied by changing the initial concentration from 5 mg/L to 60 mg/L. The other factors were fixed at, time 60 min, pH 2.7 and adsorbent dosage 5 mg. From the presented results in Figure 3.9, it can be seen that the uptake capacity of Pb^{2+} ions at 5 mg/L concentration was 47.7 mg/g whereby after increasing the Pb^{2+} concentration to 60 mg/L the uptake capacity increased to 225.05 mg/g. This might be attributed to the increase in the driving force of the mass transfer which lead to an increase in the uptake capacity of Pb^{2+} ions from water solution.

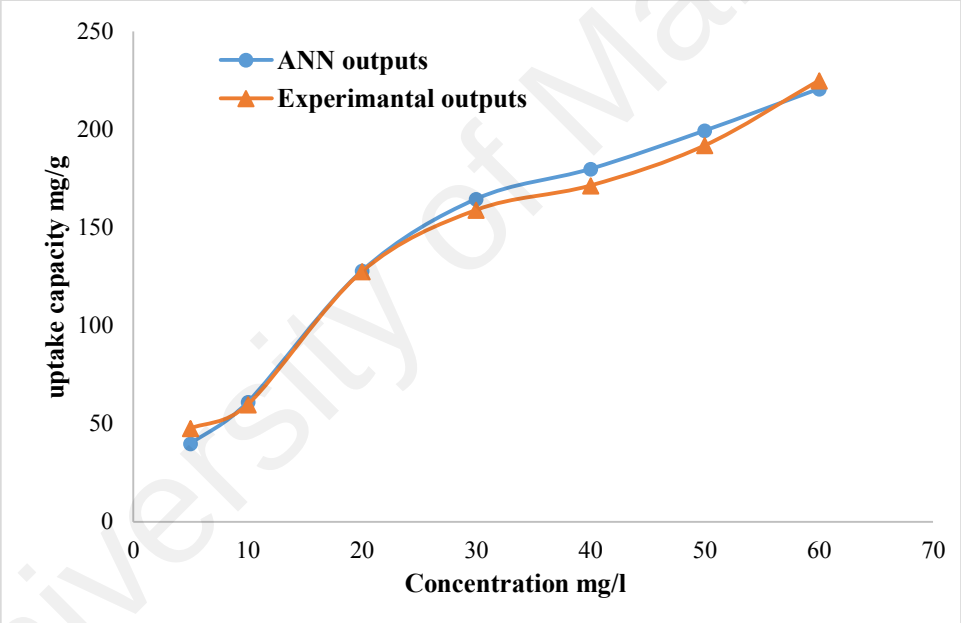

Figure 3. 9: Experimental and ANN output as the function of initial concentration

At low concentration, the Pb^{2+} ions interact at the adsorbent active site whereas at higher Pb^{2+} concentration, the adsorbent active site will be saturated and the removal percentage will be lower (Hamza et al., 2013). The obtained data from the experimental work are trained and predicted by using the ANN modelling techniques. The ANN model

prediction was found to be satisfactory for the experimental data observation. The experimental and predicted output of the ANN are presented in Figure 9.

3.5.9 The effect of contact time

The contact time being one of the involved parameters in the experimental work, the contact time effect is studied with varying the contact time from 5 min to 120 min. The other involved parameters are kept as constant, initial concentration 5 mg/L, adsorbent dosage 5 mg and pH 5.

The uptake capacity at 5 min time is 31.98 mg/g whereby, at 80 min the uptake capacity reached to 48.1 mg/g, the maximum uptake capacity at the equilibrium time is 49.3 mg/g. It is clear from the results presented in Figure10, that 90% removal occurred at 80 min (Nassereldeen A Kabbashi et al., 2009). This is due to the availability of vacant sites at the adsorbent surface hence, the adsorption rate will be higher at the beginning of the reaction. The ANN model was used for the modeling and prediction of the obtained results; it can be seen from Figure 10 that the ANN model predicted the experimental data satisfactorily.

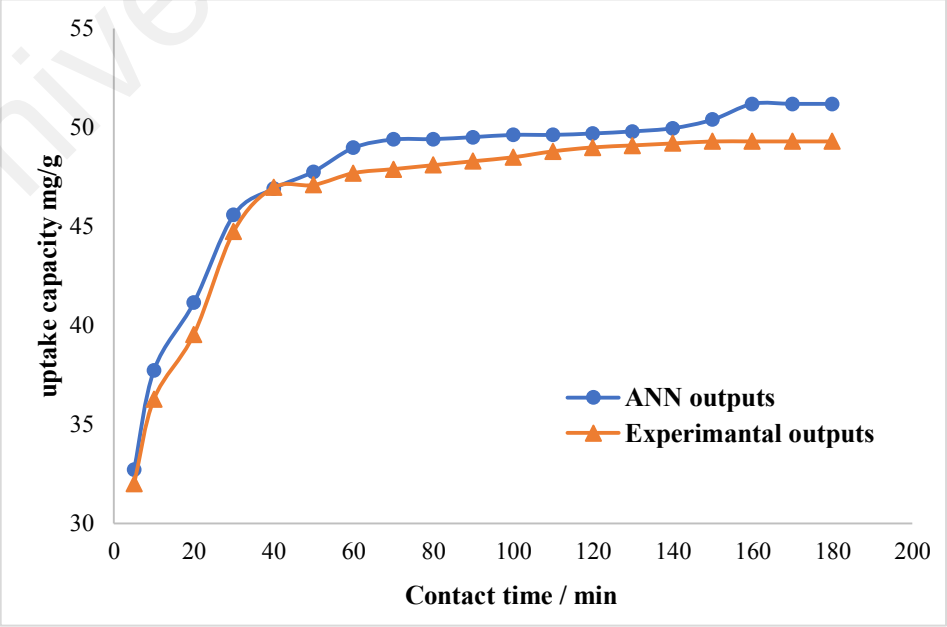

Figure 3. 10: Experimental and ANN output as the function of contact time

3.6 Conclusion

The artificial neural network (ANN) has been successfully used to predict the removal of the Pb^{2+} from aqueous solution by using DES functionalized CNTs. The (tansig) transfer function was used in this study for modeling. Two different neural network types were developed in this work, the (BP-ANN) and (LR-ANN). Both models are created with same aim function and restriction with the same structure of dataset. The optimal topology of ANN was obtained during training phase using (trainbr) algorithm. The results showed that the network with 10 neurons in each hidden layer with three hidden layers, showed the best performance. Moreover, the supervised (multi-layer feed-forward neural network) used in this study.

The (MSE) of the (BP-ANN) model prediction is 1.66×10^{-4} with the (R^2) of 0.9956. The favourable features of the ANN modeling technique was originate to have many criteria such as generalization, efficiency and simplicity, which make it a preferable choice for the modeling of complex systems, such as removal of Pb^{2+} ions from water processes.

CHAPTER 4: LEAD REMOVAL FROM WATER USING DES FUNCTIONALIZED CNTS: ANN MODELING APPROACH

4.1 Introduction

The need for a fresh water is highly important to life. Researchers have reported that heavy metal ions, such as Pb, As, Cr and Cd, have deleterious effects on human life. Metal ions arrive in water resources in different ways from various industries. Several metal ions are poisonous even at low concentrations and can cause harm if they accumulate in a living organism (K. Jiang, Sun, Sun, & Li, 2006; Karnib, Kabbani, Holail, & Olama, 2014; Mendoza-Castillo et al., 2015). Lead elements are typically found in small quantities in the earth's upper layer. Lead generates a variety of diseases and disorders in the human body. Therefore, environmental protection agencies and researchers worldwide are engaged in treating water to remove these ions. The World Health Organization (WHO) recommends 0.01 mg/L as the maximum allowable limit of lead in drinking water (Mazumder et al., 1997). The allowable lead ion concentration in industrial wastewater is 3.0 mg/L (Bahadir, Bakan, Altas, & Buyukgungor, 2007). Various remediation methods have been used to remove heavy metals from aqueous solution, including precipitation (Monique Bissen & Fritz H. Frimmel, 2003), reverse osmosis (Ning, 2002), coagulation (Ratna Kumar, Chaudhari, Khilar, & Mahajan, 2004), oxidation (Thomas M. Gihring, Gregory K. Druschel, R. Blaine McCleskey, Robert J. Hamers, & Jillian F. Banfield, 2001), ion exchange (J. Kim & Benjamin, 2004) and adsorption. The adsorption process has advanced in terms of design simplicity, operation and cost (Tseng, Wu, Wu, & Juang, 2014). The effectiveness of adsorption primarily depends on the selection of an appropriate processing condition, including the mass of sorbent, pH, system temperature and process duration (E. Lourie & Gjengedal, 2011).

Many studies have been performed using various materials as adsorbents to extract metal cations, such as activated carbon (J. P. Chen & Wu, 2004), clay minerals (J. U. K. Oubagaranadin & Z. V. P. Murthy, 2010), biomaterials (V. K. Gupta et al., 2006) and pistachio shells (Yetilmezsoy & Demirel, 2008b). However, these adsorbents have proven unsatisfactory. Researchers have proposed carbon nanotubes (CNTs) as the most effective adsorbents for removing numerous pollutants. Their large surface area and diameter and their shorter equilibrium time compared to other materials contribute to their effective application (Ibrahim et al., 2016). CNTs have been successfully used to extract various heavy metals, for instance chromium, copper, zinc, lead, cadmium, arsenic and mercury (Ihsanullah et al., 2016). However, functionalization is the key to improving the capability of CNTs. Conventional functionalization typically involves harsh acids, non-environmentally friendly chemicals and complicated processes. Thus, the need for environmentally friendly functionalization agents with simple chemical processes is crucial (AlOmar, Alsaadi, Hayyan, Akib, & Hashim, 2016).

Recently, deep eutectic solvents (DESs) have received substantial research interest because of their wide applicability. DESs were first introduced as a low-cost means to replace ionic liquids (ILs). DESs have many advantages over ILs in terms of the availability of the raw martials and their ease of synthesis with minimum environmentally harmful waste (AlOmar, Hayyan, et al., 2016). Therefore, DESs have been adopted in many areas of science. Recently, DESs have been used in several nanotechnology fields as a medium for nanoparticle synthesis (M. H. Chakrabarti et al., 2015; P. H. Chen et al., 2014; Jia et al., 2015; Xu et al., 2016), as electrolytes in nanostructure sensors (Zheng et al., 2014), as electrolytes in nanoparticle deposition (Abbott et al., 2009; C. Gu & J. Tu, 2011; Renjith et al., 2014) and as CNT functionalization agents (AlOmar, Alsaadi, Hayyan, Akib, & Hashim, 2016; AlOmar, Alsaadi, Hayyan, et al., 2017). AlOmar et al. (2016) used choline chloride-based DESs as novel CNT functionalization agents to

prepare a sufficient adsorbent of Pb^{+2} ions. DESs generally consist mainly of hydrogen bond donner (HBD) and salt, both compounds are in solid form at room temperature whereby, their mixture convert as a liquid phase. The melting point of the mixture is less than the melting points of the individual compounds (Abbott, Boothby, et al., 2004). In contrast, DES has several advantages comparing to the conventional ILs such as, diversity of physical properties and different molar ratios and cheaper price of compounds.

The adsorption process is a complicated due to the nonlinear relationship of the involved variables to the adsorption capacity of CNTs. Modeling this type of process is complex when using linear correlation methods. The artificial neural network (ANN) represents an alternative modeling method. ANN is a powerful tool for recognizing the relationships between the inputs and outputs using training process. Because of the expense of the CNTs used in the experiments and the complicated process of preparing the experiments, the ANN modeling method is useful for formulating knowledge, describing the process and extending experimental results. Scaling up from the research facility to the industrial level is simpler when process models are used. In contrast, heuristic models are recommended for collecting information without performing additional experimental research. These kinds of models are designed to recognize the complex, nonlinear relationships between variables and are easier to use.

This study aims to develop useful applicable model using the proposed artificial network system, the feed-forward neural network (FF-NN) and the adaptive neuro-fuzzy inference system (ANFIS) to predict Pb^{2+} ions removal from water using DES-functionalized CNTs, a set of experimental data prepared at a laboratory scale. The performance and efficacy of the FF-NN model are compared to those of the ANFIS model. The sensitivity study of the involved parameters is examined in this research.

Three kinetics models are applied to the predicted results to assess the rate of the adsorption reaction.

4.2 Experiment and methods

4.2.1 Experimental

In a previous study, a novel Pb^{2+} adsorbent was prepared based on pristine CNTs oxidized with $KMnO_4$ and then functionalized by choline chloride: tri ethylene glycol (salt:HBD) 1:2 DES (TEG) (AlOmar, Alsaadi, Hayyan, et al., 2016a). The preparation of the adsorbent was performed in two stages. The primary oxidation involved sonication of pristine-CNTs (P-CNTs) with KMnO4 for 2 h @ 65 °C. Subsequently, the resulting oxidized CNTs (K-CNTs) were sonicated with DES for 3 h @ 65 °C to produce KTEG-CNTs. The adsorbent was comprehensively characterized by observing the RAMAN shift using Raman spectroscopy. The functional groups associated with the functionalization process were analyzed using FT-IR. The surface charge, surface area and surface morphology were investigated using the Zeta potential, BET surface area FESEM and TEM, respectively. The structural phase was also investigated by conducting an XRD profile. Additionally, a batch adsorption study was performed at an ambient condition. The adsorption capacity of KTEG-CNTs was understood as a response to four variables: initial concentration, adsorbent dosage, pH value and contact time. A total of 158 experimental results based on different conditions were used to study the influence of each parameter on the adsorption capacity and the interaction among the parameters.

4.2.2 Artificial neural network (ANN)

The artificial neural network (ANN) has been considered a less complicated model of sophisticated biological networks. An alternative modeling technique, artificial neural network (ANN) has been used to represent the nonlinear function relationship among variables. Artificial neural network (ANN) techniques do not require mathematical

induction since an ANN analyzes examples and recognizes patterns in a series of inputs and outputs of a dataset without prior assumptions regarding their characteristics and interrelations (Sumantra Mandal et al., 2009). The special ability of an ANN to generalize and identify the pattern of any nonlinear, complex development makes it an influential modeling tool. Neural networks can extract complicated data that cannot be observed by a human or a computer technique. Several studies have recently been conducted on water quality prediction models (Chibole, 2013; G. Wu & Xu, 2011). Additionally, research has been performed on; for example, modeling fermentation media optimization (Kiran M. Desai et al., 2008) and modeling a microwave-assisted extraction method (Moghaddam & Khajeh, 2011).

A feed-forward back-propagation neural network (BP-NN) was used in this study as a gradient descent technique to minimize network error. Each layer in the BP-NN has several neurons, and each neuron transmits input values and processes to the next layer. As illustrated in Figure 4.1, the value of the inputs variable is multiplied by the connection weights w_{ii}, which connect the input to the hidden layer. The FF-BP model consists of input layers, hidden layers and one output layer in a multilayer neural network.

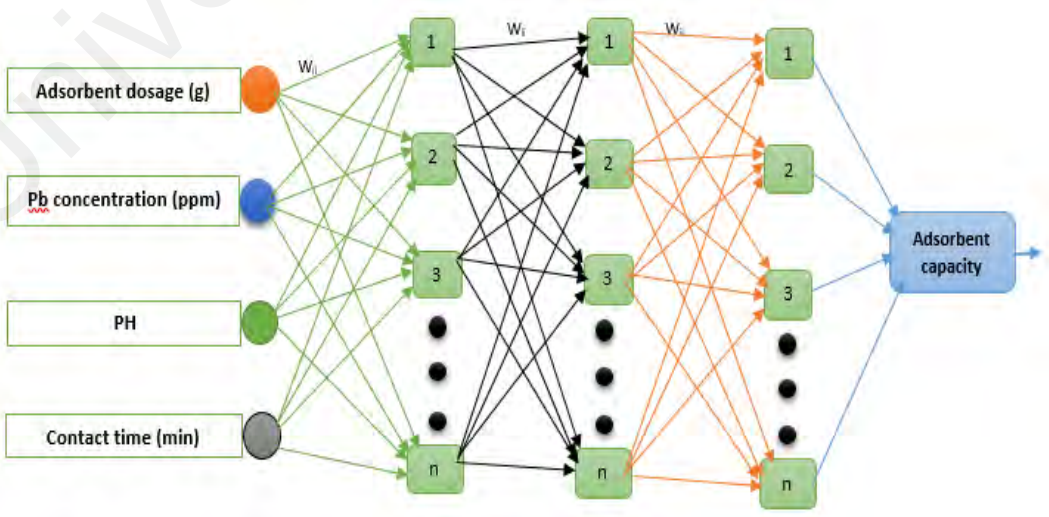

Figure 4. 1: Feed-forward back-propagation neural network structure

Because the FB-NN is a supervisory learning algorithm technique, the method used to select the optimal parameters is to adjust the network weight value (A. H. El-Shafie & El-Manadely, 2011). "Optimal" refers to the difference between target values or actual values t_k and the network output z_k that achieves the minimum or the target such that:

$$E = \frac{1}{2}\sum_{k=1}^{k}(z_k - t_k)^2 \tag{4.1}$$

Here, z_k = ANN output, and t_k is the target output T. The training process is a procedure whereby, the ANN connecting weights are modified by a continuous procedure of stimulation on the condition that the network is fixed.

The input data are normalized in a range of 0 to 1 to avoid over-fitting of the network. It is realized that all the units of a similar layer do not connect with one another. The connections among the developed layers can be expressed by the coefficient of weight (A. El-Shafie et al., 2007).

The weighted signals and bias from the input neurons are summed by the hidden neurons and then projected through the transfer function. In the BP-NN algorithm, the inputs are forwarded into the network until the end of the network. The output is initiated and compared to the target value. Finally, the error is calculated (Hemmat Esfe et al., 2015; Kurt & Kayfeci, 2009).

Back-propagation learning is used to create the relationship between the target outputs and the input data, which are typically assigned with a random initial weight and later updated by comparing the results of the actual values with the target values. In the diverse research that uses neural computations, different transfer functions are used depending on the problem nonlinearity and data complexity to design a proper network.

4.2.3 ANFIS Architecture and Development

The adaptive neuro-fuzzy inference system (ANFIS) technique is a feed-forward multilayer network that uses fuzzy logic and a neural network learning system to format the input data space to the output data space. The ANFIS learning system consists of five layers, each layer consists of several nodes, and a node is defined by its function. The squares identify the adaptive nodes, which signify the sets of parameters that are modifiable in the nodes. The circles signify the fixed nodes, which represent the sets of parameters that are immovable in the system. The output from the past layer becomes the information of the following layer. There are two types of fuzzy inference systems (FISs); the Assilian and Mamdani type (1975) and the Sugeno and Takagi type (1985). The consequence parameter definition is an important difference between the two FISs. The results parameter in the Sugeno FIS is either a constant coefficient (Jang et al., 1997) (i.e., the zero-order Sugeno FIS) or a linear equation (i.e., the first-order Sugeno FIS).

The procedures of the ANFIS can be summarized to assist comprehension. It is considered that the system contains four inputs, i.e., contact time (T), concentration of Pb^{+2} (C), pH (PH) and adsorbent dosage (AD), and one output removal efficiency (Q). The rule base consists of four fuzzy if-then rules. The four rules can be written as follows:

Rule 1:

If AD is A_1*, C is* B_1*, PH is* C_1 *and T is* D_1*,*

then $f1 = p_1 \times AD + q_1 \times C + s_1 \times PH + m_1 \times T + g_1$

Rule 2:

If AD is A2, C is B2, PH is C2 and T is D2,

then $f_2 = p_2 \times AD + q_2 \times C + s_2 \times PH + m_2 \times T + g_2$

Where q_i, p_i, s_i, m_i and g_i (i = 1,2,3…) are considered the linear parameters in the consequential part of the Sugeno fuzzy system. The ANFIS constriction is illustrated in Figure 4.2, and the ANFIS model description is as follows:

Layer 1: the input node. The input node of the first layer produces the membership grades for the input and output O_{i1}, which is calculated by the following:

$$Oi1 = \mu A_i(AD)\ (i = 1, 2) \quad (4.2)$$

$$Oi1 = \mu B_{i-2}(C)\ (i = 3, 4) \quad (4.3)$$

$$Oi1 = \mu C_{i-4}(pH)\ (i = 5, 6) \quad (4.4)$$

$$Oi1 = \mu D_{i-6}(T)\ (i = 7, 8) \quad (4.5)$$

Where AD, C, pH and T are the inputs to node I, and A_i, B_i, C_i and D_i are the linguistic labels categorized by the appropriate membership functions (m_{fs}) μAi, μBi, μCi and μDi, respectively.

Layer 2: the node rules. The layer outputs, termed firing strengths O_{i2}, are the corresponding degrees transferred from the previous layer output (Layer 1).

$$O_{i2} = wi = \mu A_i(AD)\mu B_i(C)\ \mu C_i(pH)\ \mu D_i(T),\ (i = 1, 2, 3....) \quad (4.6)$$

Layer 3: the nodes average. The purpose of the third layer is to compute the ratios of all the i_{th} rules' firing strengths to sum the firing strength of the rules. Accordingly, $\overline{w}$ i is considered a regularized firing strength.

$$O_{i3} = \overline{w} = \frac{w_i}{\sum_i w_i} \quad (4.7)$$

Layer 4: the resulting node. At this layer, the node function calculates the contribution of all the ith rules and transfers the summed contribution to the total output. The function can be written as follows:

$$O_{i4} = \overline{w}_i f_i = \overline{w}_i (p_i \times AD + q_i \times C + s_i \times pH + m_i \times T + g_i),\ i = 1, 2 \quad (4.8)$$

Where $\overline{w}_i$ denotes the Layer 3 output, whereby (p_i, q_i, s_i, mi and g_i) are the parameter set. The parameters in this layer are stated as the consequent parameters.

Layer 5: the output node. This layer is the output layer. It calculates the total output by adding all the received indications. Therefore, a de-fuzzification procedure converts all the fuzzy rules outcomes into a crisp output.

$$O_{i5} = Q\sum_i \overline{w}_i f_i = \frac{\sum_i w_i f_i}{\sum_i w_i} \quad (4.9)$$

There is no limited rule designed for constructing the ANFIS system. However, a common context can be constructed based on earlier successful engineering applications. The ANFIS target is to specify and simplify the form relationship.

$$Y = f(X_1, X_2, \cdots, X_n) \quad (4.10)$$

Where Y is the variable of output and $X_1, X_2, ..., X_n$ are the input variables. In this paper, the removal capacity (Q) can be distinguished as the function of AD, C, PH and T. The input and the output (i.e., removal efficiency) relationship can be written as follows:

$$Q = f(AD, C, PH, T) \quad (4.11)$$

The utilized data are divided into three sets. The first one is the training set. Most of the data are used in this section to train the ANFIS. The second set is a checking set and used to verify the defined ANFIS, which prevents over-fitting the network. The third set is the testing set, which is used to ascertain model accuracy and performance. In this study, 158 experimental results are used, which were divided as follows: 73 % for training, 12 % for checking and 15 % for testing.

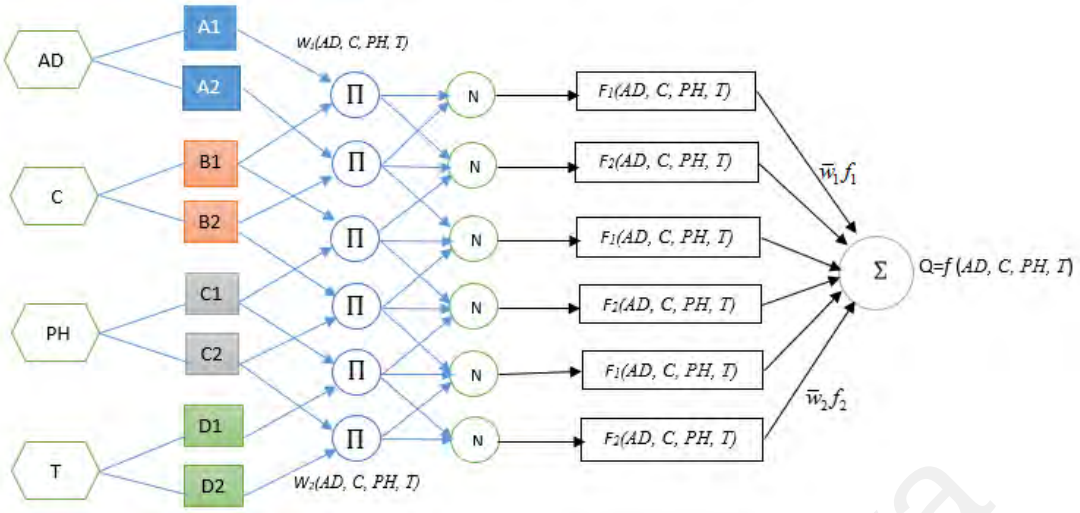

Figure 4. 2: Architecture of ANFIS

4.2.4 Model Evaluation Indicators

Two competing neural networks were developed. For the modeling in this study, the ANFIS and the FF-NN were used, an assessment of multi-criteria was performed. The performance of the ANFIS and FF-NN models was determined by comparing the actual data with the simulated dataset. The behavior of each model was examined employing the root mean square error (RMSE), relative error (RE), mean square error (MSE), relative root mean square error (RRMSE) and the mean absolute percentage error (MAPE). The formulas used to calculate these indicators are as follows:

$$MSE = \frac{1}{n}\sum_{i=1}^{n}\left(D_{a(t)} - D_{f(t)}\right)^2 \tag{4.12}$$

$$RMSE = \left[\frac{1}{n}\sum_{t=1}^{n}\left(D_{a(t)} - D_{f(t)}\right)^2\right]^{\frac{1}{2}} \tag{4.13}$$

$$RRMSE = \left[\frac{1}{n}\sum_{t=1}^{n}\left(\frac{D_{a(t)} - D_{f(t)}}{D_{a(t)}}\right)^2\right]^{\frac{1}{2}} \tag{4.14}$$

$$MAPE = \frac{1}{n}\sum_{t=1}^{n}\left|\frac{\left(D_{a(t)} - D_{f(t)}\right)}{D_{a(t)}}\right| \times 100 \tag{4.15}$$

$$RE = \frac{D_{a(t)} - D_{f(t)}}{D_{a(t)}} \times 100 \tag{4.16}$$

Where;

$D_{a(t)}$ = the actual value.

$D_{f(t)}$ = the simulated value.

Generally, MSE, RMSE, RE, MAPE and RRMSE equations were selected to indicate model performance, which was based on the result obtained by comparing the evaluated error of the actual and simulated results. The best model is considered the model with the smallest error.

4.3 Results and discussion

In this study, two modeling systems were used: the FF-NN and ANFIS systems. Various indicators were used to evaluate the two proposed methods. A comparison of the two methods was performed. Based on the comparison, the best model was adopted for a sensitivity study that used all the parameters involved in the experimental research: pH, adsorbent dosage and initial concentration. In addition, the adsorption rate was investigated using three kinetics models.

4.3.1 ANFIS versus FF-NN Performance

The feed-forward neural network (FF-NN) and the adaptive neuro-fuzzy inference system (ANFIS) modeling techniques presented in the methods section were used for the modeling in this study. “Accuracy” was defined as how closely a predicted value matches an actual value, whereas “precision” referred to how closely predicted values match one another. It was clear that the ANFIS model performed better than the FF-NN model according to the following indicators: MSE, RMSE, RRMSE and MAPE. The goal of the

training section was to decrease the error function by creating a range of connection and initial values to help the network achieve an output nearly equal to the target values.

The FF-NN was trained using the Bayesian regularization (TRAINBR) algorithm, which is considered the fastest algorithm in the MATLAB toolbox and is recommended as the best choice for the supervised algorithm. Additionally, it does not require a large memory compared to other algorithms. The optimum neuron number in each hidden layer was recognized by trial and error by changing the number of neurons in the hidden layer from 2 to 20. Moreover, the number in the hidden layers of the model was identified by trial and error to determine the optimal network structure. The optimum model architecture was identified based on the minimum values of the MSE. Therefore, the optimal network structure contains 4 inputs, 15 neurons in each hidden layer with 3 hidden layers Figure 4.1, and one output. Figure 4.3 compares the data obtained using the FF-NN with the experimental data. The figure shows a good compatibility between the experimental and predicted data.

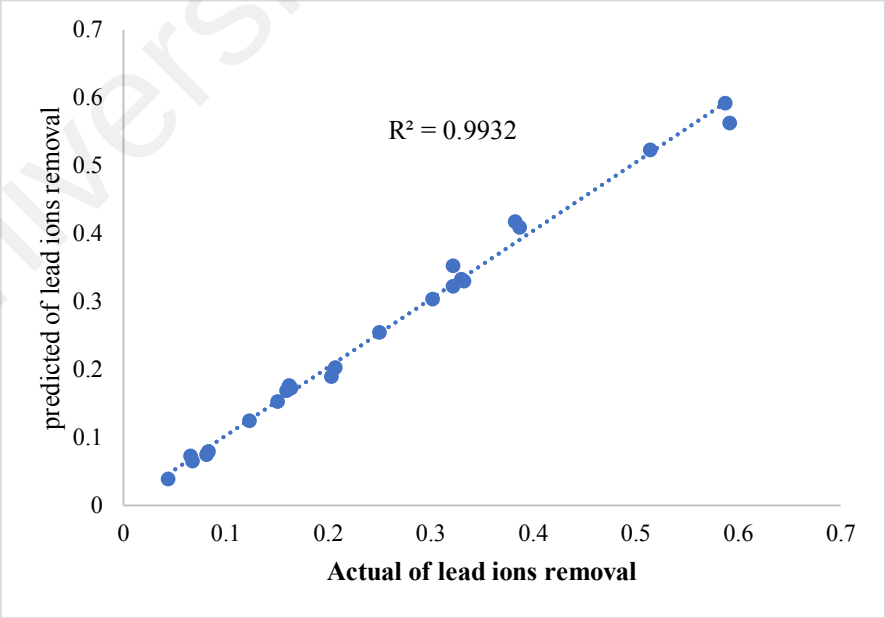

Figure 4. 3: The R^2 of ANN

Selecting the optimal network structure is the most significant problem in ANFIS training. The ANFIS structure consists of five layers Figure 2. The optimum architecture of the ANFIS system was identified based on the minimum values of testing-set error. Using the membership function for the input and linear type, which is applied for the output while generating the FIS, the optimal method was identified. As presented in Table 4.1, the minimum testing error obtained for the ANFIS model was 6.14×10^{-5} (MSE). Consequently, the ANFIS model system with a linear output MF type, 3 MFs for the input, gbellmf as MF type and 100 epochs was designated the optimal model structure. To verify its accuracy, the ANFIS model was used to simulate 22 results, which were not used in the training or validation procedures. The comparison between the actual and predicted data is presented in Figure 4.4.

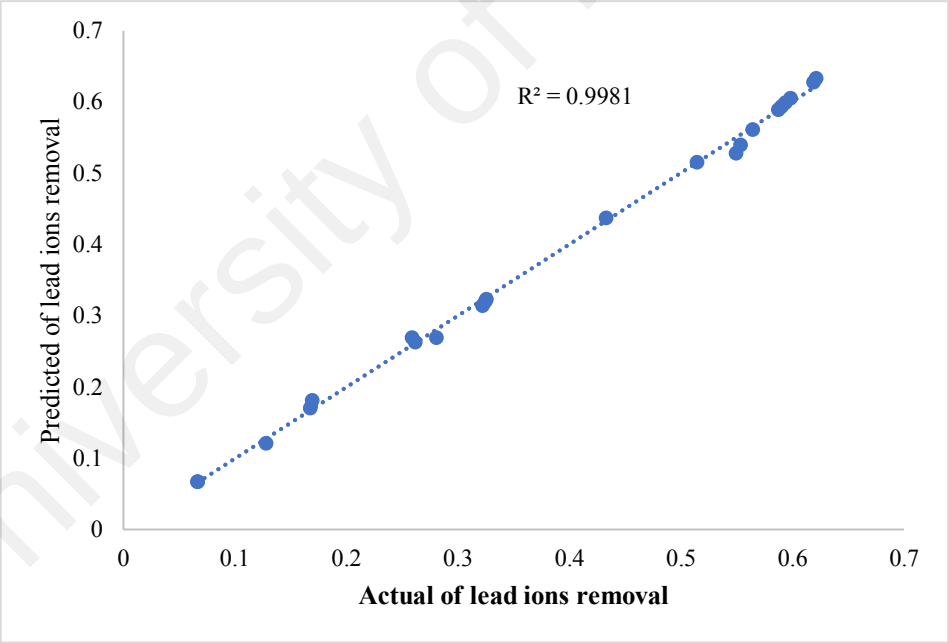

Figure 4. 4: The R^2 of ANFIS

The determination coefficient for the testing dataset R^2 is 0.9981, which indicates a superior performance of ANFIS model compared to the FF-NN model. The data scatter is nearly along a 45° line, which indicates the superior performance of the ANFIS model.

Regarding to the MSE values for the ANFIS and FF-NN models listed in Table 4.1, the MSE of ANFIS was 6.14×10^{-5}.

Table 4. 1: Evaluation indicators

	ANFIS	FFNN
MSE	6.14×10^{-5}	1.86×10-4
RMSE	6.47×10^{-3}	1.36×10^{-2}
RRMSE	5.91×10^{-3}	5.74×10^{-2}
MAPE	2.02	4.53

This outcome is a practical value and reflects accuracy and high efficacy compared to the MSE of the FF-NN, which was 1.86 10^{-4}. The ANFIS model can be used to simulate the connection between the input variables and thus to investigate the adsorbent capacity of a functionalized carbon nanotube. The MAPE value for the ANFIS model was 2.02 %. In contrast, the MAPE value for the FF-NN model was 4.53 %. This outcome demonstrates that the ANFIS model is more accurate than the FF-NN model. Additionally, the ANFIS model produced RMSE and RRMSE values of 6.47×10^{-3} and 5.91×10^{-3}; respectively, whereas the FF-NN results were 1.36×10^{-2} and 5.74×10^{-2}, respectively. Consequently, these criteria confirm that the ANFIS model performed better than the FF-NN model. Relative error is an error indicator in modeling prediction. It compares actual values to predicted values.

Figure 4.5 shows the relative error percentages for the ANFIS and FF-NN models. A total of 22 results were used for both models to test their accuracy. The maximum error value for the FF-NN model was 11.62 % as opposed to 7.07 % for the ANFIS model.

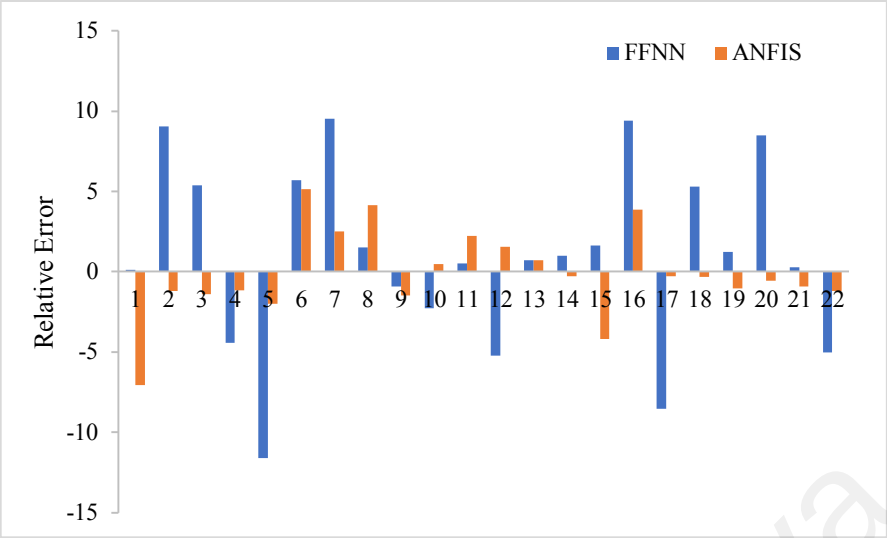

Figure 4. 5: Illustrates the accuracy of the hybrid model

The results were calculated using equation (16) and indicate that the ANFIS model is more accurate than the FF-NN model. This outcome demonstrates the reliability and effectiveness of the proposed approach to extracting features from input data. The hybrid ANFIS model can provide perfect prediction of KTEG-CNTs as a Pb^{2+} absorber from water. The ANFIS model was used for the sensitivity analysis.

4.3.2 Sensitivity analysis

4.3.2.1 pH study

The pH is one of the most influential factors in the adsorption process. It affects the interactions between the adsorbent surface and Pb^{2+} ions. In addition, pH influences the quantity and the adsorbent surface-active sites. It also affects the solubility of metals ions in solution (Salisu et al., 2016). Here, the effect of pH on the adsorption process is determined using 12.5 mg of adsorbent dosage to remove 5 mg/L of Pb^{2+} from contaminated water at 5 minutes' contact time. The pH value ranged from 1 to 10. Based on the results shown in Figure 6, by increasing the pH values, the adsorption capacity

increases to pH 5. Additionally, by increasing the pH to 6, the adsorption capacity remains nearly steady.

At a pH higher than 7.0, the adsorption capacity is increased when the dominant species of Pb^{2+} are $Pb(OH)^{+}$ and $Pb(OH)_2$. This complexation might be caused by the extensive presence of OH- at this pH level, which results in precipitation (V. K. Gupta et al., 2011).

Additionally, the adsorbent active sites affect the adsorption process, where by increasing the pH, the presence of H^{+} decreases because of the extensive presence of OH^{-}, which plays a significant role in consuming the H^{+}. As a result, the competition on the adsorbent active sites decreases, and the adsorption capacity increases. The agreement of the ANFIS model predictions as a function of pH is presented in Figure 4.6. It can be noted that the results obtained using the proposed ANFIS model indicate nearly the same behavior as the experimental data. This outcome demonstrates the accuracy of the proposed model.

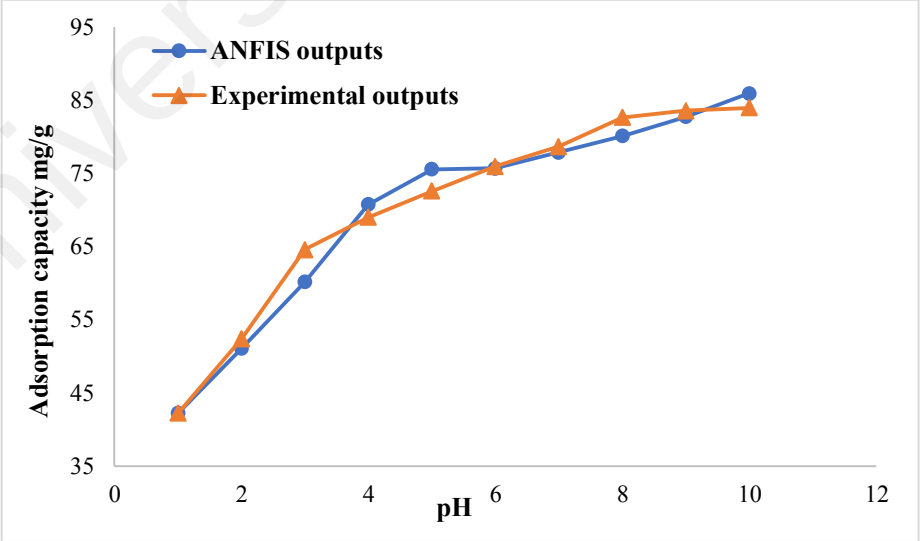

Figure 4. 6: Agreement between ANFIS outputs and Experimental outputs with various pH values

4.3.2.2 Initial concentration study

The effect of the initial concentration on the adsorption capacity was investigated by varying the initial concentration of lead from 5 to 60 mg/L. The initial concentration effect was examined at 2.7 pH, a 15-min contact time and a 5-mg adsorbent dosage. The initial concentration of lead increased from 5 to 10 mg/L, and the uptake capacity increased from 32.48 to 49.57 mg/g, whereas by increasing the initial concentration from 10 to 20 mg/L, the uptake capacity increased from 49.75 to 101.05 mg/g. This outcome might be attributed to the increase in the driving force of the mass transfer, which resulted in an increase in the quantity of Pb^{2+} adsorbed from water solution. At low concentration, Pb^{2+} interacts at the adsorbent active sites, whereas at a higher Pb^{2+} concentration, the adsorbent active sites are saturated, and the removal percentage is lower (Banerjee, Sarkar, & Banerjee, 2016). The data obtained from the experimental research were trained and predicted using ANFIS modeling. The ANFIS model prediction was found satisfactory for the experimental data. The experimental and predicted outputs of the ANFIS are presented in Figure 4.7.

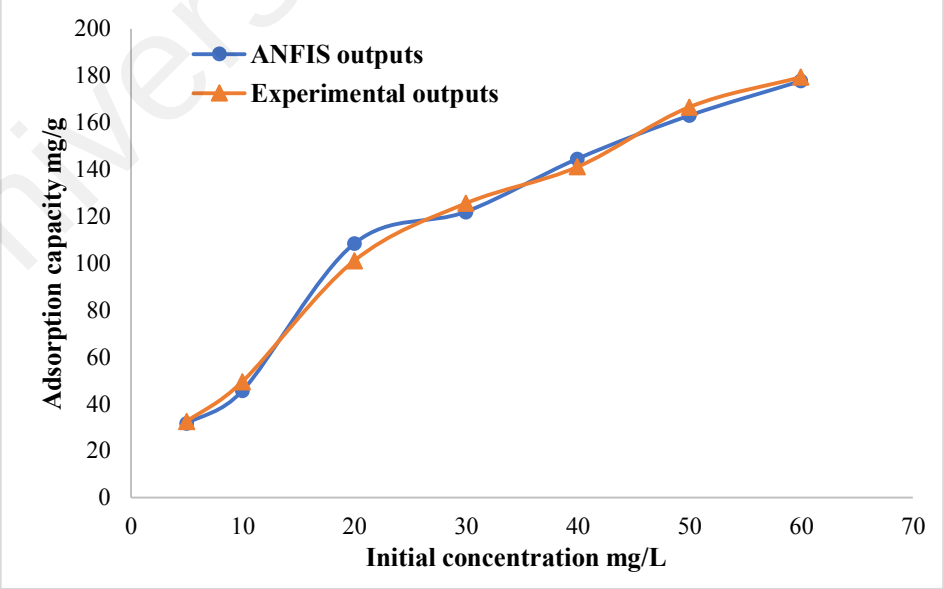

Figure 4. 7: Experimental and ANFIS output as the function of initial concentration

4.3.2.3 Adsorbent dosage study

Adsorbent dosage is an important factor involved in the adsorption process. The effect of the adsorbent dosage on Pb^{2+} removal was examined at pH 3.0, an initial concentration of 20 mg/L of Pb^{2+} and a contact time of 15 min. The KTEG-CNTs adsorption capacity decreased from 123.94 mg/g to 76.292 mg/g when the adsorbent dosage was increased from 5 mg to 12.5 mg. It decreased from 44.425 mg/g to 23.584 mg/g when the adsorbent dosage was increased from 20 mg to 30 mg. The decrease in the uptake capacity accompanied by the increase in the adsorbent dosage might be attributed to increasing the adsorbent surface area following an increase in the number of active sites (B. Das et al., 2014). The data obtained from the experiment were trained and predicted using the ANFIS model. The ANFIS model prediction was found satisfactory for the experimental data. The experimental and predicted output of the ANFIS are presented in Figure 4.8.

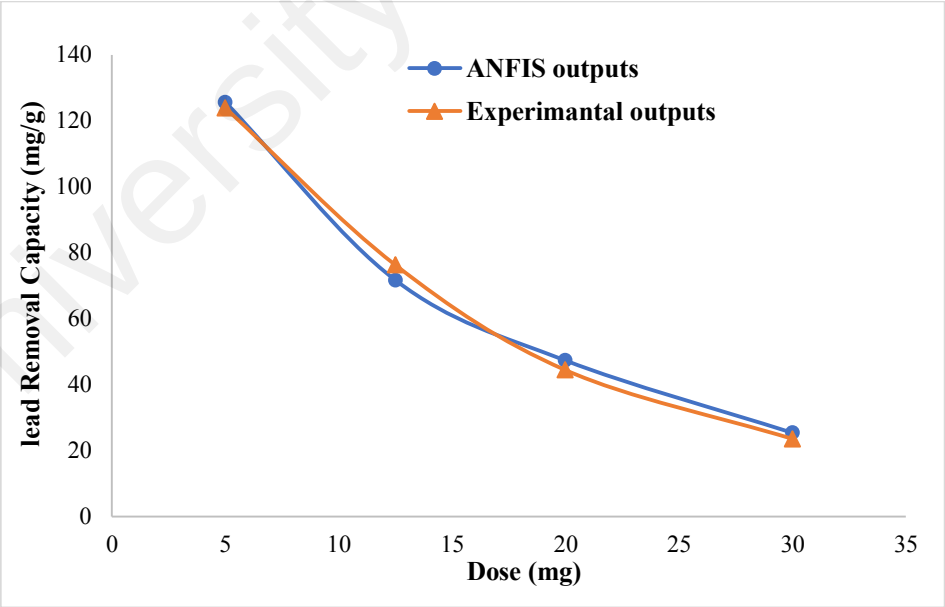

Figure 4. 8: Experimental and ANFIS output as the function of adsorbent dosage

4.3.2.4 Adsorption kinetics study

It is important to determine the kinetics of the adsorption reaction rates of any adsorption system. In this study, three kinetic models were used (i.e., pseudo-first-order, pseudo-second-order and intraparticle diffusion models) to investigate the mechanism and rate of the adsorption process. The kinetic study was performed at three initial concentrations (C_0 mg/L) values of 8, 12 and 18 mg/L and an adsorbent dosage of 5 mg. pH and contact time were regarded as variable. pH is one of the most influential factors in the adsorption process. Therefore, three pH values were used: 2.7, 6 and 8.

The adsorption kinetics for lead ion removal from water by KTEG-CNTs was studied applying the proposed ANFIS model to determine the adsorption rate and to confirm the accuracy and usability of the proposed ANFIS model. Table 4.2 presents the results for the three models that were used.

Table 4. 2: Adsorption kinetics and correlation coefficient

		Pseudo-first-order $ln(q_e–q_t)$ *vs time (t)*	Pseudo-second-order $(t/q_t$ *vs t)*	Intraparticle $(q_t$ *vs* $t^{0.5})$
PH	C_0 mg/L	R^2	R^2	R^2
2.7	8	0.972	0.998	0.861
2.7	12	0.226	0.990	0.956
2.7	18	0.679	0.991	0.951
6	8	0.524	0.995	0.982
6	12	0.946	0.998	0.994
6	18	0.888	0.999	0.986
8	8	0.433	0.997	0.861
8	12	0.753	0.999	0.956
8	18	0.707	0.999	0.951

The correlation coefficient (R^2) for the pseudo-first-order model was in the range of 0.226 to 0.972. However, for the pseudo-second-order model, it was in the range of 0.990 to 0.999, and for the intraparticle diffusion model, it was in the range of 0.861 to 0.994. Based on these results, the adsorption data were described well by the pseudo-second-order model. The model outcome for the simulated data resembles the model outcome for the experimental data (AlOmar, Alsaadi, Hayyan, et al., 2016a). Figure 9 a, b and c shows the pseudo-second-order kinetic model with different values of pH and initial concentration. It is obvious from Figure 4.9 that by increasing the initial concentration of Pb^{2+} the value of (t/q) is decreased. That is, the metal uptake capacity is proportional to the initial concentration, which is the driving force for mass transfer (Geetha et al., 2015).

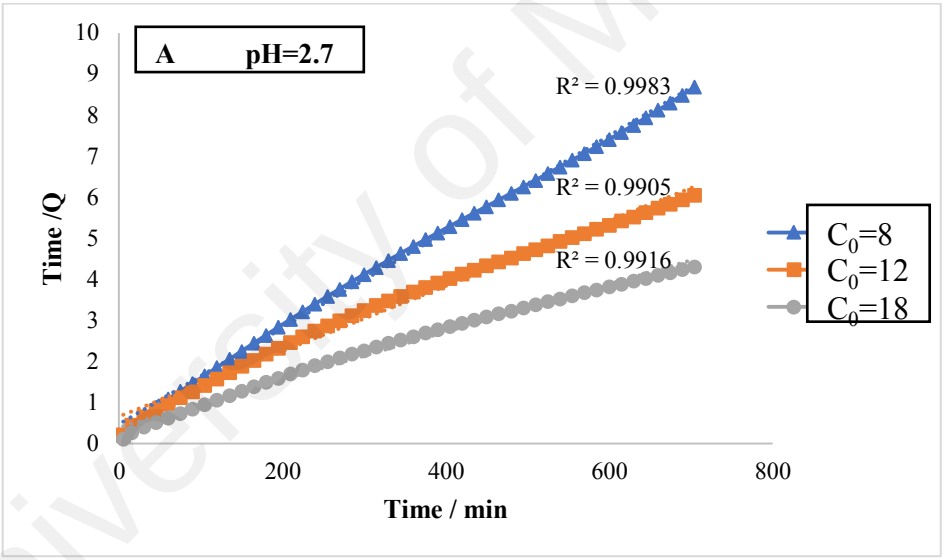

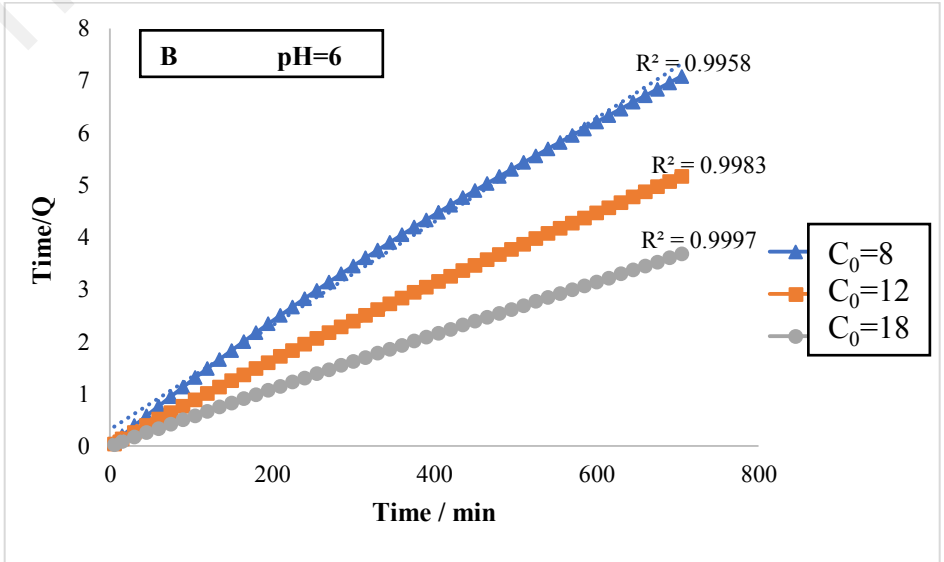

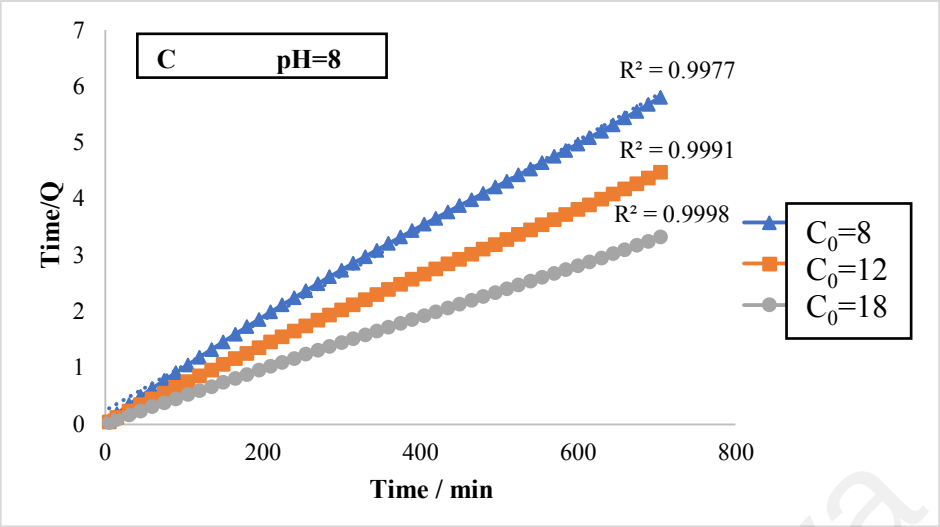

Figure 4. 9: Pseudo-second-order adsorption kinetics at different pH and initial concentrations

4.4 Conclusion

FF-NN and ANFIS techniques were successfully used to predict the removal of Pb^{2+} from an aqueous solution using DES-functionalized CNTs. The effect of various pH values on the adsorption of lead ions from water was investigated. A kinetics study was performed using different values of initial concentration and various pH values. Three different kinetics models were used to study the adsorption reaction rate. The pseudo-second-order kinetics model described the adsorption data sufficiently. The development of the two systems was such that we could obtain the optimal topology of both models during the training section. The models were created with the same purpose and their performance was compared. The performance of the ANFIS model was better than that of the FF-NN model in terms of accuracy. The ANFIS model was found to perform excellently in the prediction of the adsorption capacity of lead ions.

The prediction value of the ANFIS model was close to the real values: $R^2 = 0.998$, MSE = 6.14×10^{-5}, RMSE = 6.47×10^{-3}, RRMSE = 5.91×10^{-3} and MAPE = 2.02. This outcome indicates that the ANFIS system can model the adsorption capacity of lead ions

using DES-functionalized CNTs. One benefit of the proposed modeling technique is its simplification of the process used by researchers to recognize the significant effect of each parameter involved in removal efficiency.

CHAPTER 5: THE MODELLING OF ARSENIC REMOVAL FROM WATER BY DEEP EUTECTIC SOLVENTS FUNCTIONALIZED CNTS: ARTIFICIAL NEURAL NETWORK (ANN) APPROACH

5.1 Introduction

Arsenic is one of the extensively distributed metals in nature in water, soil and air. The water pollution arises due to the change of the environmental condition and industrial activities that brings significant consideration of specialists on its remediation skills. An earlier study demonstrates that ten millions of individuals are comprehensively exposed to poisonous substantial metals per day (Briggs, 2003). Arsenic is one of the most poisonous heavy metals and its availability in water makes the water not desirable for drinking. The accumulation of arsenic can affect the human health such as kidney, blood cell, lesion of skin, lung, brain, stomach and even cancer (Cheng, Fu, Dionysiou, & Tang, 2016; Hung, Nekrassova, & Compton, 2004; Sharma & Sohn, 2009). Therefore, the world health organization (WHO) determined the maximum allowable arsenic amount at the drinking water is 0.01 mg/l (G. Liu, Zhang, Talley, Neal, & Wang, 2008). Different techniques have been used for the removal of arsenic from water such as ion exchange (An, Liang, & Zhao, 2011), oxidation-precipitation (Tresintsi, Simeonidis, Vourlias, Stavropoulos, & Mitrakas, 2012), coagulation and filtration (Baskan & Pala, 2010) and adsorption (Pattanayak, Mondal, Mathew, & Lalvani, 2000). However, the performance of these techniques are not sufficient enough; therefore, the need for a new method is vitally important. Nevertheless, the adsorption method gained a high interest and considered as one of the most appropriate methods due to the ability of removing a small amount of heavy metals from a large amount of water solution. The effectiveness of adsorption is majorly dependent on the selection of appropriate process condition, including the mass of sorbent, pH, system temperature and the process duration (E. Lourie & Gjengedal, 2011). Several studies have been done by using different type of

materials to remove the arsenic ions from water for example, clay minerals (J. U. K. Oubagaranadin & Z. Murthy, 2010), activated carbon (J. P. Chen & S. Wu, 2004) and biomaterials (V. Gupta, A. Rastogi, V. Saini, & N. Jain, 2006). However, the use of traditional adsorbents have a drawbacks such as small adsorption capacity and low adsorption efficiency (Rao et al., 2007). Consequently, the need for the high efficient adsorbents is necessary to remove the arsenic ions from water solution. Therefore, researchers work on finding a new promising material. Carbon nanotube (CNTs) have different properties which make it convenient to several applications in electronics, optics, water treatment, nanotechnology and some of material science fields (Atieh et al., 2011). The nanoparticle is used as the most effectual adsorbent material for the removal of several pollutants, due to their special features such as, catalytic potential, large surface area, small size and high reactivity (Ali, 2012). The most and effective material used in the water treatment field is carbon nanotube (CNTs) for the removal of several types of pollutants (Abbas et al., 2016; Ibrahim et al., 2016). However, there are some limitations in the CNTs application due to various flaws in solubility, difficulty in manipulation, and aggregation. In contrast, CNTs have a great property by interaction with other compounds and have a greater interaction after surface functionalization (Thostenson, Ren, & Chou, 2001).

The oxidative functionalization of CNTs surface can increase the surface charge of CNTs, and this need to use a strong acid which is environmentally harmful. Therefore, finding a new kind and environmentally friendly material is crucial for the new application development(Hayyan, Abo-Hamad, et al., 2015; Martinez et al., 2003).

The deep eutectic solvents (DESs) is one of the ionic liquid analogues which is presented by Abbot et al. in 2003 (Abbott et al., 2003) as a cheaper replacement for developed ionic liquids (ILs). Generally, DESs made up from two or more compounds.

Deep eutectic solvents (DESs) are identified as liquid combination formed by the complexation of hydrogen bond acceptors (HBA) and hydrogen bond donors (HBD) (Abbott, Boothby, et al., 2004; Gorke et al., 2008). The malting point of the mixed compounds are lesser than the individual compound (Abbott, Boothby, et al., 2004). In contrast, DES has several advantages comparing to the conventional ILs such as, diversity of physical properties and different molar ratios, easy to synthesis and cheaper price of compounds. Recently, DESs were reported in many applications; examples of such are the uses of ChCL-based DES as a functional additive for starch-based plastics (Leroy et al., 2012), the synthesis of zeolite analogues (Cooper et al., 2004), mediums for the deposition of specific metals in electro and electroless plating of metals (Abbott, Capper, McKenzie, & Ryder, 2007; Abbott et al., 2008). And most recently, in nanotechnology applications (Abo-Hamad, Hayyan, AlSaadi, & Hashim, 2015).

The adsorption process is complicated due to many variables involved which can affect the adsorption efficiency. The conventional linear method for modelling of this kinds of processes is difficult, artificial neural network (ANN) techniques is the alternative for mapping the nonlinear relationship between variables and output professionally, can identify and reproduce non-linear relationship between inputs during training procedure in various input-output schemes (Giri, Patel, & Mahapatra, 2011). Recently, ANNs technique are used for various engineering applications. ANNs consist of a massive parallel architecture which can solve the complicated problems by the assistance of highly connected neurons organised in layers. ANN considered as a powerful tool in identifying the relationships between the parameters especially at the non-linear and complex relationships. Experiments have been successfully performed to use ANN to model the adsorption of arsenic (K. H. Cho, Sthiannopkao, Pachepsky, Kim, & Kim, 2011; Giri et al., 2011; Podder & Majumder, 2016).

5.1.1 Problem Statement

The use of the conventional ionic liquids (ILs) is considered as environmentally harmful due to the use of strong acids and higher cost comparing to the deep eutectic solvent (DES). The use of DES has many advantages over ILs such as the diversity of physical properties and easy to synthesis. In general, the adsorption process is complicated due to the effect of many variables involved in the process, due to that the use of ANN techniques can recognize the relationship between variables such as adsorbent dosage, concentration of the heavy metals, pH and contact time. Artificial intelligence (AI) process is powerful technique that has been used successfully for the engineering applications since decreases the required time and cost for the experimental work. The advantages of the modeling techniques are formulating the knowledge, describing the process and extending the experimental results.

5.1.2 Objective

One hydrogen bond donor (HBD) which is glycerol (Gly) and one type of phosphonium based salts are used which is methyltriphennylos phosphonium bromide (MTPB) to prepare the DES, the salts is mixed with (Gly) to produce the DESs. Therefore, the CNTs were pre-oxidized with $KMnO_4$ and subsequently functionalized by the synthesized DESs. The functionalized CNTs are used to remove the As^{3+} from water. Four variables will be considered during the experimental work such as, adsorbent dosage, heavy metal concentration, pH and processing time.

The artificial neural network (ANN) modeling technique will be used in this study to create an ANN model to establish the relationship that exists between the variables, and to predict the adsorption capacity of the DES-CNTs for As^{3+} removal from water solution based on the experimental data set prepared in the lab scale.

5.2 Experimental and methodology

5.2.1 Chemicals and materials

The materials used in the experimental work are multi-wall carbon nanotube (MWCNTs) with specification of D 6-9 nm ×L5 μm, >95% carbon, potassium permanganate ($KMnO_4$), Gly, hydrochloric acid (36.5-38%), and sodium hydroxide pellets were all provided by SIGMAALDRICH. The arsenic standard solution of 1000 mg/L and MTPB with >99% purity were provided by Merck, Germany.

5.2.2 Synthesis of DESs

The synthesising of DES was the result of stirring a mixture of Gly and MTPB at molar ratio of 3:1 HBD: salt at 400 rpm and temperature of 80 ºC. The mixing time was 3 h until the DES turn into homogenous mixture without precipitation (AlOmar, Hayyan, et al., 2016). The produced DES will be referred as (m) in this study. The prepared DES is kept in controlled environment to avoid the effect of the humidity.

5.2.3 Functionalization of MWCNTs by M-DES

After drying the pristine MWCNTs (P-CNTs) at 100 ºC overnight. 7 ml of $KMnO_4$ was added to 200 mg of P-CNTs and sonicated for 2 h at 65 ºC to produce K-CNTs (AlSaadi, Al Mamun, Alam, Amosa, & Atieh, 2016). The functionalization by m-DES was conducted by mixing 200 mg of K-CNTs with 7 ml of m-DES under sonication for 3 h at 65 ºC to produced mK-CNTs. Later, a filtration process was performed by washing the functionalized CNT using distilled water and filtered by PTFE 0.45 μm membrane until the pH of the filtered water reached neutral.

5.2.4 Characterization of functionalized CNTs

The characterization of the P-CNTs, K-CNTs and mK-CNTs adsorbent was done by using Fourier transform infrared (FTIR) to recognize the surface modification. The

Raman spectroscopy also used to find the Raman shift spectra to recognize the degree of functionalization. The zeta potential also used to study the partials surface charge.

5.2.5 Adsorption experiments

The prepared mK-CNTs adsorbent was used in this study to remove the As^{3+} from water. Batch adsorption study was conducted using various amount of adsorbent (20, 30 and 40 mg), arsenic concentration (1, 3 and 5 mg/L) and different values of pH (3, 5 and 8). A 50 ml of contaminated water in a 250-ml flask, the flasks were shaking at 180 rpm using a mechanical system at room temperature. The number of samples prepared in this study are 213 sample. The concentrations of arsenic were tested at different time to study the equilibrium time of adsorption.

5.3 Back propagation neural network (BPNN)

Recently, a significant improvement in the artificial neural network (ANN) techniques used in different fields for the prediction of difficult and complicated systems. ANN system able to improve the predicting ability of models at time the statistical and mathematical procedure are complicated to predict and formulate with anticipated accuracy. In this study, the sorption efficiency estimation by using analytical and mathematical tools is complicated due to the complexity and non-linear relationship between the variable of arsenic (III) removal. Consequently, in this study the ANN techniques have been used for prediction reason due to the high ability of ANN to perceive the input and output professionally in the complicated situation.

The backpropagation neural network (BP-NN) structure containing of three different layers such as input layer which receive the inputs from the source, hidden layer which process the received signals from the input layer and output layer which deliver the results have been predicted in this study, the structure of the feed-forward back-propagation presented in Figure5.1.

There are two stages in the neural network functioning the first stage is training, and the second stage is testing. The structure of the network can be presented as B-R-N, the input layer presented by B which is identified by the number of input variables. Whereby, the hidden neuron of hidden layer is presented by R, the number of output layer neuron is presented by N the number of the output layer neuron is depending on the number of desired output. An output sources deliver information to input layer, the inputs number depending on the output sources variable, the input layer sends the information to the hidden layer and do all the processing on the information and send them to the output layer, the output layer creates the result and send it to an external receptor.

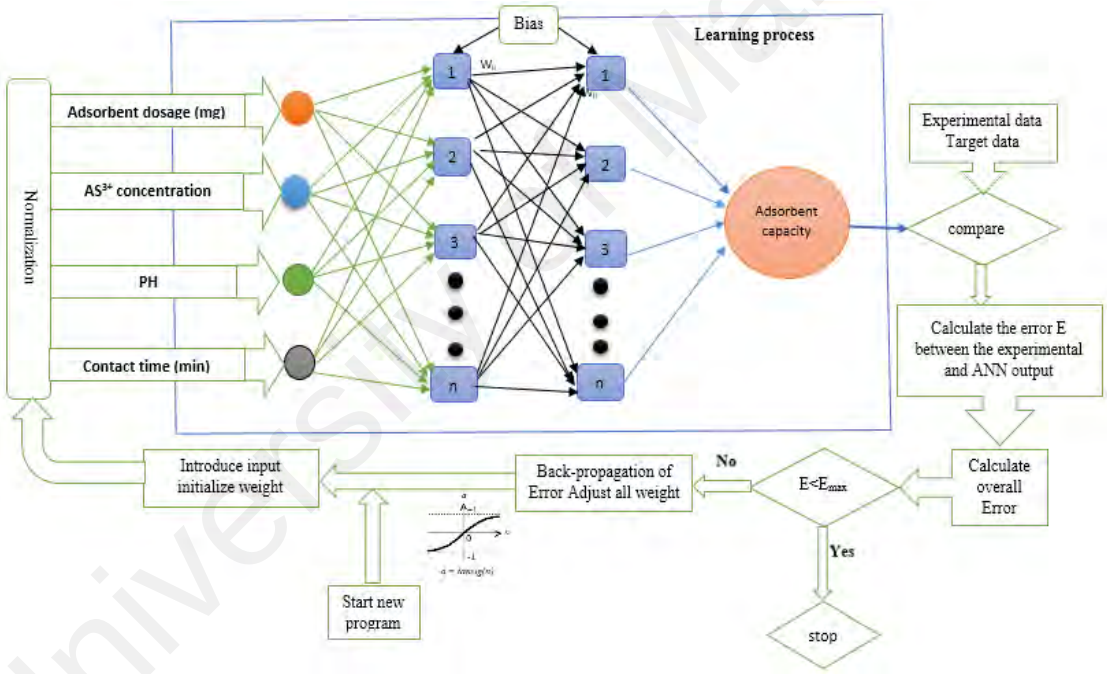

Figure 5. 1: Feed-forward back-propagation neural network structure

The interaction between the layers is called as weight (W_{ii}) the weight factor can modify the values of the transferred signals, the sigmoid transfer function (*f*) also modify the total of the information. In the same way, the output layer signals also modified by the weight factor (W_{ii}) of the k_{th} layer. All the modified information by sigmoid transfer

function (f) are combined at the output layer (Strik, Domnanovich, Zani, Braun, & Holubar, 2005).

Let $I_s = (I_{s1}, I_{s2}, I_{s3....}I_{sI})$, S = 1, 2, 3,…, N is S_{th} manner among N input manner. Where W_{kj} and W_{ji} are the connection weight between j_{th} hidden neuron to i_{th} input neuron, and k_{th} output neuron to j_{th} hidden neuron, respectively. The output neuron form of the input layer is:

$$D_{si} = I_{si} \quad \text{i= 1,2,3,….,B} \tag{5.1}$$

$$D = f(\sum_{i=1}^{I} w_{ji} D_{si}) \text{ , i = 1, 2, 3, …,R} \tag{5.2}$$

The output layer neuron is:

$$D_{sk} = f\left(\sum_{j=0}^{R} w_{kj} D_{sj}\right) \text{ , k = 1, 2, 3, …,N} \tag{5.3}$$

There are plenty of Feed-forward Back-propagation Neural Network (FBNN) transfer function in the backpropagation unit. The following transfer function selected principles used as a monotonous non-decreasing, differentiable and continuous function. In this work, the most universal binary logistic sigmoid transfer function is used and it is written as following:

$$f(x) = \frac{1}{1+e^{-x}} \tag{5.4}$$

The concentration of metals, adsorbent dosage, pH, and contact time are the input variables used in the ANN model are shown in Table 5.1.

The efficiency of adsorbent is the desired from the output of the network. Two hundred and thirteen experimental data are prepared in lab scale and used for the modeling. The used data are separated into two sets, training set and testing set, (88 %) of the data are used for the training and (12 %) are used for the testing.

Table 5. 1: The range of input and output parameters

Parameters	Minimum	Maximum
Adsorbent Dosage (mg)	20	40
Initial Concentration of As^{3+} (mg/L)	1	5
PH	3	8
Contact Time (min)	1	310
Uptake Capacity (mg/g) (output)	0	3.82

There are two types of learning methods, the supervised and unsupervised methods, in this study the supervised technique has been used. The predicted results are compared with the experimental used data by using the mean square error to calculate the occurred error between the predicted data and the desired data. The maximum value of mean square error limited based on the user desire, if the value is not in the limit prescribed, then its backpropagation the output to the input, and the weight is adjusted until the iteration number meet the prescribed limit. The mean square error E_s is defined as:

$$E_s = \sum_{i=1}^{n} \frac{1}{2}\left(Q_{si} - D_{si}\right)^2 \tag{5.5}$$

Where Q_{si} is the desired value, and D_{si} is the is the predicted output.

The mean square error value is supervised at the training stage. At the initial training phase, the value of the error is usually decreased, the training error start to rise when the overfitting starts to happen. The training stops when the error of training begins to increase and the minimum value of error at training are returned.

5.3.1 Model evaluation indicators

Different indicators will be used to evaluate the ANN model, by using the actual and predicted results, to examine the accuracy of ANN model. The behaviour of ANN model carried out by employing various indicators such as the relative root mean square error (RRMSE), mean square error (MSE), root mean square error (RMSE), mean absolute

percentage error (MAPE) and relative error (RE). The formulas of the maintained indicators are as following:

$$RRMSE = \left[\frac{1}{n} \sum_{t=1}^{n} \left(\frac{D_{a(t)} - D_{f(t)}}{D_{a(t)}} \right)^2 \right]^{\frac{1}{2}} \tag{5.6}$$

$$MSE = \frac{1}{n} \sum_{i=1}^{n} \left(D_{a(t)} - D_{f(t)} \right)^2 \tag{5.7}$$

$$RMSE = \left[\frac{1}{n} \sum_{t=1}^{n} \left(D_{a(t)} - D_{f(t)} \right)^2 \right]^{\frac{1}{2}} \tag{5.8}$$

$$MAPE = \frac{1}{n} \sum_{t=1}^{n} \left| \frac{\left(D_{a(t)} - D_{f(t)} \right)}{D_{a(t)}} \right| \times 100 \tag{5.9}$$

$$RE = \frac{D_{a(t)} - D_{f(t)}}{D_{a(t)}} \times 100 \tag{5.10}$$

Where:

$D_{f(t)}$ = the simulated value.

$D_{a(t)}$ = the actual value.

Generally, RRMSE, MSE, RMSE, MAPE and RE indicators were selected to evaluate the performance of models, all the indicators are based on the obtained result by comparing the evaluated error of the actual and simulated results. The model with smallest error considered as the best model.

5.4 Result and dissection

5.4.1 Hybrid material characterization

The Raman spectroscopy has the capability to indicate the functionalization degree for the Carbon materials, by comparing the intensity of D band (I_D) with the G band (I_G), I_D/I_G (Aitchison, Ginic-Markovic, Matisons, Simon, & Fredericks, 2007). In this work, the I_D/I_G for the P-CNTs found 1.11, by adding the $KMNO_4$ the I_D/I_G ratio reached to 1.16. Afterward, with functionalization by m-DES, the surface deformation of CNTs has been increased by bring in a new functional group in sp^3 directions, resulting in the development of the I_D/I_G ratio of the mK-CNTs to 1.22. These results were in agreement with the FT-IR analysis where the functionalization with $KMnO_4$ increased the hydrophilicity of the CNTs surface by introducing O-H functional groups. By contrast, the m-DES increased the hydrophilicity of the surface where the O-H presence was completely disappeared. In addition, the PO^{-3} presence at wave number range of 450-500 cm^{-1}. The absolute zeta potential was increased significantly after the functionalization m-DES where it's reached 39.78 mV. It is well known that the surface area of an adsorbent is of high influence on the adsorption efficiency; herein, the surface area was increased after each functionalization step. The surface area of P-CNTs, K-CNTs, mK-CNTs was 123.5, 158.9 and 205.5 respectively (AlOmar, Alsaadi, Hayyan, Akib, & Hashim, 2016).

5.4.2 Influence of pH

The pH of solution is a function of the arsenic ions removal, in order to study the pH influence, the pH values were varied in this study in the range of 3.0 to 8.0 with fixing all the involved parameters in the experimental work. Two initial concentrations of arsenic 1 mg/L and 3 mg/L were used in order to examine the effect of pH with different initial concentration.

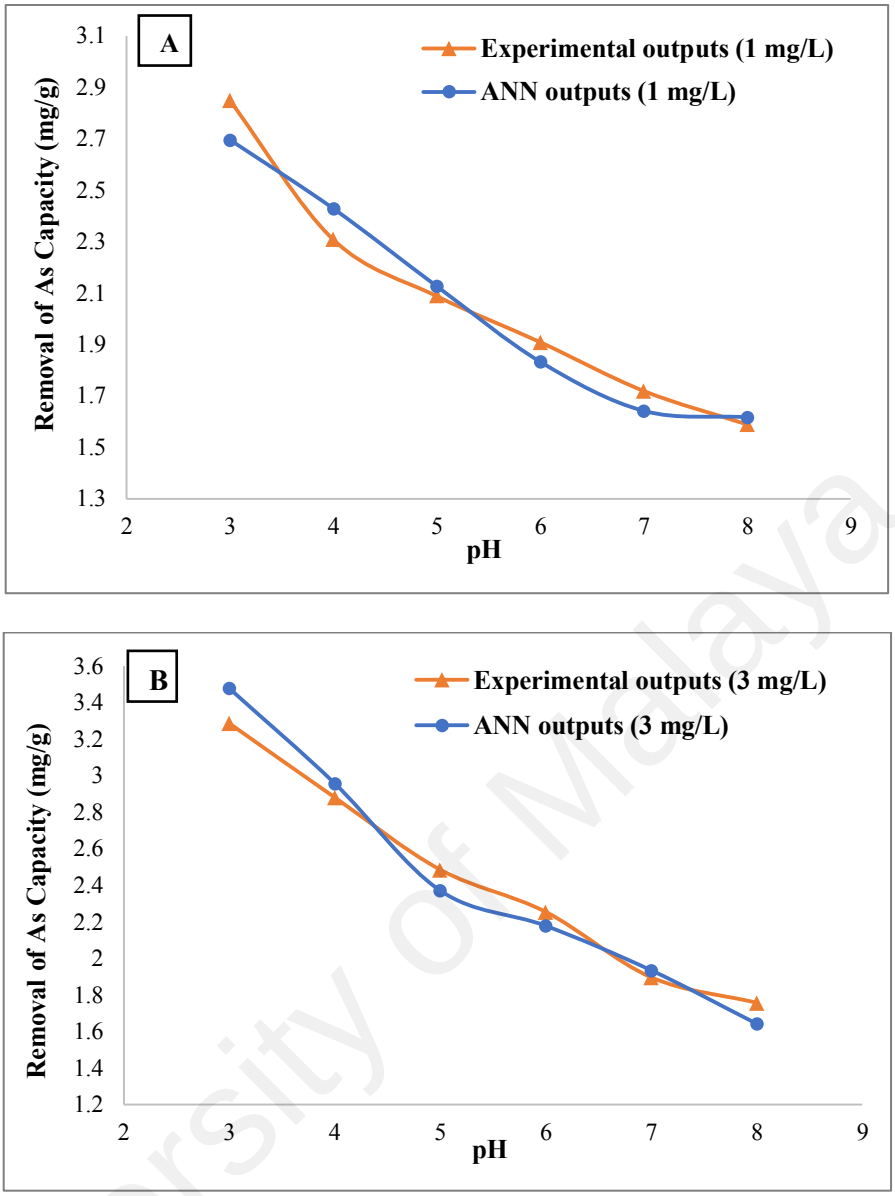

Figure 5. 2: ANN and experimental outputs as pH function (a) at 1 mg/L initial concentration, (b) at 3 mg/L initial concentration

The relationship between the pH and the adsorption efficiency can be clarified by the mechanism of the electrostatic attraction between the arsenic species and the negative charged adsorbents. The adsorbents are highly protonated at lower pH value thus, will result in a high attraction electrostatic, which lead to a higher attraction between the negatively adsorbent charged and anion resulting in a higher adsorption capacity. Where by, at higher value of pH the adsorbent capacity is decreasing. The process might happen due to, the ionization of adsorbent acidic or repulsive force might happen between the

arsenic ions and the adsorbent negatively charged. The ANN technique is used for the modeling and prediction of the obtained data from the experimental work, the prediction results shows a good agreement with the experimental result trend. The ANN outputs and the experimental results as the function of pH versus the uptake capacity are presented in Figure 5.2 A, B.

5.4.3 Effect of adsorbent dosage

Adsorbent dose is one of the important factors involved in the adsorption process, the adsorbent dose effect on the As^{3+} removal is examined at pH 5.0, with 1 mg/L and 3 mg/L As^{3+} initial concentration by keeping the other involved factors as constant. The As^{3+} removal capacity is decreased from 2.164 mg/g to 1.883 mg/g by increasing the adsorbent dosage from 20 mg to 30 mg and 1.883mg/g to 1.761 mg/g by increasing the adsorbent dosage from 30 mg to 40 mg at initial concentration of 3 mg/L. While at initial concentration of 1 mg/L, the uptake capacity decreased from 2.164 mg/g to 1.315 mg/g with increasing the adsorbent dosage from 20 mg to 30 mg, whereby, increasing the adsorbent dosage from 30 mg to 40 mg the uptake capacity decreased from 1.315 mg/g to 1.264 mg/g. The decreasing in the uptake capacity with increasing in the adsorbent dosage might be attributed with increasing the adsorbent surface area following in an increase of more active sites (B. Das et al., 2014; M. S. Kumar & Phanikumar, 2013). The obtained data from the experimental work are trained and predicted by using the ANN modeling techniques. The ANN model prediction found satisfactory for the experimental data observation. The experimental and predicted output of the ANN are presented in Figure 5.3 a, b; at 1 and 3 mg/L initial concentration.

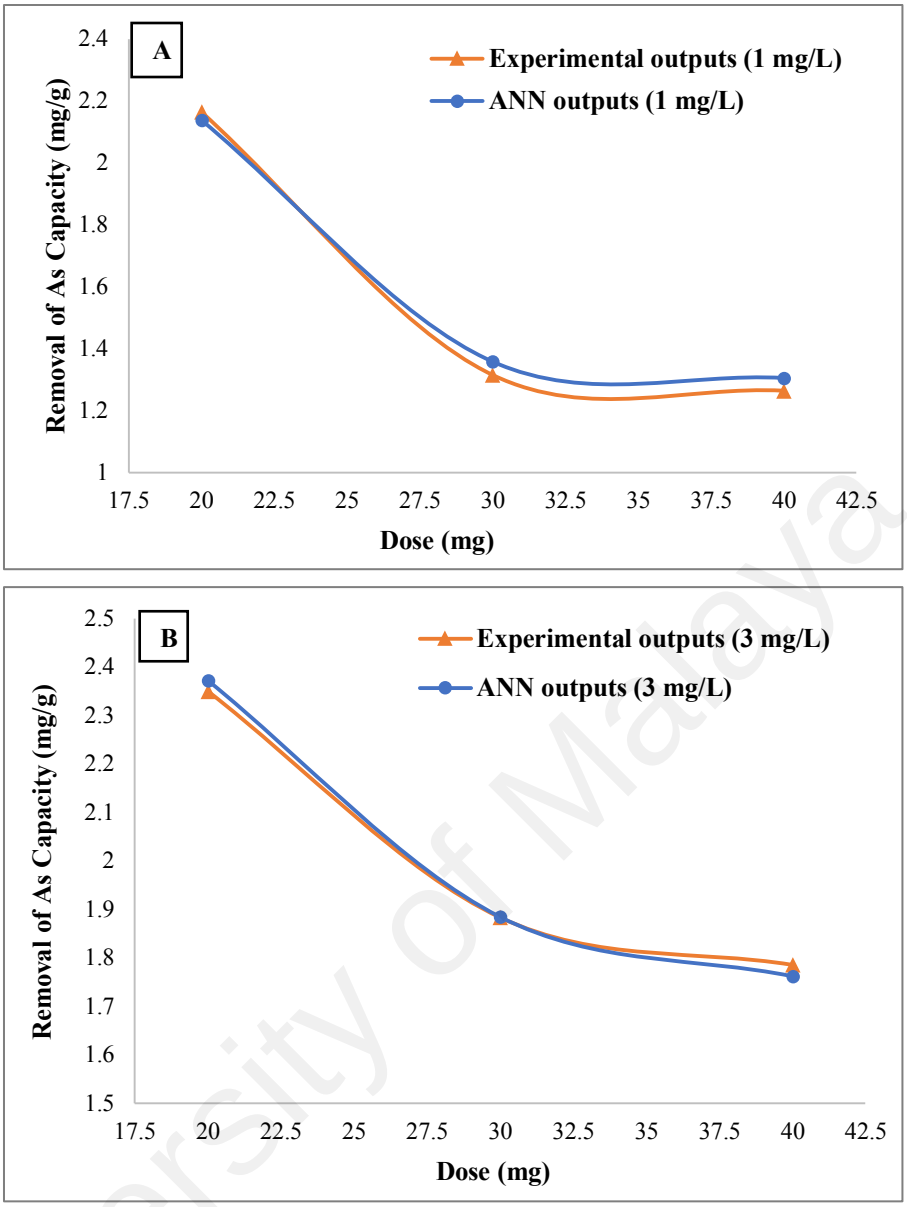

Figure 5. 3: Experimental and ANN output as the function of adsorbent dosage (a) at 1 mg/L initial concentration, (b) at 3 mg/L initial concentration

5.4.4 Effect of initial concentration

The effect of the initial concentration on the adsorption capacity is studied by varying the arsenic initial concentration from (1 mg/L to 5 mg/L), the initial concentration effect studied at 3 and 5 pH, all the other involved parameters are fixed, contact time 120 min and adsorbent dosage 30 mg. At pH 3, the initial arsenic concentration increased from 1 to 3 mg/L and the uptake capacity increased from 1.29 to 2.08 mg/g respectively;

whereas, with increasing the initial concentration from 3 to 5 mg/L the uptake capacity increased from 2.08 to 3.66 mg/g. Whereby, at pH 5, there uptake capacity increases from 2.25 to 3.35 mg/g when increasing the initial concentration from 1 to 3 mg/g respectively. While, with increasing the initial concentration from 3 to 5 mg/L the uptake capacity increased from 3.35 to 3.75 mg/g respectively. This might be attributed due to the increase in the driving force of the mass transfer which led to an increase in the uptake capacity of As^{3+} ions from water solution. At low concentration, the As^{3+} ions interact at the adsorbent active site; whereas, at higher As^{3+} concentration, the adsorbent active site will be saturated and the removal percentage will be lower (Banerjee et al., 2016). The obtained data from the experimental work are trained and predicted by using the ANN modeling techniques. The ANN model prediction found satisfactory for the experimental data observation. The experimental and predicted output of the ANN are presented in Figure 5.4 a, b.

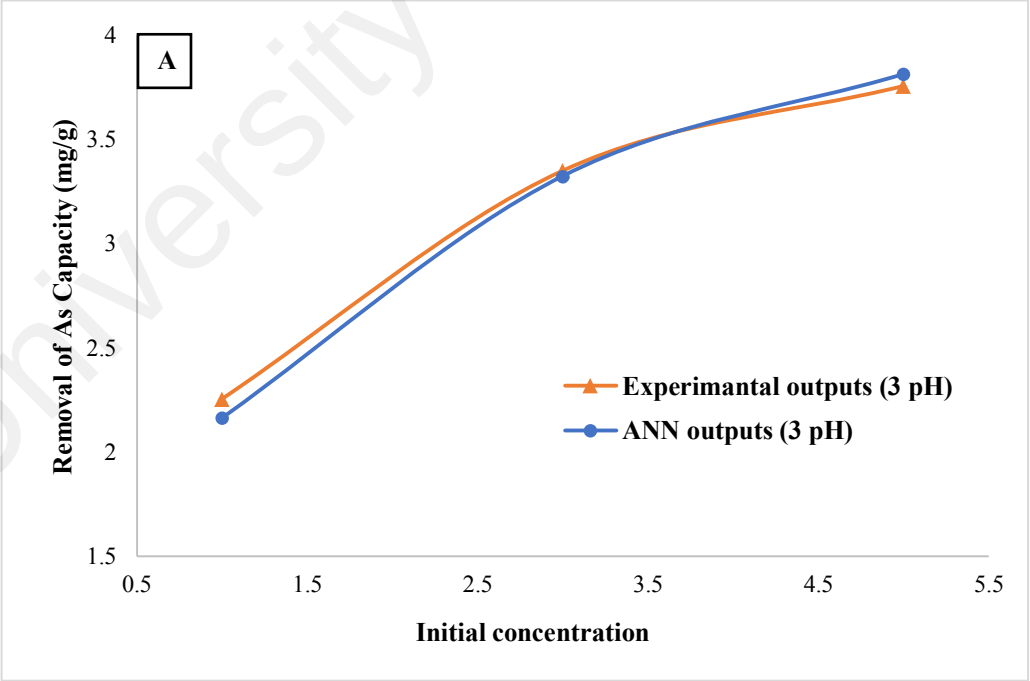

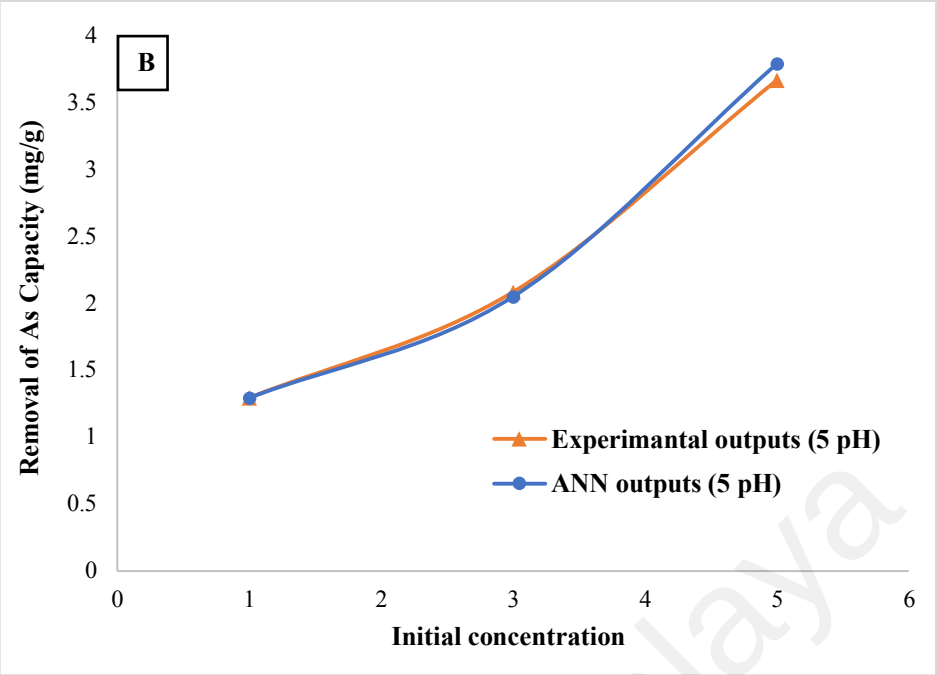

Figure 5. 4: Experimental and ANN output as the function of initial concentration

5.4.5 Adsorption kinetics study

The adsorption kinetic study is an important study as it gives a significant information about the mechanism and pathway of the adsorption reactions, also can provide an information about the solute removal rate (Ayoob, Gupta, & Bhakat, 2007). In this work, three kinetic models were used namely pseudo-first-order, pseudo-second-order and intraparticle diffusion model to investigate the mechanism and rate of the adsorption process. The kinetic study performed with 1 mg/L initial concentration, 30 mg adsorbent dosage and 180 rpm agitation speed, with, 5 and 8 pH. The equilibrium time of the experiment was after 240 minutes. The coefficients of correlation (R^2) values were used as the conformity indicator between the experiment and the predicted by each kinetic model.

The ANN technique is used for the modeling and prediction of the obtained data from the experimental work, the three kinetics models used for the experimental data also

applied on the ANN outputs. The pseudo-second order describe the adsorption kinetics of this study comparing to the intraparticle diffusion and pseudo-first order models. The pseudo-second order R^2 at pH 5 is 0.9972 for the experiment data and 0.9973 for the ANN outputs whereby, for pH 8 the R^2 of the pseudo-second order was 0.9939 for the experimental data and 0.9962 for the ANN outputs the R^2 for all the three kinetics models used are summarised in Table 5.2.

Table 5. 2: Adsorption kinetics and correlation coefficient

		Pseudo-first-order $ln(q_e–q_t)$ *vs time (t)*		Pseudo-second-order $(t/q_t$ *vs t)*		Intraparticle $(q_t$ *vs* $t^{0.5})$	
PH	C_0 mg/L	Experimental R^2	ANN output R^2	Experimental R^2	ANN output R^2	Experimental R^2	ANN output R^2
5	1	0.831	0.8225	0.9972	0.9973	0.901	0.919
8	1	0.919	0.926	0.9917	0.9904	0.89	0.8731

The ANN model shows a good agreement with the experimental work, the experiment and ANN results are presented in Figure 5.5.

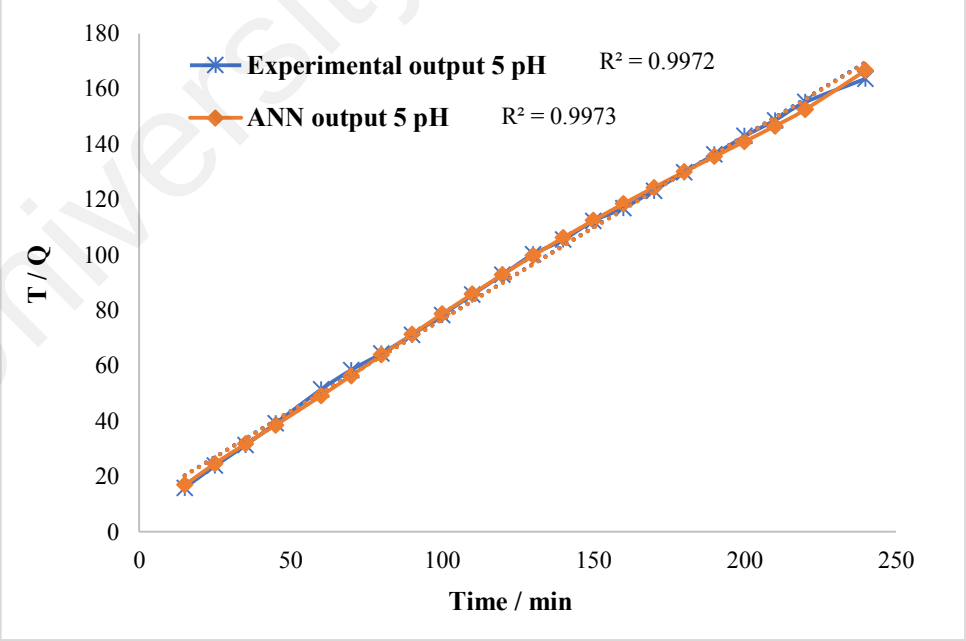

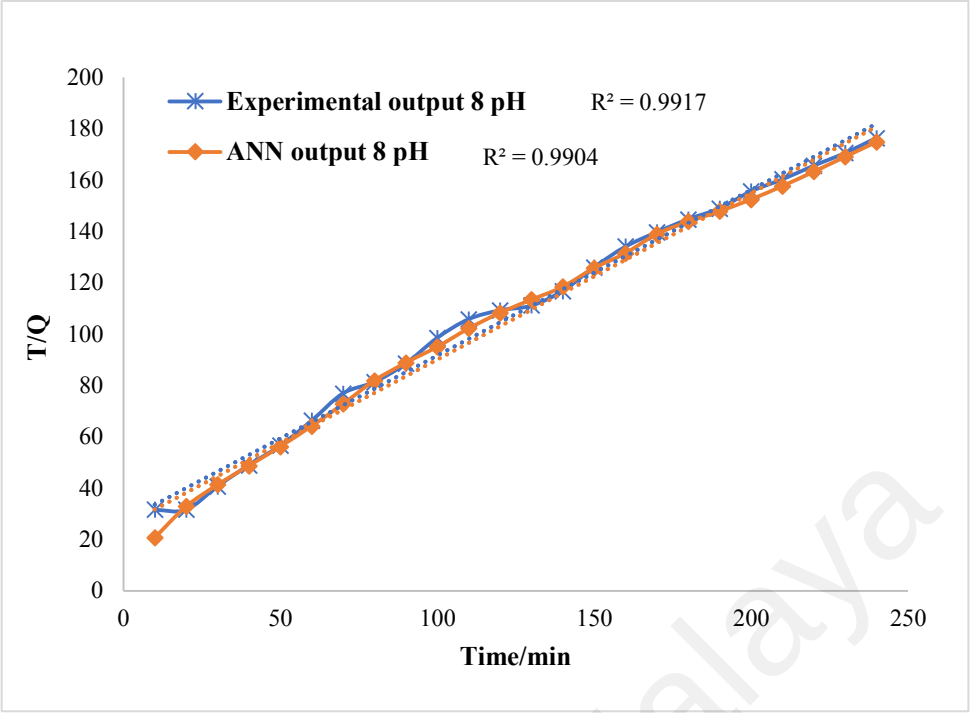

Figure 5. 5: Experimental and ANN output Pseudo-second-order adsorption kinetics at different pH value

5.4.6 Arsenic removal prediction

The artificial neural network back-propagation (ANN-BP) was used for the prediction of arsenic removal efficiency by using the functionalized carbon nanotube (CNTs) material. The parameters used in this study are arsenic concentration (1 mg/L, 3 mg/L and 5 mg/L), pH (3 to 8), adsorbent dosage (20 mg to 40 mg) and contact time until the equilibrium of reaction. Two hundred and thirteen (213) combinations were prepared in lab scale and divided into two sets training and testing set, one hundred eighty-eight (188) data were used for the training and twenty-five (25) data were used for the testing. The MATLAB R2014a programme was used in this study. The optimum hidden layers used for the model creation are two hidden layers with 10 neurons in each hidden layer with one input layer and one output layer. The (trainbr) was selected to update the bias and weight value correspond to the momentum and the tangent sigmoid transfer function (tansig) was selected as transfer function for the network. The nodes number at the hidden

layer were selected by training and testing the network with different neuron number and checking the value of the mean square error (MSE) of the testing set. The network performance is depending on the net input, weight of (trainbr) and tangent sigmoid transfer function (tansig). The minimum value of mean square error (MSE) achieved is (1.54×10^{-4}) at the testing phase, with correlation coefficient (R^2) of (0.9968), which shows a good agreement between the actual and the predicted data, the correlation coefficient plot for the testing set is presented in Figure 5.6. Different indicators were used to evaluate the created model such as relative root mean square error (RRMSE), root mean square error (RMSE), mean square error (MSE) and mean absolute percentage error (MAPE), the results of all the used indicators are presented in Table 5.3.

Table 5. 3: Evaluation indicators

Evaluation indicators	FFNN
MSE	1.54×10^{-4}
RMSE	1.24×10^{-2}
RRMSE	2.16×10^{-2}
MAPE	1.71

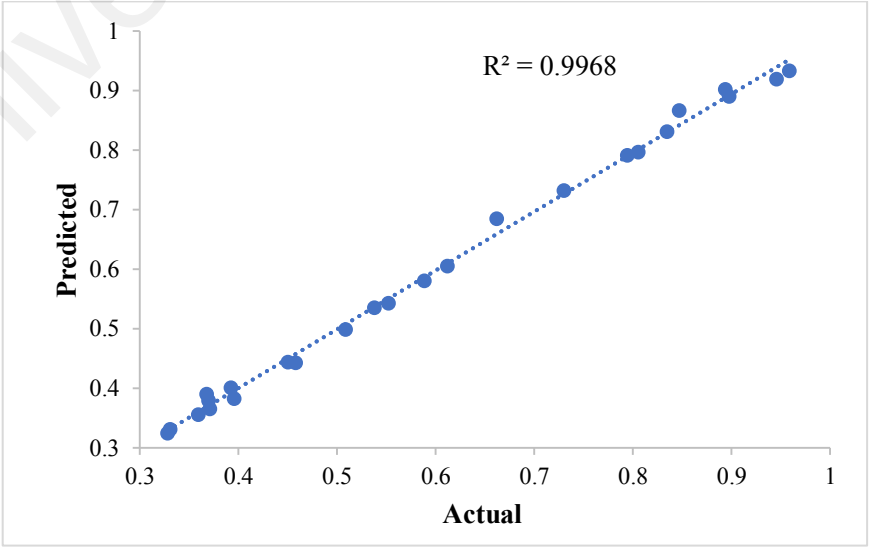

Figure 5. 6: Correlation coefficient of actual and predicted arsenic removal (testing data)

The relative error is one of the error indicators in the modelling prediction it compares the actual values to predicted values Figure 5.7 shows the relative error percentage of the model, the maximum error value for the FFNN model is 5.97 %. The best prediction performance is depending on the neural network training. This study is meant to get the mathematical approach benefit at the real-time experiment. The ANN model`s development is becoming the issues and challenges of the real-time experiment. This work currently under development phase to obtain a better feedback from the neural network in the hazardous ions removal.

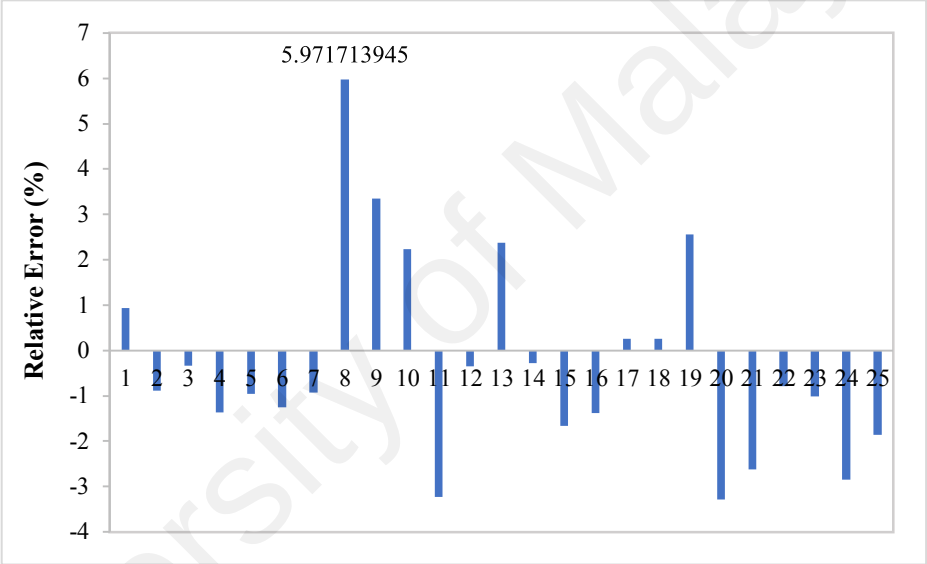

Figure 5. 7: Illustrates the accuracy of the hybrid model on the testing data

5.5 Conclusion

In this work, a novel adsorbent was developed by using two DESs systems for the CNTs functionalization. The adsorbent was characterized by using Zeta potential, Raman spectroscopy and FTIR. The adsorbent surface area increased after the functionalization by mK-CNTs. The experimental work has been carried out for the removal of arsenic from water solution. The new adsorbent found as an effective material for arsenic removal from water. Three kinetics models were used in this study which are Pseudo-

first-order, Pseudo-second-order and the Intraparticle with different values of pH, the pseudo-second order describe the adsorption kinetics of this study. The ANN technique was used successfully for the prediction of arsenic removal from water by using m-DES functionalized-CNTs (mK-CNTs). A three layers' neural network designed for the prediction of arsenic removal capacity from water, the feed-forward back-propagation algorithm was used in this study. Various indicators were used to evaluate the accuracy of ANN model such as (RRMSE, MSE, RMSE, MAPE and RE). The ANN output showed a good agreement with the experimental data, the best correlation coefficient R^2 is (0.9968) at the testing phase. This study conclude that the ANN system is able to predict the adsorption capacity of arsenic from water.

CHAPTER 6: BTPC BASED DES-FUNCTIONALIZED CNTS FOR AS^{3+} REMOVAL FROM WATER: (NARX) NEURAL NETWORK APPROACH

6.1 Introduction

The presence of heavy metal ions in water is considered as a major problem due to their non-biodegradability, toxicity and human health complications. Arsenic is one of the heavy metals, known as a carcinogenic material to humans. It can be found in polluted groundwater as a results of industrial waste discharge, rock weathering, pesticides and arsenical herbicides used for agricultural purposes (Xia, Shen, Xu, Liang, & Zhou, 2014).The exposure and consumption of arsenic polluted drinking water causes numerous health problems in several countries such as Bangladesh (G. A. Wasserman et al., 2004), Bengal (Mazumder et al., 1997) and China (S.-X. Wang et al., 2007). Due to the serious health problems related to arsenic in drinking water, the world health organization (WHO2001) determined the maximum allowable arsenic in the drinking water as 0.01 mg/L (A. H. Smith, Lopipero, Bates, & Steinmaus, 2002). Many chemical, biological and physical processes have been utilized for heavy metal treatment such as precipitation, ion-exchange, reverse osmosis, biosorption, filtration and adsorption (Ahmadi et al., 2015; D.-W. Cho, Song, Kim, Schwartz, & Jeon, 2015; Ding, Hu, Morales, & Gao, 2014; X. Luo et al., 2015; N. Mubarak, Sahu, Abdullah, Jayakumar, & Ganesan, 2015a). Adsorption is the most suitable technique due to its cost effectiveness, feasible operation and high removal efficiency (Hu, Shi, & Jing, 2015; Kamble et al., 2007; Kocabaş-Ataklı & Yürüm, 2013; N. Mubarak, Sazila, Nizamuddin, Abdullah, & Sahu, 2017; M. L. P. Ramos et al., 2016). In addition, this method has the ability to remove small concentrations of heavy metals from a large amount of water solutions. The effectiveness of adsorption mainly dependents on the selection of appropriate process conditions such as the mass of sorbent, pH, system temperature and the process duration (E. Lourie & Gjengedal, 2011).Various studies have been conducted using different

materials like clay minerals, biomaterials and activated carbon for heavy metal ions removal from water (J. P. Chen & S. Wu, 2004; V. Gupta et al., 2006; J. U. K. Oubagaranadin & Z. Murthy, 2010), Table 6.1 summarize some of the recent studies for arsenic removal using different adsorbents. However, the use of traditional adsorbents have common drawbacks such as small adsorption capacity and low adsorption efficiency(Rao et al., 2007). Consequently, the need for highly efficient adsorbents is necessary to remove the arsenic ions from water solution. Therefore, the development of new adsorbent becomes the major interest of researchers in water treatment technology.

Table 6. 1: Arsenic (As^{3+}) removal using different adsorbents

Adsorbent	Adsorption capacity	Ref.
PAMAM/CNT nanocomposite	2800 mg/g	(Hayati et al., 2016)
GO/$CuFe_2O_4$	51.64 mg/g	(L.-K. Wu et al., 2018)
Iron nanoparticles	15.50 mg/g	(Jain & Agarwal, 2017)
ZnFe-MMOs	176.3 mg/g	(G. Di et al., 2017)
CeO_2/Fe_2O_3/graphene nanocomposite	101.41 mg/g	(Sahu, Mahapatra, & Patel, 2017)

Nanoparticles are one of the most popular adsorbents for several pollutants, owing to their features such as, catalytic potential, small size, large surface area and high reactivity (Ali, 2012). Carbon nanotubes (CNTs) possess different properties from other material used, which make them suitable for many applications in electronics, water treatment (N. Mubarak, Sahu, Abdullah, Jayakumar, & Ganesan, 2015b), optics, nanotechnology and other material science fields (Atieh et al., 2011). The CNTs was used for the removal of different heavy metals Zn^{2+} (N. Mubarak et al., 2013; N. Mubarak, Sahu, Abdullah, & Jayakumar, 2014; Thines et al., 2014), Cd^{2+} (Ruthiraan et al., 2015), Pb^{2+} (N. M. Mubarak, Sahu, Abdullah, & Jayakumar, 2016) . However, carbon nanotubes have some limitations ascribed to various flaws in solubility, difficulty in manipulation and aggregation. Hence, surface modification of carbon nanotubes have magnificent affinity by interfacing with other compounds (N. Mubarak, Sahu, Wong, et al., 2015; Sun et al.,

2002; Thostenson, Ren, & Chou, 2001). The CNTs surface charge can be enhanced by the oxidative functionalization. However, this method requires the use of strong acids, which is not environmentally friendly. Therefore, the need for an environmentally friendly modification technique is crucial for the widespread application of CNTs (Hayyan, Abo-Hamad, et al., 2015; Martinez et al., 2003).

Deep eutectic solvents (DESs) are identified as liquid combination formed by the complexation of hydrogen bond acceptors (HBA) and hydrogen bond donors (HBD) (Abbott, Boothby, et al., 2004; Gorke et al., 2008; Q. Zhang et al., 2012). DESs are new green solvents with many advantages as compared to the ionic liquids (ILs) (Xu, Wang, Huang, Li, & Wen, 2015). The prime advantages of DESs over conventional ILs are the diversity of physical properties and different molar ratios, easy to synthesis and cheaper price of raw materials. The DESs are synthesized of two or more inexpensive, non-flammable and usually non-toxic components which are able to connect together via hydrogen-bonding (Paiva et al., 2014). The components mixture have a lower melting point than the individual compounds (Abbott, Boothby, et al., 2004). Recently, DESs were reported in many applications; examples of such are the uses of ChCL-based DES as a functional additive for starch-based plastics (Leroy et al., 2012), the synthesis of zeolite analogues (Cooper et al., 2004), mediums for the deposition of specific metals in electro and electroless plating of metals (Abbott et al., 2007; Abbott et al., 2008); recently, in nanotechnology applications (Abo-Hamad et al., 2015).

In general, the adsorption process is considered as a complicated heavy metal removal technique due to the influence of many variables(Ruthiraan et al., 2015) such as, contact time, adsorbent dosage, pH and initial heavy metal concentration. The conventional linear method for modelling this kind of process is hectic. On the other hand, artificial neural networks (ANNs) modelling technique which is known as a robust black-box modelling tool is capable of transforming a given data set into its target outputs (Fayaed, El-Shafie,

& Jaafar, 2013a). The ANN capability to generalize and learn the behaviour of any non-linear and complex process makes it a robust tool. ANNs consist of a massive parallel numerical architecture which can solve the complicated problems by the assistance of highly connected neurons organised in layers. Recently, ANNs technique are used for various engineering applications (Fayaed, El-Shafie, & Jaafar, 2011, 2013b). Some studies recommended the NARX neural network is suitable for nonlinear systems modelling (Çoruh, Geyikçi, Kılıç, & Çoruh, 2014; McAvoy & Werbos, 1992). The novelty of this work is using the DES as a functionalization agent of CNTs for the removal of arsenic ions from water, and using the artificial neural network modelling technique for modelling and mapping the adsorption process.

The objective of this study was to synthesis a DES by mixing glycerol (Gly) with Benzyl triphenyl-phosphonium chloride (BTPC) for CNTs functionalization. Subsequently, the DES-functionalized CNTs was utilized as an adsorbent for arsenic removal from water. Furthermore, the NARX neural network was used for modelling and establishing the relationship that exists between the operational variables.

6.2 Experimental and methodology

This section describes the materials used in DESs Synthesis, MWCNTs Functionalization by DES and the functionalized CNTs characterization. The materials used in the experimental work are hydrochloric acid (36.5-38%), Glycerol(Gly), potassium permanganate ($KMnO_4$), multi-wall carbon nanotube (MWCNTs) with specification of L5 μm × D 6-9 nm, >95% carbon, and sodium hydroxide pellets were all provided by SIGMAALDRICH. Arsenic standard solution of 1000 mg/L and benzyltriphenyl-phosphonium chloride (BTPC)>99% purity was provided by Merck, Germany.

The DES synthesis was performed by mixing benzyltriphenyl-phosphonium chloride (BTPC) and Glycerol(Gly) at molar ratio of 16:1 HBD: slat (AlOmar, Hayyan, et al., 2016), at 80 ºC temperature for 3 hours until the DES becomes homogenous. The produced DES is referred to as B in this study. The prepared DES is kept in a tightly controlled environment to avoid the effect of the humidity.

The first step of the functionalization was by drying the pristine MWCNTs (P-CNTs) at 100 ºC overnight. Then, 200 mg of the dried P-CNTs was mixed with 7 ml of $KMnO_4$ and sonicated for 2 h at 65 ºC to produce K-CNTs. The functionalization of B-DES was done by mixing 7 ml of the prepared B-DES with 200 mg of K-CNTs and sonicating them at 65 ºC for 3 h to produce BK-CNTs. After that, the filtration process was performed by washing the functionalized CNT using distilled water and filtered by PTFE 0.45 µm membrane until the pH of the filtered water reached neutral. Later, the washed functionalized CNT was dried over night at 100 ºC before using it for the removal.

The Raman spectroscopy, Fourier transform infrared (FTIR) and zeta potential were used for the characterization of P-CNTs, K-CNTs and BK-CNTs adsorbent. The Raman shift obtained to identify the degree of functionalization using a Renishaw System 2000 Raman Spectrometer. The (FTIR) was used to identify the surface chemical modification of the adsorbent using Fourier transform infrared (FTIR) spectroscopy via a PerkinElmer® FTIR spectrometer USA with a range of 400-4,000 wave number and four times repetition. Zetasizer (Malvern, UK) was used to recognize the adsorbent partial surface charge by measuring the zeta potential. The surface area of the adsorbent was measured using A fully Automated Gas Sorption System (micromeritics ASAP2020, TRISTAR II 3020 Kr®, USA) (AlOmar, Alsaadi, Hayyan, Akib, & Hashim, 2016).

6.2.1 Adsorption experiments

The functionalized BK-CNTs was used for arsenic removal from water solution. The experiments were conducted with various dosages of BK-CNTs adsorbent (20 to 40 mg), arsenic concentration (1 to 5 mg/L), with different pH values (3 to 8). 50 ml of contaminated water was poured in a 250-ml flasks; the flasks were shaked at 180 rpm using a mechanical system at room temperature. A total of 198 samples were prepared in this study. The arsenic concentrations were tested at different interval of times to study the adsorption equilibrium dynamics using the Inductively coupled plasma (ICP) with an OES OPTIMA7000DV PerkinElmer® USA.

6.2.2 NARX neural network modelling and evaluation indicators

Among the many black-box modelling strategies, the artificial neural network is a powerful tool for capturing the linear or non-linear relationship between the input and output process variables (Agami, Atiya, Saleh, & El-Shishiny, 2009). The NARX neural network is a dynamic network which contains various layers with a back-propagation connections (Sheng Chen, Billings, & Grant, 1990).The NARX neural network is well known for its high speed of convergence as well as high degree of generalization.

A NARX neural network was trained and used in this study for modelling the adsorption capacity of the BK-CNTs adsorbent. NARX is a recurrent dynamic network, it consists of feedback connections with several layers. The iterative training process are used in the NARX models whereby the weights and biases are adjusted iteratively to improve the performance of the model at each step. When including the information from the exogenous inputs, the NARX models get an extra degree of freedom as compared with other networks. This improves the accuracy of the models and decreases the number of parameters required for the model. The NARX outputs during the training are presented in equation 1.

$$y(t) = f\left[u(t-n_u),....u(t-1),\ u(t),\ y(t-n_y),....\ y(t-1)\right] \quad (6.1)$$

Where:

f is the non-linear function.

u(t) is the network inputs at time t.

y(t) is the network outputs at time t.

n_u and n_y are the order of inputs and outputs.

During the training, the outputs of the network are regressed on the target of the actual values as long as they are accessible and, the values of the actual target are feed-back to the network. This basically makes a better learning and training, and the network acts as feed-forward network which is always steady. The resulting system known as NARX network, when the *f* approach is with the multi-layer perception (Sheng Chen et al., 1990). In this paper, two-layers of NARX were used (Figure 6.1) for the prediction of the adsorption capacity (Q_e) of the BK-CNTs. The input layer of the network consists of 4 inputs (time, adsorbent dosage, pH and initial concentration) and one output layer (Q_e). In Figure 6.1, b_h is the network bias, w_{ij} is the network weight and z is the delay element.

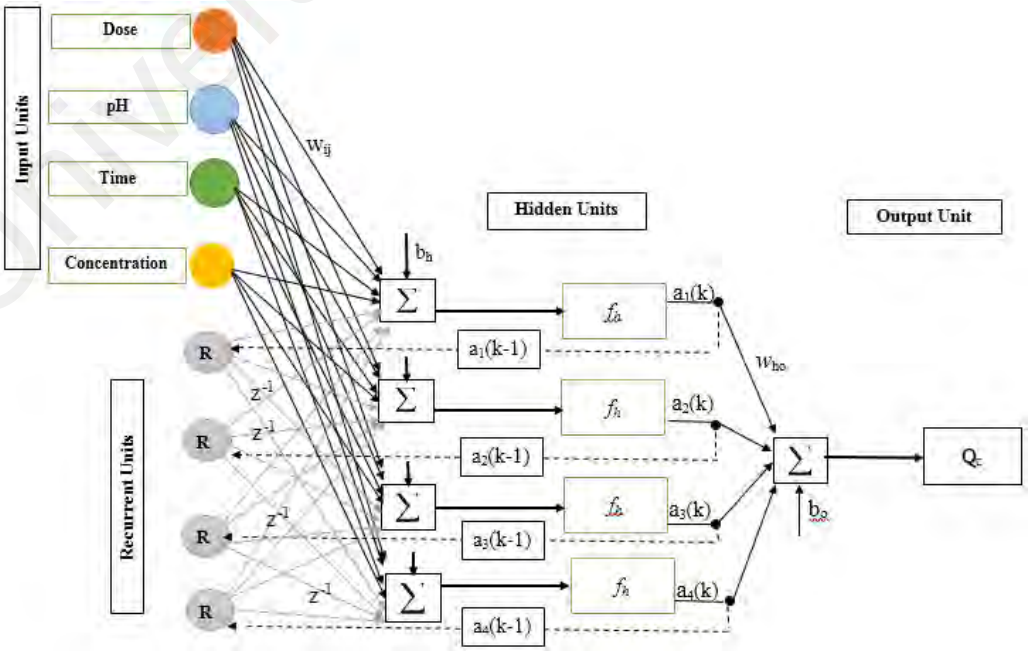

Figure 6. 1: The NARX neural network structure

Various indicators were employed in this study for the evaluation of the NARX model using the predicted and actual results to check the reliability of the NARX model. These indicators are the relative root mean square error (RRMSE), mean square error (MSE), root mean square error (RMSE), mean absolute percentage error (MAPE) and relative error (RE).

$$RRMSE = \left[\frac{1}{n} \sum_{t=1}^{n} \left(\frac{D_a(t) - D_f(t)}{D_a(t)} \right)^2 \right]^{\frac{1}{2}} \tag{6.2}$$

$$MSE = \frac{1}{n} \sum_{i=1}^{n} \left(D_a(t) - D_f(t) \right)^2 \tag{6.3}$$

$$RMSE = \left[\frac{1}{n} \sum_{t=1}^{n} \left(D_a(t) - D_f(t) \right)^2 \right]^{\frac{1}{2}} \tag{6.4}$$

$$MAPE = \frac{1}{n} \sum_{t=1}^{n} \left| \frac{\left(D_a(t) - D_f(t) \right)}{D_a(t)} \right| \times 100 \tag{6.5}$$

$$RE = \frac{D_a(t) - D_f(t)}{D_a(t)} \times 100 \tag{6.6}$$

Where:

$D_f(t)$ = the predicted value at time t.

$D_a(t)$ = the actual value at time t.

The RRMSE, MSE, RMSE, MAPE and RE are the indicators that were used for evaluating the model performance. The aim of using different indicators is to confirm the

accuracy of the model. All the indicators are based on the obtained results by comparing the error between the actual and predicted results.

6.3 Results and Discussion

In this study, a new adsorbent was prepared (BK-CNTs), and used for arsenic removal from water. The NARX neural network was used for the modelling of the adsorption capacity and different indicators were utilized to evaluate the proposed neural network model. A sensitivity study of all parameters involved in the experimental work i.e. pH, adsorbent dosage and initial concentration were implemented. In addition, the adsorption rate order was investigated using three different kinetic models.

6.3.1 Characterization of hybrid material

Studying the electric charge of any adsorbents is crucial due to its influence on the adsorption efficiency. The zeta potential is considered as the electrical potential between the bulk fluid and the surface across the dielectrical layer attached to the suspended particles in a solution. This potential is a source of balancing electrostatic forces that keep the micro or nano-particles stable in suspension or emulsion. Herein, the absolute zeta potential has increased from 5.5 to 48.34 mV for P-CNTs and BK-CNTs respectively. In addition, the Raman spectra shows that the I_D/I_G ratio also increased from 1.11 for the P-CNTs to 1.14 for BK-CNTs indicating the presence of new functional groups in sp3 direction resulted from the functionalization effect of B-DES. These functional groups play a significant role in increasing the adsorption capacity of BK-CNTs. FTT-IR results were in accordance with Raman results. The sp^3 direction functionization was observed by OH stretching appeared in the peaks around 3400 cm^{-1}. However, in the region between (3000–3600 cm^{-1}), the OH and CH may overlap. In addition, the presence of phosphonium functional groups in a form of PO_4^{-3} are shown by the bend at 500–600 cm^{-1}. The CCl bond is located in the range of 600–800 cm^{-1}.

It is well known that the surface area of the adsorbent provides huge effect on the adsorption system. The introduction of B-DES as functionalization agent of CNTs increased the surface area significantly from 123.5 to 174.7 m^2/g. This significant increment is reflected in the maximum adsorption capacity of BK-CNTs (AlOmar, Alsaadi, Hayyan, Akib, & Hashim, 2016).

6.3.2 NARX modelling and performance

Selection of the right NARX network structure with good productivity and accuracy is a complicated task, which includes many aspects such as the selection of the proper number of hidden layers and neurons number at the hidden layer. In general, the NARX network structure contains input layer(s), hidden layer(s) and output layer(s). The network selection has been done based on the network performance and productivity, using the MSE value during the training phase.

The parameters used in this work are arsenic concentration (1 to 5 mg/L), adsorbent dosage (20 to 40 mg), pH (3 to 8), and contact time until the equilibrium of reaction. Hundred and ninety-eight (198) combinations were prepared in lab scale and divided into two sets training and testing set, one hundred and seventy-three (173) data were used for the training and twenty-five (25) data points for the testing set. The MATLAB R2014a computational platform was used in the current study to code and optimize the network structure. The optimum hidden layers used for the model creation are two hidden layers with 8 neurons in each hidden layer with one input layer with 4 nodes and one output layer with one node. The back-propagation training algorithm (*trainbr)* was selected to update the bias and weight vectors values corresponding to the momentum and the tangent sigmoid transfer function (*tansig*) was selected as the neurones transfer function for the network. The nodes numbers at the hidden layer were selected by training and testing the network using different neuron numbers and checking the value of the mean square error (MSE) of the testing set. The network performance depends on the net input,

weight of trainbr and tangent sigmoid transfer function tansig. The minimum value of mean square error (MSE) achieved was (6.37×10^{-4}) at the testing phase, with correlation coefficient (R^2) of (0.9818), which shows a good agreement between the actual and the predicted data, the correlation coefficient plot for the testing set is presented in Figure 6.2.

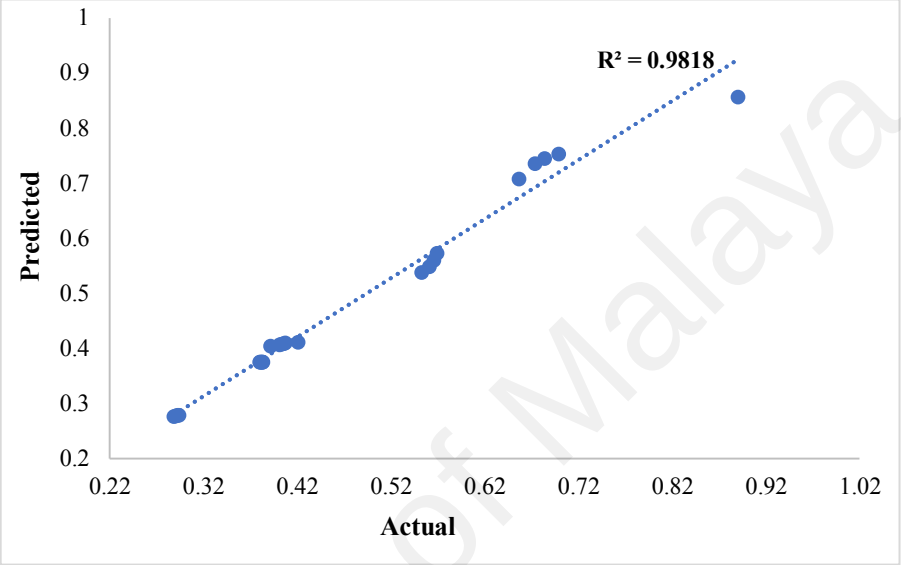

Figure 6. 2: Correlation coefficient of actual and predicted arsenic removal (testing dataset)

Different indicators were used to evaluate the trained model such as the relative root mean square error (RRMSE), the root mean square error (RMSE), the mean square error (MSE) and the mean absolute percentage error (MAPE). The results of all these indicators are presented in Table 6.2.

Table 6. 2: Evaluation indicators

Indicators	NARX
MSE	6.37×10^{-4}
RMSE	5.05×10^{-2}
RRMSE	8.30×10^{-3}
MAPE	3.25

The relative error compares the actual values to predicted values. Figure 6.3 shows the percentage relative error of the model, the maximum relative error value for the NARX model was 9.32 %.

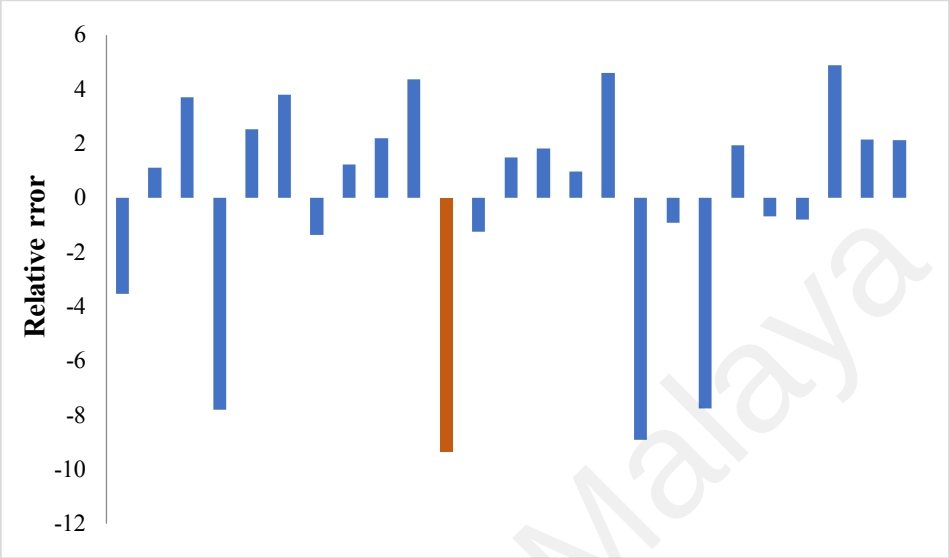

Figure 6. 3: Illustrates the accuracy of the hybrid model based on the testing dataset

The best prediction performance depends on the accuracy of the neural network training. The prepared NARX model used for the sensitivity study involved parameters in the experimental work (initial concentration, adsorbent dosage and pH). Moreover, the kinetic models were applied one the NARX outputs in order to check the model accuracy.

6.3.3 Sensitivity study

6.3.3.1 Effect of initial arsenic concentration

The effect of initial arsenic (As^{3+}) concentration on the adsorption was studied by varying the As^{3+} concentration from 1 to 5 mg/L, while all the other parameters such as pH (6), adsorbent dosage (30 mg) and time (120 min) were kept constant at their nominal levels indicated. The As^{3+} adsorption capacity is inversely proportional to the As^{3+} initial concentration. The adsorption capacity increases with increasing the initial metals

concentration at fixed amount of adsorbent dosage. When the initial As^{3+} concentration was increased from 1 to 3 mg/L, the adsorption capacity also increased from 1.57 to 2.83 mg/g. Whereas, increasing the initial As^{3+} concentration from 3 to 5 mg/L resulted in an increase of the adsorption capacity 2.83 to 5.25 mg/g. This might be attributed to the increase in the mass transfer driving force which led to an increase in the uptake capacity of As^{3+} ions from water solution. At low concentration, the As^{3+} ions interact with the adsorbent active sites. On the other hand, at higher As^{3+} concentration, the adsorbent active sites are saturated and the removal percentage decreases (Banerjee et al., 2016). The NARX model prediction results was found in a good agreement with the experimental adsorption data. The experimental and the NARX outputs are presented in Figure 6.4.

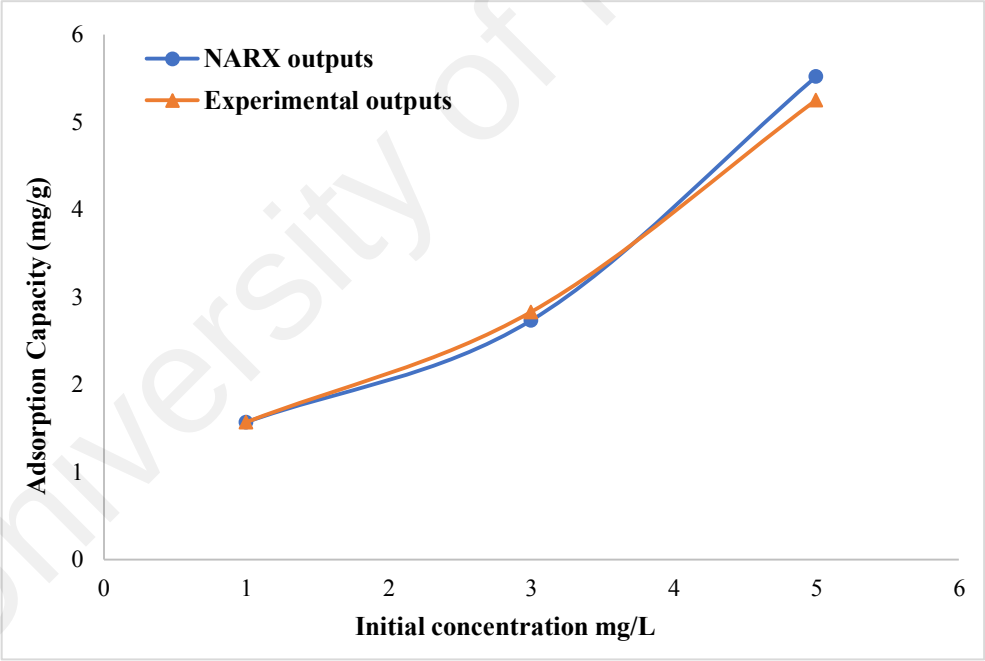

Figure 6. 4: Experimental and NARX outputs as the function of initial concentration

6.3.3.2 Effect of aqueous solution pH

The aqueous solution pH is one of the most important parameters in controlling the adsorption and ion exchange processes. It is known that the pH can affect the functional groups (i.e. amino groups, phosphate and carboxyl) protonation in the biomass, as well as the metal chemistry (i.e. its solubility) (Kazemipour, Ansari, Tajrobehkar, Majdzadeh, & Kermani, 2008; Witek-Krowiak, Szafran, & Modelski, 2011). The effect of pH was examined by varying its values from 3 to 8, and fixing all the other involved parameters such as, adsorbent dosage (20 mg), initial concentration (3 mg/L) and contact time (80 min) on their nominal levels indicated.

It can be observed in Figure 6.5 that the adsorption capacity of BK-CNTs was increased with the increase of pH value until pH 6. Thereafter, the adsorption capacity became almost steady with increasing pH from 6 to 7. It is well known that at pH more than 7.0, the dominant species of $As^{3+}$are As $(OH)^{+}$. This complexation may occur due to the extensive presence of OH^{-} at this pH level which resulted in a precipitation form (V. K. Gupta et al., 2011). In addition, the decrease of H^{+} plays a significant role in the mechanism of As^{3+} adsorption due to the decrease of competition of the adsorbent active sides. The NARX-based ANN model prediction results showed a good agreement with the experimental result trend. The NARX outputs and the experimental results as the function of pH versus the uptake capacity are presented in Figure 6.5.

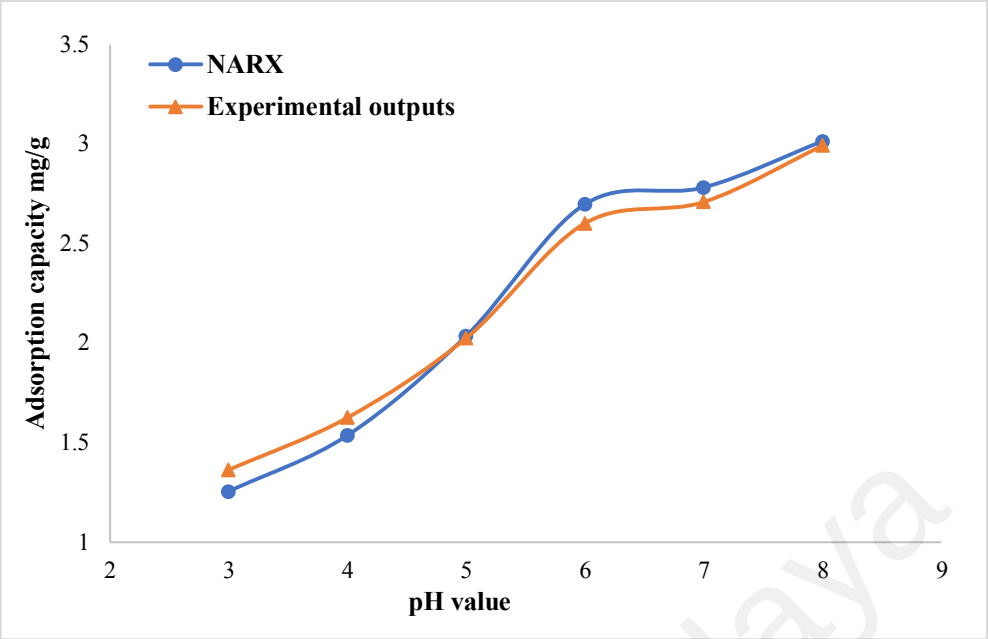

Figure 6. 5: NARX outputs and experimental data as pH function

6.3.3.3 Effect of adsorbent dosage

The effect of adsorbent dosage was studied by varying the adsorbent dosage from 20 to 40 mg under a fixed time of (80 min), initial concentration of (3 mg/L) and pH of (6). Figure 6 indicates that the adsorption capacity of As^{3+} ions was decreased by the increase in the BK-CNTs adsorbent dosage value. The adsorption capacity for 20 mg dosage was 2.85 mg/g; however, as the BK-CNTs adsorbent was increased to 30 and 40 mg the adsorption capacity was decreased to 2.01 and 1.73 mg/g, respectively. The decrease in the arsenic uptake as the adsorbent dosage increases might be attributed to the increase of more active sites due to the addition of adsorbent surface area, which is similar to other reported studies (B. Das et al., 2014). The NARX model prediction was found satisfactory for the experimental data observation as shown in Figure 6.6.

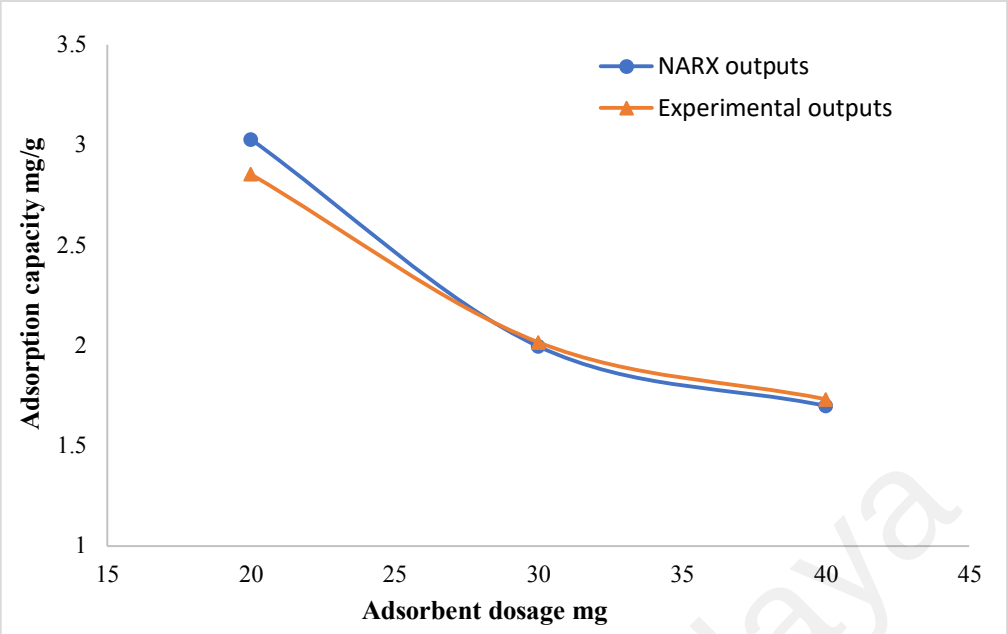

Figure 6. 6: Experimental and NARX outputs as the function of adsorbent dosage

6.3.3.4 Adsorption kinetics study

Three adsorption kinetic models were implemented in this study to investigate the As^{3+} adsorption rate and mechanism as well as the solute removal rate (Ayoob et al., 2007). The intraparticle diffusion, pseudo first order and pseudo second order models were used in this work. The kinetic studies were performed at different pH values (3, 5.5 and 8) and initial concentration (1 and 3 mg/L) with constant adsorbent dosage (40 mg) and agitation speed (180 rpm) and the results are presented in Figure 6.7 A – C.

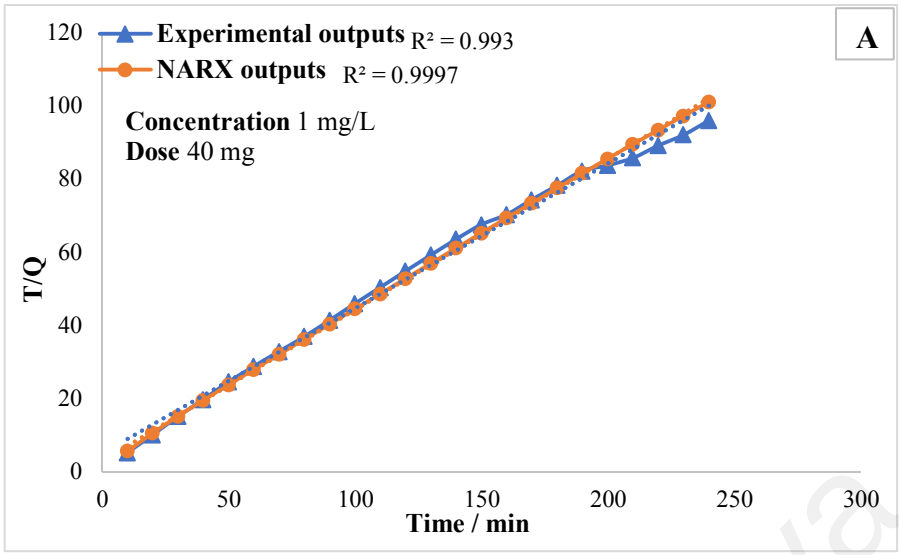

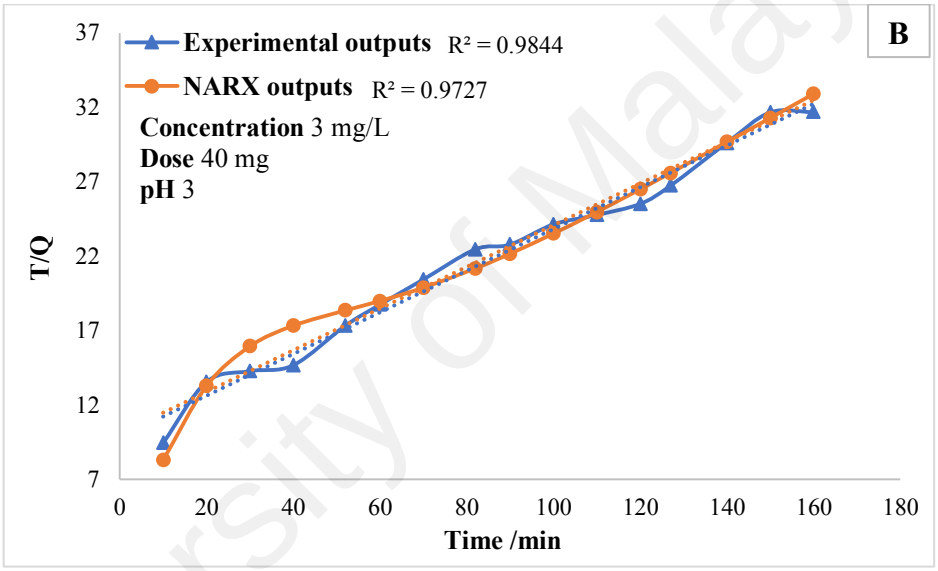

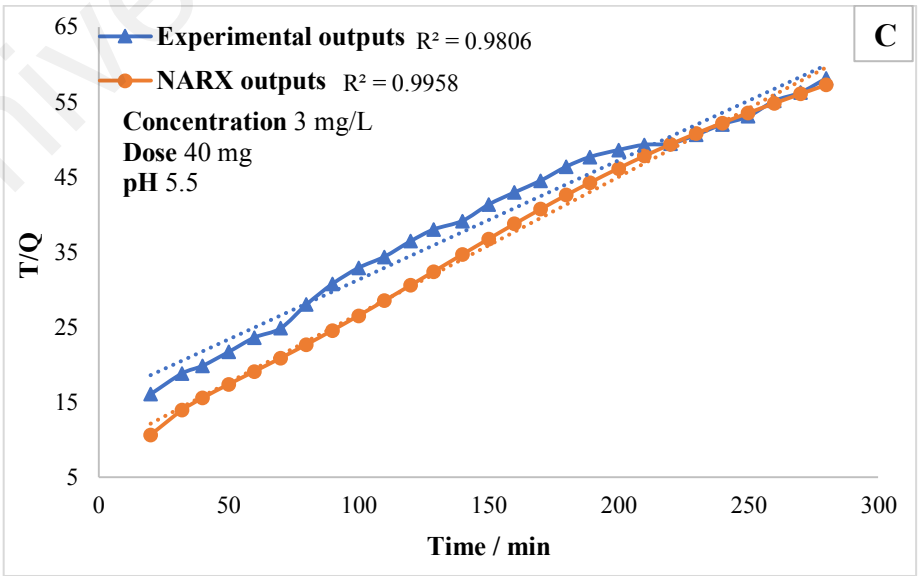

Figure 6. 7: A, B and C: Kinetics study

The correlation coefficient (R^2) were used as the conformity indicator of the kinetic models between the experiment and the predicted adsorption values for each kinetic model. The pseudo second order best described the adsorption kinetics of the system. The results of the proposed models are presented in Table 2. The kinetics study results reveal that the amount of BK-CNTs adsorbent and its concentration are associated with the rate determination step, which indicates that the rate limiting step involves chemisorption. The same behaviour was reported elsewhere (Veličković et al., 2013).

The three kinetics models used for modelling the experimental data were also applied on the NARX outputs. The pseudo second order best described the adsorption kinetics of this study as compared to the intraparticle diffusion and pseudo-first order models. The results of the kinetics study are presented in Table 6.3. The NARX model shows a good agreement with the experimental work. This can improve the high accuracy of the NARX model.

Table 6. 3: Adsorption kinetics and correlation coefficient

		Pseudo-first-order $ln(q_e–q_t)$ **vs time (t)**		**Pseudo-second-order** t/q_t **vs t**		**Intraparticle** q_t **vs** $t^{0.5}$	
PH	**C_0 mg/L**	**Experimental R^2**	**NARX output R^2**	**Experimental R^2**	**NARX outputs R^2**	**Experimental R^2**	**NARX outputs R^2**
3	3	0.7083	0.7141	0.9944	0.9927	0.8137	0.82787
5.5	3	0.6203	0.6129	0.9906	0.9958	0.8507	0.8714
8	1	0.7083	0.7859	0.993	0.9997	0.7345	0.7906

6.4 Conclusion

A new adsorbent was developed using a deep eutectic solvent system as a functionalization agent of carbon nanotubes. The functionalized CNTs showed a better result in the arsenic removal as compared to the pristine CNTs. The adsorption capacity has increased with the increase in initial concentration, contact time, and pH whereas it decreased with increasing the adsorbent dosage. The experimental data was best

described by pseudo second order kinetic model. Comparing the experiment results with the NARX model outputs using different indicators such as MSE 6.37×10^{-4}, RMSE 5.05×10^{-2}, RRMSE 8.30×10^{-3} and MAPE 3.25. It can be concluded that the NARX model was able to predict the amount of arsenic removal from water sufficiently with correlation coefficient R^2 0.9818 which is acceptable value.

CHAPTER 7: ARSENIC REMOVAL FROM WATER USING N, N-DIETHYLETHANOL AMMONIUM CHLORIDE-BASED DES-FUNCTIONALIZED CNTS: (NARX) NEURAL NETWORK APPROACH

7.1 Introduction

The presence of heavy metal ions in water is considered as a major problem due to their non-biodegradability, toxicity and human health complications. Arsenic is one of the heavy metals, known as a carcinogenic material to humans. It can be found in polluted groundwater as a results of industrial waste discharge, rock weathering, pesticides and arsenical herbicides use for agricultural purposes (Xia et al., 2014). The exposure and consumption of arsenic polluted drinking water causes numerous health problems in several countries such as Bangladesh (G. A. Wasserman et al., 2004), Bengal (Mazumder et al., 1997) and China (S.-X. Wang et al., 2007). Due to the serious health problems related to arsenic in drinking water, the World Health Organization (WHO 2001) determined the maximum allowable arsenic in the drinking water as 10 µg/L (A. H. Smith et al., 2002). Several hundreds of mg/L of arsenic concentration are available in the ground water. Consequently, millions of people are affected due to the high contaminated drinking water with arsenic (Argos et al., 2010). Many chemical, biological and physical processes have been utilized for heavy metal treatment such as precipitation, ion-exchange, reverse osmosis, biosorption, filtration and adsorption (Ahmadi et al., 2015; D.-W. Cho et al., 2015; Ding et al., 2014; X. Luo et al., 2015). Adsorption is the most suitable technique due to its cost effectiveness, feasible operation and high removal efficiency (Hu et al., 2015; Kamble et al., 2007; Kocabaş-Ataklı & Yürüm, 2013; M. L. P. Ramos et al., 2016). In addition, this method has the ability to remove small concentrations of heavy metals from a large amount of water solutions. The effectiveness of adsorption mainly dependents on the selection of appropriate process conditions such as the mass of sorbent, pH, system temperature and the process duration (E. Lourie &

Gjengedal, 2011).Various studies have been conducted using different materials like clay minerals, biomaterials and activated carbon for heavy metal ions removal from water (J. P. Chen & S. Wu, 2004; V. Gupta et al., 2006; J. U. K. Oubagaranadin & Z. Murthy, 2010). However, the use of traditional adsorbents have common drawbacks such as small adsorption capacity and low adsorption efficiency (Rao et al., 2007). Consequently, the need for highly efficient adsorbents is necessary to remove the arsenic ions from water solution. Therefore, the development of new adsorbent becomes the major interest of researchers in water treatment technology.

Nanoparticles are one of the most popular adsorbent for several pollutants, owing to their features such as, catalytic potential, small size, large surface area and high reactivity (Ali, 2012). Carbon nanotubes (CNTs) possess different properties from other material used, which make them suitable for many applications in electronics, water treatment, optics, nanotechnology and other material science fields (Atieh et al., 2011). However, carbon nanotubes have some limitations ascribed to various flaws in solubility, difficulty in manipulation and aggregation. Hence, surface modification of carbon nanotubes have magnificent affinity by interfacing with other compounds (Sun et al., 2002; Thostenson, Ren, & Chou, 2001). The CNTs surface charge can be enhanced by the oxidative functionalization. However, this method requires the use of strong acids, which is not environmentally friendly. Therefore, the need for an environmentally friendly modification technique is crucial for the widespread application of CNTs (Hayyan, Abo-Hamad, et al., 2015; Martinez et al., 2003).

Deep eutectic solvents (DESs) are identified as liquid combination formed by the complexation of hydrogen bond acceptors (HBA) and hydrogen bond donors (HBD) (Abbott, Boothby, et al., 2004; Gorke et al., 2008; Q. Zhang et al., 2012). DESs are new green solvents with many advantages as compared to the ionic liquids (ILs) (Xu et al., 2015). The prime advantages of DESs over conventional ILs are the diversity of physical

properties and different molar ratios, easy to synthesis and cheaper price of raw materials. The DESs are synthesized two or more inexpensive materials, non-flammable and usually non-toxic components which are able to connect together via hydrogen-bonding (Paiva et al., 2014). The components mixture have a lower melting point than the individual compounds(Abbott, Boothby, et al., 2004).

Recently, DESs were reported in many applications; examples of such are the uses of ChCL-based DES as a functional additive for starch-based plastics (Leroy et al., 2012), the synthesis of zeolite analogues (Cooper et al., 2004), mediums for the deposition of specific metals in electro and electroless plating of metals (Abbott et al., 2007; Abbott et al., 2008). And most recently, in nanotechnology applications (Abo-Hamad et al., 2015).

In general, the adsorption process is considered as a complicated for heavy metal removal due to the influence of many variables such as, contact time, adsorbent dosage, pH and initial heavy metal concentration. The conventional linear method for modelling this kind of process is hectic. On the other hand, artificial neural networks (ANNs) modelling technique which is known as a robust black-box modelling tool is capable of transforming a given data set into its target outputs. The ANN capability to generalize and learn the behaviour of any non-linear and complex process makes it a powerful tool. ANNs consist of a massive parallel numerical architecture which can solve the complicated problems by the assistance of highly connected neurons organised in layers. Recently, ANNs technique are used for various engineering applications (Fayaed et al., 2013a; Fiyadh et al., 2017). Some studies recommended the NARX neural network is suitable for nonlinear systems modelling (Çoruh et al., 2014; McAvoy & Werbos, 1992).

The objective of this study was to synthesis a DES by mixing glycerol (Gly) with N,N-diethylethanol ammonium chloride, for CNTs functionalization. Subsequently, the DES-functionalized CNTs was utilized as an adsorbent for arsenic removal from water.

Furthermore, the NARX neural network was used for modelling and establishing the relationship that exists between the operational variables.

7.2 Experimental and methodology

This section describes the materials used in DESs Synthesis, MWCNTs Functionalization by DES and the functionalized CNTs characterization. The materials used in the experimental work are hydrochloric acid (36.5-38%), Glycerol (Gly), potassium permanganate ($KMnO_4$), multi-wall carbon nanotube (MWCNTs) with specification of L5 μm × D 6-9 nm, >95% carbon, and sodium hydroxide pellets were all provided by SIGMA ALDRICH. Arsenic standard solution of 1000 mg/L and N,N-diethylethanol ammonium chloride (DAC)>99% purity were provided by Merck, Germany.

The DES synthesis was performed by mixing N,N- diethylethanol ammonium chloride (DAC) and Glycerol (Gly) at molar ratio of 2:1 HBD: slat (AlOmar, Hayyan, et al., 2016), at 80 ºC temperature for 3 hours until the DES becomes homogenous. The produced DES is referred to as D in this study. The prepared DES is kept in a tightly controlled environment to avoid the effect of the humidity.

The first step of the functionalization was by drying the pristine MWCNTs (P-CNTs) at 100 ºC overnight. Then, 200 mg of the dried P-CNTs was mixed with 7 ml of $KMnO_4$ and sonicated for 2 h at 65 ºC to produce K-CNTs. The functionalization of D-DES was done by mixing 7 ml of the prepared D-DES with 200 mg of K-CNTs and sonicating them at 65 ºC for 3 h to produce DK-CNTs. After that, the filtration process was performed by washing the functionalized CNT using distilled water and filtered by PTFE 0.45 μm membrane until the pH of the filtered water reached neutral. Later, the washed functionalized CNT was dried over night at 100 ºC before using it for the removal.

The Raman spectroscopy, Fourier transform infrared (FTIR) and zeta potential were used for the characterization of P-CNTs, K-CNTs and DK-CNTs adsorbent. The Raman shift obtained to identify the degree of functionalization using a Renishaw System 2000 Raman Spectrometer. The (FTIR) was used to identify the surface chemical modification of the adsorbent using Fourier transform infrared (FTIR) spectroscopy via a PerkinElmer® FTIR spectrometer USA with a range of 400-4,000 wave number and four times repetition. Zetasizer (Malvern, UK) was used to recognize the adsorbent partial surface charge by measuring the zeta potential. The surface area of the adsorbent was measured using a fully Automated Gas Sorption System (micromeritics ASAP2020, TRISTAR II 3020 Kr®, USA) (AlOmar, Alsaadi, Hayyan, Akib, & Hashim, 2016).

7.2.1 Adsorption experiments

The functionalized BK-CNTs was used for arsenic removal from water solution. The experiments were conducted with various dosages of DK-CNTs adsorbent (20 to 40 mg), arsenic concentration (1 to 5 mg/L), with different pH values (3 to 8) the pH of solution was controlled using NaOH and HCl. 50 ml of contaminated water was poured in a 250-ml flasks; the flasks were shaked at 180 rpm using a mechanical system at room temperature. The number of samples prepared in this study were 156 sample. The arsenic concentrations were tested at different interval of times to study the adsorption equilibrium time using the Inductively coupled plasma (ICP) with an OES OPTIMA 7000DV PerkinElmer® USA.

7.2.2 NARX neural network modelling and evaluation indicators

Artificial neural network is a tool that can generate and capture the linear and non-linear relationship between the dependent and independent variables (Agami et al., 2009). The NARX neural network is a dynamic network which contains various layers with a back-propagation connection (Sheng Chen et al., 1990). The NARX neural network is well known for its high speed of convergence as well as high degree of generalization.

The NARX neural network was trained and used in this study for modelling the adsorption capacity of the DK-CNTs adsorbent. NARX is a recurrent dynamic network, it consists of feedback connections with several layers. The iterative training process are used in the NARX models whereby the weights and biases are adjusted iteratively to improve the performance of the model at each step. When including the information from the exogenous inputs, the NARX models get an extra degree of freedom compared with other networks. This improves the accuracy of the models and decreases the number of parameters required for the model. The NARX outputs during the training are presented in equation 1.

$$y(t) = f(u(t-n_u),....u(t-1),u(t),y(t-n_y),....y(t-1)) \quad (7.1)$$

Where:

f is the non-linear function.

$u_{(t)}$ is the network inputs at time t.

$y_{(t)}$ is the network outputs at time t.

n_u and n_y are the order of inputs and outputs.

During the training, the outputs of the network regressed on the target of the actual values as long as they are accessible. At the training process, the values of the actual target are feed-back to the network. This basically makes a better learning and training, and the network acts as feed-forward network which is always steady. The resulting system known as NARX network, when the *f* approach is with the multi-layer perception (Sheng Chen et al., 1990). In this paper, two-layers of NARX were used presented in (Figure 7.1) for the prediction of the adsorption capacity (Q_c) of the DK-CNTs.

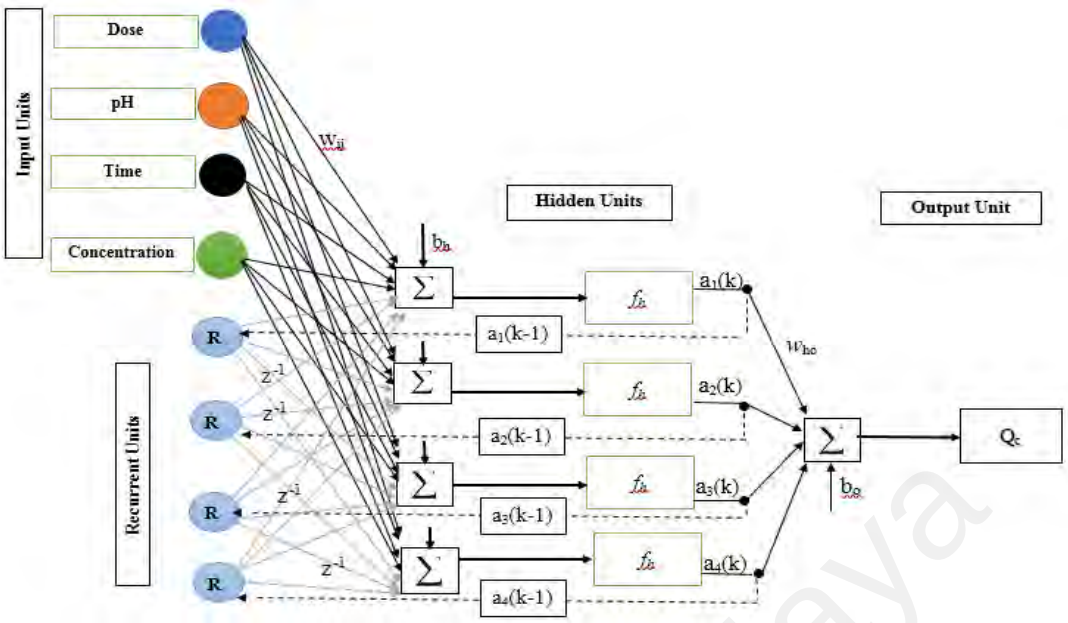

Figure 7. 1: The NARX neural network structure

The input layer of the network consists of 4 inputs (time, adsorbent dosage, pH and initial concentration) and one output layer (Q_c). In Figure 7.1, b_h is the network bias, w_{ij} is the network weight and z is the delay element.

Various indicators were employed in this study for the evaluation of the NARX model using the predicted and actual results to check the reliability of the NARX model. These indicators are the relative root mean square error (RRMSE), mean square error (MSE), root mean square error (RMSE), mean absolute percentage error (MAPE) and relative error (RE).

$$RRMSE = \left[\frac{1}{n} \sum_{t=1}^{n} \left(\frac{D_{a(t)} - D_{f(t)}}{D_{a(t)}} \right)^2 \right]^{\frac{1}{2}} \tag{7.2}$$

$$MSE = \frac{1}{n} \sum_{i=1}^{n} \left(D_{a(t)} - D_{f(t)} \right)^2 \tag{7.3}$$

$$RMSE = \left[\frac{1}{n} \sum_{t=1}^{n} \left(D_{a(t)} - D_{f(t)} \right)^2 \right]^{\frac{1}{2}} \quad (7.4)$$

$$MAPE = \frac{1}{n} \sum_{t=1}^{n} \left| \frac{\left(D_{a(t)} - D_{f(t)} \right)}{D_{a(t)}} \right| \times 100 \quad (7.5)$$

$$RE = \frac{D_{a(t)} - D_{f(t)}}{D_{a(t)}} \times 100 \quad (7.6)$$

Where:

$D_{f(t)}$ = the predicted value.

$D_{a(t)}$ = the actual value.

The RRMSE, MSE, RMSE, MAPE and RE are the indicators that were used for evaluating the model performance. The aim of using different indicators is to confirm the accuracy of the model. All the indicators are based on the obtained results by comparing the error between the actual and predicted results.

7.3 Results and Discussion

In this study, a new adsorbent was prepared (DK-CNTs), and used for arsenic removal from water. The NARX neural network was used for the modelling of the adsorption capacity and different indicators were utilized to evaluate the proposed neural network model. A sensitivity study of the involved parameters in the experimental work i.e. pH, adsorbent dosage and initial concentration were implemented. In addition, the adsorption rate order was investigated using three different kinetic models.

7.3.1 Characterization of hybrid material

Studying the electric charge of any adsorbents is crucial due to its influence on the adsorption efficiency. The zeta potential is considered as the electrical potential between the bulk fluid and the surface across the dielectrical layer attached to the suspended

particles in a solution. This potential is a source of balancing electrostatic forces that keep the micro or nano-particles stable in suspension or emulsion. Herein, the absolute zeta potential has increased from 5.5 to -37.6 mV for P-CNTs and DK-CNTs respectively. In addition, the Raman spectra shows that the I_D/I_G ratio also increased from 1.11 for the P-CNTs to 1.2 for DK-CNTs indicating the presence of new functional groups in sp^3 direction resulted from the functionalization effect of D-DES. These functional groups play a significant role in increasing the adsorption capacity of DK-CNTs. FTT-IR results were in accordance with Raman results. The sp^3 direction fictionization was observed by OH stretching appeared in the peaks around 3400 cm^{-1}. The N–H stretches in the range of 3,207 cm^{-1}. In addition, the presence of the presence of C–Cl bonds may overlap with other CO groups between 600 and 700 cm^{-1}.

It is well known that the surface area of the adsorbent provides huge effect on the adsorption system. The introduction of D-DES as functionalization agent of CNTs increased the surface area significantly from 123.5 to 200.5 m^2/g. This significant increment is reflected in the maximum adsorption capacity of DK-CNTs (Mohamed Khalid AlOmar, 2017).

7.3.2 NARX modelling and performance

Selection of the right NARX network structure with good productivity and accuracy is a complicated task, which includes many points such as the selection of the proper number of hidden layers and neurons number at the hidden layer. In general, the NARX network structure contains input layer(s), hidden layer(s) and output layer(s). The network selection has been done based on the network performance and productivity, using the MSE value during the training phase.

The parameters used in this work were arsenic concentration (1 to 5 mg/L), adsorbent dosage (20 to 40 mg), pH (3 to 8), and contact time until the equilibrium of reaction.

Hundred and sixty-five (156) combinations were prepared in lab scale and divided into two sets training and testing set, one hundred thirty-six (136) data were used for the training and twenty (20) data were used for the testing. The MATLAB R2014a computational platform was used in the current study to code and optimize the network structure. The optimum hidden layers used for the model creation are two hidden layers with 10 neurons in each hidden layer with one input layer consist of 4 nodes and one output layer with one node. The back-propagation training algorithm (*trainlm*) was selected to update the bias and weight vectors values corresponding to the momentum and the tangent sigmoid transfer function (*tansig*) was selected as the neurones transfer function for the network. The nodes numbers at the hidden layer were selected by training and testing the network using different neuron number and checking the value of the mean square error (MSE) of the testing set. The network performance is depending on the net input, weight of trainlm and tangent sigmoid transfer function tansig. The minimum value of mean square error (MSE) achieved was (4.75×10^{-4}) at the testing set, with correlation coefficient (R^2) of (0.9922), which shows a good agreement between the actual and the predicted data, the correlation coefficient plot for the testing set is presented in Figure 7.2.

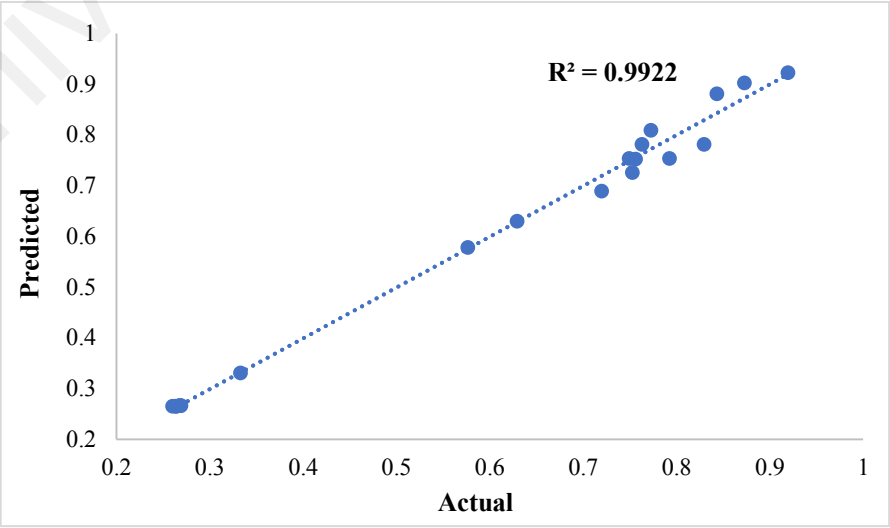

Figure 7. 2: Correlation coefficient of actual and predicted normalized arsenic removal (testing dataset)

Different indicators were used to evaluate the trained model such as the relative root mean square error (RRMSE), the root mean square error (RMSE), the mean square error (MSE) and mean absolute percentage error (MAPE). The results of all these indicators are presented in Table 7.1.

Table 7. 1: Evaluation indicators

	NARX
MSE	4.75×10^{-4}
RMSE	4.87×10^{-3}
RRMSE	2.78×10^{-3}
MAPE	2.05

The relative error is one of the indicators used in the modelling prediction it compares the actual values to predicted values Figure 7.3 shows the percentage relative error of the model, the maximum relative error value for the NARX model was 5.79 %.

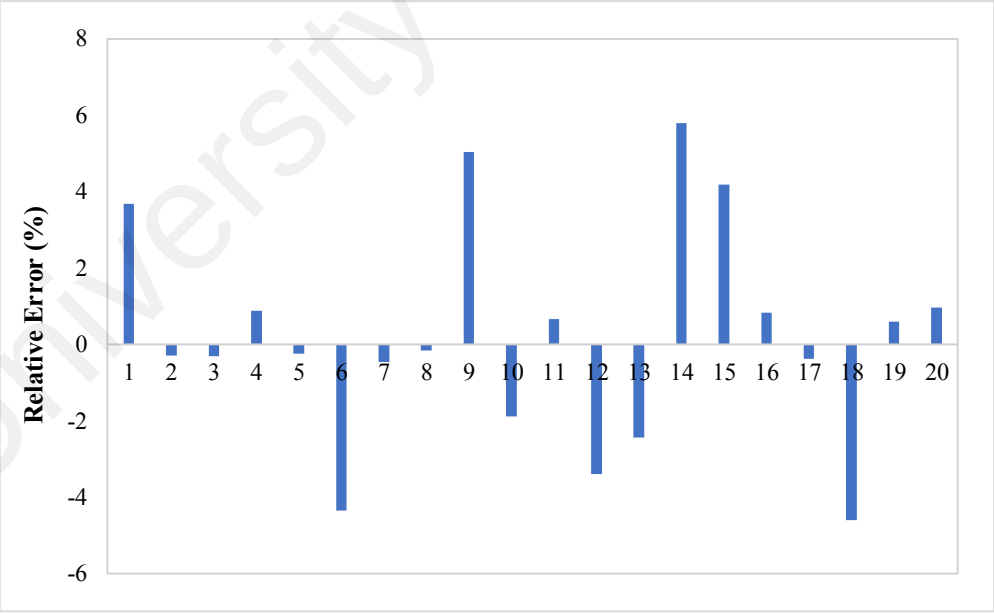

Figure 7. 3: Illustrates the accuracy of the hybrid model based on the testing dataset

The best prediction performance depends on the accuracy of the neural network training. This study is meant to get the mathematical approach benefit at the real-time experiment. The NARX model development is becoming a challenge for the real-time experiment. The prepared NARX model used for the sensitivity study involved parameters in the experimental work (initial concentration, adsorbent dosage and pH). Moreover, the kinetic models were applied one the NARX outputs in order to check the model accuracy.

7.3.3 Sensitivity study

7.3.3.1 Initial concentration

The effect of initial concentration on the adsorption was studied by varying the As^{3+} concentration from 1 to 5 mg/L, while all the other parameters such as pH (3), adsorbent dosage (20 mg) and time (5 min) were kept constant at their nominal levels indicated. The As^{3+} adsorption percentage is inversely proportional to the As^{3+} initial concentration. The adsorption capacity increases with increasing the initial metals concentration at fixed amount of adsorbent dosage. When the initial As^{3+} concentration was increased from 1 to 3 mg/L, the adsorption capacity also increased from 2.18 to 3.56 mg/g. Whereas, increasing the initial As^{3+} concentration from 3 to 5 mg/L the adsorption capacity increased from 3.56 to 5.64 mg/g. This might be attributed to the increase in the driving force of the mass transfer which led to an increase in the uptake capacity of As^{3+} ions from water solution. At low concentration, the As^{3+} ions interact with the adsorbent active sites. On the other hand, at higher As^{3+} concentration, the adsorbent active site are saturated and the removal percentage decreases (Banerjee et al., 2016). The obtained experimental data are trained using the NARX modelling techniques. The NARX model prediction results was found in a good agreement with the experimental data observation. The experimental and the NARX outputs are presented in Figure 7.4.

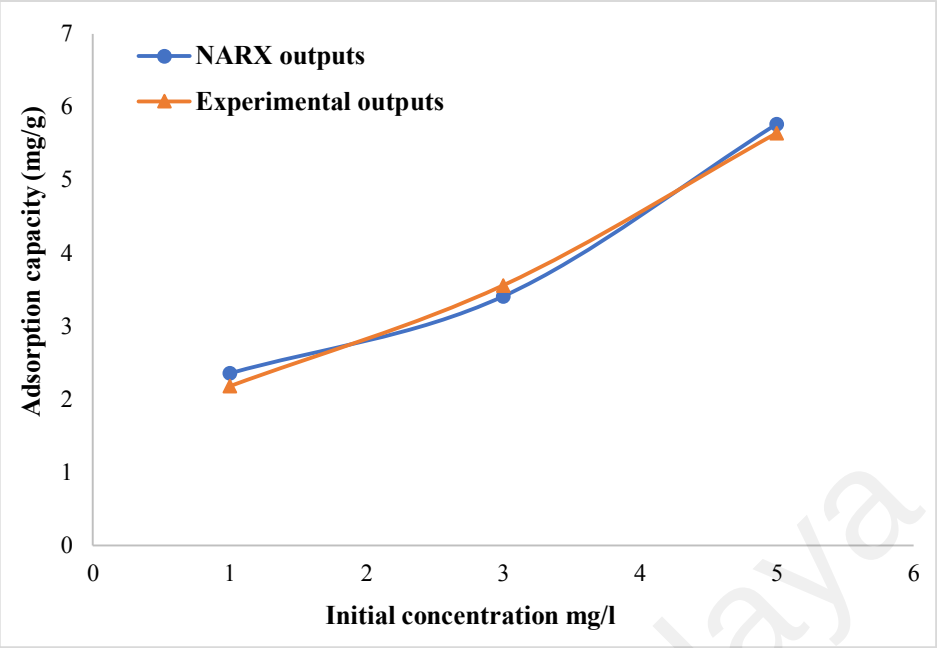

Figure 7. 4: Experimental and NARX outputs as the function of initial concentration

7.3.3.2 pH effect

The aqueous solution pH is one of the most important parameters in controlling the adsorption and ion exchange. It is known that the pH can affect the functional groups (i.e amino groups, phosphate and carboxyl) protonation in the biomass, also the metal chemistry (i.e. its solubility) (Kazemipour et al., 2008; Witek-Krowiak et al., 2011). The effect of pH was examined by varying its values from 3 to 8, and fixing all the other involved parameters such as, adsorbent dosage (20 mg), initial concentration (1 mg/L) and contact time (50 min) on their nominal levels indicated.

It can be observed in Figure 5 that the adsorption capacity of DK-CNTs was increased with the increase of pH value until pH 6. Thereafter, the adsorption capacity became almost steady with increasing pH from 6 to 8. This increase may be due to the presence of negative charge of the oxygen containing functional groups such as carboxylic group and the concentration of the negative electron charges enhanced by the presence of OH^- in the solution. This pattern of negative charge intensive distribution on the surface of the

adsorbent that may be responsible for metal binding. It is well known that at pH more than 7.0, the dominant species of As^{3+}. This complexation may occur due to the extensive presence of OH^- at this pH level which resulted in a precipitation form this phenomenon also stated by(V. K. Gupta et al., 2011). In addition, the decreasing of H^+ plays a significant role in the mechanism of As^{3+} adsorption due to the decrease of competition of the active sides of the adsorbent. The NARX technique was used for the modelling and prediction of the obtained data from the experimental work. The NARX-based ANN model prediction results showed a good agreement with the experimental result trend. The NARX outputs and the experimental results as the function of pH versus the uptake capacity are presented in Figure 7.5.

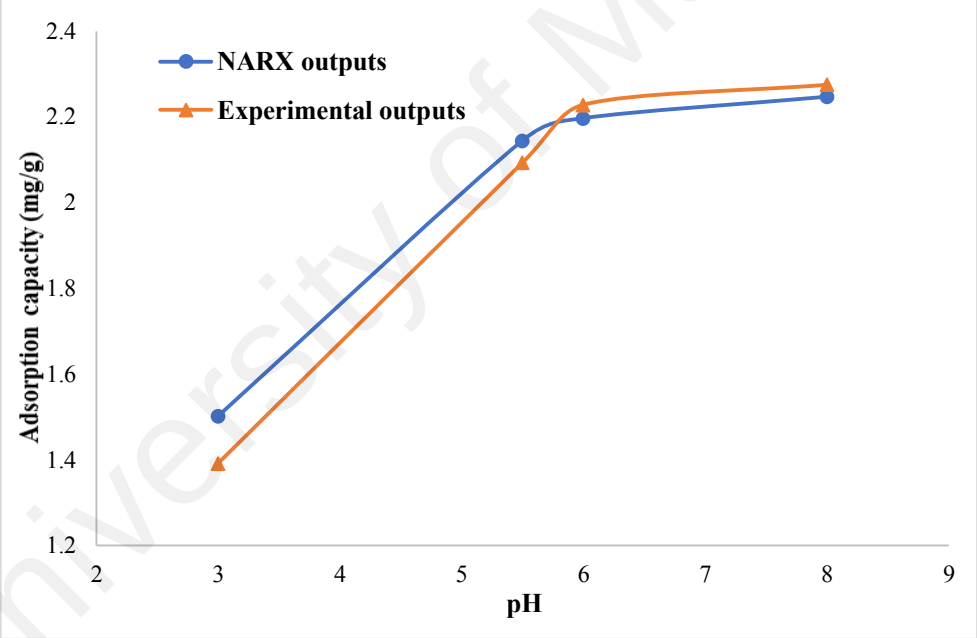

Figure 7. 5: NARX outputs and experimental data as pH function

7.3.3.3 Adsorbent dosage study

The effect of adsorbent dosage was studied by varying the adsorbent dosage from 20 to 40 mg under fixed time of (90 min), initial concentration of (3 mg/L) and pH of (6). It is obtained from Figure 6 that the adsorption capacity of As^{3+}ions decreased by increasing

the DK-CNTs adsorbent dosage value. The adsorption capacity for 20 mg dosage was 7.56 mg/g then, as the DK-CNTs adsorbent was increased to 30 and 40 mg the adsorption capacity was decreased to 6.23 and 5.89 mg/g, respectively. The decrease in the arsenic uptake capacity as the adsorbent dosage increases might be attributed to the increase of more active sites due to the addition of adsorbent surface area, it is also reported by (B. Das et al., 2014). The obtained experimental data were trained and predicted by using the NARX modelling techniques. The NARX model prediction was found satisfactory for the experimental data observation. The experimental and predicted outputs of the NARX are presented in Figure 7.6.

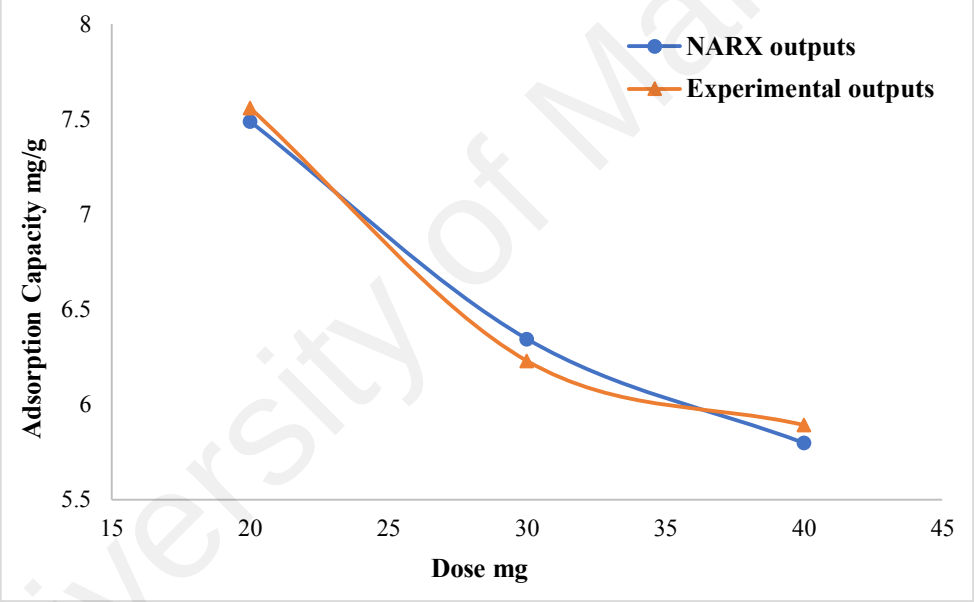

Figure 7. 6: Experimental and NARX outputs as the function of adsorbent dosage

7.3.3.4 Adsorption kinetics study

Three adsorption kinetic models were implemented in this study to investigate the As^{3+} adsorption rate and mechanism as well as the solute removal rate (Ayoob et al., 2007). The intraparticle diffusion, pseudo first order and pseudo second order models were used in this work. The kinetic studies were achieved at different pH values (3, 5.5

and 8) and initial concentration (1 and 3 mg/L) with different adsorbent dosage (20 and 30 mg) and agitation speed (180 rpm). The correlation coefficient (R^2) were used as the conformity indicator of the kinetic models between the experiment and the predicted adsorption values for each kinetic model. The pseudo second order best described the adsorption kinetics of the system the results are presented in Figure 7.7 A – H, time over adsorption capacity (T/Q). The results of the intraparticle diffusion, pseudo first order are presented in Table 7.2. The kinetics study results reveal that the amount of DK-CNTs adsorbent and its concentration are associated with the rate determination step, which indicates that the rate limiting step involves chemisorption. The same behaviour was reported elsewhere (Veličković et al., 2013).

Table 7. 2: Adsorption kinetics and correlation coefficient

			Pseudo-first-order $ln(q_e–q_t)$ vs time (t)		Pseudo-second-order $(t/q_t vs\ t)$		Intraparticle $(q_t vs\ t^{0.5})$	
Dose mg	PH	C_0 mg/L	Experimental R^2	NARX output R^2	Experimental R^2	NARX outputs R^2	Experimental R^2	NARX outputs R2
20	3	1	0.8925	0.9052	0.9973	0.9979	0.7471	0.7172
20	8	1	0.5483	0.5997	0.9983	0.9988	0.6496	0.6244
20	3	3	0.656	0.6819	0.9711	0.963	0.7931	0.7311
20	5.5	3	0.7858	0.7017	0.9562	0.9897	0.6775	0.6884
30	5.5	3	0.8939	0.8682	0.9978	0.9909	0.5338	0.5848
30	8	3	0.6758	0.6069	0.9905	0.9945	0.7542	0.795
30	3	1	0.756	0.7888	0.9994	0.9974	0.5921	0.5229
30	5.5	1	0.8102	0.8608	0.9999	0.9994	0.674	0.6838

NARX neural network technique was used for modelling and prediction of the obtained data from the experimental work. The three kinetics models used for modelling the experimental data were also applied on the NARX outputs. The pseudo second order best described the adsorption kinetics of this study as compared to the intraparticle diffusion and pseudo-first order models. The results of the kinetics study are presented in

Table 7.2. The NARX model shows a good agreement with the experimental work, this can improve the high accuracy of the NARX model.

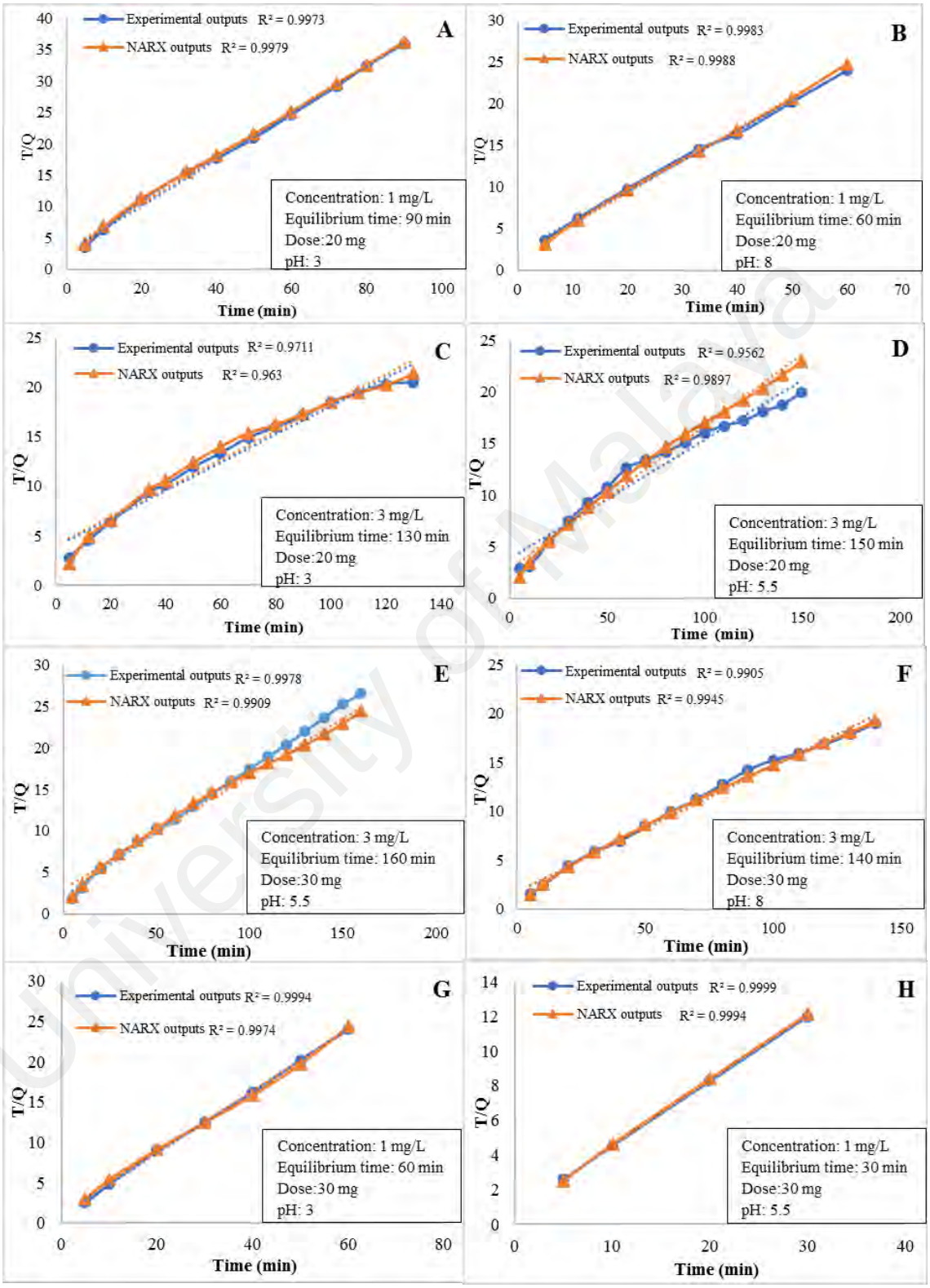

Figure 7. 7 A – H: Kinetics study

7.4 Conclusion

A new adsorbent was developed using deep eutectic solvent system as functionalization agent of carbon nanotubes. The functionalized CNTs showed a better result in the arsenic removal compared to the pristine CNTs. The amount of arsenic removal increased with the increasing of contact time, pH and initial concentration, whereas the arsenic removal decreased with increasing adsorbent dosage. Comparing the experiment results with the NARX model outputs, it can be concluded that the NARX model able to predict the amount of arsenic removal from water sufficiently with acceptable error. The minimum value of mean square error (MSE) achieved was (4.75 10^{-4}) at the testing set, with correlation coefficient (R^2) of (0.9922), which shows a good agreement between the actual and the predicted data, other indicators was used such as, the RMSE 4.87×10^{-3}, RRMSE 2.78×10^{-3} and MAPE 2.05. All these indicators approved the high accuracy of the NARX model.

CHAPTER 8: MERCURY REMOVAL FROM WATER USING TETRA-N-BUTYL AMMONIUM BROMIDE (TAB) BASED DES-FUNCTIONALIZED CNTS:(NARX) NEURAL NETWORK APPROACH

8.1 Introduction

Mercury is known as one of the toxic heavy metals, it can be found in water and wastewater. With its long and short terms on the impact of human health, it can be distributed at large areas, it can contaminate both local and distant lakes and rivers, also can affect the central of nerve system, young children and infants at highest risk and putting the children in utero. The major problem of mercury (Hg^{2+}) pollution is in many countries such as China, Iraq, Japan and Brazil (S. K. Das, Das, & Guha, 2007; G.-B. Jiang, Shi, & Feng, 2006). Mercury go into the water and wastewater by many ways including chlor-alkali manufacturing process, tattoo inks, paints and mining (Leopold, Foulkes, & Worsfold, 2010; Mousavi, Chávez, Ali, & Cabaniss, 2011). It is well realized that water pollution by mercury is the source of public health problems, even at low concentration at the drinking water (Blue, Van Aelstyn, Matlock, & Atwood, 2008). The World Health Organization determined the maximum allowable mercury concentration in the drinking water is 2.0 mg/L (S.-X. Li, Feng-Ying, Yang, & Jian-Cong, 2011).

Different methods were used to remove mercury from water solution such as ion exchange (Chiarle et al., 2000), coagulation (Henneberry et al., 2011), and oxidation-precipitation (Tresintsi et al., 2012). However, these techniques have some limitations include efficiency and costs, the adsorption technique has been used for the removal of various heavy metals (AlOmar, Alsaadi, Hayyan, Akib, & Hashim, 2016; Jingming Gong et al., 2012; Ricardo et al., 2018). Many studies were performed utilizing different materials type to remove mercury ions from water including activated carbon (J. P. Chen & S. Wu, 2004) clay minerals (J. U. K. Oubagaranadin & Z. Murthy, 2010), and

biomaterials (V. Gupta et al., 2006). However, the use of traditional materials have some limitations such as small adsorption capacity and low adsorption efficiency (Rao et al., 2007). Therefore, the need for new adsorbent with high efficient is necessary for mercury ions removal from water solution.

Carbon nanotube (CNTs) have different properties from other materials which make it convenient to several applications in nanotechnology, electronics, water treatment, optics and some fields of material science (Atieh et al., 2011). CNTs is the most effective material were used for the removal of different pollutants from water solution (Abbas et al., 2016; AlOmar, Alsaadi, Hayyan, et al., 2016a). The CNTs application have some limitations such as aggregation, difficulty in manipulation and various flaws in solubility. On the other hand, CNTs have an advantage which can interact with other compounds after surface modification (AlOmar, Alsaadi, Hayyan, et al., 2016a; Thostenson, Ren, & Chou, 2001). The CNTs oxidative functionalization is the way to increase the CNTs surface charge, this way required a strong acid unfavourable environmentally. Therefore, the need for new environmentally friendly functionalization agent is crucial (Hayyan, Abo-Hamad, et al., 2015; Martinez et al., 2003).

Deep eutectic solvents (DESs) which is one of the ionic liquid analogy, the DESs used as the ionic liquid (ILs) replacement as cheaper material and environmentally friendly, the DESs were presented by Abbot et al. in 2003 (Abbott et al., 2003). The DESs use have some benefit comparing to the use of ILs including cheaper price, easy to synthesis, verity of physical properties and can be used in different molar ratios. The DESs are usually made of more than two non-toxic components, non-flammable and inexpensive materials which have the ability to connect by hydrogen-bond (AlOmar, Alsaadi, Hayyan, Akib, & Hashim, 2016; Paiva et al., 2014).

Generally, the adsorption process is considered as one of the effective method for heavy metals removal but, due to the influence of many variables such as, contact time, adsorbent dosage, pH and initial heavy metal concentration considered as complicated to understand the relationships between the involved variables. The use of the conventional linear method for modelling this kind of process is hectic. Therefore, artificial neural networks (ANNs) techniques are a robust tool which can recognize a given data set into their target outputs. The ANN capability to generalize and learn the behaviour of any non-linear and complex process makes it a robust tool. Recently, ANNs technique are used for various engineering applications (Fiyadh et al., 2017; Ghosal & Gupta, 2016; León-Roque, Abderrahim, Nuñez-Alejos, Arribas, & Condezo-Hoyos, 2016; Pivetta et al., 2013; Rudnitskaya, Ehlert, Legin, Vlasov, & Büttgenbach, 2001; Zafar et al., 2016).

The aims of this study are to synthesis a deep eutectic solvents (DESs) using tetra-n-butyl ammonium bromide (TAB) and glycerol (Gly) as hydrogen bond donor (HBD), the (TAB) is used as functionalization agent of CNTs. Then, the functionalized CNTs were utilized as adsorbent to remove mercury ions from water. Moreover, NARX neural network is used for the modelling of the adsorption process. The Neurosolution tool is also used in the sensitivity study to investigate the effect of every parameter involved in the adsorption process.

8.2 Methods and experiments

The materials and chemicals used in this study were multi-wall carbon with D × L 6-9 nm × 5µm > 95% (carbon) specification hydrochloric acid (36.5-38 %), sodium hydroxide pellets, potassium permanganate, nitric acid (65 %), sulfuric acid (95 – 97 %), Gly and TAB all were supplied from SIGMAALDRICH. Mercury stander solution of 1000 mg/L was supplied from MERCK.

To synthesize the DESs, the TAB was mixed with Gly as a (HBD) using magnetic stirring at 80 ºC with 400 rpm, the mixing time until the DESs become a liquid with no precipitation to prepare (T-DES). The details of molar ratio, characterization and synthesis are based on (AlOmar, Hayyan, et al., 2016). The pristine CNTs (P-CNTs) surface was functionalized by oxidation with $KMnO_4$ using the sonication technique at 65 ºC for 2 h (AlSaadi et al., 2016), the functionalized CNTs is denoted by k-CNTs in this study. Later, the k-CNTs was functionalized with the prepared T-DES by mixing 7 ml of the T-DES with 200 mg of k-CNTs by sonication at 65 ºC for 3 h, the result of the mixture denoted by Tk-CNTs, each functionalization step was followed by washing step with distal water using PTFE 0.45 μm membrane and vacuum pump until the pH of the filtered water reach to neutral. Later, the washed functionalized Tk-CNTs was dried over night at 100 ºC before using it for the removal.

The Fourier transform infrared (FTIR), Raman spectroscopy and zeta potential are used for the P-CNTs, k-CNTs and Tk-CNTs adsorbents. To identify the adsorbent surface chemical modification the Fourier transform infrared (FTIR) spectroscopy was used, via PerkinElmer® FTIR spectrometer USA with a range from 400-4,000 wave number and four times repetition. The Raman shift obtained to identify the degree of functionalization using a Renishaw System 2000 Raman Spectrometer. The Zetasizer (Malvern, UK) was used to identify the adsorbent partial surface charge by measuring the zeta potential. The surface area of the adsorbent was measured using a fully Automated Gas Sorption System (micromeritics ASAP2020, TRISTAR II 3020 Kr®, USA) (AlOmar, Alsaadi, Hayyan, Akib, & Hashim, 2016).

8.2.1 Adsorption experiments

The functionalized Tk-CNTs was used for the removal of mercury from water solution. The experimental work was conducted with different values of pH (3, 5.5, 6 and 8), mercury concentration (1, 3 and 5 mg/L) and adsorbent dosages of Tk-CNTs (5, 20

and 30 mg). A 50 ml of contaminated water was poured in a 250-ml flask, the flasks were shacked at 180 rpm using a mechanical system at room temperature. A total of 163 samples were prepared in this study at different conditions. The mercury concentrations were tested at different interval of times to study the adsorption equilibrium dynamics using the Inductively coupled plasma (ICP) with an OES OPTIMA7000DV PerkinElmer® USA.

8.2.2 Modelling and evaluation of NARX neural network

The NARX neural network is a recurrent dynamic network, and it is a nonlinear autoregressive network with an exogenous input, it consists of several layers and an output feedback connection (Sheng Chen et al., 1990). By comparing the NARX network with other networks, the NARX network has a high convergence speed and generalization degree. In the NARX neural network the iterative training process are used, the biases and weight are modified iteratively to progress the model performance in each step.

During the training, the outputs of the network are regressed on the target of the actual values as long as they are accessible and, the values of the actual target are feed-back to the network. This basically makes a better learning and training, and the network acts as feed-forward network which is always steady.

When including the information from the exogenous inputs, the NARX models get an extra degree of freedom as compared with other networks. This improves the accuracy of the models and decreases the number of parameters required for the model. The NARX outputs during the training are presented in equation 8.1.

$$y(t) = f\left[u(t-n_u),....u(t-1),\ u(t),\ y(t-n_y),....\ y(t-1)\right] \tag{8.1}$$

Where:

f is the non-linear function.

u(t) is the network inputs at time t.

y(t) is the network outputs at time t.

n_u and n_y are the order of inputs and outputs.

The resulting system known as NARX network, when the *f* approach is with the multi-layer perception (Sheng Chen et al., 1990). A NARX neural network was trained and used in this study for modelling the adsorption capacity of the Tk-CNTs adsorbent for mercury removal from water. In this work, two-layers of NARX were used presented in Figure 8.1, for the prediction of the adsorption capacity (Q_c) of the Tk-CNTs.

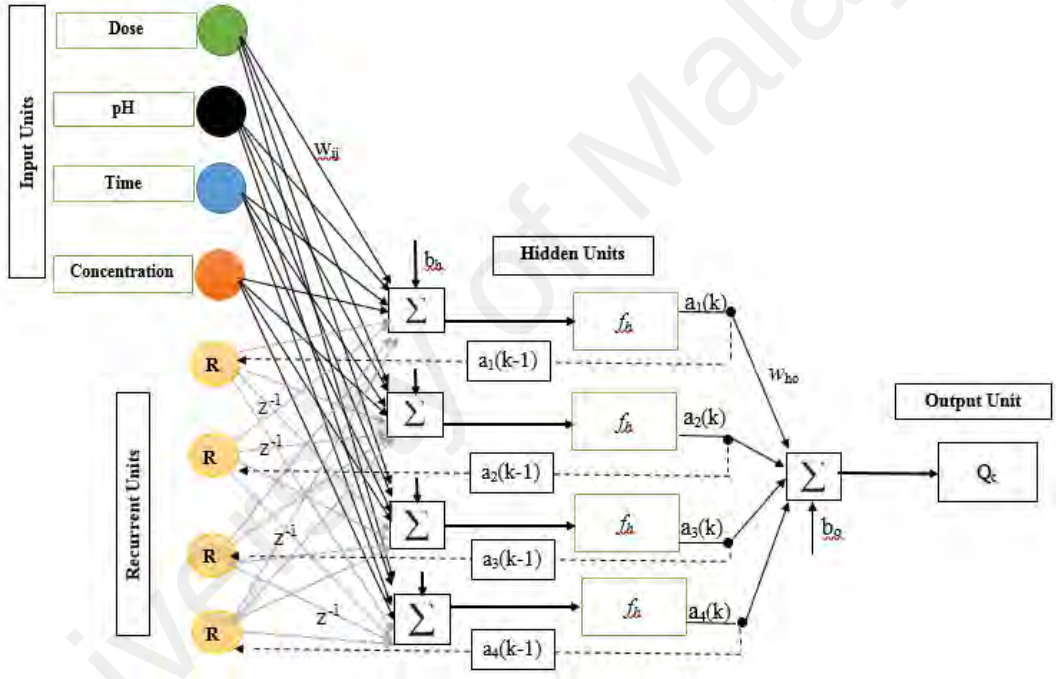

Figure 8. 1: The NARX neural network structure

The input layer of the network consists of 4 inputs (time, adsorbent dosage, pH and initial concentration) and one output layer (Q_c). In Figure 8.1, b_h is the network bias, w_{ij} is the network weight and z is the delay element. A total of 163 datasets were fed for the modelling of NARX network. The NARX neural network development includes various steps including the experimental data required for the training, the network testing, the

testing data are not included in the training part. The trainbr was select for the network training using the MATLAB R2014b; in this work different configurations are tested to find the suitable network structure with the best performance. The optimum network structure used for the model creation are two hidden layers with 10 neurons in each hidden layer with one input layer with 4 nodes and one output layer with one node, the tangent sigmoid transfer function (*tansig*) was selected as the network transfer function.

Various indicators were employed in this study for the evaluation of the NARX model using the predicted and actual results to check the reliability of the NARX model. These indicators are the relative root mean square error (RRMSE), mean square error (MSE), root mean square error (RMSE), mean absolute percentage error (MAPE) and relative error (RE).

$$RRMSE = \left[\frac{1}{n} \sum_{t=1}^{n} \left(\frac{D_a(t) - D_f(t)}{D_a(t)} \right)^2 \right]^{\frac{1}{2}} \tag{8.2}$$

$$MSE = \frac{1}{n} \sum_{i=1}^{n} \left(D_a(t) - D_f(t) \right)^2 \tag{8.3}$$

$$RMSE = \left[\frac{1}{n} \sum_{t=1}^{n} \left(D_a(t) - D_f(t) \right)^2 \right]^{\frac{1}{2}} \tag{8.4}$$

$$MAPE = \frac{1}{n} \sum_{t=1}^{n} \left| \frac{\left(D_a(t) - D_f(t) \right)}{D_a(t)} \right| \times 100 \tag{8.5}$$

$$RE = \frac{D_a(t) - D_f(t)}{D_a(t)} \times 100 \tag{8.6}$$

Where:

$D_f(t)$ = the predicted value at time t.

$D_a(t)$ = the actual value at time t.

The RRMSE, MSE, RMSE, MAPE and RE are the indicators that were used for evaluating the model performance. The aim of using different indicators is to confirm the accuracy of the model. All the indicators are based on the obtained results by comparing the error between the actual and predicted results.

8.3 Results and discussion

The Tk-CNTs adsorbent was used for the removal of mercury from water solution, NARX neural network method was proposed for the modelling of the Tk-CNTs adsorption capacity and studying the influence of every involved parameter in the experimental work on the Tk-CNTs adsorption capacity. The sensitivity analysis on the model system input-output parameters has been carried out in order to assess the effectiveness of the input parameters on the proposed system model output. Therefore, evaluation of the model performance considering various possible combinations of the model input parameters was scrutinizing. Furthermore, the adsorption rate order was investigated using three different kinetic models.

8.3. 1 Characterization of hybrid material

Studying the adsorbent electrical charge is important due to its effect on the efficiency of adsorbents. The Zeta potential measure the electrical potential between the surfaces across the dielectrical layer attached to the suspended particles in a solution and the bulk fluid. This potential is the balancing electrostatic forces source that keeps the nano-particles or micro stable in emulsion or suspension. The zeta potential was used on the P-CNTs and the Tk-CNTs, the absolute value of the zeta potential is increased from 5.5 the P-CNTs to 59.7 for the Tk-CNTs. Moreover, Raman spectra result showed an increase in the I_D/I_G ratio from 1.11 for the P-CNTs to 1.175 for the Tk-CNTs, which shows the effect of the new functional groups in sp^3 direction resulted from the functionalization

effect of T-DES. The functional group is the key to increase to adsorption capacity of the Tk-CNTs adsorbent. The result of the FTT-IR showed a good agreement with the Raman spectra result, the sp3 direction functionization was observed by OH stretching appeared in the peaks around 3172 cm^{-1}. However, in the region between (3000–3600 cm^{-1}), the OH and CH may overlap. In addition, the presence of of C-Br has been detected in the range of 550-650 cm^{-1}. It is known that the adsorbent surface area has an influence on the adsorption process, thus using the T-DES as a CNTs functionalization agent increased the adsorbent surface area from 123 to 204 m^2/g and the poor size dimeter increased from 20.49 to 124.87 Å. This increment will result in an increase in the adsorption capacity of the Tk-CNTs adsorbent (AlOmar, Alsaadi, Jassam, Akib, & Hashim, 2017).

8.3.2 NARX modelling and performance

The adsorption of mercury from water solution using functionalized CNTs was modelled using the artificial neural network by MATLAB R2014a software. A total of 163 data set prepared in lab scale was fed to the NARX network to model the adsorption capacity of Tk-CNTs adsorbent. Different parameters were involved in the experimental work and later included in the modelling such as, adsorbent dosage (5, 20 and 30 mg), mercury ions concentration (1, 3 and 5 mg/L), pH (3, 5.5, 6 and 8) and contact time at different intervals. Hundred and sixty-three (163) dataset were prepared in lab scale, (143) of the data were used for the training of the network and 20 data were used for the testing set.

The selection of the proper NARX network structure with high accuracy and productivity is hectic task, due to the effect that many factors are included such as the number of hidden layer, the neurons at each layer and the transfer function type. In this work, different number of nodes, hidden layer and transfer function type were used to select the optimum structure, the network selection structure was based on the network

productivity and performance, using the MSE value during the training step initially later, the network performance was tested based on the testing set using different indicators.

Based on the best performance obtained from the training and the testing, two hidden layers with 10 neurons at each hidden layer with one input layer consist of 4 nodes and one output layer with one node. The back-propagation training algorithm (trainbr) was selected to update the bias and weight vectors values corresponding to the momentum and the tangent sigmoid transfer function (tansig) was selected as the neurones transfer function for the network. The network performance depends on the net input, weight of trainbr and tangent sigmoid transfer function tansig. Different indicators were used to evaluate the trained model such as the relative root mean square error (RRMSE), the root mean square error (RMSE), the mean square error (MSE) and the mean absolute percentage error (MAPE). The results of the used indicators are presented in Table 8.1.

Table 8. 1: Evaluation indicators

	NARX
MSE	4.28×10^{-6}
RMSE	2.07×10^{-3}
RRMSE	1.77×10^{-2}
MAPE	1.15

The minimum value of mean square error (MSE) achieved was (4.28×10^{-6}) at the testing phase, with correlation coefficient (R^2) of (0.9998), which indicate a good agreement between the actual and the predicted data, the correlation coefficient R^2 plot for the testing set is presented in Figure 8.2. The relative error (RE) was used as an indicator to compare the actual values to predicted values. Figure 8.3 shows the results of the relative error of the model, the maximum relative error value for the NARX model was 3.49 %. The best prediction performance depends on the accuracy of the neural network training. The prepared NARX model was tested using the sensitivity study with

involving all the parameters included in the experimental work (initial concentration, adsorbent dosage and pH).

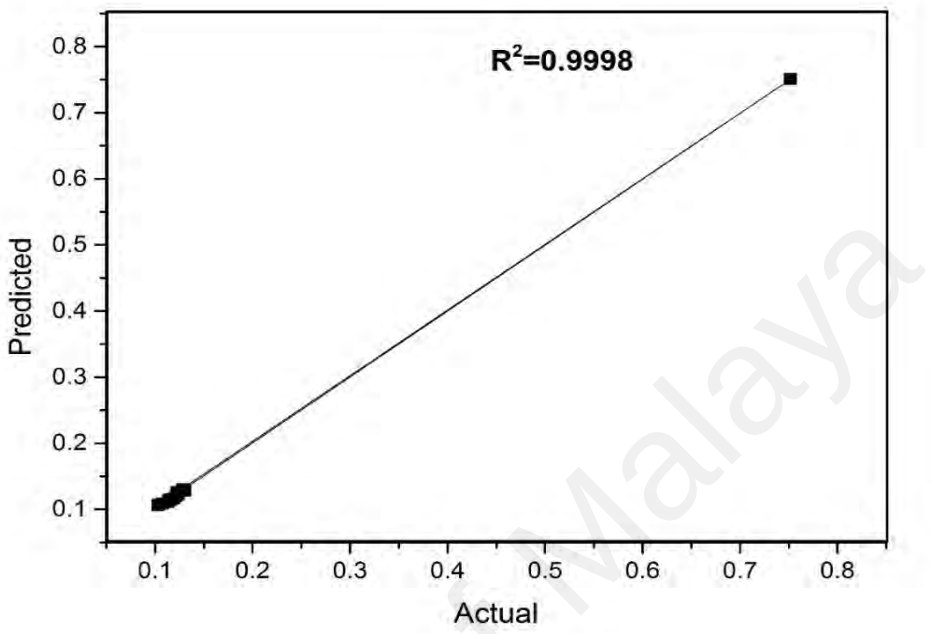

Figure 8. 2: Correlation coefficient of actual and predicted mercury removal (testing dataset)

Figure 8. 3: Illustrates the accuracy of the hybrid model based on the testing dataset

8.3.3 Sensitivity study

8.3.3.1 Effect of adsorbent dosage

The Tk-CNTs adsorbent dosage can affect the heavy metals adsorption, the effect of Tk-CNTs adsorbent was studied by varying the dose from 5 to 30 mg. The other involved parameters were fixed to pH (6), mercury concentration (5 mg/L) and time (120 min). Based on the obtained results presented in Figure 8.4, the adsorption capacity is decreased but the total of mercury ions removal is increased. The diminution in the adsorption density maybe attributed to the fact that some adsorbent site remains not saturated during the adsorption progression (Bandaru et al., 2013; B. Das et al., 2014). It is obtained from the experimental work that the adsorption capacity for 5 mg dosage was 12.79 mg/g then, as the Tk-CNTs adsorbent was increased to 20 and 30 mg the adsorption capacity was decreased to 7.85 and 6.70 mg/g, respectively. The obtained experimental data were trained and predicted by using the NARX modelling techniques. The NARX model prediction was found satisfactory for the experimental data observation. The experimental and predicted outputs of the NARX are presented in Figure 8.4.

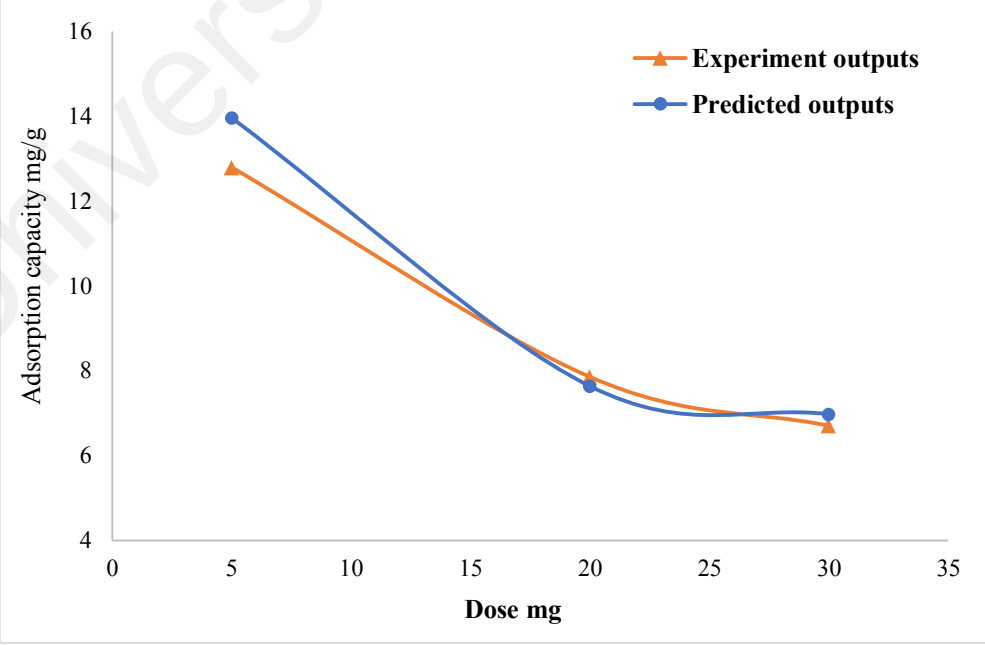

Figure 8. 4: Experimental and NARX outputs as the function of adsorbent dosage

8.3.3.2 Effect of aqueous solution pH

The solution pH has a strong effect in the adsorption process of heavy metals, it is known that the pH can affect the functional groups (i.e. amino groups, phosphate and carboxyl) protonation in the biomass, as well as the metal chemistry (i.e. its solubility) (Kazemipour et al., 2008; Witek-Krowiak et al., 2011). To study the effect of pH on the removal of Hg^{2+} ions using the Tk-CNTs adsorbent an experimental work was conducted using different values of pH and keeping the other involved parameters as constant. The other involved parameters were fixed such as amount of adsorbent dosage (20 mg), Hg^{2+} ions concentration (3 mg/L) and contact time (70 min).

The relationship between the adsorption capacity and the pH can be defined by the electrostatic mechanism between the adsorbent negative charge and the mercury species. From the results presented at Figure 8.5, the higher adsorption capacity is at lower value of pH, at pH 3 the adsorption capacity was 137.14 mg/g, but at higher value of pH (5.5) the adsorption capacity decreased to 80.75 mg/g. Moreover, by increasing the pH value to 6 and 8 the adsorption capacity decreased to 72.05 and 67.40 respectively. This is due to the fact that with low value of pH, the adsorbent active sites are protonated highly, which lead to a higher attraction between the anion and the adsorbent negatively charged resulting in a higher adsorption capacity. Whereby, at higher value of pH the adsorbent capacity is decreased, this process might happen due to the ionization of adsorbent acidic or repulsive force might happen between the mercury ions and the adsorbent negatively charged. The NARX network was used for the modelling and prediction of the Tk-CNTs adsorption capacity using the data obtained from the experimental work, the predicted results showed a good agreement with the experimental result. The NARX outputs and the experimental results as the function of pH versus the adsorption capacity are presented in Figure 8.5.

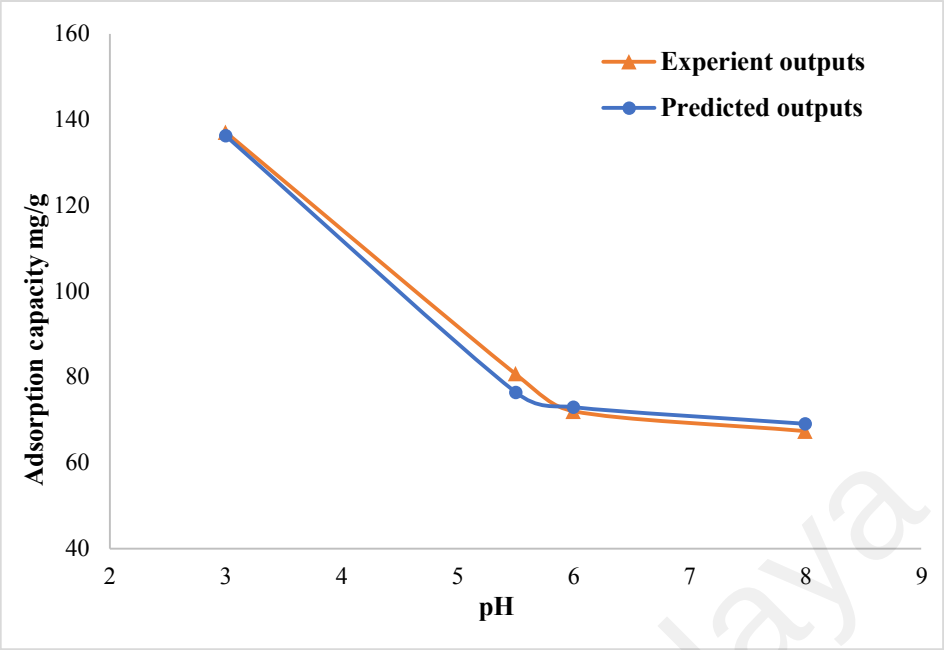

Figure 8. 5: NARX outputs and experimental data as pH function

8.3.3.3 Effect of initial mercury concentration

The relationship between the mercury ions concentration and the uptake capacity can be present clearly by the experimental work. By increasing the mercury initial concentration in the solution and fixing the adsorbent dosage, the percentage removal of mercury ions will decrease due to the limited active sites of adsorbents. Whereby, with low concentration of mercury ions in the solution the adsorption capacity will decrease due to the availability of active sites of adsorbents.

To study the effect of mercury concentration, different amounts of mercury concentration were used (1, 3 and 5 mg/L) and the other involved parameters were fixed such as the adsorbent dosage (20 mg), contact time (120 min), pH (6). In this work, the experimental results reveal that by increasing the mercury concentration in the water solution the adsorption capacity increases as well. At 1 mg/L ions concentration the adsorption capacity was 4.92 mg/g whereby, increasing the ions concentration to 3 and 5 the adsorption capacity increased to 10.17 and 20.97 mg/g respectively. The increase in

the adsorption capacity with the increase of ions concentration can cause a higher collision probability between the adsorbents active sites and the adsorbent molecules, higher active sites occupation and thus higher adsorption capacity (Zabihi, Asl, & Ahmadpour, 2010). The obtained experimental data are trained using the NARX modelling techniques. The NARX model prediction results was found in a good agreement with the experimental data observation. The experimental and the NARX outputs are presented in Figure 8.6.

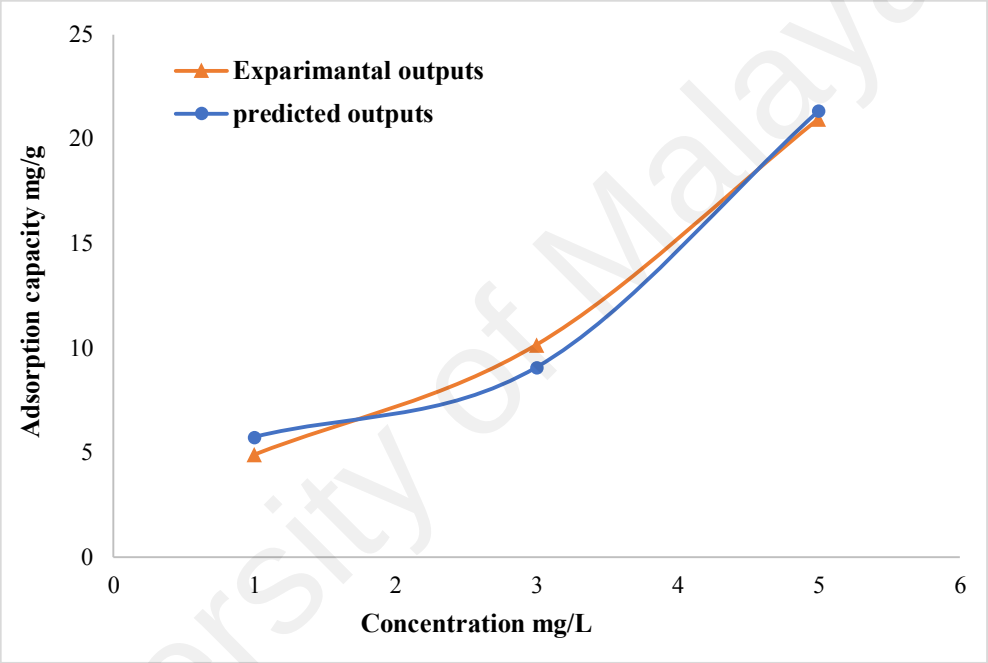

Figure 8. 6: Experimental and NARX outputs as the function of initial concentration

8.3.3.4 Influence of Parameter

The main purpose of carrying out the sensitivity analysis is to identify the parameters significance and evaluate the parameters influence, in the systems such as the adsorption system it is challenging to explore the system behaviour using the traditional methods. The sensitivity analysis of the adsorption process has been carried out in order to study the influence of the input parameters such as the adsorbent dosage, pH, contact time and

initial concentration on the accuracy of predicted output value. In other way, the sensitivity analysis attempt to examine how the input parameters could influence positively or negatively on the change of the output value. As a result of performing the sensitivity analysis and identify the weight of each model input parameters on the system model output accuracy is to optimize the system design and to qualify the system uncertainty. In addition, the sensitivity analysis for the adsorption process could provide a deep understanding on the different input parameters influence and the difference on the outputs. To conduct an effectively sensitivity analysis study, it needs to be conducted with different input parameters with different number of trial runs. Based on the sensitivity analysis results presented in Figure 8.7, the influence of the initial concentration of mercury ions on the adsorption capacity of Tk-CNTs adsorbent was 49.5%, which shows the higher influence because, the concentration is the driving force of the mass transfer between the media and the surface of the adsorbents, therefore, it has a significant effect on the adsorption capacity. Whereby, the contact time was 41.3 % this is due to the fact that the contact time is the adsorption uptake, it is obviously high because it is logically the main operating parameter. The influence of adsorbent dosage and pH was 5.4 % and 3.8 % respectively.

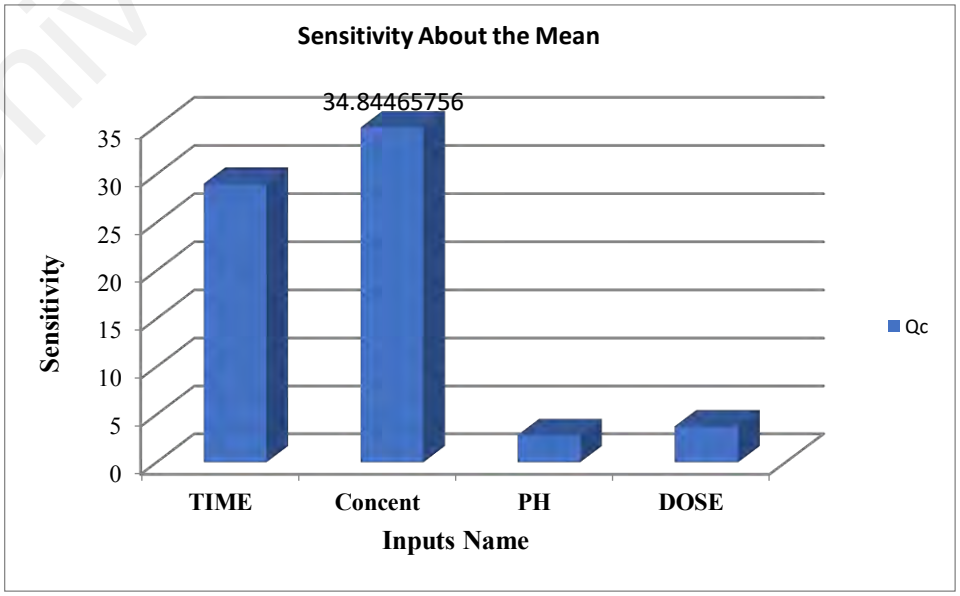

Figure 8. 7: Influence of parameters

8.3.3.5 Adsorption kinetics study

In this work, the kinetics of mercury removal using the Tk-CNTs adsorbent was examined using three well known reaction models such as, Pseudo first-order, Pseudo second order and Intraparticle diffusion, the kinetics models were applied to know the Tk-CNTs adsorption behaviour. The conditions of kinetic study were, adsorbent dose 20 mg, initial mercury ions concentration 5 mg/L and the pH value were varied 3, 6 and 8, different time intervals were used and the correlation coefficient R^2 was used as conformity indicator in this work. Based on the results presented in Figure 8.8, the Tk-CNTs adsorption kinetics fit to the pseudo-second order model with higher value of correlation coefficient R^2 comparing to the intraparticle diffusion and pseudo-first order models (C. Zhang et al., 2012). The results of the intraparticle diffusion and pseudo first order are presented in Table 8.2.

Table 8. 2: Adsorption kinetics and correlation coefficient

			Pseudo-first-order $ln(q_e–q_t)$ *vs time (t)*		Pseudo-second-order $(t/q_t$ *vs t)*		Intraparticle $(q_t$ *vs* $t^{0.5})$	
Dose mg	PH	C_0 mg/L	Experimental R^2	NARX output R^2	Experimental R^2	NARX outputs R^2	Experimental R^2	NARX outputs R^2
20	3	5	0.9121	0.9148	0.9975	0.9985	0.9205	0.9226
20	6	5	0.8599	0.8971	0.99	0.9923	0.9246	0.9256
20	8	5	0.624	0.5873	0.9994	0.9928	0.5951	0.5657

NARX neural network technique was used for modelling and prediction of the obtained data from the experimental work. The three kinetics models used for modelling the experimental data were also applied on the NARX outputs. The pseudo second order is the best described the adsorption kinetics of this study as compared to the intraparticle diffusion and pseudo-first order models. The results of the kinetics study are presented in Table 8.2, the NARX model shows a good agreement with the experimental work, this can improve the high accuracy of the NARX model.

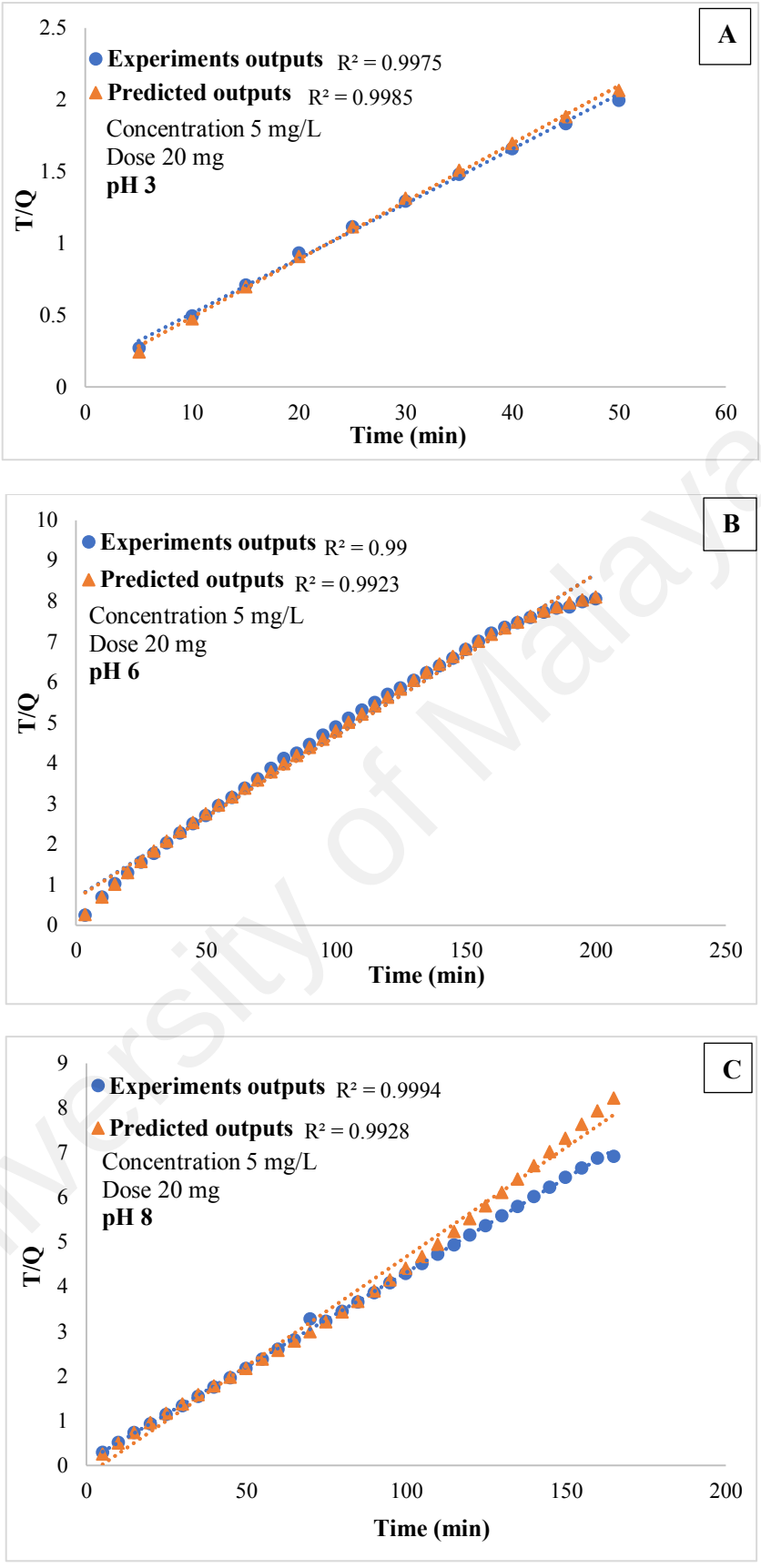

Figure 8. 8 A, B and C: Pseudo second order adsorption kinetics study

8.4 Conclusion

A successful adsorbent for mercury removal was prepared using tetra-n-butyl ammonium bromide (ATB) based DES as CNTs functionalization agent. A NARX neural network modelling technique was used successfully. Different indicators were used to evaluate the NARX model, the NARX model was able to map the adsorption process accurately. The effect of different parameters including mercury ions concentration, pH, amount of adsorbent dosage and contact time was studied. Three kinetics models such as Pseudo first-order, Pseudo second order and Intraparticle diffusion were applied on the experimental and predicted data, the Pseudo second order was the best described. A sensitivity study was conducted using different parameters.

CHAPTER 9: ALLYL TRIPHENYL PHOSPHONIUM BROMIDE-BASED DES-FUNCTIONALIZED CNTS FOR MERCURY REMOVAL FROM WATER: ARTIFICIAL NEURAL NETWORK MODELLING APPROACH

9.1 Introduction

The most toxic heavy metal is mercury, it has a serious influence on the human health and the environment (Rice, Walker Jr, Wu, Gillette, & Blough, 2014). The mercury poisoning effect is mostly on the renal disorders and neurological, mercury easily passes through the brain barrier and influence the brain. The high mercury concentration is the source of impairment the function of kidney and pulmonary (Davodi, Ghorbani, & Jahangiri, 2017). Mercury availability and toxicity are described in the chemical form that it is found. Mercury can be released from different sources, due to its long-rang, bioaccumulability, and high toxicity the removal of mercury gain a huge concern (Pacyna et al., 2010). The mercury (Hg^0) element is highly insoluble and volatile in water; therefore, it is problematic to be removed using a traditional method (Hsi, Lee, Hwang, & Chen, 2010).

However, different techniques were used to remove mercury ions from water solutions including membrane separation (Lopes et al., 2007), flotation, reverse osmosis (Chojnacki, Chojnacka, Hoffmann, & Gorecki, 2004; Evangelista, DeOliveira, Castro, Zara, & Prado, 2007), chemical precipitation (Huttenloch, Roehl, & Czurda, 2003), mechanical filtration (Biester, Schuhmacher, & Müller, 2000), ion exchange (Oehmen, Viegas, Velizarov, Reis, & Crespo, 2006), and adsorption (Pattanayak et al., 2000). These traditional methods have some drawback; therefore, the need to use a better method with high efficiency is required. The adsorption was proved as a cost-effective and efficient method, it is recommended strongly (Oubagaranadin, Sathyamurthy, & Murthy, 2007). The effectiveness of adsorption is majorly dependent on the selection of appropriate

process condition, including the mass of sorbent, pH, system temperature and the process duration (E. Lourie & Gjengedal, 2011). Many adsorbent have been used for heavy metals removal including activated carbon (Kadirvelu, Kavipriya, Karthika, Vennilamani, & Pattabhi, 2004), magnetic adsorbent (Azari et al., 2017), low cost natural materials (Davis, 1993; Sreedhar, Madhukumar, & Anirudhan, 1999), biomaterials, clay minerals (V. Gupta et al., 2006; J. U. K. Oubagaranadin & Z. Murthy, 2010) and carbon nanotubes (CNTs) (Abbas et al., 2016).

A high efficiency of adsorption material with high sensitivity and surface area for Hg^{2+} detection and absorption is required. Carbon nanotubes (CNTs) have different physicochemical properties from other materials used as adsorbents that make it suitable for many applications in water treatment, nanotechnology, electrics, optic and other material science fields (Atieh et al., 2011). Regardless, the some limitations of CNTs such as the difficulty of manipulations, aggregation and solubility, the CNTs have a great property by interaction with other compounds by surface functionalization (Sun et al., 2002; Thostenson, Ren, & Chou, 2001).

Recently, a high interest in the development of green and environmentally friendly solvents in the analytical studies. Deep eutectic solvents (DESs) have gain a huge interest as green solvent in many applications. DESs have a great superior in term of low toxicity, easy to synthesis and materials availability. Deep eutectic solvents (DESs) which is one of the ionic liquid analogy, DESs are used as the ionic liquid (ILs) replacement as cheaper material and environmentally friendly, the DESs were presented by Abbot et al. in 2003 (Abbott et al., 2003). The DESs consists of two or more safe components that are able to associate with each other by mostly occasional electrostatic, van der Waals force and hydrogen bonding (Q. Zhang et al., 2012; B.-Y. Zhao et al., 2015). The DESs melting point is lower than the individual component melting point.

The adsorption process is proposed in this study which is considered as an effective process comparing to the other techniques but, it is a complicated process due to, the influence of many variables such as contact time, adsorbent dosage, mercury concentration and pH and it has not standardized and modelled yet. Consequently, the need to use a powerful modelling technique is required, the artificial neural networks (ANNs) techniques are a robust tool which can recognize a given data set into their target outputs. The ANN capability to generalize and learn the behaviour of any non-linear and complex process makes it a robust tool. Recently, ANNs technique are used for various engineering applications (Fiyadh et al., 2017; Ghosal & Gupta, 2016; W. Li, Wei, Jiao, Qi, & Liu, 2016; Zafar et al., 2016).

The objectives of this study are; to use the deep eutectic solvents (DESs) as a combination of allyl triphenyl phosphonium bromide and glycerol (Gly) as hydrogen bond donor (HBD) as a functionalization agent of the carbon nanotubes (CNTs). To use the DESs functionalized (CNTs) as adsorbent to remove mercury ions from water. To use the layer recurrent neural network and the NARX neural network for the modelling of the adsorption process and compare their behaviours in term of accuracy and productivity.

9.2 Methods and experiments

The chemicals and materials used in this study are the multi-wall carbon nanotubes (MW-CNTs) with D × L 6-9 nm × 5μm > 95% (carbon) specifications, hydrochloric acid (36.5 – 38 %), sodium hydroxide pellets, potassium permanganate and glycerol (Gly) all were provided from SIGMA-ALDRICH. The allyl triphenyl phosphonium bromide (APB) and mercury standard solution of 1000 mg/L were provided from MERCK.

The synthesize of DESs is conducted by mixing the glycerol (Gly) as a (HBD) with the (APB) using the magnetic stirring at 80 ºC and 400 rpm, the mixing time was until

the DESs reached to a liquid state without any precipitation, the produced product referred as (A-DESs) in this study. The molar ratio details, synthesis and characterization are based on (AlOmar, Hayyan, et al., 2016). A primary oxidation was conducted to oxidize the surface of pristine CNTs (P-CNTs) with $KMnO_4$ at 65 ºC for 2 h (AlSaadi et al., 2016), the functionalized CNTs referred to as (k-CNTs). Later, 7 ml of the prepared A-DESs was sonicated with 200 mg of the k-CNTs at 65 ºC for 3 h to produce (Ak-CNTs) adsorbent. The functionalization steps were followed by washing step with distal water using vacuum pump and PTFE 0.45 µm membrane until the pH of the filtered water reach to neutral. Then, the washed functionalized Ak-CNTs adsorbent was dried at 100ºC over night before using it for the mercury ions removal.

The adsorption process was conducted with different values of the involved parameters such as pH, adsorbent dosage, mercury initial concentration and the contact time. The Ak-CNTs adsorbent was prepared to remove the mercury ions from water solution; three different amounts of Ak-CNTs adsorbent were used (10, 20 and 30) mg, the utilized mercury ion concentrations were (1, 3 and 5) mg/L, while the pH values were (3, 5.5, 6 and 8) and the contact time was until the equilibrium was achieved. Different amounts of the Ak-CNTs was added to 50 ml of Hg^{2+} stock solution into a 250 ml flack with different values of pH and mercury concentrations. The prepared flasks were placed in a mechanical system with a shaking speed of 180 rpm at a room temperate. A total of 176 samples were prepared in this study at different conditions. The mercury concentrations were tested at different interval of times to study the adsorption performance using the Inductively coupled plasma (ICP) with an OES OPTIMA7000DV PerkinElmer® USA.

The zeta potential, Fourier transform infrared (FTIR) and Raman spectroscopy are utilized for the characterization of the P-CNTs, k-CNTs and Ak-CNTs adsorbents. In order to identify the adsorbent particles surface charge by measuring the zeta potential

the Zetasizer (Malvern, UK) was used. To obtain the surface chemical modification of adsorbent the transform infrared (FTIR) spectroscopy is utilized, using PerkinElmer® FTIR spectrometer USA with a range from 400-4,000 wave number. The Raman shift is obtained to identify the degree of functionalization using the Renishaw System 2000 Raman Spectrometer.

9.2.1 Artificial neural networks

The artificial neural networks are formed from a single neuron that are connected and arranged in a way that is described by their architecture (Wunsch, Liesch, & Broda, 2018). There are three stages of the modelling are the training, validation and testing, during the training stage the dataset are fed to the network and a selected algorithm works to fit the provided dataset by adjusting the weights that connects the neurons. During the training stage a transfer functions such as sigmoid or linear works to determine the calculations that are occur during the processing of the data. The classify, sigmoid transfer functions nonlinear response qualifies the ANN to detect the nonlinear relationship during training of the dataset (Samarasinghe, 2016). The multi-layer perceptron (MLP) is the most common and simple artificial neural network used that is allocated to the feed-forward networks (FFNs). The FFNs consists of multi-layers including single input layer, single or multi-hidden layers (HL) and a single output layer. A particular feature which is the connections arrangements between the layers permits the information passes forward to the output layer only. Some of the networks uses the feedback connections which permitting the information to pass backwards or laterally within the network, that are named as recurrent neural network (RNN) (Govindaraju, 2000). The NARX neural network is a recurrent dynamic network, and it is a nonlinear autoregressive network with an exogenous input, it consists of several layers and an output feedback connection (Sheng Chen et al., 1990). In this work, the layer recurrent

neural network (LRNN) and the NARX neural network are proposed for the modelling of the adsorption capacity of the functionalized CNTs.

The layer recurrent neural network (LRNN) is a recurrent network, each layer of the network has a recurrent connection associated with hidden layer and the output layer. The tap delay associated in the network permits the network to have a dynamic response to the inputs samples of the time series (Olaofe, 2014). Moreover, the layer recurrent is similar to the distributed delay network and time delay with a finite input response. The LRNN is classified by the backward connection presence at the output of the hidden layer connected to the input of the hidden layer as a context unit. The selection of proper network structure is depending on different variables such as the type of transfer function, number of hidden layer, number of neurons at the hidden layer. The best performance of the LRNN model was by using two hidden layers, 15 neurons with a tansig transfer function.

The NARX neural network is a recurrent dynamic network, and it is a nonlinear autoregressive network with an exogenous input, it consists of several layers and an output feedback connection (Sheng Chen et al., 1990). By comparing the NARX network with other networks, the NARX network has a high convergence speed and generalization degree. In the NARX neural network the iterative training process are used, the biases and weight are modified iteratively to progress the model performance in each step. During the training, the outputs of the network are regressed on the target of the actual values as long as they are accessible and, the values of the actual target are feed-back to the network. This basically makes a better learning and training, and the network acts as feed-forward network which is always steady.

When including the information from the exogenous inputs, the NARX models get an extra degree of freedom as compared with other networks. This improves the accuracy

of the models and decreases the number of parameters required for the model. The NARX outputs during the training are presented in equation 9.1.

$$y(t) = f\left[u(t-n_u),....u(t-1),\ u(t),\ y(t-n_y),....\ y(t-1)\right] \quad (9.1)$$

Where:

f is the non-linear function.

u(t) is the network inputs at time t.

y(t) is the network outputs at time t.

n_u and n_y are the order of inputs and outputs.

The resulting system known as NARX network, when the *f* approach is with the multi-layer perception (Sheng Chen et al., 1990). A NARX neural network was trained and used in this study for modelling the adsorption capacity of the Tk-CNTs adsorbent for mercury removal from water. In this work, two-layers of NARX were used presented in Figure 9.1, for the prediction of the adsorption capacity (Q_c) of the Tk-CNTs. The input layer of the network consists of 4 inputs (time, adsorbent dosage, pH and initial concentration) and one output layer (Q_c). In Figure 9.1, b_h is the network bias, w_{ij} is the network weight and z is the delay element. A total of 176 datasets were fed for the modelling of NARX network. The NARX neural network development includes various steps including the experimental data required for the training, validation and the network testing. The training and validation data set has been developed as parallel session in order to train and validate the model before switching to the testing session which is based on unseen data input. In details, 151 records of the data were used for the training and validation of the network and 25 data were used for the testing set. The (trainbr) was select for the network training using the MATLAB R2014b; in this work different configurations are tested to find the suitable network structure with the best performance. The optimum network structure used for the model creation are three hidden layers with

10 neurons in each hidden layer with one input layer with 4 nodes and one output layer with one node, the tangent sigmoid transfer function (tansig) was selected as the network transfer function.

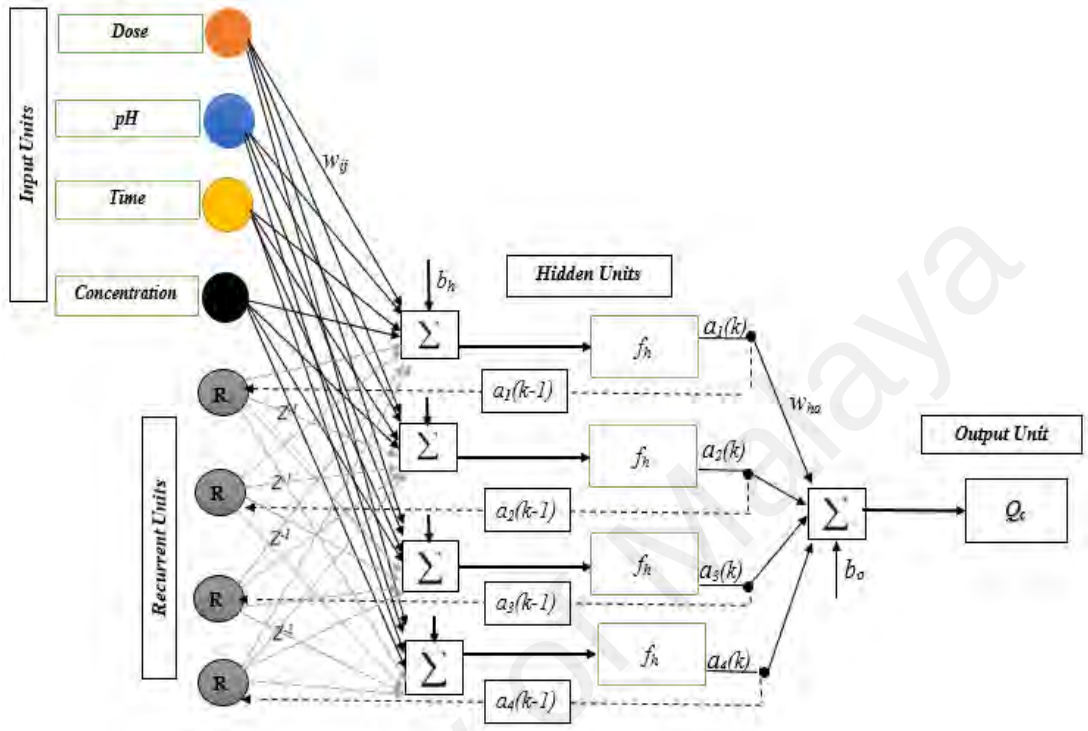

Figure 9. 1: The NARX neural network structure

Various indicators were used in this study for the evaluation of the NARX and LRNN models using the predicted and actual results to check the reliability of the NARX and LRNN models. These indicators are the relative root mean square error (RRMSE), mean square error (MSE), root mean square error (RMSE), mean absolute percentage error (MAPE) and relative error (RE).

$$RRMSE = \left[\frac{1}{n} \sum_{t=1}^{n} \left(\frac{D_a(t) - D_f(t)}{D_a(t)} \right)^2 \right]^{\frac{1}{2}} \tag{9.2}$$

$$MSE = \frac{1}{n} \sum_{i=1}^{n} \left(D_a(t) - D_f(t) \right)^2 \tag{9.3}$$

$$RMSE = \left[\frac{1}{n} \sum_{t=1}^{n} \left(D_a(t) - D_f(t) \right)^2 \right]^{\frac{1}{2}} \tag{9.4}$$

$$MAPE = \frac{1}{n} \sum_{t=1}^{n} \left| \frac{\left(D_a(t) - D_f(t) \right)}{D_a(t)} \right| \times 100 \tag{9.5}$$

$$RE = \frac{D_a(t) - D_f(t)}{D_a(t)} \times 100 \tag{9.6}$$

Where:

$D_f(t)$= the predicted value at time t.

$D_a(t)$= the actual value at time t.

The RRMSE, MSE, RMSE, MAPE and RE are the indicators that were used for evaluating the model performance. The aim of using different indicators is to confirm the accuracy of the model. All the indicators are based on the obtained results by comparing the error between the actual and predicted results.

9.3 Results and discussion

The removal of mercury ions from water solution and the NARX neural network as a modelling technique for modelling the adsorption capacity of the functionalized carbon nanotube were the focus of this study. The Ak-CNTs adsorbent was used in this study, different amounts of the adsorbent were used 5, 20 and 30 mg. The efficiency of the adsorbent was examined using various values of initial concentration (1, 3 and 5) mg/L, different values of pH (3, 5.5, 6 and 8). The contact time was used until the equilibrium state in this study. Different samples were conducted at different time using various variables values including amount of adsorbent dosage, initial concentration values and pH values therefore, the total samples prepared were 176. The effect of the involved input parameters on the adsorption capacity of Ak-CNTs was studied. The evaluation of the

model performance was conducted using different indicators such as the relative root mean square error (RRMSE), mean square error (MSE), root mean square error (RMSE), mean absolute percentage error (MAPE) and relative error (RE).

9.3.1 Characterization of hybrid material

Studying the adsorbent electrical charge is important due to its effect on the efficiency of adsorbents. The Zeta potential measure the electrical potential between the surfaces across the dielectrical layer attached to the suspended particles in a solution and the bulk fluid. This potential is the balancing electrostatic forces source that keeps the nanoparticles or micro stable in emulsion or suspension. The zeta potential was used on the P-CNTs and the Ak-CNTs, the absolute value of the zeta potential is increased from 5.5 the P-CNTs to 52.3 for the Ak-CNTs. Moreover, Raman spectra result showed an increase in the I_D/I_G ratio from 1.11 for the P-CNTs to 1.18 for the Ak-CNTs, which shows the effect of the new functional groups in sp3 direction resulted from the functionalization effect of A-DES. The functional group is the key to increase the adsorption capacity of the Ak-CNTs adsorbent. The results revealed that the O-H stretch disappeared after functionalization with A-DES. The presence of O-H is probably due to adsorbed water on the hydrophilic CNTs surface and that was noticeable in the case of K-CNTs. The functionalization with A-DES reduced the hydrophilicity and enhancing the drying process of the sample, this was the reason behind the disappearing of OH_ from the FT-IR spectrums of Ak-CNTs and P-CNTs. The presence of PO_4^{-3} was observable in the 500-600 cm^{-1} range and the C-Br stretch is also detected in the 550-650 cm^{-1} range. It is known that the adsorbent surface area has an influence on the adsorption process, thus using the A-DES as a CNTs functionalization agent increased the adsorbent surface area from 123 to 199.366 m^2/g and the poor size dimeter increased from 20.49 to 127.34 Å. This increment will result in an increase in the adsorption capacity of the Ak-CNTs adsorbent.

9.3.2 Neural network performance

The removal of mercury ions from water using the Ak-CNTs adsorbent was modelled by the artificial neural network tool using MATLAB R2014a software. The experimental data set prepared in lab scale of a total 176 data set then was fed to the neural network for modelling the adsorption capacity of Ak-CNTs adsorbent. Different parameters were involved in the experimental work and later included in the modelling such as, adsorbent dosage (5, 20 and 30 mg), mercury ions concentration (1, 3 and 5 mg/L), pH (3, 5.5, 6 and 8) and contact time at different intervals. Hundred and seventy-six (176) dataset were prepared in lab scale. A total of hundred and fifty-one (151) records of the data were used for the training and validation of the network and twenty-five (25) record were used for the testing.

In this work two neural network types were used and compared based on their productivity and performance, the best model was used for studying the effect of the parameters such as pH, adsorbent dosage, initial concentration and kinetic studies. The relative error (RE) of the NARX model presented in Figure 9.2 with a maximum error of 9.79 %, and the coefficient correlation (R^2) which is presented in Figure 9.3 with a value of 0.9701.

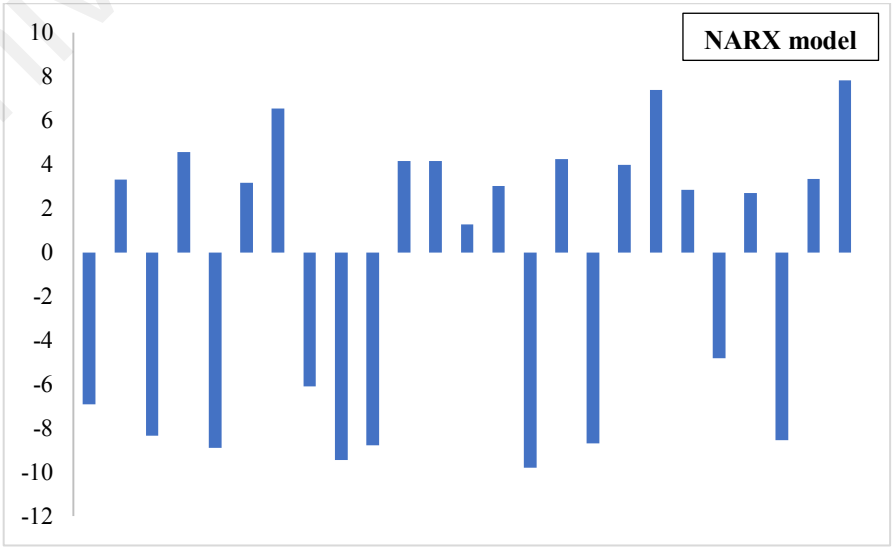

Figure 9. 2: The relative error (RE) of NARX model

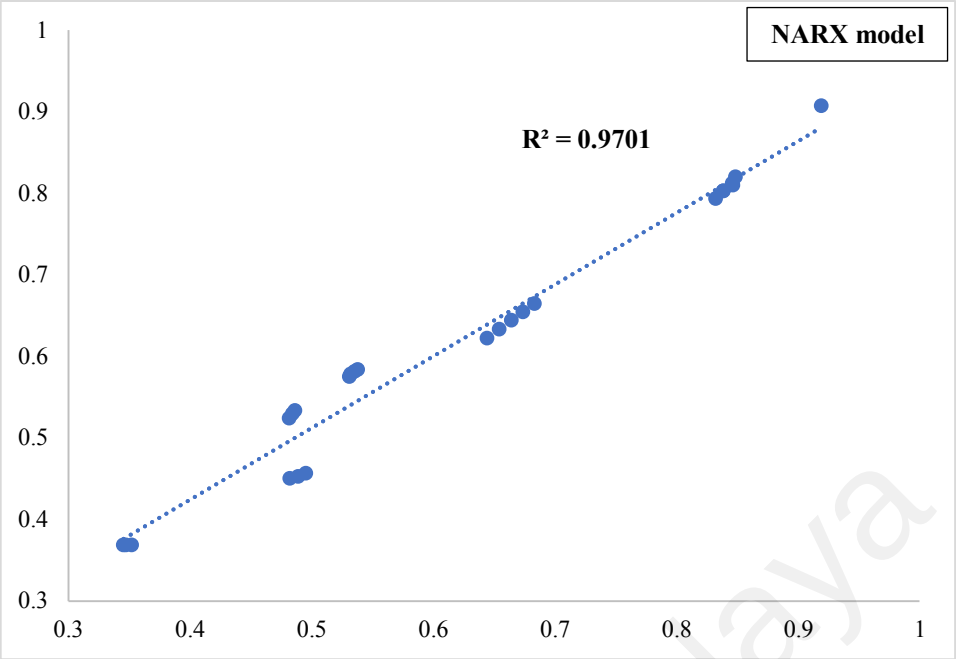

Figure 9. 3: The coefficient correlation (R^2) of NARX model

Whereby, the relative error for the LR model that is presented in Figure 9.4 with a maximum value of 15.02 %, and the coefficient correlation (R^2) which is presented in Figure 9.5 for the LR model is 0.9304. Comparing the two models relative error and the coefficient correlation, the results revel that the NARX model has the better performance. The selection of the proper model structure with high accuracy and productivity is hectic task, because of many factors are included such as the number of hidden layer, the neurons at each layer and the transfer function type.

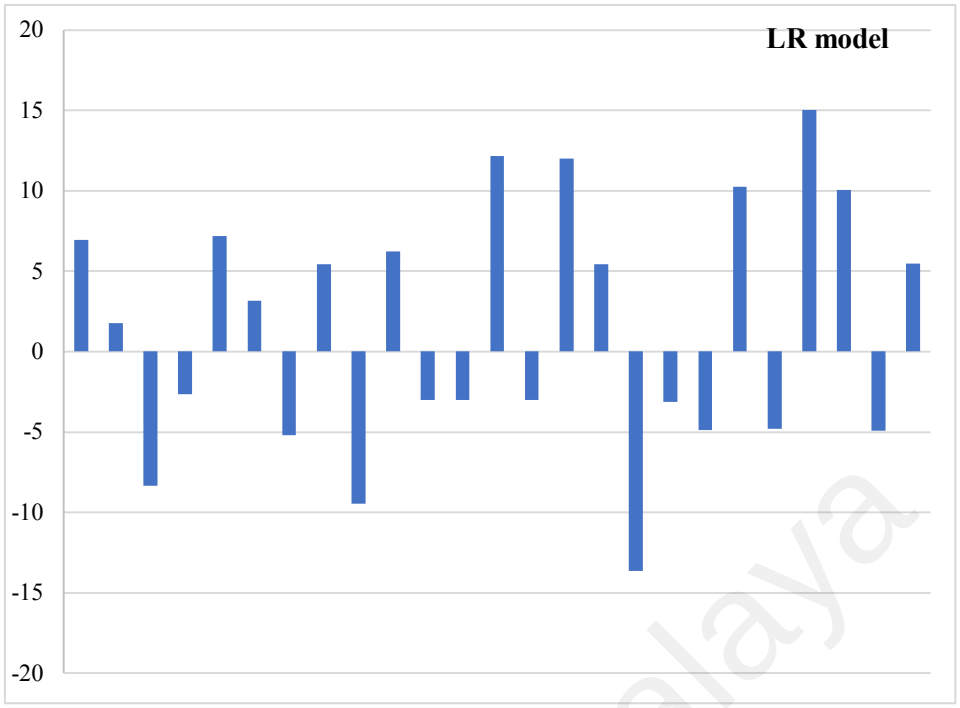

Figure 9. 4: The relative error (RE) of LR model

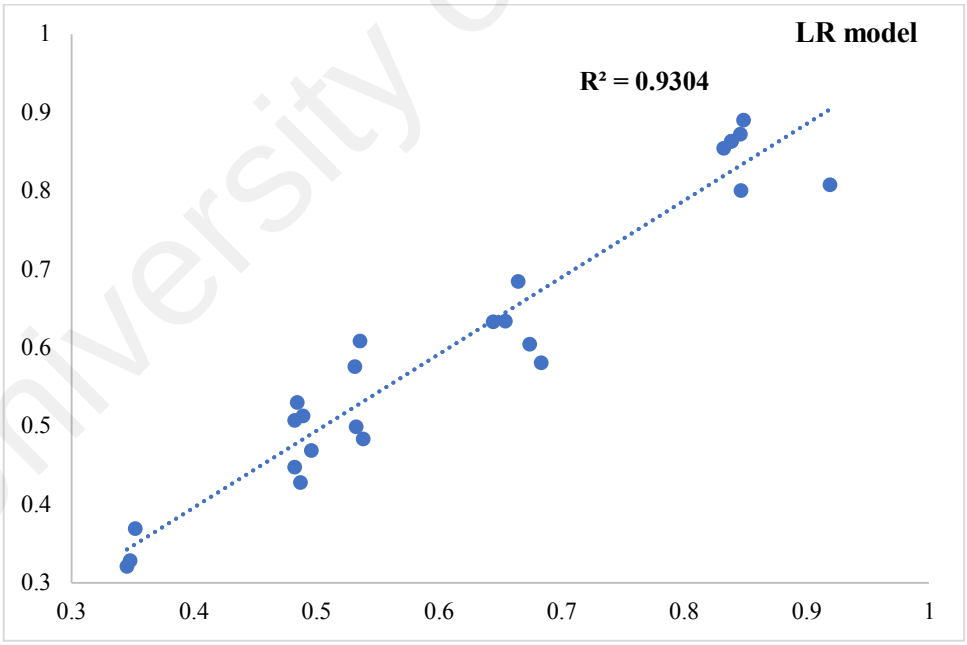

Figure 9. 5: The coefficient correlation (R^2) of LR model

In this study, different number of nodes, hidden layer and transfer function type were used to select the optimum structure, the network selection structure was based on the network productivity and performance, using the MSE value during the training step initially later, the created neural network model`s performance was tested based on the testing set using different indicators, the results are presented in Table 9.1. By comparing the obtained results which are presented in Table 9.1 from the two models, the NARX model showed a better performance than the LR model.

Table 9. 1: The performance indicators

	NARX	LR
MSE	1.15×10^{-3}	2.2×10^{-3}
RMSE	3.40×10^{-2}	4.74×10^{-2}
RRMSE	6.24×10^{-2}	7.61×10^{-2}
MAPE	5.71	6.68

9.3.3 pH effect

The pH of the solution is one of the main operational variables in the water treatment system in the industrial, economical or urban areas. Studying the effect of pH is to optimize the point of absorbance or purification. The deviation effect from this point in the work and the parameter sensitivity analysis will result in a high suggestive and performance. The effect of the pH on the Ak-CNTs (adsorbent) is presented in Figure 9.6. The effect of pH was studied with fixing the other parameters such as contact time 55 minutes, adsorbent dosage 20 mg, initial concentration 3 mg/L and the pH values were used are 3, 5.5, 6 and 8. it is known that the pH can affect the functional groups (i.e. amino groups, phosphate and carboxyl) protonation in the biomass, as well as the metal chemistry (i.e. its solubility) (Kazemipour et al., 2008; Witek-Krowiak et al., 2011). The experimental results presented that the adsorption capacity increases with increasing the pH value, at pH 3 the adsorption capacity is 2.125 mg/g whereby, at pH 5.5 the adsorption capacity increased to 3.015 mg/g and with pH 6 and 8 the adsorption capacity reached to

3.196 mg/g and 3.432 mg/g respectively. This increment is due to the oxygen negative charge presence containing a functional group such as carboxylic group and the enhancement of the negative electronic charge by the OH- presence in the solution. This negative charge pattern heavy distributed on the adsorbent surface which may be in charge of the metal building. It is known at pH greater then 7, the Hg^{2+} dominant species are $Hg(OH)^{+}$ and $Hg(OH)_2$. This complexation occurs due to the OH- existence which result in precipitation (Fiyadh et al., 2017).

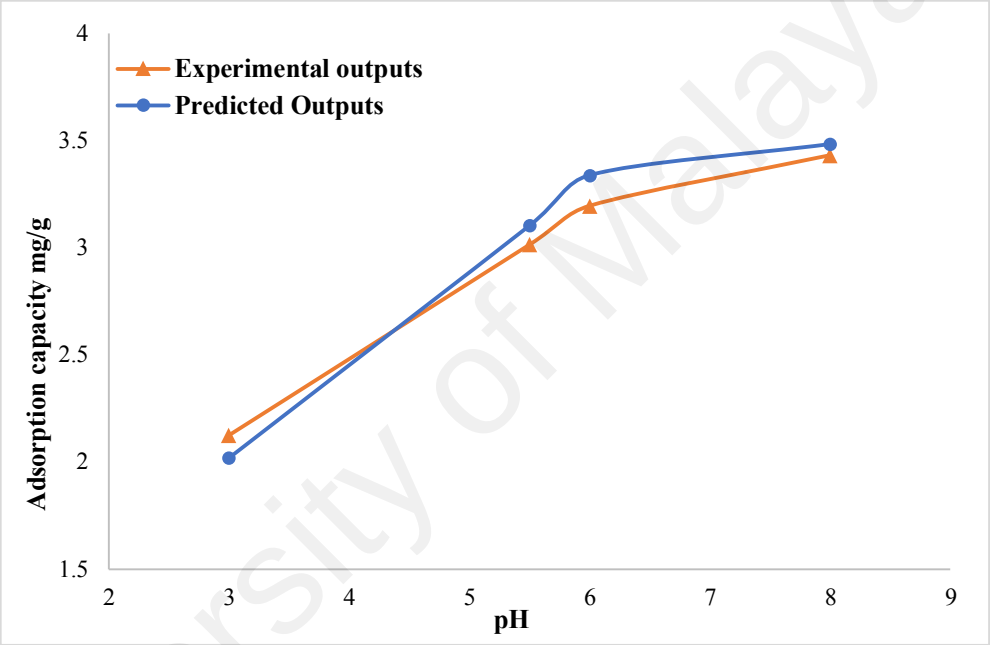

Figure 9. 6: The pH effect on the adsorption capacity

The NARX neural network modelling technique is used for the modelling of the adsorption capacity using the obtained experimental data set, by comparing the experimental results to the NARX outputs, the NARX model showed high accuracy the experimental and NARX results are presented in Figure 9.6.

9.3.4 Initial concentration effect

The Hg^{2+} initial concentration was involved in this study as one of the parameters in the experimental work, the Hg^{2+} initial concentrations used are 1, 3 and 5 mg/L. The

effect of Hg^{2+} ions concentration on the Ak-CNTs is presented in Figure 9.7. The results revel that the Hg^{2+} initial concentration had a favorable and prominent effect on the Hg^{2+} adsorbed quantity to the Ak-CNTs adsorbent.

Mercury initial concentration on the adsorption capacity is investigated with fixing the contact time to 120 minutes, adsorbent dosage 5 mg and with a pH of 5.5. In this work, the experimental results reveal that by increasing the mercury concentration in the water solution the adsorption capacity increases as well. At 1 mg/L ions concentration the adsorption capacity was 0.9935 mg/g whereby, increasing the ions concentration to 3 and 5 the adsorption capacity increased to 7.495 and 11.214 mg/g respectively. The increase in the adsorption capacity with the increase of ions concentration can cause a higher collision probability between the adsorbents active sites and the adsorbent molecules, higher active sites occupation and thus higher adsorption capacity (Zabihi et al., 2010). The experimental data obtained are trained using the NARX modelling techniques. The NARX model prediction results was found in a good agreement with the experimental data observation. The experimental and the NARX outputs are presented in Figure 9.7.

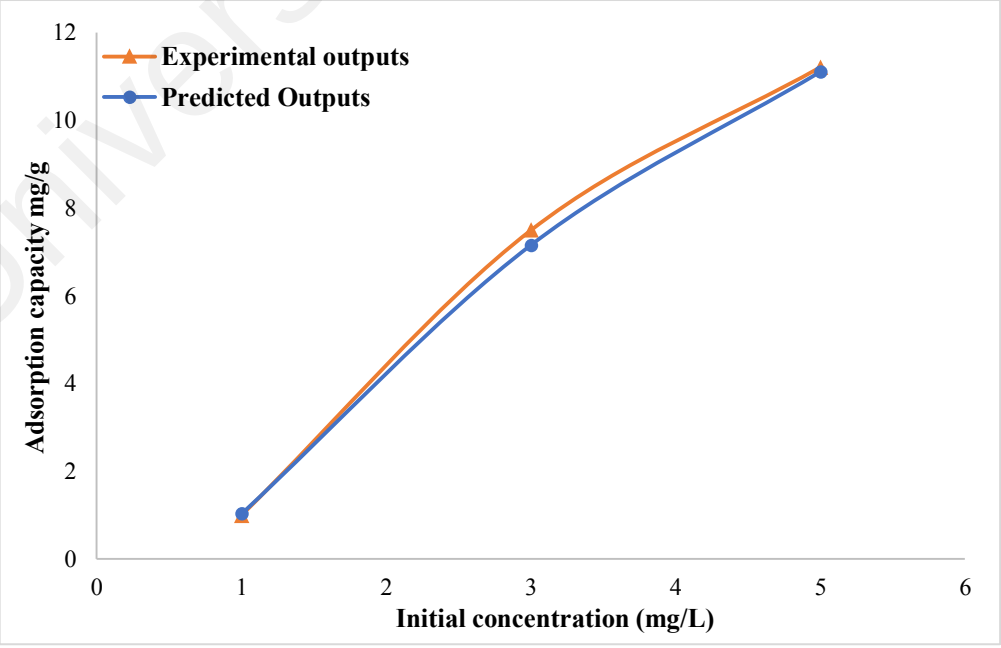

Figure 9. 7: The initial concentration effect on the adsorption capacity

9.3.5 Adsorbent dose effect

The amount of adsorbent dosage has a significant effect on the adsorption capacity, the Ak-CNTs adsorbent is used in this study for mercury removal. The amount of adsorbent dosage used in this study are 5, 20 and 30 mg, to study the effect of adsorbent dosage amount the other involved parameters in the experimental work are fixed to a contact time of 30 minutes, initial mercury concentration was 5 mg/L and with a pH of 6. Based on the obtained results presented in Figure 9.8, the adsorption capacity is decreased but the total of mercury ions removal is increased. The diminution in the adsorption density maybe attributed to the fact that some adsorbent site remains not saturated during the adsorption progression (Bandaru et al., 2013; B. Das et al., 2014). It is obtained from the experimental work that the adsorption capacity for 5 mg dosage was 13.56 mg/g then, as the Ak-CNTs adsorbent was increased to 20 and 30 mg the adsorption capacity was decreased to 8.49 and 6.47 mg/g, respectively. The obtained experimental data were used during the modelling part using NARX neural network modelling techniques. The NARX model prediction was found satisfactory for the experimental data observation. The experimental and NARX model simulation results are presented in Figure 9.8.

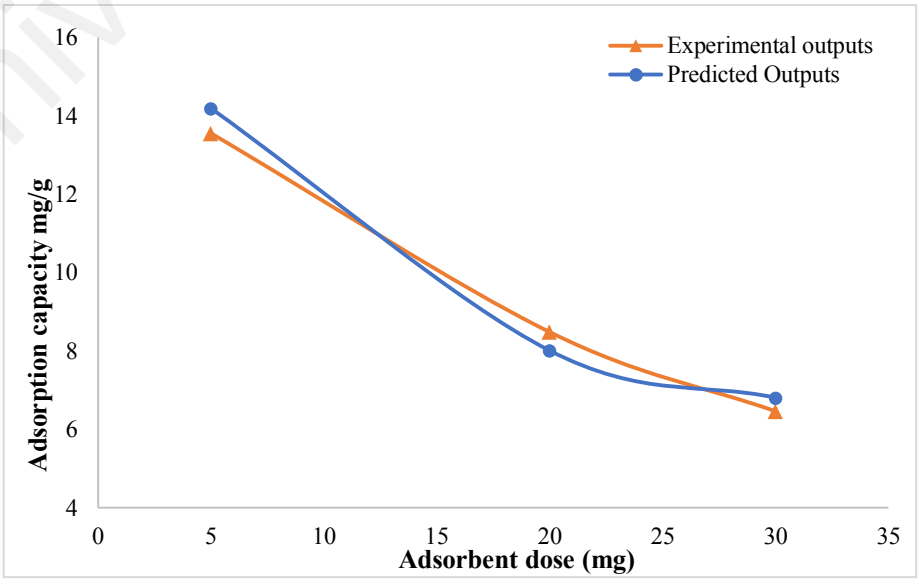

Figure 9. 8: The effect of adsorbent dosage

9.3.6 The kinetic study

The kinetic study is aimed to study the behavior of the reaction using the Ak-CNTs adsorbent, to study the reaction behavior three known kinetic models were applied including, Pseudo first-order, Pseudo second order and Intraparticle diffusion. Different parameter conditions are used in this study for the kinetic study, Figure 9.9a presented the kinetic study using adsorbent dosage of 20 mg, initial mercury concentration of 3 mg/L, pH of 3 and different interval time until the equilibrium state. Whereby, at Figure 9.9b the adsorbent dosage used is 20 mg, initial concentration 5 mg/L, pH 6 and the contact time until 162 minutes which is the equilibrium time. For Figure 9.9c the adsorption capacity used is 30 mg, initial concentration of 5 mg/L, pH 6 and the contact time until 163 minutes. Based on the results presented in Figure 9 A,B and C, the Ak-CNTs adsorption kinetics fit to the pseudo-second order model with higher value of correlation coefficient R^2 comparing to the intraparticle diffusion and pseudo-first order models (C. Zhang et al., 2012). The results of the intraparticle diffusion and pseudo first order are presented in Table 9.2. NARX neural network technique was used for modelling and prediction of the obtained data from the experimental work. The three kinetics models used for modelling the experimental data were also applied on the NARX outputs. The pseudo second order best described the adsorption kinetics of this study as compared to the intraparticle diffusion and pseudo-first order models. The results of the kinetics study are presented in Table 9.2, the NARX model shows a good agreement with the experimental work, this can improve the high accuracy of the NARX model.

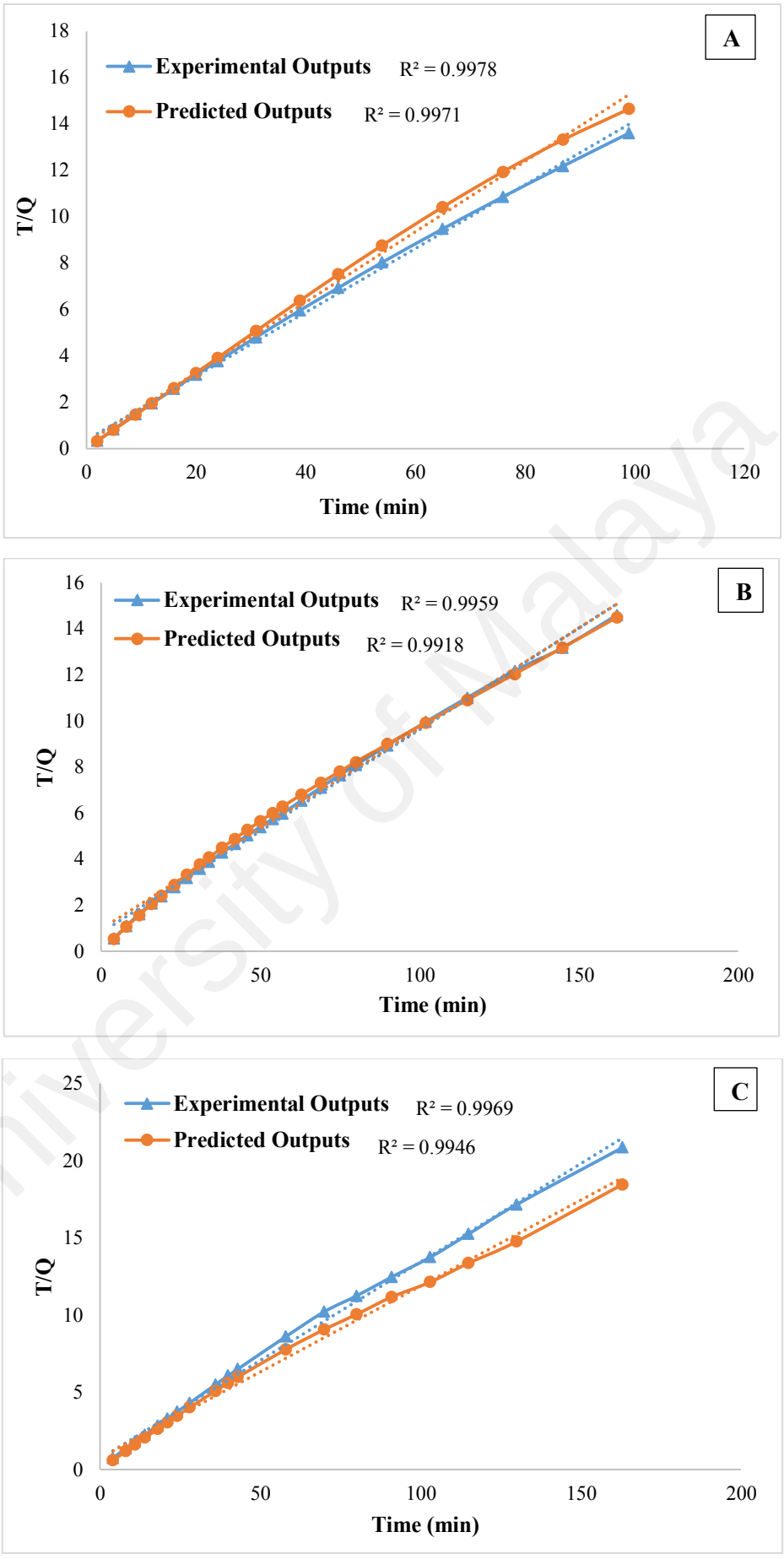

Figure 9. 9 A, B and C: The kinetic study

Table 9. 2: Adsorption kinetics and correlation coefficient

			Pseudo-first-order $ln(q_e–q_t)$ *vs time (t)*		Pseudo-second-order $(t/q_t vs\ t)$		Intraparticle $(q_t vs\ t^{0.5})$	
Dose mg	PH	C_0 mg/L	Experimental R^2	NARX output R^2	Experimental R^2	NARX outputs R^2	Experimental R^2	NARX outputs R^2
20	3	3	0.9378	0.9314	0.9978	0.9971	0.9114	0.9128
20	6	5	0.8689	0.8301	0.9959	0.9918	0.9053	0.9058
30	6	5	0.5692	0.5489	0.9969	0.9946	0.6045	0.6721

9.4 Conclusion

The functionalized carbon nanotube with deep eutectic solvents (DESs) based allyl triphenyl phosphonium bromide, was able to remove mercury ions from water solution efficiently. A comparative study between the NARX and LR models is conducted based on their performance and accuracy, the NARX model presented a better performance than the LR model. The effect of different parameters including mercury ions concentration, pH, amount of adsorbent dosage and contact time was studied. Three kinetics models such as Pseudo first-order, Pseudo second order and intraparticle diffusion were applied on the experimental and predicted data, the Pseudo second order was the best described. The maximum RE for the LR model was 15.02 %, R^2 of 0.9304 and MSE 2.2×10^{-3}. Whereby, the maximum relative error (RE) for the NARX model was 9. 79 %, R^2 of 0.9701 and MSE 1.15×10^{-3}.

CHAPTER 10: CONCLUSION AND RECOMMENDATIONS

10.1 Conclusion

In this study, different CNTs-based nano-adsorbents were successfully prepared for the removal of different heavy metals such as lead, arsenic and mercury. The pristine CNTs (P-CNTs) oxidized with $KMnO_4$ to produce (K-CNTs). For functionalization purpose, different DESs types were synthesized based on various molar ratios and salt types. Later, the prepared DESs were utilized as a functionalization agent of the (K-CNTs). The adsorption experiments were conducted using the functionalized CNTs as adsorbent for heavy metals removal. Experimental work was conducted to improve the adsorption capacity of the functionalized CNTs. The adsorption process is considered as a complicated process for the removal of heavy metal due to the influence of many variables including, adsorbent dosage, contact time, initial heavy metal concentration and pH. Therefore, artificial neural networks (ANNs) techniques were selected as a powerful tool for modelling and recognizing a given data set into their target outputs. Different algorithms were used for the modelling of the functionalized CNTs which are feed forward backpropagation neural network, layer recurrent neural network, adaptive neuro fuzzy inference system and nonlinear autoregressive network with exogenous inputs (NARX), using the input parameters (adsorbent dosage, contact time, initial heavy metal concentration and pH) and one output response (adsorption capacity). Different indicators were adopted to evaluate the neural network models such as the (RRMSE), (MSE), (RMSE), (MAPE) and (RE). The kinetic study was performed for all the adsorptions systems. Several significant findings were concluded from this study as following:

1- The (DES) is a great replacement of the ionic liquids (ILs) due to their low price, flammability, recyclability, biodegradability, lack of significant toxicity

and availability. Six DESs systems were synthesized successfully with various phosphonium and ammonium-based salts.

2- The oxidation with $KMnO_4$ was performed successfully by sonicating 7 ml of 1 mol $KMnO_4$ with 200 mg of the P-CNTs at 65 °C for 2 h. The developed adsorbent was characterized using Zeta potential, Fourier transform infrared (FTIR) and Raman spectroscopy.

3- The prepared DESs were utilized to functionalize the K-CNTs successfully under sonication for 3 h at 65 °C.

4- The functionalized CNTs with DESs were used successfully as adsorbents for heavy metal ions including As^{3+}, Pb^{2+} and Hg^{2+}.

5- Three well known kinetic models were applied such as, Pseudo first-order, Pseudo second order and Intraparticle diffusion, the kinetics models, the Pseudo second order was the best describe.

6- For the removal of Pb^{+2} the KTEG-CNTs adsorbent was used, 158 points were taken to study the influence of each parameter and the interaction among them on the adsorption capacity. Three ANN types were designed for the Pb^{+2} removal, the (FFBP), (ANFIS) and (LR). The methods were compared based on their predictive proficiency in terms of the (MSE), (RMSE), (RRMSE), (MAPE) and (R^2) based on the testing dataset. The maximum RE was 7.078% and the MSE was 6.14×10^{-5} for the ANFIS with R^2 of 0.9981. The pseudo-second-order kinetic model was well fitted to the simulated data.

7- For the arsenic (As^{3+}) removal, three adsorbents were used which are mK-CNTs, BK-CNTs and DK-CNTs. Two ANN types were designed for the As^{3+}removal, the feed-forward back-propagation (FFBP) and the nonlinear autoregressive network with exogenous inputs (NARX) neural network. The effect of operational parameters such as initial concentration, adsorbent

dosage, pH and contact time are studied to investigate the optimum conditions for maximum arsenic removal. The pseudo-second order best described the adsorption kinetics. The best model relative error value for the NARX model was 5.79%, with correlation coefficient (R^2) of (0.9922).

8- For the removal of mercury from water solution using Tk-CNTs adsorbent was described, the NARX neural network modelling technique was used for the modelling of the Tk-CNTs adsorption capacity using different parameters based on experimental data. The effect of different parameters including mercury ions concentration, pH, amount of adsorbent dosage and contact time was studied. Three kinetics models such as Pseudo first-order, Pseudo second order and Intraparticle diffusion were applied on the experimental and predicted data, the Pseudo second order was the best to describe the system. A sensitivity study was conducted using different parameters. Different indicators are used to determine the efficiency and accuracy of the NARX neural network model which are (MSE), (RMSE), (RRMSE), (MAPE), (RE) and correlation coefficient R^2. The value of the maximum relative error was 3.49 %, the correlation coefficient R^2 was (0.9998) and the MSE was 4.28×10^{-6}. Based on the used indicators, the NARX model was able to predict the mercury ions removal from water by comparing the NARX model results with the experimental data.

10.2 Recommendations

This research included many stages. From the experience of these stages, different recommendations can be proposed for further studies. The first stage of this research was the DES synthesis. The second stage was the functionalization processes. The third stage focused on the removal of various heavy metals. The final stage was on the use of the

artificial neural network (ANN) as a modelling technique. The proposed recommendations for further work are as following:

1- Different potential DESs could be discovered using organic or metal salts.
2- The use of metal-based DESs as a functionalization agent has an interesting research pathway.
3- The DESs as functionalization agent could be use with other carbon-based nanomaterials, i.e., SWCNTs, graphene and other CNTs types that were synthesised using different substrates such as activated carbon impregnated CNTs.
4- The DES-CNTs success as adsorbent for the removal of Hg^{2+}, Pb^{2+} and As^{3+} showed a great performance; therefore, these adsorbent could be used for the removal of different heavy metals such as Fe, Ni, Cr and Cd.
5- A deep study could be performed to inspect the optimum adsorption process conditions.
6- A competition study can be carried out to determine the performance of each adsorbent with competitive ions.
7- Apply the used artificial neural network algorithms for the modelling of different heavy metals adsorbents.
8- There are many neural network algorithms could be applied for the modelling of the DES-CNTs adsorbent.

REFERENCES

Abbas, A., Al-Amer, A. M., Laoui, T., Al-Marri, M. J., Nasser, M. S., Khraisheh, M., & Atieh, M. A. (2016). Heavy metal removal from aqueous solution by advanced carbon nanotubes: critical review of adsorption applications. *Separation and Purification Technology, 157*, 141-161.

Abbott, A. P., Boothby, D., Capper, G., Davies, D. L., & Rasheed, R. K. (2004). Deep eutectic solvents formed between choline chloride and carboxylic acids: versatile alternatives to ionic liquids. *Journal of the American Chemical Society, 126*(29), 9142-9147.

Abbott, A. P., Capper, G., Davies, D. L., & Rasheed, R. K. (2004). Ionic liquid analogues formed from hydrated metal salts. *Chemistry-A European Journal, 10*(15), 3769-3774.

Abbott, A. P., Capper, G., Davies, D. L., Rasheed, R. K., & Tambyrajah, V. (2003). Novel solvent properties of choline chloride/urea mixtures. *Chemical Communications*(1), 70-71.

Abbott, A. P., Capper, G., McKenzie, K. J., & Ryder, K. S. (2007). Electrodeposition of zinc–tin alloys from deep eutectic solvents based on choline chloride. *Journal of Electroanalytical Chemistry, 599*(2), 288-294.

Abbott, A. P., El Ttaib, K., Frisch, G., McKenzie, K. J., & Ryder, K. S. (2009). Electrodeposition of copper composites from deep eutectic solvents based on choline chloride. *Physical Chemistry Chemical Physics, 11*(21), 4269-4277.

Abbott, A. P., Griffith, J., Nandhra, S., O'Connor, C., Postlethwaite, S., Ryder, K. S., & Smith, E. L. (2008). Sustained electroless deposition of metallic silver from a choline chloride-based ionic liquid. *Surface and Coatings Technology, 202*(10), 2033-2039.

Abbott, A. P., & McKenzie, K. J. (2006). Application of ionic liquids to the electrodeposition of metals. *Physical Chemistry Chemical Physics, 8*(37), 4265-4279.

Abdel-Ghani, N., Hefny, M., & El-Chaghaby, G. A. (2007). Removal of lead from aqueous solution using low cost abundantly available adsorbents. *International Journal of Environmental Science & Technology, 4*(1), 67-73.

Abo-Hamad, A., Hayyan, M., AlSaadi, M. A., & Hashim, M. A. (2015). Potential applications of deep eutectic solvents in nanotechnology. *Chemical Engineering Journal, 273*, 551-567.

Abujazar, M. S. S., Fatihah, S., Ibrahim, I. A., Kabeel, A., & Sharil, S. (2018). Productivity modelling of a developed inclined stepped solar still system based on actual performance and using a cascaded forward neural network model. *Journal of Cleaner Production, 170*, 147-159.

Agami, N., Atiya, A., Saleh, M., & El-Shishiny, H. (2009). A neural network based dynamic forecasting model for Trend Impact Analysis. *Technological Forecasting and Social Change, 76*(7), 952-962.

Aghaeinejad-Meybodi, A., Ebadi, A., Shafiei, S., Khataee, A., & Rostampour, M. (2015). Modeling and optimization of antidepressant drug fluoxetine removal in aqueous media by ozone/H 2 O 2 process: comparison of central composite design and artificial neural network approaches. *Journal of the Taiwan Institute of Chemical Engineers, 48*, 40-48.

Ahmad, M. F., Haydar, S., Bhatti, A. A., & Bari, A. J. (2014). Application of artificial neural network for the prediction of biosorption capacity of immobilized Bacillus subtilis for the removal of cadmium ions from aqueous solution. *Biochemical Engineering Journal, 84*, 83-90.

Ahmadi, Y., Eshraghi, S. E., Bahrami, P., Hasanbeygi, M., Kazemzadeh, Y., & Vahedian, A. (2015). Comprehensive Water–Alternating-Gas (WAG) injection study to evaluate the most effective method based on heavy oil recovery and asphaltene precipitation tests. *Journal of Petroleum Science and Engineering, 133*, 123-129.

Aitchison, T. J., Ginic-Markovic, M., Matisons, J. G., Simon, G. P., & Fredericks, P. M. (2007). Purification, cutting, and sidewall functionalization of multiwalled carbon nanotubes using potassium permanganate solutions. *The Journal of Physical Chemistry C, 111*(6), 2440-2446.

Akbari, M. K., Shirvanimoghaddam, K., Hai, Z., Zhuiykov, S., & Khayyam, H. (2017). Nano TiB2 and TiO2 reinforced composites: A comparative investigation on strengthening mechanisms and predicting mechanical properties via neural network modeling. *Ceramics International*.

Ali, I. (2012). New generation adsorbents for water treatment. *Chemical Reviews, 112*(10), 5073-5091.

Ali, I., & Gupta, V. (2006). Advances in water treatment by adsorption technology. *Nature protocols, 1*(6), 2661.

AlOmar, M. K., Alsaadi, M. A., Hayyan, M., Akib, S., & Hashim, M. A. (2016). Functionalization of CNTs surface with phosphonuim based deep eutectic solvents for arsenic removal from water. *Applied Surface Science, 389*, 216-226.

AlOmar, M. K., Alsaadi, M. A., Hayyan, M., Akib, S., Ibrahim, M., & Hashim, M. A. (2017). Allyl triphenyl phosphonium bromide based DES-functionalized carbon nanotubes for the removal of mercury from water. *Chemosphere, 167*, 44-52.

AlOmar, M. K., Alsaadi, M. A., Hayyan, M., Akib, S., Ibrahim, R. K., & Hashim, M. A. (2016a). Lead removal from water by choline chloride based deep eutectic solvents functionalized carbon nanotubes. *Journal of Molecular Liquids, 222*, 883-894.

AlOmar, M. K., Alsaadi, M. A., Hayyan, M., Akib, S., Ibrahim, R. K., & Hashim, M. A. J. J. o. M. L. (2016b). Lead removal from water by choline chloride based deep eutectic solvents functionalized carbon nanotubes. *222*, 883-894.

AlOmar, M. K., Alsaadi, M. A., Jassam, T. M., Akib, S., & Ali Hashim, M. (2017). Novel deep eutectic solvent-functionalized carbon nanotubes adsorbent for mercury removal from water. *Journal of colloid and interface science, 497*, 413-421.

AlOmar, M. K., Alsaadi, M. A., Jassam, T. M., Akib, S., & Hashim, M. A. (2017). Novel deep eutectic solvent-functionalized carbon nanotubes adsorbent for mercury removal from water. *Journal of colloid and interface science, 497*, 413-421.

AlOmar, M. K., Hayyan, M., Alsaadi, M. A., Akib, S., Hayyan, A., & Hashim, M. A. (2016). Glycerol-based deep eutectic solvents: Physical properties. *Journal of Molecular Liquids, 215*, 98-103.

AlSaadi, M. A., Al Mamun, A., Alam, M. Z., Amosa, M. K., & Atieh, M. A. (2016). Removal of cadmium from water by CNT–PAC composite: effect of functionalization. *Nano, 11*(01), 1650011.

An, B., Liang, Q., & Zhao, D. (2011). Removal of arsenic (V) from spent ion exchange brine using a new class of starch-bridged magnetite nanoparticles. *Water research, 45*(5), 1961-1972.

Andjelkovic, I., Nesic, J., Stankovic, D., Manojlovic, D., Pavlovic, M., Jovalekic, C., & Roglic, G. (2014). Investigation of sorbents synthesised by mechanical–chemical reaction for sorption of As (III) and As (V) from aqueous medium. *Clean Technologies and Environmental Policy, 16*(2), 395-403.

Andrews, R., Jacques, D., Qian, D., & Rantell, T. (2002). Multiwall carbon nanotubes: synthesis and application. *Accounts of Chemical Research, 35*(12), 1008-1017.

Argos, M., Kalra, T., Rathouz, P. J., Chen, Y., Pierce, B., Parvez, F., . . . Hasan, R. (2010). Arsenic exposure from drinking water, and all-cause and chronic-disease mortalities in Bangladesh (HEALS): a prospective cohort study. *The Lancet, 376*(9737), 252-258.

Arnold, M. S., Green, A. A., Hulvat, J. F., Stupp, S. I., & Hersam, M. C. (2006). Sorting carbon nanotubes by electronic structure using density differentiation. *Nature nanotechnology, 1*(1), 60-65.

Asgari, S., Sahari, M. A., & Barzegar, M. (2017). Practical modeling and optimization of ultrasound-assisted bleaching of olive oil using hybrid artificial neural network-genetic algorithm technique. *Computers and Electronics in Agriculture, 140*, 422-432.

Atieh, M. A., Bakather, O. Y., Al-Tawbini, B., Bukhari, A. A., Abuilaiwi, F. A., & Fettouhi, M. B. (2011). Effect of carboxylic functional group functionalized on carbon nanotubes surface on the removal of lead from water. *Bioinorganic chemistry and applications, 2010*.

Axtell, N. R., Sternberg, S. P., & Claussen, K. (2003). Lead and nickel removal using Microspora and Lemna minor. *Bioresource Technology, 89*(1), 41-48.

Ayoob, S., Gupta, A., & Bhakat, P. (2007). Performance evaluation of modified calcined bauxite in the sorptive removal of arsenic (III) from aqueous environment. *Colloids and Surfaces A: Physicochemical and Engineering Aspects, 293*(1), 247-254.

Azari, A., Gharibi, H., Kakavandi, B., Ghanizadeh, G., Javid, A., Mahvi, A. H., . . . Khosravia, T. (2017). Magnetic adsorption separation process: an alternative method of mercury extracting from aqueous solution using modified chitosan coated Fe3O4 nanocomposites. *Journal of Chemical Technology and Biotechnology, 92*(1), 188-200.

Bahadir, T., Bakan, G., Altas, L., & Buyukgungor, H. (2007). The investigation of lead removal by biosorption: An application at storage battery industry wastewaters. *Enzyme and Microbial Technology, 41*(1–2), 98-102.

Bandaru, N. M., Reta, N., Dalal, H., Ellis, A. V., Shapter, J., & Voelcker, N. H. (2013). Enhanced adsorption of mercury ions on thiol derivatized single wall carbon nanotubes. *Journal of Hazardous Materials, 261*, 534-541.

Banerjee, A., Sarkar, P., & Banerjee, S. (2016). Application of statistical design of experiments for optimization of As (V) biosorption by immobilized bacterial biomass. *Ecological Engineering, 86*, 13-23.

Baskan, M. B., & Pala, A. (2010). A statistical experiment design approach for arsenic removal by coagulation process using aluminum sulfate. *Desalination, 254*(1), 42-48.

Baughman, R. H., Zakhidov, A. A., & De Heer, W. A. (2002). Carbon nanotubes--the route toward applications. *Science, 297*(5582), 787-792.

Bauschlicher Jr, C. W., & Ricca, A. (2004). Binding of N H 3 to graphite and to a (9, 0) carbon nanotube. *Physical Review B, 70*(11), 115409.

Berhan, L., Yi, Y., Sastry, A., Munoz, E., Selvidge, M., & Baughman, R. (2004). Mechanical properties of nanotube sheets: Alterations in joint morphology and achievable moduli in manufacturable materials. *Journal of Applied Physics, 95*(8), 4335-4345.

Bienfait, M., Zeppenfeld, P., Dupont-Pavlovsky, N., Muris, M., Johnson, M., Wilson, T., . . . Vilches, O. (2004). Thermodynamics and structure of hydrogen, methane, argon, oxygen, and carbon dioxide adsorbed on single-wall carbon nanotube bundles. *Physical Review B, 70*(3), 035410.

Biester, H., Schuhmacher, P., & Müller, G. (2000). Effectiveness of mossy tin filters to remove mercury from aqueous solution by Hg (II) reduction and Hg (0) amalgamation. *Water research, 34*(7), 2031-2036.

Bindiganavale, S. (2009). *Study of mechanical behavior of single walled carbon nanotube reinforced matrix representative volume elements*: Lamar University-Beaumont.

Bingöl, D., Hercan, M., Elevli, S., & Kılıç, E. (2012). Comparison of the results of response surface methodology and artificial neural network for the biosorption of lead using black cumin. *Bioresource Technology, 112*, 111-115.

Bissen, M., & Frimmel, F. H. (2003). Arsenic—a review. Part II: oxidation of arsenic and its removal in water treatment. *CLEAN–Soil, Air, Water, 31*(2), 97-107.

Bissen, M., & Frimmel, F. H. (2003). Arsenic — a Review. Part II: Oxidation of Arsenic and its Removal in Water Treatment. *Acta hydrochimica et hydrobiologica, 31*(2), 97-107.

Black, B. (1999). *Arsenic: answers to questions commonly asked by drinking water professionals*: American Water Works Association.

Blue, L. Y., Van Aelstyn, M. A., Matlock, M., & Atwood, D. A. (2008). Low-level mercury removal from groundwater using a synthetic chelating ligand. *Water research, 42*(8), 2025-2028.

Briggs, D. (2003). Environmental pollution and the global burden of disease. *British Medical Bulletin, 68*(1), 1-24.

Brown, P., Jefcoat, I. A., Parrish, D., Gill, S., & Graham, E. (2000). Evaluation of the adsorptive capacity of peanut hull pellets for heavy metals in solution. *Advances in Environmental Research, 4*(1), 19-29.

Cai, W., Wang, L., Pan, Z., Zuo, J., Xu, C., & Shao, X. (2001). Application of the wavelet transform method in quantitative analysis of Raman spectra. *Journal of Raman Spectroscopy, 32*(3), 207-209.

Çelekli, A., Birecikligil, S. S., Geyik, F., & Bozkurt, H. (2012). Prediction of removal efficiency of Lanaset Red G on walnut husk using artificial neural network model. *Bioresource Technology, 103*(1), 64-70.

Chakrabarti, M., Manan, N., Brandon, N., Maher, R., Mjalli, F., AlNashef, I., . . . Nir, D. (2015). One-pot electrochemical gram-scale synthesis of graphene using deep eutectic solvents and acetonitrile. *Chemical Engineering Journal, 274*, 213-223.

Chakrabarti, M. H., Manan, N. S. A., Brandon, N. P., Maher, R. C., Mjalli, F. S., AlNashef, I. M., . . . Nir, D. (2015). One-pot electrochemical gram-scale synthesis of graphene using deep eutectic solvents and acetonitrile. *Chemical Engineering Journal, 274*, 213-223.

Chandra, V., & Kim, K. S. (2011). Highly selective adsorption of Hg 2+ by a polypyrrole–reduced graphene oxide composite. *Chemical Communications, 47*(13), 3942-3944.

Chen, H., & Wang, A. (2007). Kinetic and isothermal studies of lead ion adsorption onto palygorskite clay. *Journal of colloid and interface science, 307*(2), 309-316.

Chen, J., Hamon, M. A., Hu, H., Chen, Y., Rao, A. M., Eklund, P. C., & Haddon, R. C. (1998). Solution properties of single-walled carbon nanotubes. *Science, 282*(5386), 95-98.

Chen, J. P., & Wu. (2004). Acid/Base-Treated Activated Carbons: Characterization of Functional Groups and Metal Adsorptive Properties. *Langmuir, 20*(6), 2233-2242.

Chen, J. P., & Wu, S. (2004). Acid/base-treated activated carbons: characterization of functional groups and metal adsorptive properties. *Langmuir, 20*(6), 2233-2242.

Chen, P. H., Hsu, C.-F., Tsai, D. D.-W., Lu, Y.-M., & Huang, W.-J. (2014). Adsorption of mercury from water by modified multi-walled carbon nanotubes: adsorption behaviour and interference resistance by coexisting anions. *Environmental technology, 35*(15), 1935-1944.

Chen, S., Billings, S., & Grant, P. (1990). Non-linear system identification using neural networks. *International journal of control, 51*(6), 1191-1214.

Chen, S., Kobayashi, K., Miyata, Y., Imazu, N., Saito, T., Kitaura, R., & Shinohara, H. (2009). Morphology and melting behavior of ionic liquids inside single-walled carbon nanotubes. *Journal of the American Chemical Society, 131*(41), 14850-14856.

Cheng, Z., Fu, F., Dionysiou, D. D., & Tang, B. (2016). Adsorption, oxidation, and reduction behavior of arsenic in the removal of aqueous As (III) by mesoporous Fe/Al bimetallic particles. *Water research, 96*, 22-31.

Chiarle, S., Ratto, M., & Rovatti, M. (2000). Mercury removal from water by ion exchange resins adsorption. *Water research, 34*(11), 2971-2978.

Chibole, O. K. (2013). Modeling River Sosiani's water quality to assess human impact on water resources at the catchment scale. *Ecohydrology & Hydrobiology, 13*(4), 241-245.

Cho, D.-W., Song, H., Kim, B., Schwartz, F. W., & Jeon, B.-H. (2015). Reduction of nitrate in groundwater by Fe (0)/Magnetite nanoparticles entrapped in Ca-Alginate beads. *Water, Air, & Soil Pollution, 226*(7), 206.

Cho, K. H., Sthiannopkao, S., Pachepsky, Y. A., Kim, K.-W., & Kim, J. H. (2011). Prediction of contamination potential of groundwater arsenic in Cambodia, Laos, and Thailand using artificial neural network. *Water research, 45*(17), 5535-5544.

Chojnacki, A., Chojnacka, K., Hoffmann, J., & Gorecki, H. (2004). The application of natural zeolites for mercury removal: from laboratory tests to industrial scale. *Minerals Engineering, 17*(7-8), 933-937.

Choubineh, A., Ghorbani, H., Wood, D. A., Moosavi, S. R., Khalafi, E., & Sadatshojaei, E. (2017). Improved predictions of wellhead choke liquid critical-flow rates: modelling based on hybrid neural network training learning based optimization. *Fuel, 207*, 547-560.

Coleman, J. N., Khan, U., & Gun'ko, Y. K. (2006). Mechanical reinforcement of polymers using carbon nanotubes. *Advanced Materials, 18*(6), 689-706.

Collins, P. G., & Avouris, P. (2000). Nanotubes for electronics. *Scientific american, 283*(6), 62-69.

Cooper, E. R., Andrews, C. D., Wheatley, P. S., Webb, P. B., Wormald, P., & Morris, R. E. (2004). Ionic liquids and eutectic mixtures as solvent and template in synthesis of zeolite analogues. *Nature, 430*(7003), 1012-1016.

Çoruh, S., Geyikçi, F., Kılıç, E., & Çoruh, U. (2014). The use of NARX neural network for modeling of adsorption of zinc ions using activated almond shell as a potential biosorbent. *Bioresource Technology, 151*, 406-410.

Cui, H., Li, Q., Gao, S., & Shang, J. K. (2012). Strong adsorption of arsenic species by amorphous zirconium oxide nanoparticles. *Journal of Industrial and Engineering Chemistry, 18*(4), 1418-1427.

Cvjetko Bubalo, M., Vidović, S., Radojčić Redovniković, I., & Jokić, S. (2015). Green solvents for green technologies. *Journal of Chemical Technology and Biotechnology, 90*(9), 1631-1639.

Das, B., Mondal, N., Bhaumik, R., & Roy, P. (2014). Insight into adsorption equilibrium, kinetics and thermodynamics of lead onto alluvial soil. *International Journal of Environmental Science and Technology, 11*(4), 1101-1114.

Das, S. K., Das, A. R., & Guha, A. K. (2007). A study on the adsorption mechanism of mercury on Aspergillus versicolor biomass. *Environmental science & technology, 41*(24), 8281-8287.

Davis, A. P. (1993). *Hazardous and industrial wastes; proceedings of the Twenty-Fifth Mid-Atlantic Industrial Waste Conference.* Paper presented at the Mid-Atlantic Industrial Waste Conference, 25.

Davodi, B., Ghorbani, M., & Jahangiri, M. (2017). Adsorption of mercury from aqueous solution on synthetic polydopamine nanocomposite based on magnetic nanoparticles using Box–Behnken design. *Journal of the Taiwan Institute of Chemical Engineers, 80*, 363-378.

Desai, K. M., Survase, S. A., Saudagar, P. S., Lele, S., & Singhal, R. S. (2008). Comparison of artificial neural network (ANN) and response surface methodology (RSM) in fermentation media optimization: case study of fermentative production of scleroglucan. *Biochemical Engineering Journal, 41*(3), 266-273.

Desai, K. M., Survase, S. A., Saudagar, P. S., Lele, S. S., & Singhal, R. S. (2008). Comparison of artificial neural network (ANN) and response surface methodology (RSM) in fermentation media optimization: Case study of fermentative production of scleroglucan. *Biochemical Engineering Journal, 41*(3), 266-273.

Deshmukh, R. R., Rajagopal, R., & Srinivasan, K. (2001). Ultrasound promoted C–C bond formation: Heck reaction at ambient conditions in room temperature ionic liquids. Chemical Communications(17), 1544-1545.

Di, G., Zhu, Z., Zhang, H., Zhu, J., Lu, H., Zhang, W., . . . Küppers, S. (2017). Simultaneous removal of several pharmaceuticals and arsenic on Zn-Fe mixed metal oxides: Combination of photocatalysis and adsorption. *Chemical Engineering Journal, 328*, 141-151.

Di, Z.-C., Ding, J., Peng, X.-J., Li, Y.-H., Luan, Z.-K., & Liang, J. (2006). Chromium adsorption by aligned carbon nanotubes supported ceria nanoparticles. *Chemosphere, 62*(5), 861-865.

Dillon, A. C., Jones, K., Bekkedahl, T., & Kiang, C. (1997). Storage of hydrogen in single-walled carbon nanotubes. *Nature, 386*(6623), 377.

Dimitrova, S., & Mehandgiev, D. (1998). Lead removal from aqueous solutions by granulated blast-furnace slag. *Water research, 32*(11), 3289-3292.

Ding, Z., Hu, X., Morales, V. L., & Gao, B. (2014). Filtration and transport of heavy metals in graphene oxide enabled sand columns. *Chemical Engineering Journal, 257*, 248-252.

Duncan, T. V. (2011). Applications of nanotechnology in food packaging and food safety: barrier materials, antimicrobials and sensors. *Journal of colloid and interface science, 363*(1), 1-24.

Ebbesen, T., & P M, A. (1992). Large-scale synthesis of carbon. *Nature, 358*, 16.

El-Shafie, A., Taha, M. R., & Noureldin, A. (2007). A neuro-fuzzy model for inflow forecasting of the Nile river at Aswan high dam. *Water Resources Management, 21*(3), 533-556.

El-Shafie, A. H., & El-Manadely, M. S. (2011). An integrated neural network stochastic dynamic programming model for optimizing the operation policy of Aswan High Dam. *Hydrology Research, 42*(1), 50.

El-Sheikh, A. H., Al-Degs, Y. S., Al-As' ad, R. M., & Sweileh, J. A. (2011). Effect of oxidation and geometrical dimensions of carbon nanotubes on Hg (II) sorption and preconcentration from real waters. *Desalination, 270*(1), 214-220.

Esfahani, A. R., Hojati, S., Azimi, A., Farzadian, M., & Khataee, A. (2015). Enhanced hexavalent chromium removal from aqueous solution using a sepiolite-stabilized zero-valent iron nanocomposite: impact of operational parameters and artificial neural network modeling. *Journal of the Taiwan Institute of Chemical Engineers, 49*, 172-182.

Esfe, M. H., Afrand, M., Yan, W.-M., & Akbari, M. (2015). Applicability of artificial neural network and nonlinear regression to predict thermal conductivity modeling

of Al 2 O 3–water nanofluids using experimental data. *International Communications in Heat and Mass Transfer, 66*, 246-249.

Esfe, M. H., Bahiraei, M., Hajmohammad, M. H., & Afrand, M. (2017). Rheological characteristics of MgO/oil nanolubricants: Experimental study and neural network modeling. *International Communications in Heat and Mass Transfer, 86*, 245-252.

Esumi, K., Ishigami, M., Nakajima, A., Sawada, K., & Honda, H. (1996). Chemical treatment of carbon nanotubes. *Carbon, 34*(2), 279-281.

Evangelista, S. M., DeOliveira, E., Castro, G. R., Zara, L. F., & Prado, A. G. (2007). Hexagonal mesoporous silica modified with 2-mercaptothiazoline for removing mercury from water solution. *Surface Science, 601*(10), 2194-2202.

Fan, J., Shi, Z., Tian, M., Wang, J., & Yin, J. (2012). Unzipped multiwalled carbon nanotube oxide/multiwalled carbon nanotube hybrids for polymer reinforcement. *ACS applied materials & interfaces, 4*(11), 5956-5965.

Fausett, L., & Fausett, L. (1994). *Fundamentals of neural networks: architectures, algorithms, and applications*: Prentice-Hall.

Fayaed, S. S., El-Shafie, A., & Jaafar, O. (2011). Performance of artificial neural network and regression techniques for simulation model in reservoir inter-relationships. *International Journal of Physical Sciences, 6*(34), 7738-7748.

Fayaed, S. S., El-Shafie, A., & Jaafar, O. (2013a). Adaptive neuro-fuzzy inference system–based model for elevation–surface area–storage interrelationships. *Neural Computing and Applications, 22*(5), 987-998.

Fayaed, S. S., El-Shafie, A., & Jaafar, O. (2013b). Integrated artificial neural network (ANN) and stochastic dynamic programming (SDP) model for optimal release policy. *Water Resources Management, 27*(10), 3679-3696.

Feng, Q., Zhang, Z., Ma, Y., He, X., Zhao, Y., & Chai, Z. (2012). Adsorption and desorption characteristics of arsenic onto ceria nanoparticles. *Nanoscale research letters, 7*(1), 84.

Férey, G. (2008). Hybrid porous solids: past, present, future. *Chemical Society Reviews, 37*(1), 191-214.

Fischer, J. E. (2002). Chemical doping of single-wall carbon nanotubes. *Accounts of Chemical Research, 35*(12), 1079-1086.

Fiyadh, S. S., AlSaadi, M. A., AlOmar, M. K., Fayaed, S. S., Hama, A. R., Bee, S., & El-Shafie, A. (2017). The modelling of lead removal from water by deep eutectic solvents functionalized CNTs: artificial neural network (ANN) approach. *Water Science and Technology, 76*(9), 2413-2426.

Fu, F., & Wang, Q. (2011). Removal of heavy metal ions from wastewaters: a review. *Journal of Environmental Management, 92*(3), 407-418.

Gad, S., & Pham, T. (2014). Mercury. Encyclopedia of Toxicology: Oxford Academic Press: Oxford, UK.

Geetha, P., Latha, M. S., Pillai, S. S., & Koshy, M. (2015). Nanoalginate based biosorbent for the removal of lead ions from aqueous solutions: Equilibrium and kinetic studies. *Ecotoxicology and Environmental Safety, 122*, 17-23.

Genuino, D. A. D., Bataller, B. G., Capareda, S. C., & de Luna, M. D. G. (2017). Application of artificial neural network in the modeling and optimization of humic acid extraction from municipal solid waste biochar. *Journal of Environmental Chemical Engineering, 5*(4), 4101-4107.

Ghaedi, A. M., & Vafaei, A. (2017). Applications of artificial neural networks for adsorption removal of dyes from aqueous solution: A review. *Advances in Colloid and Interface Science*.

Ghorbel-Abid, I., & Trabelsi-Ayadi, M. (2015). Competitive adsorption of heavy metals on local landfill clay. *Arabian Journal of Chemistry, 8*(1), 25-31.

Ghosal, P. S., & Gupta, A. K. (2016). Enhanced efficiency of ANN using non-linear regression for modeling adsorptive removal of fluoride by calcined Ca-Al-(NO 3)-LDH. *Journal of Molecular Liquids, 222*, 564-570.

Ghosh, M. K., Poinern, G. E. J., Issa, T. B., & Singh, P. (2012). Arsenic adsorption on goethite nanoparticles produced through hydrazine sulfate assisted synthesis method. *Korean Journal of Chemical Engineering, 29*(1), 95-102.

Gihring, T. M., Druschel, G. K., McCleskey, R. B., Hamers, R. J., & Banfield, J. F. (2001). Rapid arsenite oxidation by Thermus aquaticus and Thermus thermophilus: field and laboratory investigations. *Environmental science & technology, 35*(19), 3857-3862.

Gihring, T. M., Druschel, G. K., McCleskey, R. B., Hamers, R. J., & Banfield, J. F. (2001). Rapid Arsenite Oxidation by Thermus aquaticus and Thermus thermophilus: Field and Laboratory Investigations. *Environmental science & technology, 35*(19), 3857-3862.

Giri, A., Patel, R., & Mahapatra, S. (2011). Artificial neural network (ANN) approach for modelling of arsenic (III) biosorption from aqueous solution by living cells of Bacillus cereus biomass. *Chemical Engineering Journal, 178*, 15-25.

GK, P., Nale, J., & Muluneh, W. Modelling Reference Evapotranspiration Using Artificial Neural Network: A Case Study of Ameleke watershed, Ethiopia.

Goel, J., Kadirvelu, K., Rajagopal, C., & Garg, V. K. (2005). Removal of lead (II) by adsorption using treated granular activated carbon: batch and column studies. *Journal of Hazardous Materials, 125*(1), 211-220.

Gogotsi, Y. (2006). *Nanotubes and nanofibers*: CRC press.

Goldman, L. R., Shannon, M. W., & Health, C. o. E. (2001). Technical report: mercury in the environment: implications for pediatricians. *Pediatrics, 108*(1), 197-205.

Gong, J., Feng, J., Liu, J., Jiang, Z., Chen, X., Mijowska, E., . . . Tang, T. (2014). Catalytic carbonization of polypropylene into cup-stacked carbon nanotubes with high performances in adsorption of heavy metallic ions and organic dyes. *Chemical Engineering Journal, 248*, 27-40.

Gong, J., Wang, X., Shao, X., Yuan, S., Yang, C., & Hu, X. (2012). Adsorption of heavy metal ions by hierarchically structured magnetite-carbonaceous spheres. *Talanta, 101*, 45-52.

Gorke, J. T., Srienc, F., & Kazlauskas, R. J. (2008). Hydrolase-catalyzed biotransformations in deep eutectic solvents. *Chemical Communications*(10), 1235-1237.

Govindaraju, R. S. (2000). Artificial neural networks in hydrology. I: Preliminary concepts. *Journal of hydrologic Engineering, 5*(2), 115-123.

Gu, C.-D., & Tu, J.-P. (2011). Thermochromic behavior of chloro-nickel (II) in deep eutectic solvents and their application in thermochromic composite films. *RSC Advances, 1*(7), 1220-1227.

Gu, C., & Tu, J. (2011). One-Step Fabrication of Nanostructured Ni Film with Lotus Effect from Deep Eutectic Solvent. *Langmuir, 27*(16), 10132-10140.

Gupta, A., Vidyarthi, S., & Sankararamakrishnan, N. (2014). Enhanced sorption of mercury from compact fluorescent bulbs and contaminated water streams using functionalized multiwalled carbon nanotubes. *Journal of Hazardous Materials, 274*, 132-144.

Gupta, K., Bhattacharya, S., Chattopadhyay, D., Mukhopadhyay, A., Biswas, H., Dutta, J., . . . Ghosh, U. C. (2011). Ceria associated manganese oxide nanoparticles: synthesis, characterization and arsenic (V) sorption behavior. *Chemical Engineering Journal, 172*(1), 219-229.

Gupta, V., Rastogi, A., Saini, V., & Jain, N. (2006). Biosorption of copper (II) from aqueous solutions by Spirogyra species. *Journal of colloid and interface science, 296*(1), 59-63.

Gupta, V. K., Agarwal, S., & Saleh, T. A. (2011). Synthesis and characterization of alumina-coated carbon nanotubes and their application for lead removal. *Journal of Hazardous Materials, 185*(1), 17-23.

Gupta, V. K., Rastogi, A., Saini, V. K., & Jain, N. (2006). Biosorption of copper(II) from aqueous solutions by Spirogyra species. *Journal of colloid and interface science, 296*(1), 59-63.

Haddon, R. C. (2002). Carbon nanotubes: ACS Publications.

Hamad, K., Khalil, M. A., & Shanableh, A. (2017). Modeling roadway traffic noise in a hot climate using artificial neural networks. *Transportation Research Part D: Transport and Environment, 53*, 161-177.

Hamid, H. A., Jenidi, Y., Thielemans, W., Somerfield, C., & Gomes, R. L. (2016). Predicting the capability of carboxylated cellulose nanowhiskers for the remediation of copper from water using response surface methodology (RSM) and artificial neural network (ANN) models. *Industrial Crops and Products, 93*, 108-120.

Hamon, M. A., Chen, J., Hu, H., Chen, Y., Itkis, M. E., Rao, A. M., . . . Haddon, R. C. (1999). Dissolution of single-walled carbon nanotubes. *Advanced Materials, 11*(10), 834-840.

Hamza, I. A., Martincigh, B. S., Ngila, J. C., & Nyamori, V. O. (2013). Adsorption studies of aqueous Pb (II) onto a sugarcane bagasse/multi-walled carbon nanotube composite. *Physics and Chemistry of the Earth, Parts A/B/C, 66*, 157-166.

Han, R., Zou, W., Li, H., Li, Y., & Shi, J. (2006). Copper (II) and lead (II) removal from aqueous solution in fixed-bed columns by manganese oxide coated zeolite. *Journal of Hazardous Materials, 137*(2), 934-942.

Hassett-Sipple, B., Swartout, J., & Schoeny, R. (1997). Mercury study report to Congress. Volume 5. Health effects of mercury and mercury compounds: Environmental Protection Agency, Research Triangle Park, NC (United States). Office of Air Quality Planning and Standards.

Hawari, A. H., & Mulligan, C. N. (2006). Biosorption of lead (II), cadmium (II), copper (II) and nickel (II) by anaerobic granular biomass. *Bioresource Technology, 97*(4), 692-700.

Hayati, B., Maleki, A., Najafi, F., Daraei, H., Gharibi, F., & McKay, G. (2016). Synthesis and characterization of PAMAM/CNT nanocomposite as a super-capacity adsorbent for heavy metal (Ni 2+, Zn 2+, As 3+, Co 2+) removal from wastewater. *Journal of Molecular Liquids, 224*, 1032-1040.

Hayyan, A., Mjalli, F. S., AlNashef, I. M., Al-Wahaibi, Y. M., Al-Wahaibi, T., & Hashim, M. A. (2013). Glucose-based deep eutectic solvents: Physical properties. *Journal of Molecular Liquids, 178*, 137-141.

Hayyan, M., Abo-Hamad, A., AlSaadi, M. A., & Hashim, M. A. (2015). Functionalization of graphene using deep eutectic solvents. *Nanoscale research letters, 10*(1), 324.

Hayyan, M., Hashim, M. A., Hayyan, A., Al-Saadi, M. A., AlNashef, I. M., Mirghani, M. E., & Saheed, O. K. (2013). Are deep eutectic solvents benign or toxic? *Chemosphere, 90*(7), 2193-2195.

Hayyan, M., Looi, C. Y., Hayyan, A., Wong, W. F., & Hashim, M. A. (2015). In vitro and in vivo toxicity profiling of ammonium-based deep eutectic solvents. *PloS one, 10*(2), e0117934.

Hayyan, M., Mjalli, F. S., Hashim, M. A., & AlNashef, I. M. (2010). A novel technique for separating glycerine from palm oil-based biodiesel using ionic liquids. *Fuel Processing Technology, 91*(1), 116-120.

Hazrati, H., Moghaddam, A. H., & Rostamizadeh, M. (2017). The influence of hydraulic retention time on cake layer specifications in the membrane bioreactor: Experimental and artificial neural network modeling. *Journal of Environmental Chemical Engineering*.

Hemmat Esfe, M., Afrand, M., Yan, W.-M., & Akbari, M. (2015). Applicability of artificial neural network and nonlinear regression to predict thermal conductivity modeling of Al2O3–water nanofluids using experimental data. *International Communications in Heat and Mass Transfer, 66*, 246-249.

Henneberry, Y. K., Kraus, T. E., Fleck, J. A., Krabbenhoft, D. P., Bachand, P. M., & Horwath, W. R. (2011). Removal of inorganic mercury and methylmercury from surface waters following coagulation of dissolved organic matter with metal-based salts. *Science of The Total Environment, 409*(3), 631-637.

Hirsch, A., & Vostrowsky, O. (2007). Functionalization of carbon nanotubes. *Functional organic materials: syntheses, strategies and applications*, 1-57.

Ho, Y., & McKay, G. (1999). The sorption of lead (II) ions on peat. *Water research, 33*(2), 578-584.

Hone, J., Whitney, M., Piskoti, C., & Zettl, A. (1999). Thermal conductivity of single-walled carbon nanotubes. *Physical Review B, 59*(4), R2514.

Hong, N., Zhu, P., & Liu, A. (2017). Modelling heavy metals build-up on urban road surfaces for effective stormwater reuse strategy implementation. *Environmental pollution, 231*, 821-828.

Hopfield, J. J. (1982). Neural networks and physical systems with emergent collective computational abilities. *Proceedings of the national academy of sciences, 79*(8), 2554-2558.

Hsi, H.-C., Lee, H.-H., Hwang, J.-F., & Chen, W. (2010). Mercury speciation and distribution in a 660-megawatt utility boiler in Taiwan firing bituminous coals. *Journal of the Air & Waste Management Association, 60*(5), 514-522.

Hu, S., Shi, Q., & Jing, C. (2015). Groundwater arsenic adsorption on granular TiO2: integrating atomic structure, filtration, and health impact. *Environ. Sci. Technol, 49*(16), 9707-9713.

Huang, Z.-H., Zhang, F., Wang, M.-X., Lv, R., & Kang, F. (2012). Growth of carbon nanotubes on low-cost bamboo charcoal for Pb (II) removal from aqueous solution. *Chemical Engineering Journal, 184*, 193-197.

Hung, D. Q., Nekrassova, O., & Compton, R. G. (2004). Analytical methods for inorganic arsenic in water: a review. *Talanta, 64*(2), 269-277.

Hussein, A. K. (2015). Applications of nanotechnology in renewable energies—A comprehensive overview and understanding. *Renewable and Sustainable Energy Reviews, 42*, 460-476.

Huttenloch, P., Roehl, K. E., & Czurda, K. (2003). Use of copper shavings to remove mercury from contaminated groundwater or wastewater by amalgamation. *Environmental science & technology, 37*(18), 4269-4273.

Ibrahim, R. K., Hayyan, M., AlSaadi, M. A., Hayyan, A., & Ibrahim, S. (2016). Environmental application of nanotechnology: air, soil, and water. *Environmental Science and Pollution Research, 23*(14), 13754-13788.

Ihsanullah, Abbas, A., Al-Amer, A. M., Laoui, T., Al-Marri, M. J., Nasser, M. S., . . . Atieh, M. A. (2016). Heavy metal removal from aqueous solution by advanced

carbon nanotubes: Critical review of adsorption applications. *Separation and Purification Technology, 157*, 141-161.

Iijima, S. (1991). Helical microtubules of graphitic carbon. *Nature, 354*(6348), 56.

Imamoglu, M., & Tekir, O. (2008). Removal of copper (II) and lead (II) ions from aqueous solutions by adsorption on activated carbon from a new precursor hazelnut husks. *Desalination, 228*(1-3), 108-113.

Ince, R. (2004). Prediction of fracture parameters of concrete by artificial neural networks. *Engineering Fracture Mechanics, 71*(15), 2143-2159.

Jain, A., & Agarwal, M. (2017). Kinetic equilibrium and thermodynamic study of arsenic removal from water using alumina supported iron nano particles. *Journal of Water Process Engineering, 19*, 51-59.

Ji, L., Chen, W., Duan, L., & Zhu, D. (2009). Mechanisms for strong adsorption of tetracycline to carbon nanotubes: a comparative study using activated carbon and graphite as adsorbents. *Environmental science & technology, 43*(7), 2322-2327.

Jia, H., An, J., Guo, X., Su, C., Zhang, L., Zhou, H., & Xie, C. (2015). Deep eutectic solvent-assisted growth of gold nanofoams and their excellent catalytic properties. *Journal of Molecular Liquids, 212*, 763-766.

Jiang, G.-B., Shi, J.-B., & Feng, X.-B. (2006). Mercury pollution in China: ACS Publications.

Jiang, K., Sun, T.-h., Sun, L.-n., & Li, H.-b. (2006). Adsorption characteristics of copper, lead, zinc and cadmium ions by tourmaline. *Journal of Environmental Sciences, 18*(6), 1221-1225.

Justi, K. C., Fávere, V. T., Laranjeira, M. C., Neves, A., & Peralta, R. A. (2005). Kinetics and equilibrium adsorption of Cu (II), Cd (II), and Ni (II) ions by chitosan functionalized with 2 [-bis-(pyridylmethyl) aminomethyl]-4-methyl-6-formylphenol. *Journal of colloid and interface science, 291*(2), 369-374.

Kabbashi, N. A., Atieh, M. A., Al-Mamun, A., Mirghami, M. E., Alam, M., & Yahya, N. (2009). Kinetic adsorption of application of carbon nanotubes for Pb (II) removal from aqueous solution. *Journal of Environmental Sciences, 21*(4), 539-544.

Kabbashi, N. A., Atieh, M. A., Al-Mamun, A., Mirghami, M. E. S., Alam, M. D. Z., & Yahya, N. (2009). Kinetic adsorption of application of carbon nanotubes for Pb(II) removal from aqueous solution. *Journal of Environmental Sciences, 21*(4), 539-544.

Kadirvelu, K., Kavipriya, M., Karthika, C., Vennilamani, N., & Pattabhi, S. (2004). Mercury (II) adsorption by activated carbon made from sago waste. *Carbon, 42*(4), 745-752.

Kadirvelu, K., Thamaraiselvi, K., & Namasivayam, C. (2001). Removal of heavy metals from industrial wastewaters by adsorption onto activated carbon prepared from an agricultural solid waste. *Bioresource Technology, 76*(1), 63-65.

Kamble, S. P., Jagtap, S., Labhsetwar, N. K., Thakare, D., Godfrey, S., Devotta, S., & Rayalu, S. S. (2007). Defluoridation of drinking water using chitin, chitosan and lanthanum-modified chitosan. *Chemical Engineering Journal, 129*(1), 173-180.

Kaneko, K. (1994). Determination of pore size and pore size distribution: 1. Adsorbents and catalysts. *Journal of membrane science, 96*(1-2), 59-89.

Karimi, M., Eshraghi, M., & Jahangir, V. (2016). A facile and green synthetic approach based on deep eutectic solvents toward synthesis of CZTS nanoparticles. *Materials Letters, 171*, 100-103.

Karnib, M., Kabbani, A., Holail, H., & Olama, Z. (2014). Heavy Metals Removal Using Activated Carbon, Silica and Silica Activated Carbon Composite. *Energy Procedia, 50*, 113-120.

Karousis, N., Tagmatarchis, N., & Tasis, D. (2010). Current progress on the chemical modification of carbon nanotubes. *Chemical Reviews, 110*(9), 5366-5397.

Kazemipour, M., Ansari, M., Tajrobehkar, S., Majdzadeh, M., & Kermani, H. R. (2008). Removal of lead, cadmium, zinc, and copper from industrial wastewater by carbon developed from walnut, hazelnut, almond, pistachio shell, and apricot stone. *Journal of Hazardous Materials, 150*(2), 322-327.

Kewalramani, M. A., & Gupta, R. (2006). Concrete compressive strength prediction using ultrasonic pulse velocity through artificial neural networks. *Automation in Construction, 15*(3), 374-379.

Khajeh, M., Sarafraz-Yazdi, A., & Moghadam, A. F. (2017). Modeling of solid-phase tea waste extraction for the removal of manganese and cobalt from water samples by using PSO-artificial neural network and response surface methodology. *Arabian Journal of Chemistry, 10*, S1663-S1673.

Khajeh, M. M. a. M. (2011). "Comparison of Response Surface Methodology and Artificial Neural Network in Predicting the Microwave-Assisted Extraction Procedure to Determine Zinc in Fish Muscles" *Food and Nutrition Sciences, Vol. 2*(No. 8,), pp. 803-808.

Khalil, B., Ouarda, T., & St-Hilaire, A. (2011). Estimation of water quality characteristics at ungauged sites using artificial neural networks and canonical correlation analysis. *Journal of Hydrology, 405*(3), 277-287.

Khandanlou, R., Masoumi, H. R. F., Ahmad, M. B., Shameli, K., Basri, M., & Kalantari, K. (2016). Enhancement of heavy metals sorption via nanocomposites of rice straw and Fe 3 O 4 nanoparticles using artificial neural network (ANN). *Ecological Engineering, 91*, 249-256.

Kim, E.-J., Lee, C.-S., Chang, Y.-Y., & Chang, Y.-S. (2013). Hierarchically structured manganese oxide-coated magnetic nanocomposites for the efficient removal of heavy metal ions from aqueous systems. *ACS applied materials & interfaces, 5*(19), 9628-9634.

Kim, J., & Benjamin, M. M. (2004). Modeling a novel ion exchange process for arsenic and nitrate removal. *Water research, 38*(8), 2053-2062.

Kim, S. E., & Seo, I. W. (2015). Artificial Neural Network ensemble modeling with conjunctive data clustering for water quality prediction in rivers. *Journal of Hydro-Environment Research, 9*(3), 325-339.

Kiparissides, C., & Kammona, O. (2015). Nanotechnology advances in diagnostics, drug delivery, and regenerative medicine *The nano-micro interface: bridging the micro and nano worlds*: Wiley-VCH Verlag GmbH & Co. KGaA Weinheim, Germany.

Kobya, M., Demirbas, E., Senturk, E., & Ince, M. (2005). Adsorption of heavy metal ions from aqueous solutions by activated carbon prepared from apricot stone. *Bioresource Technology, 96*(13), 1518-1521.

Kocabaş-Ataklı, Z. Ö., & Yürüm, Y. (2013). Synthesis and characterization of anatase nanoadsorbent and application in removal of lead, copper and arsenic from water. *Chemical Engineering Journal, 225*, 625-635.

Kothari, R., & Agyepong, K. (1996, 3-6 Jun 1996). *On lateral connections in feed-forward neural networks.* Paper presented at the Neural Networks, 1996., IEEE International Conference on.

Koziol, K., Vilatela, J., Moisala, A., Motta, M., Cunniff, P., Sennett, M., & Windle, A. (2007). High-performance carbon nanotube fiber. *Science, 318*(5858), 1892-1895.

Kumar, M. S., & Phanikumar, B. (2013). Response surface modelling of Cr6+ adsorption from aqueous solution by neem bark powder: Box–Behnken experimental approach. *Environmental Science and Pollution Research, 20*(3), 1327-1343.

Kumar, P. R., Chaudhari, S., Khilar, K. C., & Mahajan, S. (2004). Removal of arsenic from water by electrocoagulation. *Chemosphere, 55*(9), 1245-1252.

Kurt, H., & Kayfeci, M. (2009). Prediction of thermal conductivity of ethylene glycol–water solutions by using artificial neural networks. *Applied Energy, 86*(10), 2244-2248.

Lee, J.-W., Suh, C., Hong, Y.-S. T., & Shin, H.-S. (2011). Sequential modelling of a full-scale wastewater treatment plant using an artificial neural network. *Bioprocess and biosystems engineering, 34*(8), 963.

Lee, S.-C. (2003). Prediction of concrete strength using artificial neural networks. *Engineering Structures, 25*(7), 849-857.

León-Roque, N., Abderrahim, M., Nuñez-Alejos, L., Arribas, S. M., & Condezo-Hoyos, L. (2016). Prediction of fermentation index of cocoa beans (Theobroma cacao L.) based on color measurement and artificial neural networks. *Talanta, 161*, 31-39.

Leopold, K., Foulkes, M., & Worsfold, P. (2010). Methods for the determination and speciation of mercury in natural waters—a review. *Analytica chimica acta, 663*(2), 127-138.

Leroy, E., Decaen, P., Jacquet, P., Coativy, G., Pontoire, B., Reguerre, A.-L., & Lourdin, D. (2012). Deep eutectic solvents as functional additives for starch based plastics. *Green Chemistry, 14*(11), 3063-3066.

Li, S.-X., Feng-Ying, Z., Yang, H., & Jian-Cong, N. (2011). Thorough removal of inorganic and organic mercury from aqueous solutions by adsorption on Lemna minor powder. *Journal of Hazardous Materials, 186*(1), 423-429.

Li, W., Wei, S., Jiao, W., Qi, G., & Liu, Y. (2016). Modelling of adsorption in rotating packed bed using artificial neural networks (ANN). *Chemical Engineering Research and Design, 114*, 89-95.

Li, X., Hou, M., Han, B., Wang, X., & Zou, L. (2008). Solubility of CO2 in a choline chloride+ urea eutectic mixture. *Journal of Chemical & Engineering Data, 53*(2), 548-550.

Li, Y.-H., Wang, S., Luan, Z., Ding, J., Xu, C., & Wu, D. (2003). Adsorption of cadmium (II) from aqueous solution by surface oxidized carbon nanotubes. *Carbon, 41*(5), 1057-1062.

Li, Y.-H., Wang, S., Wei, J., Zhang, X., Xu, C., Luan, Z., . . . Wei, B. (2002). Lead adsorption on carbon nanotubes. *Chemical physics letters, 357*(3), 263-266.

Lin, D., Tian, X., Li, T., Zhang, Z., He, X., & Xing, B. (2012). Surface-bound humic acid increased Pb 2+ sorption on carbon nanotubes. *Environmental pollution, 167*, 138-147.

Lin, T., Bajpai, V., Ji, T., & Dai, L. (2003). Chemistry of carbon nanotubes. *Australian journal of chemistry, 56*(7), 635-651.

Liu, G., Zhang, X., Talley, J. W., Neal, C. R., & Wang, H. (2008). Effect of NOM on arsenic adsorption by TiO 2 in simulated As (III)-contaminated raw waters. *Water research, 42*(8), 2309-2319.

Liu, P. (2005). Modifications of carbon nanotubes with polymers. *European Polymer Journal, 41*(11), 2693-2703.

Liu, Y., Yan, J., Yuan, D., Li, Q., & Wu, X. (2013). The study of lead removal from aqueous solution using an electrochemical method with a stainless steel net electrode coated with single wall carbon nanotubes. *Chemical Engineering Journal, 218*, 81-88.

Long, R. Q., & Yang, R. T. (2001). Carbon nanotubes as superior sorbent for dioxin removal. *Journal of the American Chemical Society, 123*(9), 2058-2059.

Lopes, C., Otero, M., Coimbra, J., Pereira, E., Rocha, J., Lin, Z., & Duarte, A. (2007). Removal of low concentration Hg2+ from natural waters by microporous and layered titanosilicates. *Microporous and Mesoporous Materials, 103*(1-3), 325-332.

López-Salas, N., Jardim, E. O., Silvestre-Albero, A., Gutiérrez, M., Ferrer, M., Rodríguez-Reinoso, F., . . . del Monte, F. (2014). Use of Eutectic Mixtures for Preparation of Monolithic Carbons with CO2-Adsorption and Gas-Separation Capabilities. *Langmuir, 30*(41), 12220-12228.

Lourie, E., & Gjengedal, E. (2011). Metal sorption by peat and algae treated peat: Kinetics and factors affecting the process. *Chemosphere, 85*(5), 759-764.

Lourie, O., Wagner, H. D., Zhang, Y., & Iijima, S. (1999). Dependence of Elastic Properties on Morphology in Single-Wall Carbon Nanotubes. *Advanced Materials, 11*(11), 931-934.

Lu, C., & Chiu, H. (2006). Adsorption of zinc (II) from water with purified carbon nanotubes. *Chemical Engineering Science, 61*(4), 1138-1145.

Lu, C., Chung, Y.-L., & Chang, K.-F. (2005). Adsorption of trihalomethanes from water with carbon nanotubes. *Water research, 39*(6), 1183-1189.

Lu, X., & Chen, Z. (2005). Curved pi-conjugation, aromaticity, and the related chemistry of small fullerenes. *Chemical Reviews, 105*(10), 3643-3696.

Luo, C., Tian, Z., Yang, B., Zhang, L., & Yan, S. (2013). Manganese dioxide/iron oxide/acid oxidized multi-walled carbon nanotube magnetic nanocomposite for enhanced hexavalent chromium removal. *Chemical Engineering Journal, 234*, 256-265.

Luo, X., Zhang, Z., Zhou, P., Liu, Y., Ma, G., & Lei, Z. (2015). Synergic adsorption of acid blue 80 and heavy metal ions (Cu 2+/Ni 2+) onto activated carbon and its mechanisms. *Journal of Industrial and Engineering Chemistry, 27*, 164-174.

Ma, P.-C., Siddiqui, N. A., Marom, G., & Kim, J.-K. (2010). Dispersion and functionalization of carbon nanotubes for polymer-based nanocomposites: a review. *Composites Part A: Applied Science and Manufacturing, 41*(10), 1345-1367.

Ma, P. C., Kim, J.-K., & Tang, B. Z. (2006). Functionalization of carbon nanotubes using a silane coupling agent. *Carbon, 44*(15), 3232-3238.

Majumdar, S. S., Das, S. K., Chakravarty, R., Saha, T., Bandyopadhyay, T. S., & Guha, A. K. (2010). A study on lead adsorption by Mucor rouxii biomass. *Desalination, 251*(1–3), 96-102.

Mak, M. S., Rao, P., & Lo, I. M. (2009). Effects of hardness and alkalinity on the removal of arsenic (V) from humic acid-deficient and humic acid-rich groundwater by zero-valent iron. *Water research, 43*(17), 4296-4304.

Mąka, H., Spychaj, T., & Kowalczyk, K. (2014). Imidazolium and deep eutectic ionic liquids as epoxy resin crosslinkers and graphite nanoplatelets dispersants. *Journal of Applied Polymer Science, 131*(12).

Mallat, S. G. (1989). A theory for multiresolution signal decomposition: the wavelet representation. *IEEE transactions on pattern analysis and machine intelligence, 11*(7), 674-693.

Mandal, B. K., & Suzuki, K. T. (2002). Arsenic round the world: a review. *Talanta, 58*(1), 201-235.

Mandal, S., Mahapatra, S., Sahu, M., & Patel, R. (2015). Artificial neural network modelling of As (III) removal from water by novel hybrid material. *Process Safety and Environmental Protection, 93*, 249-264.

Mandal, S., Sivaprasad, P. V., Venugopal, S., & Murthy, K. P. N. (2009). Artificial neural network modeling to evaluate and predict the deformation behavior of stainless steel type AISI 304L during hot torsion. *Applied Soft Computing, 9*(1), 237-244.

Mansoori, G. A., & Soelaiman, T. F. (2005). Nanotechnology—an introduction for the standards community. *Journal of ASTM International, 2*(6), 1-22.

Martinez, M., Callejas, M., Benito, A., Cochet, M., Seeger, T., Anson, A., . . . Chauvet, O. (2003). Modifications of single-wall carbon nanotubes upon oxidative purification treatments. *Nanotechnology, 14*(7), 691.

Martinson, C. A., & Reddy, K. (2009). Adsorption of arsenic (III) and arsenic (V) by cupric oxide nanoparticles. *Journal of colloid and interface science, 336*(2), 406-411.

Mazumder, D. G., Mandal, B., Chowdhury, T., Samanta, G., Basu, G., Chowdhury, P., . . . Chakraborti, D. (1997). Chronic arsenic toxicity in West Bengal. *Curr Sci, 72*(1), 114-117.

McAvoy, T. J., & Werbos, P. (1992). Long-term predictions of chemical processes using recurrent neural networks: A parallel training approach. *Industrial & Engineering Chemistry Research, 31*(5), 1338-1352.

McCulloch, W. S., & Pitts, W. (1943). A logical calculus of the ideas immanent in nervous activity. *The bulletin of mathematical biophysics, 5*(4), 115-133.

Mendoza-Castillo, D. I., Rojas-Mayorga, C. K., García-Martínez, I. P., Pérez-Cruz, M. A., Hernández-Montoya, V., Bonilla-Petriciolet, A., & Montes-Morán, M. A. (2015). Removal of heavy metals and arsenic from aqueous solution using textile wastes from denim industry. *International Journal of Environmental Science and Technology, 12*(5), 1657-1668.

Mittal, G., Dhand, V., Rhee, K. Y., Park, S.-J., & Lee, W. R. (2015). A review on carbon nanotubes and graphene as fillers in reinforced polymer nanocomposites. *Journal of Industrial and Engineering Chemistry, 21*, 11-25.

Mjalli, F. S., Al-Asheh, S., & Alfadala, H. E. (2007). Use of artificial neural network black-box modeling for the prediction of wastewater treatment plants performance. *Journal of Environmental Management, 83*(3), 329-338.

Mobasherpour, I., Salahi, E., & Ebrahimi, M. (2012). Removal of divalent nickel cations from aqueous solution by multi-walled carbon nano tubes: equilibrium and kinetic processes. *Research on Chemical Intermediates, 38*(9), 2205-2222.

Moghaddam, M. G., & Khajeh, M. (2011). Comparison of response surface methodology and artificial neural network in predicting the microwave-assisted extraction procedure to determine zinc in fish muscles. *Food and Nutrition Sciences, 2*(08), 803.

Mohamed Khalid AlOmar, M. A. A., Mustafa Mohammed Aljumaily, Shatirah Akib, Taha M. Jassam, Mohd Ali Hashim. (2017). N,N-Diethylethanolammonium chloride-based DES-functionalized carbon nanotubes for arsenic removal from aqueous solution. *Desalination and Water Treatment, 74*, 163-173.

Mohan, D., Gupta, V., Srivastava, S., & Chander, S. (2001). Kinetics of mercury adsorption from wastewater using activated carbon derived from fertilizer waste. *Colloids and Surfaces A: Physicochemical and Engineering Aspects, 177*(2), 169-181.

Mohmood, I., Lopes, C. B., Lopes, I., Ahmad, I., Duarte, A. C., & Pereira, E. (2013). Nanoscale materials and their use in water contaminants removal—a review. *Environmental Science and Pollution Research, 20*(3), 1239-1260.

Mota-Morales, J. D., Gutiérrez, M. C., Ferrer, M. L., Jiménez, R., Santiago, P., Sanchez, I. C., . . . Luna-Bárcenas, G. (2013). Synthesis of macroporous poly (acrylic acid)–carbon nanotube composites by frontal polymerization in deep-eutectic solvents. *Journal of Materials Chemistry A, 1*(12), 3970-3976.

Mousavi, A., Chávez, R. D., Ali, A.-M. S., & Cabaniss, S. E. (2011). Mercury in natural waters: a mini-review. *Environmental Forensics, 12*(1), 14-18.

Mubarak, N., Alicia, R., Abdullah, E., Sahu, J., Haslija, A. A., & Tan, J. (2013). Statistical optimization and kinetic studies on removal of Zn 2+ using functionalized carbon nanotubes and magnetic biochar. *Journal of Environmental Chemical Engineering, 1*(3), 486-495.

Mubarak, N., Sahu, J., Abdullah, E., & Jayakumar, N. (2014). Removal of heavy metals from wastewater using carbon nanotubes. *Separation & Purification Reviews, 43*(4), 311-338.

Mubarak, N., Sahu, J., Abdullah, E., Jayakumar, N., & Ganesan, P. (2015a). Microwave assisted multiwall carbon nanotubes enhancing Cd (II) adsorption capacity in aqueous media. *Journal of Industrial and Engineering Chemistry, 24*, 24-33.

Mubarak, N., Sahu, J., Abdullah, E., Jayakumar, N., & Ganesan, P. (2015b). Novel microwave-assisted multiwall carbon nanotubes enhancing Cu (II) adsorption capacity in water. *Journal of the Taiwan Institute of Chemical Engineers, 53*, 140-152.

Mubarak, N., Sahu, J., Wong, J., Jayakumar, N., Ganesan, P., & Abdullah, E. (2015). Overview on the functionalization of carbon nanotubes (pp. 82-101): CRC Press, Boca Raton, FL, USA.

Mubarak, N., Sazila, N., Nizamuddin, S., Abdullah, E., & Sahu, J. (2017). Adsorptive Removal of Phenol from Aqueous Solution by Using Carbon Nanotubes and Magnetic BioChar. *NanoWorld J, 3*(2), 32-37.

Mubarak, N. M., Sahu, J. N., Abdullah, E. C., & Jayakumar, N. S. (2016). Rapid adsorption of toxic Pb (II) ions from aqueous solution using multiwall carbon nanotubes synthesized by microwave chemical vapor deposition technique. *Journal of Environmental Sciences, 45*, 143-155.

Müller, B., Zumbuehl, A., Walter, M. A., Pfohl, T., Cattin, P. C., Huwyler, J., & Hieber, S. E. (2015). Translational medicine: nanoscience and nanotechnology to improve patient care. *The nano-micro interface: bridging the micro and nano worlds*, 289-310.

Nabipour, M., & Keshavarz, P. (2017). Modeling surface tension of pure refrigerants using feed-forward back-propagation neural networks. *International Journal of Refrigeration, 75*, 217-227.

Nejad, F. P., & Jaksa, M. B. (2017). Load-settlement behavior modeling of single piles using artificial neural networks and CPT data. *Computers and Geotechnics, 89*, 9-21.

Netzer, A., & Hughes, D. (1984). Adsorption of copper, lead and cobalt by activated carbon. *Water research, 18*(8), 927-933.

Ng, J. C. (2005). Environmental contamination of arsenic and its toxicological impact on humans. *Environmental Chemistry, 2*(3), 146-160.

Ngueta, G., Prévost, M., Deshommes, E., Abdous, B., Gauvin, D., & Levallois, P. (2014). Exposure of young children to household water lead in the Montreal area (Canada): The potential influence of winter-to-summer changes in water lead levels on children's blood lead concentration. *Environment international, 73*, 57-65.

Ni, H.-G., & Wang, J.-Z. (2000). Prediction of compressive strength of concrete by neural networks. *Cement and Concrete Research, 30*(8), 1245-1250.

Ning, R. Y. (2002). Arsenic removal by reverse osmosis. *Desalination, 143*(3), 237-241.

Niyogi, S., Hamon, M., Hu, H., Zhao, B., Bhowmik, P., Sen, R., . . . Haddon, R. (2002). Chemistry of single-walled carbon nanotubes. *Accounts of Chemical Research, 35*(12), 1105-1113.

Nriagu, J. O. (1988). A silent epidemic of environmental metal poisoning? *Environmental pollution, 50*(1-2), 139-161.

Oehmen, A., Viegas, R., Velizarov, S., Reis, M. A., & Crespo, J. G. (2006). Removal of heavy metals from drinking water supplies through the ion exchange membrane bioreactor. *Desalination, 199*(1-3), 405-407.

Oh, J.-H., & Lee, J.-S. (2014). Synthesis of gold microstructures with surface nanoroughness using a deep eutectic solvent for catalytic and diagnostic applications. *Journal of nanoscience and nanotechnology, 14*(5), 3753-3757.

Olalere, O. A., Abdurahman, N. H., bin Mohd Yunus, R., & Alara, O. R. (2017). Multi-response optimization and neural network modeling for parameter precision in heat reflux extraction of spice oleoresins from two pepper cultivars (Piper nigrum). *Journal of King Saud University-Science*.

Olaofe, Z. O. (2014). A 5-day wind speed & power forecasts using a layer recurrent neural network (LRNN). *Sustainable Energy Technologies and Assessments, 6*, 1-24.

Orumwense, F. F. (1996). Removal of lead from water by adsorption on a kaolinitic clay. *Journal of Chemical Technology and Biotechnology, 65*(4), 363-369.

Oubagaranadin, J. U. K., & Murthy, Z. (2010). Isotherm modeling and batch adsorber design for the adsorption of Cu (II) on a clay containing montmorillonite. *Applied Clay Science, 50*(3), 409-413.

Oubagaranadin, J. U. K., & Murthy, Z. V. P. (2010). Isotherm modeling and batch adsorber design for the adsorption of Cu(II) on a clay containing montmorillonite. *Applied Clay Science, 50*(3), 409-413.

Oubagaranadin, J. U. K., Sathyamurthy, N., & Murthy, Z. (2007). Evaluation of Fuller's earth for the adsorption of mercury from aqueous solutions: a comparative study with activated carbon. *Journal of Hazardous Materials, 142*(1-2), 165-174.

Pacyna, E. G., Pacyna, J., Sundseth, K., Munthe, J., Kindbom, K., Wilson, S., . . . Maxson, P. (2010). Global emission of mercury to the atmosphere from anthropogenic sources in 2005 and projections to 2020. *Atmospheric Environment, 44*(20), 2487-2499.

Paiva, A., Craveiro, R., Aroso, I., Martins, M., Reis, R. L., & Duarte, A. R. C. (2014). Natural deep eutectic solvents–solvents for the 21st century. *ACS Sustainable Chemistry & Engineering, 2*(5), 1063-1071.

Park, M. J., Lee, J. K., Lee, B. S., Lee, Y.-W., Choi, I. S., & Lee, S.-g. (2006). Covalent modification of multiwalled carbon nanotubes with imidazolium-based ionic liquids: effect of anions on solubility. *Chemistry of Materials, 18*(6), 1546-1551.

Patel, H. A., Byun, J., & Yavuz, C. T. (2012). Arsenic removal by magnetic nanocrystalline barium hexaferrite. *Journal of Nanoparticle Research, 14*(7), 881.

Pattanayak, J., Mondal, K., Mathew, S., & Lalvani, S. (2000). A parametric evaluation of the removal of As (V) and As (III) by carbon-based adsorbents. *Carbon, 38*(4), 589-596.

Payne, K. B., & Abdel-Fattah, T. M. (2005). Adsorption of arsenate and arsenite by iron-treated activated carbon and zeolites: effects of pH, temperature, and ionic strength. *Journal of Environmental Science and Health, 40*(4), 723-749.

Peng, X., Li, Y., Luan, Z., Di, Z., Wang, H., Tian, B., & Jia, Z. (2003). Adsorption of 1, 2-dichlorobenzene from water to carbon nanotubes. *Chemical physics letters, 376*(1), 154-158.

Phadtare, S. B., & Shankarling, G. S. (2010). Halogenation reactions in biodegradable solvent: Efficient bromination of substituted 1-aminoanthra-9, 10-quinone in deep eutectic solvent (choline chloride: urea). *Green Chemistry, 12*(3), 458-462.

Pimentel, P. M., González, G., Melo, M. F. A., Melo, D. M. A., Silva Jr, C. N., & Assunção, A. L. C. (2007). Removal of lead ions from aqueous solution by retorted shale. *Separation and Purification Technology, 56*(3), 348-353.

Pivetta, T., Isaia, F., Trudu, F., Pani, A., Manca, M., Perra, D., . . . Havel, J. (2013). Development and validation of a general approach to predict and quantify the synergism of anti-cancer drugs using experimental design and artificial neural networks. *Talanta, 115*, 84-93.

Podder, M., & Majumder, C. (2016). The use of artificial neural network for modelling of phycoremediation of toxic elements As (III) and As (V) from wastewater using Botryococcus braunii. *Spectrochimica Acta Part A: Molecular and Biomolecular Spectroscopy, 155*, 130-145.

Podstawczyk, D., Witek-Krowiak, A., Dawiec, A., & Bhatnagar, A. (2015). Biosorption of copper (II) ions by flax meal: Empirical modeling and process optimization by response surface methodology (RSM) and artificial neural network (ANN) simulation. *Ecological Engineering, 83*, 364-379.

Polo-Luque, M., Simonet, B., & Valcárcel, M. (2013). Functionalization and dispersion of carbon nanotubes in ionic liquids. *TrAC Trends in Analytical Chemistry, 47*, 99-110.

Pombeiro, H., Santos, R., Carreira, P., Silva, C., & Sousa, J. M. (2017). Comparative assessment of low-complexity models to predict electricity consumption in an

institutional building: Linear regression vs. fuzzy modeling vs. neural networks. *Energy and Buildings, 146*, 141-151.

Popov, V. N. (2004). Carbon nanotubes: properties and application. *Materials Science and Engineering: R: Reports, 43*(3), 61-102.

Ramos, M. A., Yan, W., Li, X.-q., Koel, B. E., & Zhang, W.-x. (2009). Simultaneous oxidation and reduction of arsenic by zero-valent iron nanoparticles: Understanding the significance of the core− shell structure. *The Journal of Physical Chemistry C, 113*(33), 14591-14594.

Ramos, M. L. P., González, J. A., Albornoz, S. G., Pérez, C. J., Villanueva, M. E., Giorgieri, S. A., & Copello, G. J. (2016). Chitin hydrogel reinforced with TiO 2 nanoparticles as an arsenic sorbent. *Chemical Engineering Journal, 285*, 581-587.

Ramsden, J. (2009). *Essentials of nanotechnology*: BookBoon.

Rao, G. P., Lu, C., & Su, F. (2007). Sorption of divalent metal ions from aqueous solution by carbon nanotubes: a review. *Separation and Purification Technology, 58*(1), 224-231.

Ratna Kumar, P., Chaudhari, S., Khilar, K. C., & Mahajan, S. P. (2004). Removal of arsenic from water by electrocoagulation. *Chemosphere, 55*(9), 1245-1252.

Renjith, A., Roy, A., & Lakshminarayanan, V. (2014). In situ fabrication of electrochemically grown mesoporous metallic thin films by anodic dissolution in deep eutectic solvents. *Journal of colloid and interface science, 426*, 270-279.

Ricardo, A. I. C., Sánchez-Cachero, A., Jiménez-Moreno, M., Bernardo, F. J. G., Martín-Doimeadios, R. C. R., & Ríos, Á. (2018). Carbon nanotubes magnetic hybrid nanocomposites for a rapid and selective preconcentration and clean-up of mercury species in water samples. *Talanta, 179*, 442-447.

Rice, K. M., Walker Jr, E. M., Wu, M., Gillette, C., & Blough, E. R. (2014). Environmental mercury and its toxic effects. *Journal of preventive medicine and public health, 47*(2), 74.

Richter, M., Berndt, H., Eckelt, R., Schneider, M., & Fricke, R. (1999). Zeolite-mediated removal of NO x by NH 3 from exhaust streams at low temperatures. *Catalysis today, 54*(4), 531-545.

Roy, P., Mondal, N., & Das, K. (2014). Modeling of the adsorptive removal of arsenic: a statistical approach. *Journal of Environmental Chemical Engineering, 2*(1), 585-597.

Ru, C. (2000). Effect of van der Waals forces on axial buckling of a double-walled carbon nanotube. *Journal of Applied Physics, 87*(10), 7227-7231.

Rudnitskaya, A., Ehlert, A., Legin, A., Vlasov, Y., & Büttgenbach, S. (2001). Multisensor system on the basis of an array of non-specific chemical sensors and artificial neural networks for determination of inorganic pollutants in a model groundwater. *Talanta, 55*(2), 425-431.

Rumelhart, D. E., Hinton, G. E., & McClelland, J. L. (1986). A general framework for parallel distributed processing. *Parallel distributed processing: Explorations in the microstructure of cognition, 1*, 45-76.

Ruthiraan, M., Mubarak, N. M., Thines, R. K., Abdullah, E. C., Sahu, J. N., Jayakumar, N. S., & Ganesan, P. (2015). Comparative kinetic study of functionalized carbon nanotubes and magnetic biochar for removal of Cd2+ ions from wastewater. *Korean Journal of Chemical Engineering, 32*(3), 446-457.

Sabour, M. R., & Amiri, A. (2017). Comparative study of ANN and RSM for simultaneous optimization of multiple targets in Fenton treatment of landfill leachate. *Waste Management, 65*, 54-62.

Sadrzadeh, M., Mohammadi, T., Ivakpour, J., & Kasiri, N. (2008). Separation of lead ions from wastewater using electrodialysis: comparing mathematical and neural network modeling. *Chemical Engineering Journal, 144*(3), 431-441.

Sadrzadeh, M., Mohammadi, T., Ivakpour, J., & Kasiri, N. (2009). Neural network modeling of Pb 2+ removal from wastewater using electrodialysis. *Chemical Engineering and Processing: Process Intensification, 48*(8), 1371-1381.

Sahu, U. K., Mahapatra, S. S., & Patel, R. K. (2017). Application of Box–Behnken Design in response surface methodology for adsorptive removal of arsenic from aqueous solution using CeO 2/Fe 2 O 3/graphene nanocomposite. *Materials Chemistry and Physics*.

Saito, R., Dresselhaus, G., & Dresselhaus, M. S. (1998). *Physical properties of carbon nanotubes*: World scientific.

Salam, M. A. (2013). Coating carbon nanotubes with crystalline manganese dioxide nanoparticles and their application for lead ions removal from model and real water. *Colloids and Surfaces A: Physicochemical and Engineering Aspects, 419*, 69-79.

Salisu, A., Sanagi, M. M., Abu Naim, A., Wan Ibrahim, W. A., & Abd Karim, K. J. (2016). Removal of lead ions from aqueous solutions using sodium alginate-graft-poly(methyl methacrylate) beads. *Desalination and Water Treatment, 57*(33), 15353-15361.

Samarasinghe, S. (2016). *Neural networks for applied sciences and engineering: from fundamentals to complex pattern recognition*: CRC Press.

Sánchez, A. S., Rodrigues, D. A., Fontes, R. M., Martins, M. F., de Araújo Kalid, R., & Torres, E. A. (2017). Wave resource characterization through in-situ measurement followed by artificial neural networks' modeling. *Renewable Energy*.

Sarangi, A., & Bhattacharya, A. K. (2005). Comparison of Artificial Neural Network and regression models for sediment loss prediction from Banha watershed in India. *Agricultural Water Management, 78*(3), 195-208.

Sekar, M., Sakthi, V., & Rengaraj, S. (2004). Kinetics and equilibrium adsorption study of lead (II) onto activated carbon prepared from coconut shell. *Journal of colloid and interface science, 279*(2), 307-313.

Selvakumar, R., Jothi, N. A., Jayavignesh, V., Karthikaiselvi, K., Antony, G. I., Sharmila, P., . . . Swaminathan, K. (2011). As (V) removal using carbonized yeast cells containing silver nanoparticles. *Water research, 45*(2), 583-592.

Sharma, V. K., & Sohn, M. (2009). Aquatic arsenic: toxicity, speciation, transformations, and remediation. *Environment international, 35*(4), 743-759.

Shetty, G. R., & Chellam, S. (2003). Predicting membrane fouling during municipal drinking water nanofiltration using artificial neural networks. *Journal of membrane science, 217*(1), 69-86.

Shirazian, S., Kuhs, M., Darwish, S., Croker, D., & Walker, G. M. (2017). Artificial neural network modelling of continuous wet granulation using a twin-screw extruder. *International journal of pharmaceutics, 521*(1), 102-109.

Shojaeimehr, T., Rahimpour, F., Khadivi, M. A., & Sadeghi, M. (2014). A modeling study by response surface methodology (RSM) and artificial neural network (ANN) on Cu 2+ adsorption optimization using light expended clay aggregate (LECA). *Journal of Industrial and Engineering Chemistry, 20*(3), 870-880.

Singh, B., Lobo, H., & Shankarling, G. (2011). Selective N-alkylation of aromatic primary amines catalyzed by bio-catalyst or deep eutectic solvent. *Catalysis letters, 141*(1), 178-182.

Singha, B., Bar, N., & Das, S. K. (2015). The use of artificial neural network (ANN) for modeling of Pb (II) adsorption in batch process. *Journal of Molecular Liquids, 211*, 228-232.

Šipoš, T. K., Miličević, I., & Siddique, R. (2017). Model for mix design of brick aggregate concrete based on neural network modelling. *Construction and Building Materials, 148*, 757-769.

Smedley, P. L., & Kinniburgh, D. G. (2001). United Nations Synthesis Report on Arsenic in Drinking-Water. *British Geological Survey*, 1-61.

Smith, A. H., Lopipero, P. A., Bates, M. N., & Steinmaus, C. M. (2002). Arsenic epidemiology and drinking water standards. *Science, 296*(5576), 2145-2146.

Smith, E. L., Abbott, A. P., & Ryder, K. S. (2014). Deep eutectic solvents (DESs) and their applications. *Chemical Reviews, 114*(21), 11060-11082.

Sobhani, J., Najimi, M., Pourkhorshidi, A. R., & Parhizkar, T. (2010). Prediction of the compressive strength of no-slump concrete: A comparative study of regression, neural network and ANFIS models. *Construction and Building Materials, 24*(5), 709-718.

Sonawane, Y. A., Phadtare, S. B., Borse, B. N., Jagtap, A. R., & Shankarling, G. S. (2010). Synthesis of diphenylamine-based novel fluorescent styryl colorants by knoevenagel condensation using a conventional method, biocatalyst, and deep eutectic solvent. *Organic letters, 12*(7), 1456-1459.

Sounthararajah, D., Loganathan, P., Kandasamy, J., & Vigneswaran, S. (2015). Adsorptive removal of heavy metals from water using sodium titanate nanofibres loaded onto GAC in fixed-bed columns. *Journal of Hazardous Materials, 287*, 306-316.

Sreedhar, M., Madhukumar, A., & Anirudhan, T. (1999). Evaluation of an adsorbent prepared by treating coconut husk with polysulphide for the removal of mercury from wastewater.

Srivastava, N., & Majumder, C. (2008). Novel biofiltration methods for the treatment of heavy metals from industrial wastewater. *Journal of Hazardous Materials, 151*(1), 1-8.

Srivastava, S., & Goyal, P. (2010). *Novel biomaterials: decontamination of toxic metals from wastewater*: Springer Science & Business Media.

Stephenson, J. J., Sadana, A. K., Higginbotham, A. L., & Tour, J. M. (2006). Highly functionalized and soluble multiwalled carbon nanotubes by reductive alkylation and arylation: the billups reaction. *Chemistry of Materials, 18*(19), 4658-4661.

Strik, D. P., Domnanovich, A. M., Zani, L., Braun, R., & Holubar, P. (2005). Prediction of trace compounds in biogas from anaerobic digestion using the MATLAB Neural Network Toolbox. *Environmental Modelling & Software, 20*(6), 803-810.

Sun, Y.-P., Fu, K., Lin, Y., & Huang, W. (2002). Functionalized carbon nanotubes: properties and applications. *Accounts of Chemical Research, 35*(12), 1096-1104.

Supply, W. U. J. W., & Programme, S. M. (2014). *Progress on drinking water and sanitation: 2014 update*: World Health Organization.

Tan, X., Yin, Q., Yang, X., Chen, S., Xu, R., Huang, X., & Dong, Y. (2012). Hyperchromic Effect and Mechanism of Carboxylic Carbon Nanotubes in Determination of Lead by Spectrophotometry. *Integrated Ferroelectrics, 137*(1), 126-133.

Tanzifi, M., Yaraki, M. T., Kiadehi, A. D., Hosseini, S. H., Olazar, M., Bhati, A. K., . . . Kazemi, A. (2018). Adsorption of Amido Black 10B from aqueous solution using polyaniline/SiO2 nanocomposite: Experimental investigation and artificial neural network modeling. *Journal of colloid and interface science, 510*, 246-261.

Tao, H.-C., Zhang, H.-R., Li, J.-B., & Ding, W.-Y. (2015). Biomass based activated carbon obtained from sludge and sugarcane bagasse for removing lead ion from wastewater. *Bioresource Technology, 192*, 611-617.

Tawabini, B. S., Al-Khaldi, S. F., Khaled, M. M., & Atieh, M. A. (2011). Removal of arsenic from water by iron oxide nanoparticles impregnated on carbon nanotubes. *Journal of Environmental Science and Health, Part A, 46*(3), 215-223.

Tchobanoglous, G., & Burton, F. L. (1991). Wastewater engineering. *Management, 7*, 1-4.

Tehlah, N., Kaewpradit, P., & Mujtaba, I. M. (2016). Artificial neural network based modeling and optimization of refined palm oil process. *Neurocomputing, 216*, 489-501.

Thines, R., Mubarak, N., Ruthiraan, M., Abdullah, E., Sahu, J., Jayakumara, N., . . . Sajuni, N. (2014). Adsorption isotherm and thermodynamics studies of Zn (II) on functionalized and non-functionalized carbon nanotubes. *Advanced Science, Engineering and Medicine, 6*(9), 974-984.

Thostenson, E. T., Ren, Z., & Chou, T.-W. (2001). Advances in the science and technology of carbon nanotubes and their composites: a review. *Composites science and technology, 61*(13), 1899-1912.

Thostenson, E. T., Ren, Z., Chou, T.-W. J. C. s., & technology. (2001). Advances in the science and technology of carbon nanotubes and their composites: a review. *61*(13), 1899-1912.

Tofighy, M. A., & Mohammadi, T. (2011). Adsorption of divalent heavy metal ions from water using carbon nanotube sheets. *Journal of Hazardous Materials, 185*(1), 140-147.

Tomić, A. Š., Antanasijević, D., Ristić, M., Perić-Grujić, A., & Pocajt, V. (2018). A linear and non-linear polynomial neural network modeling of dissolved oxygen content in surface water: Inter-and extrapolation performance with inputs' significance analysis. *Science of The Total Environment, 610*, 1038-1046.

Tong, S., Schirnding, Y. E. v., & Prapamontol, T. (2000). Environmental lead exposure: a public health problem of global dimensions. *Bulletin of the World Health Organization, 78*(9), 1068-1077.

Tresintsi, S., Simeonidis, K., Estradé, S., Martinez-Boubeta, C., Vourlias, G., Pinakidou, F., . . . Mitrakas, M. (2013). Tetravalent manganese feroxyhyte: a novel nanoadsorbent equally selective for As (III) and As (V) removal from drinking water. *Environmental science & technology, 47*(17), 9699-9705.

Tresintsi, S., Simeonidis, K., Vourlias, G., Stavropoulos, G., & Mitrakas, M. (2012). Kilogram-scale synthesis of iron oxy-hydroxides with improved arsenic removal capacity: Study of Fe (II) oxidation–precipitation parameters. *Water research, 46*(16), 5255-5267.

Tseng, R.-L., Wu, P.-H., Wu, F.-C., & Juang, R.-S. (2014). A convenient method to determine kinetic parameters of adsorption processes by nonlinear regression of pseudo-nth-order equation. *Chemical Engineering Journal, 237*, 153-161.

Turan, N. G., Mesci, B., & Ozgonenel, O. (2011). Artificial neural network (ANN) approach for modeling Zn (II) adsorption from leachate using a new biosorbent. *Chemical Engineering Journal, 173*(1), 98-105.

Turan, N. G., Mesci, B., & Ozgonenel, O. (2011). The use of artificial neural networks (ANN) for modeling of adsorption of Cu (II) from industrial leachate by pumice. *Chemical Engineering Journal, 171*(3), 1091-1097.

Tuutijärvi, T., Lu, J., Sillanpää, M., & Chen, G. (2009). As (V) adsorption on maghemite nanoparticles. *Journal of Hazardous Materials, 166*(2), 1415-1420.

Usui, Y., Aoki, K., Narita, N., Murakami, N., Nakamura, I., Nakamura, K., . . . Kato, H. (2008). Carbon Nanotubes with High Bone-Tissue Compatibility and Bone-Formation Acceleration Effects. *Small, 4*(2), 240-246.

Vakili, M., Yahyaei, M., & Kalhor, K. (2016). Thermal conductivity modeling of graphene nanoplatelets/deionized water nanofluid by MLP neural network and theoretical modeling using experimental results. *International Communications in Heat and Mass Transfer, 74*, 11-17.

Veličković, Z. S., Marinković, A. D., Bajić, Z. J., Marković, J. M., Perić-Grujić, A. A., Uskokovic, P. S., & Ristic, M. D. (2013). Oxidized and ethylenediamine-functionalized multi-walled carbon nanotubes for the separation of low concentration arsenate from water. *Separation Science and Technology, 48*(13), 2047-2058.

Venkata Ramana, D., Kumar Reddy, D. H., Kumar, B. N., Seshaiah, K., Chandra Rao, G. P., & Lu, C. (2013). Adsorption of Pb (II) from aqueous solutions by chemically modified zeolite supported carbon nanotubes: equilibrium, kinetic, and thermodynamic studies. *Separation Science and Technology, 48*(3), 403-412.

Vuković, G. D., Marinković, A. D., Čolić, M., Ristić, M. Đ., Aleksić, R., Perić-Grujić, A. A., & Uskoković, P. S. (2010). Removal of cadmium from aqueous solutions by oxidized and ethylenediamine-functionalized multi-walled carbon nanotubes. *Chemical Engineering Journal, 157*(1), 238-248.

Wang, H., Zhou, A., Peng, F., Yu, H., & Chen, L. (2007). Adsorption characteristic of acidified carbon nanotubes for heavy metal Pb (II) in aqueous solution. *Materials Science and Engineering: A, 466*(1), 201-206.

Wang, J., & Chen, C. (2006). Biosorption of heavy metals by Saccharomyces cerevisiae: A review. *Biotechnology Advances, 24*(5), 427-451.

Wang, S.-X., Wang, Z.-H., Cheng, X.-T., Li, J., Sang, Z.-P., Zhang, X.-D., . . . Wang, Z.-Q. (2007). Arsenic and fluoride exposure in drinking water: children's IQ and growth in Shanyin county, Shanxi province, China. *Environmental health perspectives*, 643-647.

Wasserman, G. A., Liu, X., Parvez, F., Ahsan, H., Factor-Litvak, P., van Geen, A., . . . Hussain, I. (2004). Water arsenic exposure and children's intellectual function in Araihazar, Bangladesh. *Environmental health perspectives*, 1329-1333.

Wasserman, P. D. (1989). *Neural computing*: Van Nostrand Reinhold, New York.

Wei, L., Fan, Y.-J., Wang, H.-H., Tian, N., Zhou, Z.-Y., & Sun, S.-G. (2012). Electrochemically shape-controlled synthesis in deep eutectic solvents of Pt nanoflowers with enhanced activity for ethanol oxidation. *Electrochimica Acta, 76*, 468-474.

Weng, C.-H., & Huang, C. (2004). Adsorption characteristics of Zn (II) from dilute aqueous solution by fly ash. *Colloids and Surfaces A: Physicochemical and Engineering Aspects, 247*(1), 137-143.

Witek-Krowiak, A., Szafran, R. G., & Modelski, S. (2011). Biosorption of heavy metals from aqueous solutions onto peanut shell as a low-cost biosorbent. *Desalination, 265*(1), 126-134.

won Seo, I., Yun, S. H., & Choi, S. Y. (2016). Forecasting water quality parameters by ANN model using pre-processing technique at the downstream of Cheongpyeong Dam. *Procedia Engineering, 154*, 1110-1115.

Wu, G., & Xu, Z. (2011). Prediction of algal blooming using EFDC model: Case study in the Daoxiang Lake. *Ecological Modelling, 222*(6), 1245-1252.

Wu, L.-K., Wu, H., Zhang, H.-B., Cao, H.-Z., Hou, G.-Y., Tang, Y.-P., & Zheng, G.-Q. (2018). Graphene oxide/CuFe2O4 foam as an efficient absorbent for arsenic removal from water. *Chemical Engineering Journal, 334*, 1808-1819.

Wunsch, A., Liesch, T., & Broda, S. (2018). Forecasting groundwater levels using nonlinear autoregressive networks with exogenous input (NARX). *Journal of Hydrology*.

Xia, S., Shen, S., Xu, X., Liang, J., & Zhou, L. (2014). Arsenic removal from groundwater by acclimated sludge under autohydrogenotrophic conditions. *Journal of Environmental Sciences, 26*(2), 248-255.

Xiong, Q., Tu, J., Ge, X., Wang, X., & Gu, C. (2015). One-step synthesis of hematite nanospindles from choline chloride/urea deep eutectic solvent with highly powerful storage versus lithium. *Journal of Power Sources, 274*, 1-7.

Xu, K., Wang, Y., Ding, X., Huang, Y., Li, N., & Wen, Q. (2016). Magnetic solid-phase extraction of protein with deep eutectic solvent immobilized magnetic graphene oxide nanoparticles. *Talanta, 148*, 153-162.

Xu, K., Wang, Y., Huang, Y., Li, N., & Wen, Q. (2015). A green deep eutectic solvent-based aqueous two-phase system for protein extracting. *Analytica chimica acta, 864*, 9-20.

Yadav, A. K., & Chandel, S. (2014). Solar radiation prediction using Artificial Neural Network techniques: A review. *Renewable and Sustainable Energy Reviews, 33*, 772-781.

Yamauchi, H., & Yamamura, Y. (1983). Concentration and chemical species of arsenic in human tissue. *Bulletin of environmental contamination and toxicology, 31*(3), 267-270.

Yang, D., Hou, M., Ning, H., Zhang, J., Ma, J., Yang, G., & Han, B. (2013). Efficient SO 2 absorption by renewable choline chloride–glycerol deep eutectic solvents. *Green Chemistry, 15*(8), 2261-2265.

Yang, J., Wei, W., Pi, S., Ma, F., Li, A., Wu, D., & Xing, J. (2015). Competitive adsorption of heavy metals by extracellular polymeric substances extracted from Klebsiella sp. J1. *Bioresource Technology, 196*, 533-539.

Yang, Y., Wang, G., Wang, B., Li, Z., Jia, X., Zhou, Q., & Zhao, Y. (2011). Biosorption of Acid Black 172 and Congo Red from aqueous solution by nonviable Penicillium YW 01: Kinetic study, equilibrium isotherm and artificial neural network modeling. *Bioresource Technology, 102*(2), 828-834.

Yang, Z., Qiao, W.-m., & Liang, X.-y. (2017). Modelling and optimization of the pore structure of carbon aerogels using an artificial neural network. *New Carbon Materials, 32*(1), 77-85.

Yasin, Y., Ahmad, F. B. H., Ghaffari-Moghaddam, M., & Khajeh, M. (2014a). Application of a hybrid artificial neural network–genetic algorithm approach to optimize the lead ions removal from aqueous solutions using intercalated tartrate-Mg–Al layered double hydroxides. *Environmental Nanotechnology, Monitoring & Management, 1–2*, 2-7.

Yasin, Y., Ahmad, F. B. H., Ghaffari-Moghaddam, M., & Khajeh, M. (2014b). Application of a hybrid artificial neural network–genetic algorithm approach to optimize the lead ions removal from aqueous solutions using intercalated tartrate-Mg–Al layered double hydroxides. *Environmental Nanotechnology, Monitoring & Management, 1*, 2-7.

Yetilmezsoy, K., & Demirel, S. (2008a). Artificial neural network (ANN) approach for modeling of Pb (II) adsorption from aqueous solution by Antep pistachio (Pistacia Vera L.) shells. *Journal of hazardous materials, 153*(3), 1288-1300.

Yetilmezsoy, K., & Demirel, S. (2008b). Artificial neural network (ANN) approach for modeling of Pb(II) adsorption from aqueous solution by Antep pistachio (Pistacia Vera L.) shells. *Journal of Hazardous Materials, 153*(3), 1288-1300.

Yi, W., Lu, L., Dian-Lin, Z., Pan, Z., & Xie, S. (1999). Linear specific heat of carbon nanotubes. *Physical Review B, 59*(14), R9015.

Yim, W., & Liu, Z. (2004). A reexamination of the chemisorption and desorption of ozone on the exterior of a (5, 5) single-walled carbon nanotube. *Chemical physics letters, 398*(4), 297-303.

Yu, F., Ma, J., & Wu, Y. (2011). Adsorption of toluene, ethylbenzene and m-xylene on multi-walled carbon nanotubes with different oxygen contents from aqueous solutions. *Journal of Hazardous Materials, 192*(3), 1370-1379.

Yu, F., Wu, Y., Ma, J., & Zhang, C. (2013). Adsorption of lead on multi-walled carbon nanotubes with different outer diameters and oxygen contents: kinetics, isotherms and thermodynamics. *Journal of Environmental Sciences, 25*(1), 195-203.

Yu, R., Chen, L., Liu, Q., Lin, J., Tan, K.-L., Ng, S. C., . . . Hor, T. A. (1998). Platinum deposition on carbon nanotubes via chemical modification. *Chemistry of Materials, 10*(3), 718-722.

Zabihi, M., Asl, A. H., & Ahmadpour, A. (2010). Studies on adsorption of mercury from aqueous solution on activated carbons prepared from walnut shell. *Journal of Hazardous Materials, 174*(1), 251-256.

Zafar, M., Van Vinh, N., Behera, S. K., & Park, H.-S. (2016). Ethanol mediated As (III) adsorption onto Zn-loaded pinecone biochar: Experimental investigation, modeling, and optimization using hybrid artificial neural network-genetic algorithm approach. *Journal of Environmental Sciences*.

Zeng, W., Song, Q., Liu, H., & Wang, T. (2010). Research on ANN-based pre-warning water bloom model of LiuHai Lake in Beijing. *Procedia Environmental Sciences, 2*, 625-635.

Zhang, B., & Govindaraju, R. S. (2003). Geomorphology-based artificial neural networks (GANNs) for estimation of direct runoff over watersheds. *Journal of Hydrology, 273*(1–4), 18-34.

Zhang, C., Sui, J., Li, J., Tang, Y., & Cai, W. (2012). Efficient removal of heavy metal ions by thiol-functionalized superparamagnetic carbon nanotubes. *Chemical Engineering Journal, 210*, 45-52.

Zhang, F.-S., Nriagu, J. O., & Itoh, H. (2005). Mercury removal from water using activated carbons derived from organic sewage sludge. *Water research, 39*(2), 389-395.

Zhang, J., Wu, T., Chen, S., Feng, P., & Bu, X. (2009). Versatile Structure-Directing Roles of Deep-Eutectic Solvents and Their Implication in the Generation of Porosity and Open Metal Sites for Gas Storage. *Angewandte Chemie International Edition, 48*(19), 3486-3490.

Zhang, J., Zhao, L., Deng, S., Xu, W., & Zhang, Y. (2017). A critical review of the models used to estimate solar radiation. *Renewable and Sustainable Energy Reviews, 70*, 314-329.

Zhang, M., Gao, B., Cao, X., & Yang, L. (2013). Synthesis of a multifunctional graphene–carbon nanotube aerogel and its strong adsorption of lead from aqueous solution. *RSC Advances, 3*(43), 21099-21105.

Zhang, Q., Vigier, K. D. O., Royer, S., & Jérôme, F. (2012). Deep eutectic solvents: syntheses, properties and applications. *Chemical Society Reviews, 41*(21), 7108-7146.

Zhang, Q., Zhang, S., & Deng, Y. (2011). Recent advances in ionic liquid catalysis. *Green Chemistry, 13*(10), 2619-2637.

Zhao, B.-Y., Xu, P., Yang, F.-X., Wu, H., Zong, M.-H., & Lou, W.-Y. (2015). Biocompatible deep eutectic solvents based on choline chloride: characterization and application to the extraction of rutin from Sophora japonica. *ACS Sustainable Chemistry & Engineering, 3*(11), 2746-2755.

Zhao, H., Baker, G. A., & Holmes, S. (2011). Protease activation in glycerol-based deep eutectic solvents. *Journal of Molecular Catalysis B: Enzymatic, 72*(3), 163-167.

Zhao, X., Jia, Q., Song, N., Zhou, W., & Li, Y. (2010). Adsorption of Pb (II) from an aqueous solution by titanium dioxide/carbon nanotube nanocomposites: kinetics, thermodynamics, and isotherms. *Journal of Chemical & Engineering Data, 55*(10), 4428-4433.

Zheng, Y., Ye, L., Yan, L., & Gao, Y. (2014). The electrochemical behavior and determination of quercetin in choline chloride/urea deep eutectic solvent electrolyte based on abrasively immobilized multi-wall carbon nanotubes modified electrode. *Int. J. Electrochem. Sci, 9*, 238-248.

Zhou, L., Ji, L., Ma, P.-C., Shao, Y., Zhang, H., Gao, W., & Li, Y. (2014). Development of carbon nanotubes/CoFe 2 O 4 magnetic hybrid material for removal of tetrabromobisphenol A and Pb (II). *Journal of Hazardous Materials, 265*, 104-114.

Zhu, H., Xu, C., Wu, D., Wei, B., Vajtai, R., & Ajayan, P. (2002). Direct synthesis of long single-walled carbon nanotube strands. *Science, 296*(5569), 884-886.

LIST OF PUBLICATIONS AND PAPERS PRESENTED

Published papers

1- **Seef Saadi Fiyadh**, Mohammed Abdulhakim AlSaadi, Mohamed Khalid AlOmar, Sabah Saadi Fayaed, Ako R. Hama, Sharifah Bee, Ahmed El-Shafie., 2017. *The modeling of lead removal from water by deep eutectic solvents functionalized CNTs: Artificial neural network (ANN) approach*. Water Science & Technology. ***ISI index***.

2- **Seef Saadi Fiyadh**, Mohammed Abdulhakim AlSaadi, Mohamed Khalid AlOmar, Sabah Saadi Fayaed, Ahmed El-Shafie, 2018. *Lead removal from water using DES functionalized CNTs: ANN modeling approach,* Desalination and water treatment. ***ISI index***.

3- **Seef Saadi Fiyadh**, Mohammed Abdulhakim AlSaadi, Mohamed Khalid AlOmar, Sabah Saadi Fayaed, Sharifa Bee, Ahmed El-Shafie. 2017. *The modelling of arsenic removal from water by deep eutectic solvents functionalized CNTs: Artificial neural network (ANN) approach.* Desalination and water treatment. ***ISI index***.

4- **Seef Saadi Fiyadh**, Mohammed Abdulhakim AlSaadi, Mohamed Khalid AlOmar, Sabah Saadi Fayaed, Farouq S. Mjalli, Ahmed El-Shafie, 2018. *BTPC based DES-functionalized CNTs for As3+ removal from water:(NARX) neural network approach*. Journal of environmental engineering. ***ISI index***.

5- **Seef Saadi Fiyadh**, Mohammed Abdulhakim AlSaadi, Mohamed Khalid AlOmar, Sabah Saadi Fayaed, Ahmed El-Shafie, 2018. *Arsenic removal from water using N, N- diethylethanol ammonium chloride based DES-functionalized CNTs: (NARX) neural network approach*. Journal of Water Supply: Research and Technology – AQUA. ***ISI index***.

6- **Seef Saadi Fiyadh**, Mohammed Abdulhakim AlSaadi, Mohamed Khalid AlOmar, Sabah Saadi Fayaed, Nuruol Syuhadaa Binti Mohd, Ahmed El-Shafie, 2018. *Review on heavy metal adsorption processes by carbon nanotubes.* Journal of Cleaner Production. ***ISI index***.

7- **Seef Saadi Fiyadh**, Mohammed Abdulhakim AlSaadi, Wan Zurina Binti Jaafar, Mohamed Khalid AlOmar, Sabah Saadi Fayaed, Ako Rashed Hama, Lai Sai Hin, Ahmed El-Shafie, 2018. *Mercury removal from water solution using tetra-n-butyl ammonium bromide (TAB) based DES-functionalized MWCNTs:(NARX) neural network approach.* Environmental Progress & Sustainable Energy. ***ISI index***.

Submitted papers (Under review)

8- **Seef Saadi Fiyadh**, Mohammed Abdulhakim AlSaadi, Wan Zurina Binti Jaafar, Mohamed Khalid AlOmar, Sabah Saadi Fayaed, Suhana Binti Koting, Lai Sai Hin, Ahmed El-Shafie, 2018. *Allyl triphenyl phosphonium bromide-based DES-functionalized CNTs for mercury removal from water: artificial neural network modelling approach*. Journal of Cleaner Production. ***ISI index***.